Università degli Studi di Padova

Dipartimento di Matematica "Tullio Levi-Civita"
Corso di Dottorato di Ricerca in Scienze Matematiche
Curricolo Matematica Computazionale
Ciclo XXXVI

Numerical Modeling of Water Distribution Systems Using the Graph p-Laplacian: Variational and Duality Methods with Applications

Coordinatore
Ch.mo Prof. Giovanni Colombo

Supervisore
Ch.mo Prof. Mario Putti
Ch.ma Prof. Antonia Larese

Dottorando
Nicola Segala

Acknowledgments

This thesis is the result of a long and tortuous journey lasted more than three years, during which I had the opportunity to meet and collaborate with many wonderful people. The support of these people made this thesis possible, so I would like to express my gratitude to all of them. First of all, I sincerely want express my gratitude to my supervisors Mario Putti and Antonia Larese who gave me the opportunity to accomplish my PhD, along with my company tutors Franco Masenello, Cristina Scarpel and Massimo Ramazzotto who constantly gave me support from a professional point of view and, more importantly, establishing a sincere friendship. Their constant encouragement, patience and suggestions have allowed me to grow in every scientific aspect. I also want to sincerely thanks Francesco Marchetti, Piero Deidda, Federico Piazzon, and Enrico Facca for the many interesting discussions that have been a continuous source of ideas for my research.

Abstract

In this thesis we discuss how to model a Water Distribution System(WDS) by means of a surrogate graph p-Laplacian model, with $1 < p < 2$.
We exhaustively discuss both numerical and theoretical aspects, within the framework of graph based inverse problems, convex analysis and Legendre duality.
As an application of the proposed techniques, we extend the results that we achieved on WDS modeling to a larger class of graph-based optimization problems.
The basic idea is that, starting mainly from data on pipe characteristics and measurements of water pressure and water fluxes inside pipes, it is possible to accurately determine an edge-based distribution of edges weights and p-values on the edges so that the corresponding weighted p-Poisson equation can be effectively used as a Digital Twin of the WDS under study. The successful completion of this part required the determination and subsequent numerical solution of an appropriately regularized inverse problem (a variant of Calderon's inverse problem) defined on the WDS graph.
The peculiar characteristics of a WDS, whereby neighboring pipes have typically the same edge-constant properties (read weights and p-values) required the use of a Total-Variation (TV) based regularization.
Thus, on the second part of this thesis we focused on the variational characterization by duality methods of TV regularizers embedded in the solution of the weighted p-Laplace inverse problem.
We discuss how to properly rewrite a convex energy functional into an equivalent saddle point formulation, to tackle the problem of finding it's minimizers from an alternative and more performing perspective. We extensively study the case of the p-Dirichlet energy for $1 < p < 2$, and of the Total Variation energy as limit case for $p \to 1$, including it's application as a regularization term in various type of inverse problems.
The derivation of these saddle point formulations is essentially based on the iteration of the Legendre transform combined with ad-hoc substitutions and transformations of the involved variables. Indeed, this is a classical technique in convex optimization theory and widely used in the variational formulation of partial differential equations.
These resulting equivalent formulations based on duality theory, leads to a class of saddle point problems that can be efficiently translated into accurate and robust numerical methods based on variant of the Dynamic-Monge-Kantorovich(DMK) equations developed earlier by the supervisors research group for the numerical solution of the L1 Optimal Transport problem. Moreover, we discuss both theoretical aspects and numerical implementation of the proposed formulation showing also the efficiency and robustness of the developed algorithms on both

classical problems and real-world examples.
On the third part of the thesis we focus on the development of numerical schemes for the nonlinear eigenvalue problem of p-Laplace operators on graphs with $1 < p$. The aim of this part is to provide a proper efficient numerical scheme in order to use eigen-information of the p-Laplace operator governing the specific WDS to develop Machine-Learning and surrogate models. A family of Energy functions, inspired again by the DMK approach, whose critical points can be proved to be variational eigenpairs of the p-Laplace operators, have been used to develop gradient-flow algorithms for the numerical calculations of p-eigenpairs.
Unfortunately, only partial results have been achieved in this topic due to two main difficulties inherently related to the nonlinear eigenvalue problem. On one hand, the non-regularity of these energy functions in the presence of eigenpairs with multiplicity greater than one may cause non-convergence of the developed gradient-based method. The second important difficulty is related to the positioning of the found p-eigenpairs within the p-spectrum. Indeed, the interpretation of the DMK equations deriving from the KKT conditions of the proposed energy functions as an appropriate weighted linear Laplace eigenproblem allowed the definition of an approximate ordering of the numerically calculated p-eigenpairs. However, a complete solution of this problem is still elusive and is left of a matter of future developments.

Contents

Introduction

This thesis is focused on modeling a water distribution system (WDS) through a surrogate p-Laplacian model. This problem can be genuinely connected to the framework of graph based machine learning and graph based inverse problems with PDE constraints.
Different techniques has been appositevely developed for the numerical solution of this problem and collected into three main chapters, which can be related but also be of independent interest.
For this reason, we provide here a brief introduction, summarizing the main concepts and ideas which are then presented in details on the relative chapters and their exhaustive introductions.
When dealing with the mathematical modeling of a Water Distribution System (WDS), it is natural to consider a graph-theoretic setting, where features such as, e.g., pipes, intersections, house services, tanks, pumps, and valves are effectively represented by means of nodes, edges and their related properties. It is natural to express the physical laws that govern the hydraulic dynamics of a WDS, such as mass and momentum balances, localized and distributed energy losses, input and control structures, demands, etc. via tools from the graph theory framework. This is explained in some details for example in [141], with predominant emphasis on topological characteristics for WDS reliability analysis.
Accurate modeling of an operational WDS is a complex task mostly attributable to the non-stationarity of the system inputs. Indeed, a considerable number of variables and parameters involved in the model may have changed during the WDS lifespan because of, e.g., pipe degradation, valve malfunctioning, varied demand, added connections, etc., and the model developed in the design phase may not be accurate forcing a re-development of the simulation model. In general, this development together with the tuning of the new parameters is problematic especially because of the frequent lack of available data [38, 122]. Therefore, aiming at recovering a detailed Physics-Based (PB) operational model of the WDS is very often an unrealistic task. This suggests the idea to look for surrogate models, namely simplified-reality models that are relatively easy to tune and capable of describing the dynamics of the WDS with sufficient (controlled) accuracy.
In the last decade, Artificial Intelligence (AI), alias Machine Learning (ML) and all its derivatives such as deep or reinforced learning, has seen a dramatic development and found extensive application in surrogate modeling of WDSs, espe-

cially within the field of leak detection [75, 86, 90]. These approaches are named Data-Driven (DD) for their extraordinary ability to approximate data without any knowledge of the underlying physical processes that generated the data. We observe that pure DD methods, where the physics-based model is replaced by machine/deep learning schemes trained on available data, turned out to be often unsatisfactory as the dynamics of the WDS pressure is completely ignored [86].

In our view, the low prediction ability of ML-based surrogate modeling is essentially based to the absence of physics in the modelling setting. Indeed, the nonlinear regime governing a WDS increases the model sensitivity to parameter variations and, as a consequence, the ill-conditioning of the related calibration inverse problem. One of the founding ideas of this thesis is that the use of a simplified but nonlinear surrogate model substantially reduces the danger of over-parametrization and increases the prediction ability of calibrated surrogate models in WDS simulations.

A typical nonlinear model problem extensively studied in the mathematical literature is the so-called weighted p-Laplacian operator, a nonlinear extension of the classical Laplacian operator. To define this operator, one starts from the water fluxes that are parallel to a pressure gradient and are characterized by a conductivity constant w multiplied by the modulus of the pressure gradient raised to the power $p-2$. The mass balance arising from such fluxes produces the so-called weighted p-Laplacian (or p-Poisson in the presence of a forcing function) equation.

One of the goals of our work is to verify if and how a WDS can be effectively described using a p-Laplacian-based surrogate modeling. For this purpose, we recast standard WDS modeling approaches within the framework of a weighted p-Laplacian operator. Once this has been established, we use synthetic and real test cases to calibrate the weight w and power p to reproduce standard modeling results and verify that the wanted prediction accuracy can be realized by the proposed p-Laplace-based surrogate model.

Hence, in this thesis, we propose a surrogate Data-Based (DB) model for for the simulation of operational WDSs, which lies *in the middle* between PB and DD approaches. Indeed, we make extensive use of collected data for model calibration, and we also take into account the physical aspect by considering a dynamics based on the weighted graph p-Laplacian operator.

As a consequence, we find out that our task can be efficiency solved by introducing a non-linear extension based on the graph p-Laplacian for the classical Calderon's inverse problem on graph [42].

Differently from the standard approach to this problem, which is essentially based on harmonic extensions, medial graphs reduction and Schur complements, we adopt the framework of the primal-adjoint method, typically used in parameter estimation for the continuous based two dimensional Calderon's problem [95], [26]. This is ultimately due to the need of adopting a sufficiently flexible approach which leads us to easily include further constraints on our parameters to

satisfy the physical lows governing a WDS i.e. the edges weights w must to be positive and the exponents p should be such that $1.4 \leq p \leq 1.8$. Due to the lack of convexity of the Calderon's inverse problem, over-parametrization typically occurs and the consequential appearance of multiple solutions force the use of Tikhonov-like regularization terms to arrive at a feasible solution [14, 30, 69].

A very efficient class of Tikhonov regularizers are based on the Total Variation of the design parameters and naturally leads to solution in the space of bounded variation functions BV. The Total Variation energy, due to it's enhancing sparsity property on the gradient, plays an important role in image denoising and signal reconstruction [26], [33], [64], [104], [115]. In the case of WDS, the Total Variation is particularly suitable as regularization term since it is natural, by construction, that there are sequences of pipes with the same diameters and materials, so that we are expecting to retrieve clustered parameters and the TV has optimal clustering properties.

Taking inspiration from the Hazen-Williams water losses formulas in WDS, we develop a Legendre duality based saddle point formulation for the p-Dirichlet energy which, in the limit case when $p = 1$ naturally interconnects the space of BV functions with the positive Radon measures. Thus, following the work of [18], [55], [59] on the L^1 Optimal Transport problem, we introduce a new variational problem which leads us to reduce the computation of the Total Variation for a function in BV as the computation of a saddle point for a Lagrangian function that can be easily discretized with the standard methods of numerical analysis.

As a case of direct interest for this thesis, we state the discrete counterpart on graph of the proposed saddle point method, where the differential structure is given by the graph signed differences matrix. We then introduce an opportune smoothed version of our saddle point formulation for the Total Variation energy which leads to a class of very efficient numerical solvers based on the DMK(Dynamic-Monge-Kantorovich) scheme [54]. This smoothed formulation can be easily incorporated as a continuous and differentiable approximation for the TV Tikhonov regularization term in our WDS p-Laplacian inverse problem.

Furthermore, in the general case when $1 < p < 2$, the proposed saddle point numerical method can be efficiently recycled as a very fast iterative linear solver for the p-Poisson problem on graphs.

As a consequence, all the proposed algorithms were implemented and integrated in our numerical algorithm based on the Calderon's p-Laplacian inverse problem for the parameters identification of the edges weights w and the esponents p in order to reproduce the piezometric heads distribution (pressure plus elevation) and the water fluxes from synthetic pressures, fluxes and demands data measurements.

In the Last part of this thesis, as an introduction for future developments, we propose a new reformulation of the p-Laplacian eigenpairs in terms of constrained weighted linear Laplacian eigenproblems. In particular, we show that from this reformulation of the p-Laplacian eigenproblem it is possible to deduce novel nu-

merical methods, which are essentially an extension of the iterative numerical solver for the p-Poisson problem that we developed for our surrogate p-Laplacian WDS model calibration.
Thus, summarizing, the content of the thesis can be divided into three main topics that are related but that can also be of independent interest.

1. In the first part we introduce the mathematical aspects of WDS modeling, the available data and the physical laws governing a pressurize network. Then, we introduce the role of the graph p-Laplacian as the main governing operator describing the dynamics of piezometric heads and fluxes giving a certain demand distribution. We enphasize the role of the various components of a WDS network such as tanks, reservoirs, pumps, valves, emitters, and their mathematical translation which in the p-Laplacian framework are essentially various type of boundary conditions. We then propose our parameter identification model which will be the core of our model calibration inverse problem, extending the notion of the Dirichlet-to-Neumann map on graphs and introducing a variant of the classical Calderon's inverse problem. Then, we describe our primal-adjoint based approach and the role of the Dirichlet-to-Neumann map to ensure the well posedness of the problem proposing moreover a topological based Line Graph Tikhonov type regularization, based on the graph Total Variation energy. Finally we present some numerical results based on synthethic data.

2. In the second part of the thesis we describe the main tool that we use for the numerical solution of our WDS data calibration model as for the p-Laplacian PDE constraint and mainly for the TV based regularization.
   In particular, we propose a duality based saddle point formulation for the p-Dirichlet energy $1 < p < 2$ and it's limit case when $p = 1$, namely the Total Variation energy, both in the continuous and in the discrete graph based setting. We also discuss how to properly rewrite, with similar arguments, a larger class of convex energy functionals into an equivalent saddle point formulation with the ultimate goal to tackle the problem of finding their minimizers from an alternative and more performing perspective.
   Our initial idea is based by observing that iterating the Legendre transform, and selecting opportunely the state and conjugate variables, we can translate the p-Dirichlet energy into a classical weighted Laplacian mixed formulation plus a mass term in the conductivity weight variable.
   Then, we further show how to extend our saddle point formulation to a larger class of convex discrete energies, providing also an example of application to the minimal surfaces discrete energy. We also state theorems and proofs for the most important results, essentially based on duality arguments and some ad hoc extensions of classical convex analysis results in [46]. Moreover, we propose novel numerical schemes based on the Dynamic-Monge-Kantorovich(DMK) scheme first developed for the L^1 optimal trans-

port problem ([55], [58], [54], [59]), and opportunely modified for the problem of computing saddle points of the proposed energies reformulations. The computation of these saddle points is proved to be equivalent to the problem of computing minimizers for the original energies, showing also the advantages of this approach.
As an application, we show how to use our proposed techniques to the numerical solution of classical problems, such as an iterative numerical solution to 1-harmonic Dirichlet problem and the p-Poisson Dirichlet problem on graphs. We also show some other applications based on using the Total Variation and the l_1 norm as Tikhonov regularization terms in some discrete optimization problems such as the classical ROF(Rudin-Osher-Fatemi) TV denoising [104] and the compressed modes for the graph Laplacian [106].

3. In the third part of the thesis we discuss the problem of computing the p-Laplacian eigenpairs. This matter has recently been investigated by different authors [21, 72, 139] leaving, however, several open problems. In the thesis, we show that it is possible to compute the p-Laplacian eigenpairs as the limit of sequences of weighted linear Laplacian eigenpairs. In particular, we observe that, for any $p \in [2, \infty]$, it is possible to reformulate the p-Laplacian eigenvalue problem as a weighted Laplacian eigenvalue problem with constraints on the weights. Based on the weighted linear reformulation of the p-Laplacian eigenvalue problem, we introduce a family of energy functions such that the cardinality of the family is equal to the dimension of the graph N, and the variables of the functions are weights on the edges and on the nodes of the graph. Enumerated the energy functions from 1 to N, we prove that any smooth saddle point of the k-th energy function corresponds to a p-Laplacian eigenpairs. In addition, we prove that the first energy function has a unique saddle point, possibly not smooth, which always corresponds to the unique first eigenpair of the p-Laplacian. Finally, based on the above results, we investigate novel numerical methods devoted to compute p-Laplacian eigenpairs in both the cases $p < \infty$ and $p = \infty$.

1 Modeling WDS via the graph p-Laplace operator

1.1 Introduction

When dealing with the mathematical modeling of a Water Distribution System (WDS), it is natural to consider a graph-theoretic setting, in which features such as, e.g., pipes, intersections, house services, tanks, pumps, and valves are effectively represented by means of nodes and edges and their related properties. Once a WDS has been defined over a graph, its modeling can take advantage of the vast literature on graph theory (see e.g. Kepner and Gilbert [85] for a recent exposition). This comprises important tools such as discrete analogues of differential operators (graph Laplacians and p-Laplacians), divergence theorems, and integration by parts, as well as linear algebra and related numerical algorithms addressing, e.g., the numerical solution of linear systems and calculation of eigenvalues and clustering. Within this framework, it becomes natural to express the physical laws that govern the hydraulic dynamics of a WDS, such as mass and momentum balances, localized and distributed energy losses, input and control structures, demands, etc. This is explained in some details for example in Yazdani and Jeffrey [141], with predominant emphasis on topological characteristics of the graph aimed at WDS reliability analysis. The latter has seen a number of recent contributions based on graph theory, among which we would like to mention [29, 31, 65, 66, 73, 97, 98, 107, 114, 127, 137]. All these works leverage on the recent advances in complex network and cluster analysis to determine aqueduct vulnerability to unforeseen and extreme conditions. However, the exploitation of graph theory results for modeling the hydrodynamics and simulating the dynamics of a WDS is not yet developed.
In the past years a wealth of WDS simulators have appeared in the specialized literature and are routinely used in engineering practice for their design and analysis (see [10] for a recent review). Various simulation approaches and techniques together with the accompanying optimization methods have been developed in order to obtain accurate simulations of WDS dynamics subject to complex demands, both in terms of design and operational strategies [39, 81, 124, 133, 144]. Among the available software [10], EPANET is a well-known package and a defacto standard for the design of a WDS. It allows a precise planning of the WDS

structure and its hydraulic dynamics, including an accurate description of all the components and corresponding parameters, and it finds widespread use in the WDS community. In this thesis it is assumed to be the reference model for WDSs. Accurate modeling of an operational WDS is a complex task mostly attributable to the uncertainty and non-stationarity of the system parameters and the forcings. Indeed, aging certainly causes changes in the behavior of WDS components because of, e.g., pipe degradation, valve malfunctioning, varied demand, added connections, etc. This leads to changes in the parameter values that best model the changed behavior of the system components. Hence, the model developed in the design phase cannot be accurate for the entire WDS lifespan and re-development or re-calibration of the simulation model is often required. In general, this development forces a re-calibration and the tuning of the system parameters, and this is often problematic especially because of the frequent lack of available data [38, 122]. Therefore, aiming at recovering a detailed Physics-Based (PB) operational WDS model is often an unrealistic task. In order to resolve this concrete issue, various *surrogate* indices have been proposed in the few last years and employed in WDS least-cost management tasks [108, 112, 126]. The aim of theses surrogate indices is to summarize in only a few numbers the status of the WDS. Along this direction, one of the first approaches can be traced back to [132], where a resilience index was designed as surrogate metric to assess the dependability of a WDS. More recently, a further index built upon Todini's ideas has been introduced in [116] and compared in [117, 125] to other reliability indices, such as the flow entropy or the flow-uniformity indices [93, 100].

The idea of surrogate metric naturally suggests to look for surrogate models, or digital twins. These are simplified-reality models that are relatively easy to tune and capable of describing the dynamics of the WDS with sufficient (controlled) accuracy. In the last decade, Artificial Intelligence (AI), alias Machine Learning (ML) and all its derivatives such as deep or reinforced learning, has seen a dramatic development and found extensive application in surrogate modeling of WDSs, especially within the field of leak detection [75, 86, 90]. These approaches are named Data-Driven (DD) for their extraordinary ability to approximate data without any knowledge of the underlying physical processes that generated the data. However, we would like observe that pure DD methods, where the physics-based model is replaced by machine/deep learning schemes trained on available data, turned out to be often unsatisfactory as the dynamics of the WDS pressure is completely ignored [86]. Indeed, being ML essentially based on articulated regression mechanisms, the prediction accuracy essentially depends on the training data. In a non-stationary regime, where training data do not contain enough information or do not reflect the changes in the WDS properties, an ML-based model can be accurate only for short extrapolation times. This is a common problem of ML and current research in AI looks for so-called "Physics-Informed" Machine Learning (PI-ML) to add to the outstanding regression capabilities of ML some physical knowledge of the system at hand [119].

In our view, the low prediction ability of ML-based surrogate modeling, traced back in the previous paragraph (and in the relevant literature) to the absence of physics in the modelling setting, can be related further to the role of the nonlinearities introduced in the mathematical modeling of friction and energy losses in a WDS. Indeed, the nonlinear regime governing a WDS has to main effects. On one hand, it increases the model sensitivity to parameter variations and, as a consequence, the ill-conditioning of the related calibration inverse problem. On the other hand, the observations used for calibration are not in general representative the entire interval of variation of the variables driving the system dynamics. This latter problem, while negligible in a linear model, becomes highly critical in the nonlinear case. The most important consequence of this is the so called over-parametrization of regression models, which leads typically to ill-conditioning and multiple solutions of both the direct and inverse (calibration) models. This forces the use of Tikhonov-like regularization terms to arrive at a computable solution [14, 30, 69]. One of the founding ideas of this thesis is that the use of a simplified but nonlinear surrogate model substantially reduces the danger of over-parametrization and increases the prediction ability of calibrated surrogate models in WDS simulations and their concrete development.

A typical nonlinear model problem extensively studied in the mathematical literature is the so-called weighted p-Laplacian operator, a nonlinear extension of the classical Laplacian operator. To define this operator, one considers water fluxes that are aligned to the pressure gradient, i.e., they are parallel and go in the same direction of the pressure gradient. The magnitude of the fluxes are characterized by a conductivity that is a nonlinear function of the pressure gradient. The resulting flux is equal to the product of a constant w multiplied by the modulus of the pressure gradient raised to the power $p-2$ times the pressure gradient. The mass balance arising from such fluxes produces the so-called weighted p-Laplacian (or p-Poisson in the presence of a forcing function) equation. The p-Laplace equation has mathematical properties that are similar to the linear Laplace equation ($p = 2$) in terms of symmetry and dissipation properties that provide well-posedness and well-conditioning of the related mathematical and numerical formulations that can be easily related to those of the linear Laplace operator. For these reasons, p-Laplace equations have been used extensively in many different applications [20, 28, 47].

One of the goals of our work is to verify if and how a WDS can be effectively described using a p-Laplacian-based surrogate modeling. For this purpose, we recast standard WDS modeling approaches within the framework of a weighted p-Laplacian operator. Once this has been established, we use synthetic and real test cases to calibrate the spatial distributions of the weight w and of the power p that best reproduce standard commercial simulations results (i.e., EPANET), and verify that the desired prediction accuracy can be realized by the proposed p-Laplace-based surrogate model.

In this chapter we propose a surrogate Data-Based (DB) model for for the sim-

ulation of operational WDSs, and note that this approach can be position *in the middle* between PB and DD approaches. Indeed, we make extensive use of collected data for model calibration, and we also take into account the physical aspects by considering a dynamics based on the weighted graph p-Laplace operator. More precisely, after motivating the introduction of such an operator within this context, we show that it is possible to tune its two parameters, i.e., the value of the exponent p and the weight w, in such a way that the outputs of an EPANET simulation can be reproduced within this simplified setting. We test the accuracy of the proposed surrogate model by varying the number and distribution of the data collected from the EPANET simulation in a small synthetic aqueduct and in a real large scale aqueduct in the Veneto Region (Italy), for which the design-phase EPANET model is available.

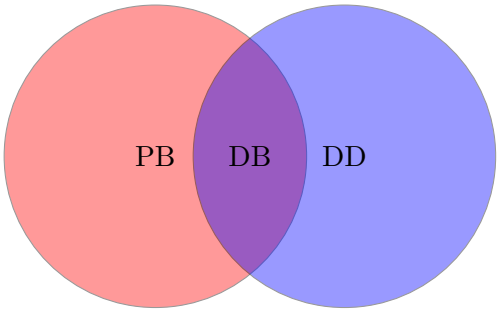

This chapter is organized as follows. First the mathematical notation is established by providing rigorous definitions of all the mathematical objects, including the p-Laplace operator, that are needed. We note here that, since the p-Laplace operator has been studied mostly within the context of PDEs, we use a notation that derives from it and make several references to the continuous case in an effort to make the presentation more streamlined. All the relevant properties of the used operators are discussed and proved if necessary. This first section will be followed by a description of a standard WDS model, discussing standard nomenclature and components of a WDS, including examples of typical equations used for localized and distributed energy losses, and types of simulations that are typically performed. The third section contains a discussion on typical data that are available to a WDS operators and what are the data that will be available in the future by the introduction modern metering technologies. Section 5 is dedicated to the discussion and mathematical formulation of the inverse problems used to calibrate the p-Laplace based model. This will include the development of the needed mathematical theory as well as of the numerical algorithms that will be used to solve the problem. Finally, Section 6 will report the numerical examples obtained on synthetic and real aqueducts.

1.2 The p-Laplace operator and the graph setting

The p-Laplacian operator is a non-linear generalization of the well-known Laplacian operator. This operator, restricted to the graph setting, has received renewed interest in the last few years because of potential application to machine learning and data science [20, 28, 47]. In the continuous case, the p-Laplacian takes the form

$$\Delta_p(\cdot) = -\operatorname{div}(|\nabla(\cdot)|^{p-2}\nabla(\cdot))\,.$$

The above equation is defined in an open domain $\Omega \subset \mathbb{R}^n$ with Lipschitz boundary and $p \in \mathbb{R}$ with $1 \leq p < \infty$. Obviously, for $p = 2$ we recover the standard Laplace operator. The p-Laplacian operator naturally arises from the Euler-Lagrange equation of the p-Dirichlet energy on $W^{1,p}(\Omega)$, defined as:

$$\mathcal{E}_p(\varphi) := \int_\Omega \frac{1}{p}|\nabla \varphi|^p\,.$$

We are also interest in the p-Poisson problem, where given a profile function $g(x) : \Gamma \longrightarrow \mathbb{R}$ defined on $\Gamma = \partial\Omega$, and a forcing term $f \in L^{p'}(\Omega)$, we consider the following variational problem:

$$\inf_{\varphi \in W_0^{1,p}(\Omega)} \int_\Omega \frac{1}{p}|\nabla \varphi + \bar{\varphi}|^p - \int_\Omega f\varphi\,, \tag{1.2.1}$$

where $\bar{\varphi}$ is a lifting function such that $\bar{\varphi}(x) = g(x)$, $\forall\, x \in \Gamma$. The Euler-Lagrange equation for problem (1.2.1) is indeed equivalent to the well-known p-Poisson PDE with Dirichlet boundary conditions:

$$\begin{aligned} \Delta_p\varphi &= f, \quad x \in \Omega, \\ \varphi(x) &= g(x), \quad x \in \Gamma. \end{aligned} \tag{1.2.2}$$

The value of p determines the regime of the non-linear diffusive dynamics, i.e., *sub-diffusive* if $p < 2$ or *super-diffusive* if $p > 2$. In particular, we highlight the following two *limit* cases and their sample applications.

- Case $p \to \infty$: eq. (1.2.2) can be related to the PDE-based formulation of the Monge-Kantorovich (MK) equations for the L^1 Optimal Transport problem, if the Euclidean distance is assumed as cost function for the optimal transportation problem [51];
- Case $p = 1$: the p-Poisson problem relates to the 1-Laplacian operator and the Total Variation (TV) energy. These lead to solutions belonging to the space of Bounded Variation (BV) functions [50, 52]. This case will be exhaustively studied in Chapter 2, where we will also study the interdependence between the p-Laplacian operator and the so-called Dynamic Monge Kantorovich (DMK) approach, which has been introduced in [55–57] to obtain approximate solutions of the above MK problem.

Although the detailed analysis of our adaptation of the DMK approach is postponed, at the end of this chapter we will present its fundamental role in providing effective numerical tools for tackling the p-Laplacian inverse problem of interest. In the graph-based setting, the p-Laplacian is defined to mimic the behavior of the continuous counterpart. Before getting into details, we recall some important ideas from the theory of graphs operators. We define a weighted directed graph as a collection of edges, nodes, and edge weights, $\mathcal{G} = (E, V, \omega)$, where E is the set of $m = |E|$ edges, V the set of $n = |V|$ nodes, and ω is a weight defined on the edges. Each edge $e_i \in E$ is characterized by the pair $e_i = v_j v_k$, with $v_j, v_k \in V$, and we write ω_i for the weight associated to the edge e_i. On a graph, we can define functions on nodes and functions on edges. We denote as $\mathcal{H}(V) = \mathbb{R}^n$ and $\mathcal{H}(E) = \mathbb{R}^m$ the Banach spaces of real-valued functions on V and E, respectively. Therefore, we can directly use the vector notation $h = [h_{v_1}, ..., h_{v_n}] \in \mathcal{H}(V)$, and write $h_v = h(v)$ for the evaluation at $v \in V$, or, equivalently, the v-th component of the vector h. With the same notation, we write $q_e = q(e)$ and $q = [q_{e_1}, ..., q_{e_m}] \in \mathcal{H}(E)$.
Assume that $i \in \{1, \dots, m\}$ is the index associated to an edge $e_i \in E$ and that $k_u, k_v \in \{1, \dots, n\}$ are the indices associated to u and v in V. We define graph gradient operator $\nabla : \mathcal{H}(V) \longrightarrow \mathcal{H}(E)$ as the $m \times n$ signed incidence matrix whose (i, j)-element is:

$$(\nabla)_{ij} = \begin{cases} -1 & \text{if } j = k_u, \\ 1 & \text{if } j = k_v, \\ 0 & \text{otherwise.} \end{cases} .$$

Although the gradient matrix relies on the edge orientations, we point out that such orientation is arbitrary and does not affect the construction of the operator. Next, we define the graph divergence operator $\operatorname{div} : \mathcal{H}(E) \longrightarrow \mathcal{H}(V)$ as the negative adjoint of the gradient, or in other words:

$$\operatorname{div} = -\nabla^T,$$

i.e., the negative transpose $n \times m$ matrix of ∇. Indeed, given $h \in \mathcal{H}(V)$, $q \in \mathcal{H}(E)$ and $e = uv \in E$, $u, v \in V$, direct calculations show that:

$$h \mapsto (\nabla h)_e = h_v - h_u, \tag{1.2.3}$$

$$q \mapsto (\operatorname{div} q)_u = \sum_{\substack{v \sim u \\ e = uv}} q_e \,, \tag{1.2.4}$$

where $v \sim u$ means that v is connected to u by an edge of the graph.
In analogy to the continuous case, we can define the weighted graph Laplacian operator for a function $h \in \mathcal{H}(V)$ as:

$$\Delta_\omega h := -\operatorname{div}(\omega \odot \nabla h) = \nabla^T Diag(\omega) \nabla h \,, \tag{1.2.5}$$

where $\omega \in \mathcal{H}(E)$ is a weight function, $\mathrm{Diag}(\omega)$ is the diagonal matrix with diagonal equal to c, and $\odot$ is the Hadamard or entrywise product:

$$\begin{aligned} u \odot v : \mathbb{R}^n \times \mathbb{R}^n &\longrightarrow \mathbb{R}^n \\ (u \odot v)_i &\mapsto u_i \cdot v_i \qquad i = 1, \dots, n\,. \end{aligned}$$

Note that (1.2.5) is the matrix-vector product of the ω-weighted graph Laplacian matrix

$$\Delta_\omega = \nabla^T Diag(\omega) \nabla\,,$$

and the vector representation of the node function $h \in \mathcal{H}(V)$.
The ω-weighted graph p-Laplacian operator, $p > 1$, can be defined as:

$$\Delta_{p,\omega} h := -\operatorname{div}(\omega^{p-1} \odot |\nabla h|^{p-2} \odot \nabla h) = \nabla^T Diag(c^{p-1} \odot |\nabla h|^{p-2}) \nabla h\,.$$

As done in the continuous case, we can associate to $\Delta_{p,\omega}$ a p-Dirichlet energy and a p-Poisson problem on graphs. First, we recall that given $q \in \mathcal{H}(E)$ and $1 \le p < \infty$ we can define the edges-based p-norm as:

$$\|q\|_{l_p} := \left(\sum_{e \in E} |q_e|^p \right)^{\frac{1}{p}},$$

while in the limit case $p = \infty$ we can consider the l_∞-norm

$$\|q\|_{l_\infty} := \sup_{e \in E} |q_e|\,.$$

Letting $p > 1$ and $\omega \in \mathcal{H}(E)^+$ be a positive weight function, we define the weighted graph p-Dirichlet energy for a function $h \in \mathcal{H}(V)$, $h_v < \infty$, $\forall\, v \in V$ as:

$$\mathtt{E}_{p,\omega}(h) := \frac{\|\omega^{\frac{p-1}{p}} \odot \nabla h\|_{l_p}^p}{p} = \sum_{e \in E} \frac{\omega_e^{p-1} |(\nabla h)_e|^p}{p}\,. \tag{1.2.6}$$

Now we want to introduce the p-Poisson equation on graphs. Before we do that, we need to define the boundary of a graph. Thus we consider a graph $\mathcal{G} = (E, V)$ and characterize the node and edge sets as the disjoint union of internal and boundary sets [63]. In other words, given a proper subset $B \subset V$ of $\mathcal{G}$, called the boundary, we have $V = (V_I \sqcup B)$ and $E = (E_I \sqcup E_B)$ where $E_I = \{uv \in E : u, v \in V_I\}$ and $E_B = \{uv \in E : u \in V_I, v \in B\}$. Now, for given functions $f \in \mathcal{H}(V_I)$ and $g \in \mathcal{H}(B)$, we can introduce the following p-Poisson problem:

$$\begin{aligned} (\Delta_{p,\omega}\, h)_v &= f_v \quad v \in V_I \\ h_v &= g_v \quad v \in B, \end{aligned} \tag{1.2.7}$$

This problem can be given a variational formulation. Indeed, for a forcing term $f \in \mathcal{H}(V_I)$ and non-homogeneous Dirichlet boundary conditions on the graph boundary B, we can consider the equivalent formulation:

$$\inf_{h \in \mathcal{H}_0^B(V)} \sum_{e \in E} \frac{\omega_e^{p-1} |(\nabla(h + \bar{h}))_e|^p}{p} - \sum_{v \in V_I} f_v h_v \,, \tag{1.2.8}$$

where $\mathcal{H}_0^B(V) := \{h \in \mathcal{H}(V) \mid h_v = 0,\ \forall\, v \in B\}$ and $\bar{h}$ is a lifting function such that $\bar{h}_v = g_v$ for all $v \in B$, and $\bar{h}_v = 0$ for all $v \in V_I$. The Euler Lagrange equation for (1.2.8) is indeed (1.2.7). Moreover, by virtue of the Poincaré inequality [91], problem (1.2.8) is strictly convex and coercive, and therefore it admits a unique minimizer. Thus (1.2.7) admits a unique solution.

We would like to remark that, in addition to the parameter p, $\Delta_{p,\omega}$ includes the positive weight ω, which, analogously to the exponent p, is a function defined on the edges of the graph and is introduced to ensures physical interpretability when using the operator in modeling physical phenomena along the graph structure. Indeed, in many situations, the weighted p-Laplacian can be employed as a surrogate of more complex non-linear operators. However, in order to obtain an *effective* model, it is necessary to carry out a fine tuning of the parameter functions p and ω. Thus, a non-linear inverse problem on graphs must be solved [9, 76, 80, 101]. In the context of partial differential equations, inverse problems are a well-established topic [8, 45, 68, 94] and are used for model-parameter identification [26, 96, 118]. Typically, inverse problems are carried out by minimizing the least squares of the difference between model solution and external observations (see [129] for an interesting discussion on linear or nonlinear least squares in the field of inverse problems in water resources). To be able to use a weighted p-Laplacian as a surrogate model of an aqueduct we need to address this problem.

We now focus our attention to properties of the graph gradient and the graph divergence operators that will be useful in the sequel. From (1.2.3), it is clear that the kernel of the graph gradient matrix are the constant functions on the nodes. On the other hand, from (1.2.4), we can easily see that a basis for the kernel of the divergence operator consists of functions defined on the edges that are constant on directed loops. As a consequence, denoting by $\bar{1} \in \mathcal{H}(V)$ the unit constant function, we also have that for any $f \in \mathcal{H}(V)$ for which there exists $q \in \mathcal{H}(E)$ such that $f = \operatorname{div} q$, then

$$\langle \bar{1}, f \rangle = \langle \bar{1}, \operatorname{div} q \rangle = -\langle \nabla\, \bar{1}, q \rangle = 0 \,,$$

where $\langle x, y \rangle = x^T y$ is the standard scalar product between vectors in $\mathbb{R}^n$. In other words, we can write the following mass balance constraint:

$$f = \operatorname{div} q \implies \sum_{v \in V} f_v = 0 \,. \tag{1.2.9}$$

An important tool that will be useful is the discrete counterpart of the divergence theorem, given in the following Proposition.

Proposition 1.2.1. *(Graph divergence theorem) Let $\mathcal{G} = (V, E)$ be a graph with boundary set B. Given two node and edge functions $\psi \in \mathcal{H}(V)$ and $\phi \in \mathcal{H}(E)$, then:*

$$\sum_{v \in B} \psi_v (\phi \cdot \vec{\nu})_v - \sum_{v \in V_I} (\operatorname{div} \phi)_v \psi_v = \sum_{e \in E} \phi_e (\nabla \psi)_e \,,$$

where, for any $v \in B$, the graph boundary normal flow map is defined as:

$$(v, \phi) \mapsto (\phi \cdot \vec{\nu})_v := -(\operatorname{div} \phi)_v, \quad \forall\, \phi \in \mathcal{H}(E),\ \forall\, v \in B.$$

Proof. The proof is obtained by means of the following direct computation:

$$-\sum_{v \in B} (\operatorname{div} \phi)_v \psi_v - \sum_{v \in V_I} (\operatorname{div} \phi)_v \psi_v = \langle \nabla^T \phi, \psi \rangle = \langle \phi, \nabla \psi \rangle = \sum_{e \in E} \phi_e (\nabla \psi)_e \,,$$

from which the thesis follows. □

Consider now the following general non-linear elliptic operator on graphs:

$$h \mapsto \nabla^T \operatorname{Diag}(\alpha(h)) \nabla h, \quad h \in \mathcal{H}(V),\ \alpha : \mathcal{H}(V) \to \mathcal{H}(E)^+ \,.$$

From Proposition 1.2.1, we can introduce the following definition of the Dirichlet to Neumann (DtN) map for a general graph elliptic operator.

Definition 1.2.2. *(Dirichlet-to-Neumann map (DtN)) Let $\mathcal{G}(V, E)$ be a directed graph with boundary B and let ∇ be the associated gradient matrix. Given some Dirichlet boundary data $g \in \mathcal{H}(B)$, a forcing term $f \in \mathcal{H}(V_I)$, and a sufficiently smooth and positive map $\alpha : \mathcal{H}(V) \to \mathcal{H}(E)^+$ such that the following Poisson problem admits a unique solution:*

$$\begin{aligned} (\nabla^T \operatorname{Diag}(\alpha(h)) \nabla h)_v &= f_v, \quad v \in V_I, \\ h_v &= g_v, \quad v \in B \,, \end{aligned}$$

define the flux $q \in \mathcal{H}(E)$ as:

$$q := -\operatorname{Diag}(\alpha(h)) \nabla h_v \,.$$

Then for any $v \in B$ the Dirichlet-to-Neumann (DtN) map is given by:

$$(g_v) \mapsto \Lambda_\alpha(g_v) := (-q \cdot \overrightarrow{\nu})_v = (\operatorname{div} q)_v = (\nabla^T \operatorname{Diag}(\alpha(h)) \nabla h)_v, \quad \forall\, v \in B \,. \tag{1.2.10}$$

Remark 1.2.3. *Differently from the continuous case where the DtN map is continuous [3](even in the case of the p-Laplacian), surprisingly in the graph case we loose many of the good properties of the continuous case. Indeed, the DtN map is proven to be continuous only on circular, critical and planar graphs [42, Th. 4.4, p. 76].*

Note that, from (1.2.9) and Proposition 1.2.1, we have the graph-based counterpart of the classical boundary conditions in elliptic PDE theory. In close analogy, we can define the following boundary conditions:

- **Dirichlet boundary conditions**: this essentially corresponds to the imposition of the grounding of the operator obtained by fixing $h_v = g_v$, $\forall\, v \in B$, where $g \in \mathcal{H}(B)$ is the given Dirichlet data. Moreover, from (1.2.9) and (1.2.10) we find immediately that the total flux injected or extracted in the graph domain by the forcing function must be balanced at the Dirichlet nodes, i.e.:

$$\sum_{v\in B} \Lambda_\alpha(g_v) = \sum_{v\in B} (\nabla^T \operatorname{Diag}(\alpha(h))\, \nabla h)_v = -\sum_{v\in V_I} f_v\,;$$

- **Neumann or flux boundary conditions**: in the continuous case these conditions impose a boundary flux:

$$\alpha(h(x))\, \nabla h(x) \cdot \overrightarrow{\nu} = g(x), \quad \forall\, x \in \Gamma = \partial\Omega\,.$$

  This condition can be translated to the graph setting by means of the graph divergence theorem (Proposition 1.2.1). Indeed, as in the continuous case, a Neumann boundary on a graph in the variational formulation is implemented directly on the Lagrangian by moving the boundary fluxes to the forcing term:

$$(\operatorname{Diag}(\alpha(h))\, \nabla h \cdot \overrightarrow{\nu})_v = (\nabla^T \operatorname{Diag}(\alpha(h))\, \nabla h)_v = f_v\,.$$

  In the case of zero Neumann boundary conditions (no flow impermeable boundary) eq. (1.2.9) requires the compatibility conditions that the forcing term f must have zero-mean to guarantee the well-posedness of the problem. The above equation has infinitely many solutions since the constant function is in the kernel of the operator. The standard method to provide a unique solution is to enforce zero mean to the solution, i.e., $\sum_{v\in V} h_v = 0$;

- **Robin type boundary conditions**: another typical class of boundary conditions are the (generalized) Robin or third type conditions, which in the continuous setting can be written as:

$$\alpha(h(x))\, \nabla h(x) \cdot \overrightarrow{\nu} = \gamma(h(x))h(x) + g(x), \quad \forall\, x \in \Gamma = \partial\Omega.$$

  By virtue of Proposition 1.2.1, given a map $\gamma : \mathcal{H}(V) \to \mathcal{H}(B)$ and a function $g \in \mathcal{H}(B)$, Robin type conditions in the graph can be written as:

$$(\operatorname{Diag}(\alpha(h))\, \nabla h \cdot \overrightarrow{\nu})_v = (\nabla^T \operatorname{Diag}(\alpha(h))\, \nabla h)_v = \gamma(h)_v h_v + g_v, \quad \forall\, v \in B. \tag{1.2.11}$$

  In this case eq. (1.2.9) implies the following conservation equation:

$$\sum_{v\in B} (\gamma(h)_v h_v + g_v) = -\sum_{v\in V_I} f_v.$$

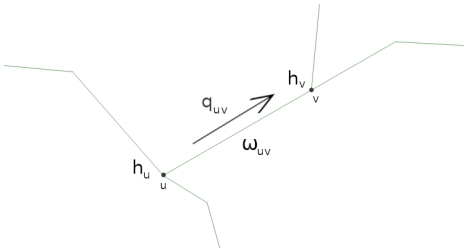

Figure 1.1: Sketch of a portion of the graph underlying a WDS model.

For further details concerning the theory of graph operators, we refer the interested reader to e.g. [42].

1.3 The WDS model

We can genuinely consider a WDS as a weighted directed graph $\mathcal{G} = (E, V, \omega)$, where edges are pipes and nodes are junctions. Positive edge weights ω embed the pipe attributes, including length, diameter, roughness coefficient etc. Figure 1.1 shows a sketch of the graph underlying a portion of a WDS.
Aside from the graph structure and operators, in the WDS model we need to consider the following functions:

- a flux function $q \in \mathcal{H}(E)$, $[q] = \left[\mathrm{L}^3/\mathrm{T}\right]$, which represents the volume of water that flows inside the pipe in unit time. This quantity is defined on edges;

- a piezometric head function $h \in \mathcal{H}(V)$, $[h] = [\mathrm{L}]$, which is defined as the pressure (in meters of water column) plus the elevation from a reference function. This quantity on a graph is defined on nodes;

- a forcing term $f \in \mathcal{H}(V)$, $[f] = \left[\mathrm{L}^3/\mathrm{T}\right]$, which represents the global flux entering or exiting the domain on the nodes, i.e.,

$$f_u = \sum_{\substack{u \sim v \\ e = uv}} q_e \,,$$

  This quantity is defined on nodes.

Next, we describe in more details how the main components of a WDS are modeled in standard commercial softwares such as EPANET, and how the are reframed into our setting (cf. [1, §3.1]).

- **Junctions** are the points of a WDS where the pipes join and water can enter or leave the network. They are the nodes of the underlying graph, whose piezometric head is described by the function h. Moreover, the amount

of water coming in or out, i.e. the required hydraulic demand on each node must be balanced by the forcing term function f with the convention (compatible with the graph divergence theorem) that $f_v > 0$ if it represents an inflow in the network, while $f_v < 0$ if it represents an outflow.

- **Pipes** convey water from one junction in the network to another. Note that each pipe is assumed to be *full*, i.e., it is always subject to a positive pressure and no water surface develops. This implies that in each moment the flux and the amount of water are uniform in all the regions of the pipe. Pipes are the edges of $\mathcal{G}$, and the flux of water flowing is quantified by the flux function q.

- **Reservoirs and Tanks. Reservoirs** are used to model components such as lakes and rivers and they represent an infinite source or sink of water that is externally provided to the WDS. On the other hand, in **tanks** the volume of stored water varies in time. In EPANET they are both modeled as points (same as junctions). In our framework, both reservoirs and tanks are represented as non-homogeneous Dirichlet boundary conditions that fix the piezometric head at a node. Note that in principle tanks represent a different type of boundary condition where the amount of stored water changes in time. They are typically implemented as a nonlinear boundary condition and take into account any transient that may occur in the WDS. For simplicity we do not consider this type of boundary conditions and add the hypothesis that the fluid is incompressible [82], that tanks behave as reservoirs, and that the water demand is stationary. While the first assumption is amply justified, the last two require careful definition of the problems to be simulated by considering temporally averaged demands and properly adapted data to absorb temporal variations in the tank. Nevertheless, we point out that it is easy in our framework to include also time varying simulations and nonlinear boundary conditions.

- **Pumps** and **valves** are typical components of a WDS, which are represented in EPANET as links in the network. The effect of pumps is modeled by imposing a proper Dirichlet condition on the piezometric head of the related node connecting the pump to the rest of the network. This pressure is easily calculated from the flow-pressure graph of the pump or, if not available, by measuring the flux and using the DtN map. On the other hand, valves can be modeled by removing the corresponding edge from the underlying graph, or by assigning a very small value to its weight ω.

- The same surrogate procedure applies to various further theoretical and empirical components that are involved in the EPANET hydraulic simulations, as for examples **minor head losses** parameters and **emitters**. Among them, **emitters** are modeled as junctions and are typically used to reproduce leaks and local dissipative phenomena. The corresponding

hydraulic demand or forcing term f is imposed to be dependent on the pressure:

$$f_v = c_v |press_v|^{\gamma_v - 2} press_v + g_v \,,$$

where c is a positive node function which, roughly speaking, represents the diameter of the leaking hole, $press_v := h_v - z_v$ is the pressure, z_v is the elevation of the junction at the node, γ_v is an exponent parameter which is typically set to be equal to 1.5 (a direct consequence of the classical Bernoulli Principle), with possible minor corrections depending on the materials, and g is a fixed distributed minimum leakage rate. Note that in our framework this is exactly a Robin type boundary condition as in (1.2.11).

In the analysis of a WDS two main types of simulations are typically considered:

- **Demand Driven Analysis (DDA)**: this is the most used approach. One fixes a distributed demand f on every node of the WDS, and then carries out the simulation with proper Dirichlet boundary conditions for the piezometric head at source junctions, typically represented as reservoirs or as tanks;
- **Pressure Dependent Analysis (PDA)**: in this approach, in addition to the a distributed demand f, a minimum pressure is required on every junction of the network. Tanks are typically used as nonlinear Dirichlet boundary conditions and the simulation is carried out multiple times by increasing the tank level of stored water (and consequently changing Dirichlet data), until the minimum required pressure is satisfied.

1.3.1 The graph p-Laplacian mathematical model of a WDS

In this section we would like to motivate the introduction of the graph p-Laplacian operator. A WDS model has to include distributed (edge) and localized (nodes) energy losses due to friction in the pipe walls and the presence of junctions and valves, respectively. These are typically simulated by imposing head losses given by empirical power-law formulas commonly used in practice and justified by considerations related to conservation of momentum (second Newton law). The main principles governing the flow of water in a WDS are:

$$\textbf{Momentum Balance} \quad -(\nabla h)_e = \frac{L_e \omega_e}{D_e C_e} |q_e|^{n_e - 1} q_e, \quad \forall\, e \in E, \tag{1.3.1}$$

$$\textbf{Mass Balance} \quad (\operatorname{div} q)_v = f_v, \quad \forall\, v \in V, \tag{1.3.2}$$

where $n_e \geq 1$ is the edge power law exponent, $L_e > 0$ and $D_e > 0$ are the length and the diameter of the pipe, $C_e > 0$ is the roughness coefficient (a unit-less coefficient which depends mainly from age, material and diameter of the pipe), and $\omega_e > 0$ is a weight on the edges which typically depends from the physical properties of the pipe and the flux regime(turbulent, laminar, etc. [1]). We point

out that in general the exponent n is chosen to be constant on the edges and, considering for example the *Hazen-Williams* formulation [1, §12.1], it varies in the interval $n_e \in [1.4, 2.5]$ for each $e \in E$.
By taking the absolute value on both sides of (1.3.1) and by setting $\ell_e := D_e C_e / L_e$ for all $e \in E$, we obtain:

$$|(\nabla h)_e| = \frac{\omega_e}{\ell_e} |q_e|^{n_e} \Longrightarrow |q_e| = |(\nabla h)_e|^{\frac{1}{n_e}} \left(\frac{\omega_e}{\ell_e}\right)^{-\frac{1}{n_e}},$$

which implies:

$$-(\nabla h)_e = |(\nabla h)_e|^{\frac{n_e-1}{n_e}} \left(\frac{\omega_e}{\ell_e}\right)^{1-\frac{n_e-1}{n_e}} q_e \,.$$

By substituting $n_e = 1/(p_e - 1)$, $\forall\, e \in E$ we then obtain:

$$q_e = -\left(\frac{\omega_e}{\ell_e}\right)^{1-p_e} |(\nabla h)_e|^{p_e-2} (\nabla h)_e \,.$$

Finally, letting $w_e := \ell_e/\omega_e$, $\forall\, e \in E$ and substituting into (1.3.2), we obtain the mixed dual formulation of our p-Laplacian-based surrogate model:

$$\begin{aligned} q_e &= -w^{p-1} \odot |\nabla h|^{p-2} \nabla h \\ (\operatorname{div} q)_v &= f_v \,, \end{aligned}$$

or, putting together the two equations above, the standard formulation:

$$(\Delta_{p,w} h)_v = f_v, \tag{1.3.3}$$

where

$$\Delta_{p,w} h = -\operatorname{div}(w^{p-1} \odot |\nabla h|^{p-2} \nabla h) = \nabla^T \operatorname{Diag}(w^{p-1} \odot |\nabla h|^{p-2}) \nabla h \,, \tag{1.3.4}$$

is the weighted p-Laplacian operator with $p \in (1.4, 1.7)$, for any edge of the graph representing the WDS.
Boundary conditions need to be added to (1.3.1), (1.3.2) or equivalently to (1.3.4) in order to get a well-posed mathematical problem.
We recall that the thesis of this chapter is that it is possible to retrieve a distribution of p and ω parameters so that the p-Laplace operator in eq. (1.3.4) can be effectively used as a surrogate model. To this aim we need to embed eq. (1.3.4) within an inverse problem framework to calculate the distribution of p and ω that best fit a given set of observed data. Our approach to the latter task will be described in Sec. 1.5. Here, instead we reformulate our surrogate model as a minimization problem suitable to be embedded in the inverse problem setting. To this aim, we note that eqs. (1.3.1) and (1.3.2) are reminiscent of a mixed dual formulation of the p-Laplace equation in (1.3.3) and is similar to the mixed

FEM formulation for elliptic PDEs introduced in [43]. Thus, we introduce the Lagrangian $\mathtt{L}_{w,p} : (\mathcal{H}(V) \times \mathcal{H}(E)) \to \mathbb{R}$:

$$\mathtt{L}_{w,p}(h,q) := -\sum_{e\in E} \frac{1}{p'_e} \frac{|q_e|^{p'_e}}{w_e} - \sum_{e\in E} q_e(\nabla h)_e - \sum_{v\in V} f_v h_v \,, \tag{1.3.5}$$

where $p'_e = \frac{p_e}{p_e-1}$ is the conjugate exponent to p. If $w_e > 0$ for all $e \in E$, eqs. (1.3.1) and (1.3.2) are exactly the Euler-Lagrange equations for the saddle point problem:

$$\inf_{h\in\mathcal{H}(V)} \sup_{q\in E} \mathtt{L}_{w,p}(h,q) \,.$$

As will be seen in Sec. 1.5, this formulation needs to include a Tikhonov-like regularization. In addition, this regularization are designed to ensure similar accuracy in the reconstruction of both the piezometric head and the fluxes, which typically converge at different speeds. For this reason we consider the following regularized Lagrangian:

$$\mathtt{L}^{\delta_q,\delta_w}_{w,p}(h,q) := -\sum_{e\in E} \frac{1}{p'_e} \frac{|q_e|^{p'_e}}{w_e+\delta_w} - \frac{1}{2}\sum_{e\in E} \frac{\delta_q |q_e|^2}{w_e+\delta_w} - \sum_{e\in E} q_e(\nabla h)_e - \sum_{v\in V} f_v h_v, \tag{1.3.6}$$

where and $0 < \delta_q << 1$ and $0 < \delta_w << 1$ are two regularization parameters. The resulting saddle point problem becomes:

$$\inf_{h\in\mathcal{H}(V)} \sup_{q\in E} \mathtt{L}^{\delta_q,\delta_w}_{w,p}(h,q) \,,$$

and the corresponding regularized Euler-Lagrange equations read now as:

$$\begin{cases} (|q_e|^{p'_e-2} + \delta_q) q_e = -(w_e+\delta_w)(\nabla h)_e, & \forall\, e \in E \\ -(\nabla^T q)_v = f_v, & \forall\, v \in V \,. \end{cases} \tag{1.3.7}$$

1.4 Available Data and general considerations

In the last years, the increased challenges mostly induced by climate change to minimize water waste has prompted for a relevant improvement in the monitoring of WDS. Several commercial devices are now available to measure water fluxes and pressures along a WDS. Among them, we make extensive use of data collected by **smart meters**, devices designed to independently measure both pressure and water fluxes. These measurement systems can be placed in strategic points of the network (e.g. pipes interconnections, valves, hydrants etc.) or directly on the final user outlet. In the latter case, the instruments monitor the service pressure and the user hydraulic demand several times per day, yielding a large dataset of observations. The monitoring is typically associated to a **district** subdivision of the municipal network. Namely, Water Industries typically subdivide the network in small connected components with global inflow and outflow accurately

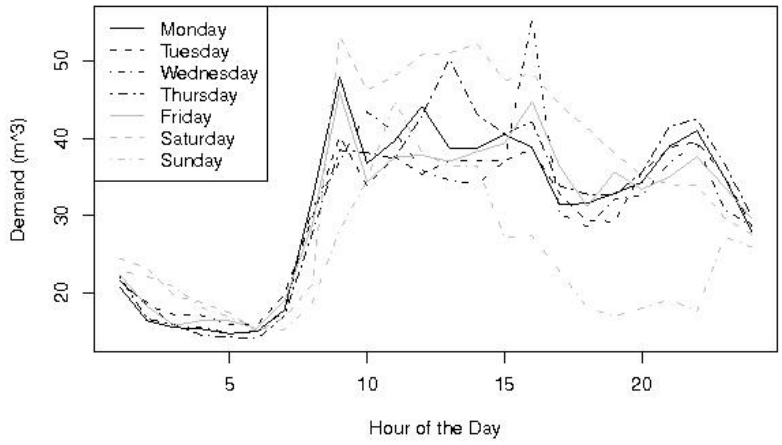

Figure 1.2: Typical daily demand curve

measured[81]. This allows a tight control on the state of the "distrectualized" portion of the WDS and the collection of a large number of data that can be used to successfully seed an inverse procedure. For example, in the city of Milan (IT), a relatively large quantity of smart meters are placed on the house services connections, and a a relevant amount of data is now available[86]. Unfortunately, generally only a small quantity of data is nowadays readily available, and for this reason we will mainly use synthetic data generated from commercial software simulations such as EPANET.

Another important measurement that is not readily available because Water Companies typically treat it as classified, is water demand, which can be defined as the total client consumption on one household junctions per unit time. The reconstruction of the water demand as a function of time is complex. Typically, it is calculated as a time series on the basis of either design parameters or of detailed measurements. When measurements are not available, an average water consumption can be evaluated. A typical periodic daily demand profile (which follows the daily habit of the users) is shown in Figure 1.2. A typical approach at evaluating a water demand pattern is to measure the minimum night flow, which represents the fixed water consumption of the network (possibly due to the presence of leaks) typically measured at 4am/5am when the user consumption is at its minimum. Appropriately rescaling the daily measured district inflow or the daily calculated demand and eventually averaging a number of daily patterns, leads to an operational daily demand that can be used for modeling purposes. This is what is known in literature as the FAVAD concept [123]. For our test cases we will use a demand that is calculated using this latter approach.

After the definition of the water demand, the identification of the surrogate model parameters can proceed on the basis of time measurements of pressure heads and water fluxes appropriately distributed along the WDS network. Because of

difficulties in having appropriate data, but most importantly because of confidentiality problems, in our simulations we will employ data from an EPANET model of the WDS at hand, which is thus assumed as the "true" solution. In the next section, we will introduce our model parameter estimation approach which is essentially based on a non-linear extension of the classical Calderon's inverse problem on graphs [42].

1.5 Retrieving p and w from the data

In this section we want to determine the distribution of the p and w parameters so that the resulting weighted p-Laplacian model can be used as a surrogate model of the WDS of interest. This task can be accomplished by solving an inverse problem, i.e., by determining the p and w distribution that minimizes the mismatch between measurements and simulation results. This can be framed within the classical theory of inverse problems (see [131] for a standard reference book) whose practical solution is typically very difficult and computationally demanding. In order to simplify our problem, we need to exploit the fact that our model is defined on a graph domain. Thus we start this section by describing our main working choices.

The most important simplification that can be done in our setting is to design our inverse problem as a Calderon-type problem. These are boundary inverse problems that try to identify the parameter distribution in the interior of the domain from boundary data. They are used normally in a variety of applied fields including geophysical prospection (e.g., electrical impedance/resistivity tomography EIT/ERT, seismic imaging, geo-radar imaging) and medical imaging (e.g., electrocardiography, electroencephalography, EIT), among others. The main advantage of a Calderon problem, besides the fact that it has been thoroughly studied, is that, in dimension stricktly larger than one, its solution is unique, albeit still severely ill-conditioned [12, 95, 136]. Indeed, for one-dimensional domains Calderon problem is not well-posed, while it is well-posed for problems whose dimension is greater or equal than two. Unfortunately, in a graph setting, [42], Calderon problem is well-posed if and only if the graph is planar and "circular", i.e., the boundary nodes can be connected by edges that form a circle without destroying the planarity. Intuitively, a graph can be imagined as an object that is in between one and two dimensions. Thus, the well posedness of Calderon problem is ensured by this conditions because it forces the graph to be embedded in a plane, thus forming a "truly" two dimensional object.

The most important characteristic that allows our problem to be casted within a Calderon boundary problem is that the boundary of a graph is just any subset of nodes. Hence we can chose to define our boundary to include instrumented nodes where measurements are available. This, together with the fact that in the p-Laplacian based model we need to identify the spatial distributions of only two parameters makes our task much more tractable.

Given some boundary observations of pressure $\{\bar{u}_m(x), x \in \Gamma, m = 1, ..., n\}$ and normal fluxes $\{\gamma_m(x), x \in \Gamma, m = 1, ..., n\}$, and given a known forcing term $\{f_m : \Omega \mapsto \mathbb{R}, x \in \Gamma, m = 1, ..., n\}$, one looks to minimize following functional:

$$\min_{w \in (L^\infty(\Omega))^+} \sum_{m=1}^{n} \int_\Gamma |w| \nabla u_m|^{p-2} \nabla u_m \cdot \vec{n} - \gamma_m|^2$$
$$s.t. \quad \begin{cases} -\Delta_{p,w} u_m & = f_m \quad x \in \Omega, \ m = 1, .., n \\ u_m(x) & = \bar{u}_m(x) \quad x \in \Gamma = \partial\Omega, \ m = 1, .., n \end{cases},$$

In a continuous setting and for the linear case $p = 2$, Calderon problem is known to be non convex and, as already remarked, ill-posed. There are particular instances, for example for the identification of the diffusion equation in dimension $d \geq 3$, Calderon inverse problem has a unique solution provided a sufficient number of boundary data are given[3]. In the graph setting, only a few results are available and only for circular planar graphs [42]. In all other general cases, to the author's best knowledge, no uniqueness results are available. This is the reason why multiple samples at each nodes are required and an opportune Tikhonov regularization strategy will be proposed in what follows.
Our approach a direct extension to the non-linear setting of the linear graph Calderon problem and are described as follows. Assume that the set of nodes is partitioned into $V = V_I \cup B$ and $V_I \cap B = \emptyset$, where V_I is the set of *internal* nodes and B is the set of *boundary(sampling)* nodes. At the same time, we also assume that the set of edges is partitioned into $E = E_I \cup E_S$ and $E_I \cap E_S = \emptyset$, where E_I are the internal edges(unsampled) and E_S is the set of sampling fluxes edges. We then define the following problem.

Problem 1 (p-Calderon problem)**.** *Let $\mathcal{G} = (E, V, w)$ be a weighted directed graph with $n = |V|$ nodes and $m = |E|$ edges. Let $B \subset V$ be the set of n_b boundary nodes where the piezometric head is sampled and E_S the set of m_s boundary edges where fluxes are sampled. Suppose moreover that we are given a $n_i \times M$ matrix $F(V_I)$ of known demand distributions on the $n_i = n - n_b$ internal nodes. Here we use the standard convention that $F(V_I)_{i,j} > 0$ if there is an inflow at node i and sampling time j, while $F(V_I)_{i,j} < 0$ if it represents an outflow.*
Our aim is to estimate the weight $w \in \mathcal{H}(E)$ and the exponent $p \in \mathcal{H}(E)$) of a weighted p-Laplace operator from the sample matrices given by:

- *the $n_b \times M$ matrix $\overline{H}(B)$ (piezometric head measurements);*
- *the $n_b \times M$ matrix $\overline{F}(B)$ (boundary demand measurements);*
- *the $m_s \times M$ matrix $\overline{Q}(E_S)$ (flux measurements).*

Such matrices contain $M \geq 1$ multiple synchronized measurements taken at different sampling times. Precisely, each column of $\overline{H}(B)$, $\overline{F}(B)$ and $\overline{Q}(E_S)$ contains

sampled piezometric heads at B, demand measurements at B, and flux measurements at E_S, respectively, at one of the M sampling times. We point out that the further necessary condition of global mass balance must be satisfied:

$$\sum_{i=1}^{n_b} \overline{F}(B)_{i,j} + \sum_{i=1}^{n_i} F(V_I)_{i,j} = 0\,, \quad \forall\, j = 1, \dots, M\,. \tag{1.5.1}$$

1.5.1 Computing gradients via the Primal-Adjoint method

Differently from the standard approach in [42] to this problem, which is essentially based on harmonic extensions, medial graphs reduction and Schur complements, we adopt the framework of the primal-adjoint method, typically used in parameter estimation for the continuous based two dimensional Calderon's problem [95], [26]. This is ultimately due to the need of adopting a sufficiently flexible approach which leads us to easily include further constraints on our parameters to satisfy the physical laws governing a WDS. Namely, we require that the edges weights w be positive and the exponent be in the range $1.4 \leq p \leq 1.8$ or equivalently $2.25 \leq p' \leq 3.5$.
Instead of the weighted p-Poisson equation as governing non linear equation for our parameter identification model, we will work with the conjugate exponent p' and use the equivalent mixed formulation defined in (1.3.1) and (1.3.2). Moreover, we will consider its regularized version defined in (1.3.7)
As already observed, there are various reasons that suggest to use this mixed formulation. First, working separately for the fluxes and the piezometric heads allows us to control better the accuracy between the simulated flux and heads and the data measurements, which are collected with different instruments and different measurement errors. Second, this formulation allows to compute easily the gradients of our design parameters w and p' since they are less interconnected (the term w^{p-1} disappears) with the result that the derived numerical scheme is far more easy to implement.
We denote as $A_{i,:}$ and $A_{:,j}$ the i-th row and the j-th column of a given matrix A. Moreover, we denote as $H(V)$ and $F(V_I)$ the $n \times M$ matrices related to the *simulated* piezometric heads and the imposed demands on the whole graph. The $m \times M$ matrix $Q(E)$ will contain the simulated fluxes. We introduce four injective functions:

- $\iota_{V_B} : \{1, \dots, n_b\} \longrightarrow \{1, \dots, n\}$,
- $\iota_{V_I} : \{1, \dots, n_i\} \longrightarrow \{1, \dots, n\}$,
- $\iota_{E_S} : \{1, \dots, m_s\} \longrightarrow \{1, \dots, m\}$,
- $\iota_{E_I} : \{1, \dots, m_i\} \longrightarrow \{1, \dots, m\}$

where $n_i = |V_I|$ and $m_i = |E_I|$, and, we recall, $n = |V|$ and $m = |E|$. The function ι_{V_B} (ι_{E_S}) maps the node $v_i \in B$ of the sample set (the edge $e_i \in E_S$)

to the same node $v_{\iota_{V_B}(i)} \in V$ of the graph set (edge $e_{\iota_{E_S}(i)} \in E$) set, and will be useful to relate the sample matrices $\overline{H}(B), \overline{Q}(E_S), \overline{F}(B)$ to the ones corresponding to the whole graph introduced above. With the same notation, the maps ι_{V_I} and ι_{E_I} acts similarly on the internal nodes and internal edges respectively. Three additional sample matrices are needed: the $n_b \times M$ sample matrix $\overline{T}(B) = \{\overline{T}(B)_{i,j} = (-Q(E)_{:,j} \cdot \vec{\nu})_{\iota_{V_B}(i)}\}$ and the $n \times M$ divergence matrix $D(V) = D(V)_{i,j} = (-\nabla^T Q(E)_{:,j})_i$, and the $m \times M$ gradient matrix $\nabla H(E) = (\nabla H(E))_{i,j} = (\nabla(H(V)_{:,j}))_i$, where $j = 1, \ldots, M$ refers to the number of independent measurements and i indexes nodes or edges that can be on the boundary or on the entire graph.
Problem 1 can now then be translated into the following discrete minimization problem:

$$\min_{p,w} \sum_{j=1}^{M} \left(\frac{1}{2} \sum_{i=1}^{n_b} \left(\overline{T}(B)_{i,j} - \overline{F}(B)_{i,j}\right)^2 + \frac{1}{2} \sum_{i=1}^{m_s} \left(Q(E)_{\iota_{E_S}(i),j} - \overline{Q}(E_S)_{i,j}\right)^2 \right)$$

5

$$\text{s.t. } \forall\, j = 1, .., M \tag{1.5.2}$$

$$\begin{aligned}
(|Q(E)_{i,j}|^{p'_i - 2} + \delta_q) Q(E)_{i,j} &= -(w_i + \delta_w)\, \nabla H(E)_{i,j} \quad \text{for } i \in \{1, \ldots, m\} \\
D(V)_{i,j} &= F(V_I)_{\iota_{V_I}^{-1}(i),j} \quad \text{for } i \notin \iota_{V_B}(\{1, \ldots, n_b\}) \\
H(V)_{\iota_{V_B}(i),j} &= \overline{H}(B)_{i,j} \quad \text{for } i = 1, \ldots, n_b \\
w_i \geq 0,\ 3.5 \geq p'_i \geq 2.25 &\quad \text{for } i \in \{1, \ldots, m\} \\
1 >> \delta_q > 0,\ 1 >> \delta_w > 0 &
\end{aligned} \tag{1.5.3}$$

The two sums in the objective function (eq. (1.5.2)) are the difference between the calculated and observed boundary fluxes and represent the consistency with respect to the samples. The first addendum exploits the DtN map while the second one requires a good approximation of the measured fluxes on edges.

Remark 1.5.1. *Compared to the classical Calderón problem, the additional parameter p needs to be tuned Unfortunately, in this case, infinite solutions may occur even in the case where both heads and fluxes are measures on all graph nodes and edges. For this reason, multiple independent measurement for each boundary node and edge are needed together with an appropriate regularization.*

The minimization process is thus governed by the following extended Lagrangian:

$$
\begin{aligned}
&\mathcal{L}(p', w, H(V), Q(E), \Phi, \Psi, \Xi, \delta_q, \delta_w) := \\
&\sum_{j=1}^{M} \left(\frac{1}{2} \sum_{i=1}^{n_b} \left(\overline{T}(B)_{i,j} - \overline{F}(B)_{i,j} \right)^2 + \frac{1}{2} \sum_{i=1}^{m_s} \left(Q(E)_{\iota_{E_S}(i),j} - \overline{Q}(E_S)_{i,j} \right)^2 \right. \\
&+ \sum_{i \notin \iota_{V_B}(\{1,\dots,n_b\})} \psi_i^j \left(D(V)_{i,j} - F(V_I)_{\iota_{V_I}^{-1}(i),j} \right) + \\
&- \sum_{i=1}^{m} \phi_i^j \left((|Q(E)_{i,j}|^{p_i'-2} + \delta_q) Q(E)_{i,j} + (w_i + \delta_w) \nabla H(E)_{i,j} \right) + \\
&\left. + \sum_{i=1}^{n_b} \xi_i^j \left(H(V)_{\iota_{V_B}(i),j} - \overline{H}(B)_{i,j} \right) \right) .
\end{aligned}
\tag{1.5.4}
$$

where $\Phi = (\phi^1, \dots, \phi^M) \in [\mathcal{H}(E)]^M$, $\Psi = (\psi^1, \dots, \psi^M) \in [\mathcal{H}(V)]^M$ and $\Xi = (\xi^1, \dots, \xi^M) \in [\mathcal{H}(B)]^M$ are set of vectors of Lagrange multipliers for each measurement. Note that by imposing $\frac{\partial \mathcal{L}}{\partial \phi^j} = 0$, $\frac{\partial \mathcal{L}}{\partial \psi^j} = 0$ and $\frac{\partial \mathcal{L}}{\partial \xi^j} = 0$ for each $j = 1, \dots, M$ we recover the *primal equations* (1.5.3).
The *adjoint equations* are defined by setting to zero the derivatives of $\mathcal{L}$ with respect to the columns $(H(V)_{:,j}, Q(E)_{:,j})$ for each $j = 1, ..., M$. To this aim, define the set of vectors of test functions $\Theta = (\theta^1, \dots, \theta^M) \in [\mathcal{H}(E)]^M$, $P = (\rho^1, \dots, \rho^M) \in [\mathcal{H}(V)]^M$. Using Proposition 1.2.1, we first impose that for any $j = 1, .., M$ the derivatives with respect to the fluxes are zero, i.e.:

$$
\frac{\partial \mathcal{L}}{\partial Q(E)_{:,j}} \cdot \Theta^j = 0, \ \forall \, \Theta^j \in \mathcal{H}(E) .
$$

This leads to:

$$
\begin{aligned}
&- \sum_{i=1}^{n_b} \left(\overline{T}(B)_{i,j} - \overline{F}(B)_{i,j} \right) N_\theta(B)_{i,j} + \\
&+ \sum_{i=1}^{m_s} \left(Q(E)_{\iota_{E_S}(i),j} - \overline{Q}(E_S)_{i,j} \right) \theta^j_{\iota_{E_S}(i)} + \sum_{i=1}^{n_b} \psi^j_{\iota_{V_B}(i)} N_\theta(B)_{i,j} + , \\
&+ \sum_{i=1}^{m} (\nabla \, \psi^j)_i \theta_i^j - \sum_{i=1}^{m} \left((p_i' - 1) |Q(E)_{i,j}|^{p_i'-2} + \delta_q \right) \phi_i^j \theta_i^j = 0
\end{aligned}
$$

where test functions are collected in the matrix $N_\theta(B) = (N_\theta(B))_{ij} = (\theta^j \cdot \vec{\nu})_{\iota_{V_B}(i)}$.
We now impose the annihilation of the partial derivatives with respect to the head:

$$
\frac{\partial \mathcal{L}}{\partial H(V)_{:,j}} \cdot \rho^j = 0, \ \forall \, \rho^j \in \mathcal{H}(V) .
$$

This yields:

$$
- \sum_{i \in \iota_{V_B}(\{1,\dots,n_b\})} N_\rho(V)_{i,j} \rho_i^j - \sum_{i \notin \iota_{V_B}(\{1,\dots,n_b\})} \left(\nabla^T (\mathrm{Diag}(w) + \delta_w \mathbb{1}) \phi^j \right)_i \rho_i^j + \sum_{i=1}^{n_b} \xi_i^j \rho^j_{\iota_{V_B}(i)} = 0 ,
$$

where the test functions together with the weights and the regularization term are collected in matrix $N_\rho(V) = (N_\rho(V))_{ij} = ((\mathrm{Diag}(w) + \delta_w \mathbb{1})\phi^j) \cdot \vec{\nu})_i$.
Now we derive the adjoint equations. On the one hand, letting θ^j such that $(N_\theta(B))_{:,j} \equiv 0$ and ρ^j such that $\rho^j_i = 0$, $\forall\, i \in \iota_{V_B}(\{1, \dots, n_b\})$ we obtain the following:

- on the edges in E_S:

$$\left((p'_i - 1)|Q(E)_{i,j}|^{p'_i - 2} + \delta_q\right) \phi^j_i + (\nabla\, \psi^j)_i = Q(E)_{i,j} - \overline{Q}(E_S)_{\iota^{-1}_{E_S}(i),j}, \quad \forall\, i \in \iota_{E_S}(\{1, \dots, m_s\})\,;$$

- on the edges in E_I:

$$\left((p'_i - 1)|Q(E)_{i,j}|^{p'_i - 2} + \delta_q\right) \phi^j_i + (\nabla\, \psi^j)_i = 0, \quad \forall\, i \in \iota_{E_I}(\{1, \dots, m_i\})\,;$$

- on the internal nodes V_I:

$$-\left(\nabla^T \left(\mathrm{Diag}(w) + \delta_w \mathbb{1}\right) \phi^j\right)_i = 0, \quad \forall\, i \notin \iota_{V_B}(\{1, \dots, n_b\})\,.$$

On the other hand, assuming $(N_\theta(B))_{:,j}$ has no zero elements, by virtue the previous three equations, we have:

$$\psi^j_{\iota_{V_B}(i)} = -\overline{F}(B)_{i,j} + \overline{T}(B)_{i,j}, \quad \forall\, i \in \{1, \dots, n_b\}\,.$$

Note that this latter equation defines the Dirichlet boundary conditions on B for the adjoint variable ψ. Finally, supposing that ρ^j has no zero elements on B we obtain the compatibility condition:

$$\xi^j_i = N_\rho(V)_{\iota_{V_B}(i),j}, \quad \forall\, i \in \{1, \dots, n_b\}.$$

In summary, letting $q^j := Q(E)_{:,j} \in \mathcal{H}(E)$, $\bar{q}^j := \overline{Q}(E_S)_{:,j} \in \mathcal{H}(E_S)$, $h^j := H(V)_{:,j} \in \mathcal{H}(V)$, $\bar{h}^j := \overline{H}(B)_{:,j} \in \mathcal{H}(B)$, $f^j := F(V_I)_{:,j} \in \mathcal{H}(V_I)$, $\bar{f}^j := \overline{F}(B)_{:,j} \in \mathcal{H}(B)$, $\forall\, j = 1, \dots, M$, we have that the primal equations can be written in compact form as:

$$\begin{cases} \left(|q^j_e|^{p'_e - 2} + \delta_q\right)) q^j_e = -(w_e + \delta_w)(\nabla\, h^j)_e, & \forall\, e \in E \\ -(\nabla^T\, q^j)_v = f^j_v, & \forall\, v \in V_I \\ h^j_v = \bar{h}^j_v, & \forall\, v \in B, \end{cases} \tag{1.5.5}$$

while the adjoint equations can be written as:

$$\begin{cases} \left((p'_e - 1)|q^j_e|^{p'_e - 2} + \delta_q\right) \phi^j_e + (\nabla\, \psi^j)_e = q^j_e - \bar{q}^j_e & \forall\, e \in E_S \\ \left((p'_e - 1)|q^j_e|^{p'_e - 2} + \delta_q\right) \phi^j_e + (\nabla\, \psi^j)_e = 0 & \forall\, e \in E_I \\ -\left(\nabla^T \left(\mathrm{Diag}(w) + \delta_w \mathbb{1}\right) \phi^j\right)_v = 0 & \forall\, v \in V_I \\ \psi^j_v = -\bar{f}^j_v - (q^j \cdot \vec{\nu})_v & \forall\, v \in B \end{cases}. \tag{1.5.6}$$

By the standard theory of optimization via adjoints, we have that the derivative of $\mathcal{L}$ with respect to the optimization parameter is exactly the partial derivative of $\mathcal{L}$ with respect to (w, p') computed on the solution $(Q(E), H(V), \Phi, \Psi)$ of the primal and adjoint equations. Thus, with simple computations we have:

$$\frac{d}{dw_i}\mathcal{L} = \partial_{w_i}\mathcal{L} = -\sum_{j=1}^{M} \phi_i^j \, \nabla H(V)_{i,j} \quad \forall\, i = 1, \dots, m\,;$$

$$\frac{d}{dp'_i}\mathcal{L} = \partial_{p'_i}\mathcal{L} = -\sum_{j=1}^{M} \phi_i^j \log\left(|Q(E)_{i,j}|\right) |Q(E)_{i,j}|^{p'_i - 2} \, Q(E)_{i,j} \quad \forall\, i = 1, \dots, m.$$

which can be rewritten in more compact form as:

$$\frac{d}{dw_e}\mathcal{L} = \partial_{w_e}\mathcal{L} = -\sum_{j=1}^{M} \phi_e^j (\nabla h^j)_e \quad \forall\, e \in E, \tag{1.5.7}$$

and

$$\frac{d}{dp'_e}\mathcal{L} = \partial_{p'_e}\mathcal{L} = -\sum_{j=1}^{M} \phi_e^j \log(|q_e^j|) q_e^j |^{p'_e - 2} q_e^j \quad \forall\, e \in E. \tag{1.5.8}$$

1.5.2 The role of the Dirichlet-to-Neumann map

In this section we discuss in more detail the role that the Dirichlet-to-Neumann map plays in guaranteeing the consistency of the model with respect to the measurements. Before delving into the discussion, we rewrite formally the primal and adjoint equations in (1.5.5) and (1.5.6) by introducing new variables. Thus, let $\mu^j \in \mathcal{H}(E)^+$ $j = 1, \dots, M$ be the positive edge function such that:

$$\mu_e^j = |q_e^j|^{p'_e - 2} \quad \forall\, e \in E\,.$$

Then, the primal equations (1.5.5) can be rewritten as the following weighted Laplacian system:

$$\begin{cases} q_e^j = -\dfrac{w_e + \delta_w}{\mu_e + \delta_q} (\nabla h^j)_e, & \forall\, e \in E \\ (\nabla^T \operatorname{Diag}\left(\dfrac{w + \delta_w}{\mu + \delta_q}\right) \nabla h^j)_v = f_v^j, & \forall\, v \in V_I \\ h_v^j = \bar{h}_v^j, & \forall\, v \in B, \end{cases}. \tag{1.5.9}$$

Analogously, the first two equations in (1.5.6) can be rewritten as:

$$\begin{cases} \left((p'_e - 1)\mu_e^j + \delta_q\right) \phi_e^j + (\nabla \psi^j)_e = q_e^j - \bar{q}_e^j, & \forall\, e \in E_S \\ \left((p'_e - 1)\mu_e^j + \delta_q\right) \phi_e^j + (\nabla \psi^j)_e = 0, & \forall\, e \in E_I \end{cases}. \tag{1.5.10}$$

We would like to remark here that the gradient $(\nabla \psi^j)_e$ of the adjoint variable ψ^j in the above equation has dimension of a flux and must not be confused with the gradient of the piezometric head $(\nabla h^j)_e$ in eq. 1.5.9. Now, in the same manner as before, we can introduce the variable $\tilde{q}^j$ defined as:

$$\begin{cases} \tilde{q}_e^j = q_e^j - \bar{q}_e^j, & \forall\, e \in E_S \\ \tilde{q}_e^j = 0, & \forall\, e \in E_I \end{cases} .$$

Then (1.5.10) rewrites as:

$$\phi_e^j = -\frac{(\nabla \psi^j)_e}{(p_e' - 1)\mu_e^j + \delta_q} + \frac{\tilde{q}_e^j}{(p_e' - 1)\mu_e^j + \delta_q} . \tag{1.5.11}$$

These observations allow us to interpret the system of adjoint equations (1.5.6) as the following weighted Laplacian system in the variable ψ^j:

$$\left(\nabla^T \operatorname{Diag}\left(\frac{w + \delta_w}{(p' - 1)\mu^j + \delta_q}\right) \nabla \psi^j\right)_v = (\nabla^T \operatorname{Diag}\left(\frac{w + \delta_w}{(p' - 1)\mu^j + \delta_q}\right) \tilde{q}^j)_v \quad \forall\, v \in V_I\,, \tag{1.5.12}$$

$$\psi_v^j = -\bar{f}_v^j - (q^j \cdot \vec{\nu})_v \qquad \forall\, v \in B\,.$$

We have now all the necessary tools to discuss the role of the Dirichlet-to-Neumann map. We first observe that the DtN performs the task of transforming head information into flux values, which can be compared with the actual demand. When the demand is met by the DtN flux, the parameter identification process terminates. The adjoint equation fulfills the task of driving the system towards the correct identification. The second observation is that the DtN map allows the simultaneous use of both sampled piezometric heads and fluxes by incorporating into the objective function the difference between the measured demand and the simulated DtN map and the difference between the simulated fluxes and the sampled fluxes on internal edges, when this information is available. Note that the DtN appears in the Dirichlet boundary conditions for ψ^j in the previous equation. Thus the adjoint equation is "forced" by the mismatch between observed and simulated demand. Indeed, eqs. (1.2.9) and (1.2.10) tell us that the solution (q^j, h^j) of the primal equation (1.5.9) satisfies:

$$\sum_{v \in B} (-q^j \cdot \vec{\nu})_v = \sum_{v \in V_I} f_v^j \quad \forall\, j = 1, \ldots, M\,,$$

i.e., the total boundary flux at Dirichlet nodes must equate the total flux on internal edges. At the same time, the mass balance equation (1.5.1) shows that the total boundary flux must be equal to the total external demand:

$$\sum_{v \in B} (-q^j \cdot \vec{\nu})_v = \sum_{v \in B} \bar{f}_v^j \quad \forall\, j = 1, \ldots, M\,.$$

These two statements are simultaneously fulfilled only when the distributions of the weight w and the exponent p are correctly identified, which occurs when the residual flux at Dirichlet nodes is zero:

$$-\bar{f}_v^j - (q^j \cdot \vec{\nu})_v = 0 \quad \forall\, v \in B\,. \tag{1.5.13}$$

For a better understanding of the identification process, suppose for simplicity that $M = 1$. In the case where $|q^j| \neq 0$ is nonzero, from (1.5.7), (1.5.8) we have that (p^*, w^*) is a local minimizer for $\mathcal{L}$ if and only if $\phi^j \equiv 0$. From the adjoint equation (1.5.8) and from (1.5.11) we have that

$$\phi^j \equiv 0 \quad \iff \quad \tilde{q}^j - \nabla\, \psi^j \equiv 0$$

if $\nabla\psi^j \equiv 0$ then $\phi^j \equiv 0$ if and only if $\tilde{q}^j \equiv 0$, which implies that the sampled fluxes are captured exactly. On the other hand, $\nabla\, \psi^j \equiv 0$ if the mismatch between the observed demand and the DtN is constant, i.e.,

$$-\bar{f}_v^j - (q^j \cdot \vec{\nu})_v = c\,, \tag{1.5.14}$$

we have that for any $v \in B$

$$\nabla^T \,\mathrm{Diag}\left(\frac{w + \delta_w}{(p'-1)\mu^j + \delta_q}\right) \tilde{q}^j \equiv 0\,. \tag{1.5.15}$$

This implies that the procedure can terminate also when the difference between observed and calculated demands is constant. Thus, we need to avoid working in the kernel of the divergence operator to ensure that (1.5.15) is zero if and only if $\tilde{q}^j \equiv 0$. Since the kernel of the divergence operator corresponds to loops in the graph, this suggests that the optimal sampling strategy is to measure the piezometric head at every junction with topological degree greater than two. Observe that, if no flux data are provided, then $\tilde{q}^j \equiv 0$ and eq. (1.5.15) is automatically satisfied. However, the price to pay in this case is that no information on internal nodes are actually provided to the identification process, which then may become less accurate. Since the objective function in problem (1.5.2) is equivalent to:

$$\sum_{j=1}^{M} \left(\sum_{v \in B} \frac{1}{2} |(-q^j \cdot \vec{\nu})_v - \bar{f}_v^j|^2 + \sum_{e \in E_S} \frac{1}{2} |\tilde{q}_e^j|^2 \right)\,, \tag{1.5.16}$$

these a posteriori considerations show that the minimization of (1.5.16), if sufficient information are provided and $|q^j| \neq 0$, will naturally converge to a solution (p^*, w^*) such that the condition (1.5.13) is satisfied and the sampled fluxes and the consistency with respect to the data is preserved or equivalently the constant c in (1.5.14) is zero and the adjoint variable ψ^j is constantly zero (see eqs. (1.5.15) and (1.5.12)).

Observe that no ambiguities arise if we have at our disposal the measured fluxes at all the boundary edges (i.e., edges that are incident to a boundary node). This

situation occurs for example when modern smart meters measuring both water pressure and flux are used at junctions. Indeed, in this case the condition $\tilde{q}^j \equiv 0$ is equivalent to condition (1.5.13) and leads to far better results in our numerical experiments.
In the case where the demand distribution f^j is such that the flux q^j is zero (or near zero) in some edges (this is the case for example when no demand or a very small demand is applied to a household service connection), then some bad behavior arises in the minimization process since $\partial_{p'^j}\mathcal{L}$ can be approximately zero without implying that ϕ^j to be close to zero in the corresponding edge. Thus the identification procedure benefits dramatically from the use of multiple observations sets obtained from different demand distributions. This is easily obtained using information at several times making sure that the demand distributions are different. We finally observe that geometrical symmetries in the graph can also become critical as multiple distribution of exponent p and w can lead to the same minimizers of Problem (1). However, this is a rare situation in the real world aqueducts.

1.5.3 The connection with the Extended Dynamic Monge Kantorovich approach

In Section 1.3 we have seen that the momentum and mass balance equations (1.3.1) and (1.3.2) are equivalent to the graph weighted p-Poisson equation reported in (1.3.3). These, in turn, are the Euler-Lagrange equations of the saddle points of the Lagrangian defined in (1.3.5). We then introduced the Tikhononv regularized Lagrangian (1.3.6) and the derived regularized momentum and mass balance equations (1.3.7), which are the core of our primal adjoint approach described in Section 1.5.1.
In this section, we discuss a gradient flow for the solution of Problem (1) inspired by the Extended Dynamic Monge Kantorovich (EDMK) [57]. For the sake of simplicity will use a compact notation as in eqs. (1.5.5) and (1.5.6). Thus, we introduce the lifting function:

$$\tilde{h}^j := \begin{cases} 0, & v \in V_I \\ \bar{h}_v^j, & v \in B \end{cases},$$

and consider the Lagrangian functional $\mathtt{L}^{\mathtt{j}\,\delta_q,\delta_w}_{w,p} : (\mathcal{H}_0^B(V) \times \mathcal{H}(E)) \to \mathbb{R}$ defined as:

$$\mathtt{L}^{\mathtt{j}\,\delta_q,\delta_w}_{w,p}({h_0}^j, q^j) := -\sum_{e\in E} \frac{1}{p'_e} \frac{|q_e^j|^{p'_e}}{w_e^j + \delta_w} - \frac{1}{2}\sum_{e\in E} \frac{\delta_q |q_e^j|^2}{w_e^j + \delta_w} - \sum_{e\in E} q_e^j \left(\nabla({h_0}^j + \tilde{h}^j)\right)_e - \sum_{v\in V} f_v^j {h_0}_v^j, \tag{1.5.17}$$

where $\mathcal{H}_0^B(V)$ is as in eq. (1.2.8). We now introduce the saddle point problem:

$$\inf_{{h_0}^j \in \mathcal{H}_0^B(V)} \sup_{q^j \in \mathcal{H}(E)} \mathtt{L}^{\mathtt{j}\,\delta_q,\delta_w}_{w,p}({h_0}^j, q^j)\,.$$

The Euler-Lagrange equations for this saddle point problem are:

$$\begin{cases} (|q_e^j|^{p'_e-2}+\delta_q)q_e^j = -(w_e+\delta_w)\left(\nabla({h_0}^j+\tilde{h}^j)\right)_e & \forall\, e\in E \\ -(\nabla^T q^j)_v = f_v^j & \forall\, v\in V_I\,, \\ {h_0}_v^j = 0, & \forall\, v\in B \end{cases} \tag{1.5.18}$$

which are equivalent to the primal equations in (1.5.5) with the non homogeneous Dirichlet boundary conditions absorbed in the definition of the lifting function. As done in Section 1.5.2, we introduce the additional variable $\mu^j \in \mathcal{H}(E)^+$, $j=1,\dots,M$ defined as:

$$\mu_e^j := |q_e^j|^{p'_e-2} \quad \forall\, e\in E\,.$$

This intermediate variable has the important role of formally reducing the primal equation into a system of equations involving a linear weighted Laplacian system. Indeed, in this case eq.(1.5.18) becomes:

$$\begin{cases} (\mu_e^j+\delta_q)q_e^j = -(w_e+\delta_w)(\nabla({h_0}^j+\tilde{h}^j))_e & \forall\, e\in E \\ -(\nabla^T q^j)_v = f_v^j & \forall\, v\in V_I\,. \\ {h_0}_v^j = 0, & \forall\, v\in B \end{cases}$$

Obviously, this additional variable becomes an extra unknown of the problem. The justification for the introduction of this new unknown will be provided in Chapter 2, Section 2.4, where, by a Legendre duality argument, we introduce an equivalent saddle point formulation for the p-Dirichlet energy on graphs that naturally involves the variable μ^j. This allows also the definition of a variational formulation for the p-Poisson problem (1.2.8). The aim of this effort is to can combine in one single optimization problem the solution of the weighted p-Poisson equation and the minimization of the objective function of the parameter identification problem.
Indeed, again, by duality, we can transform the p-Poisson variational problem into a saddle point problem involving a minimization in two variables (the variable μ and the variable h^j, in our framework) and a maximization in a third variable, which plays the role of the negative of the edge flux q^j. After the introduction of a Tykhonov regularization, by directly computing a maximizer it is possible to remove the "sup" from the problem thus arriving at a reduced optimality problem involving a double minimization.
While these statements will find rigorous justification in the next chapter, in this section we provide the description together with an intuitive rationalization of the full procedure. We start this description by considering the p-Dirichlet energy $\mathtt{E}_{p,\omega}(\varphi)$ defined in eq. (1.2.6) restricting ourselves for simplicity to the case of interest for aqueducts $1\le p<2$ but with uniform weights $\omega_e=1$, $\forall\, e\in E$. Let us introduce the family of Lagrangian functionals $\mathtt{L}_\varphi^p : (\mathcal{H}(E)^+\times\mathcal{H}(E))\to\mathbb{R}$

given by:

$$\mathtt{L}^p_\varphi(\mu,\sigma) := -\sum_{e\in E}\frac{1}{2}\mu_e|\sigma_e|^2 + \sigma\cdot\nabla\varphi + \frac{2-p}{2p}\sum_{e\in E}\mu_e{}^{\frac{p}{2-p}} \quad \varphi\in\mathcal{H}(V)\,. \tag{1.5.19}$$

It is possible to show (see Theorem 2.4.1) that the saddle point of the above family of Lagrangian functional is exactly the p-Dirichlet energy $\mathtt{E}_{p,\omega}(\varphi)$, i.e.:

$$\mathtt{E}_{p,\omega=1}(\varphi) = \inf_{\mu\in\mathcal{H}(E)^+}\sup_{\sigma\in\mathcal{H}(E)}\mathtt{L}^p_\varphi(\mu,\sigma). \tag{1.5.20}$$

The saddle point (μ^*,σ^*) is unique in the case $1<p<2$ and it satisfies the extremality relations:

$$\begin{aligned}
\mu^*_e\sigma^*_e &= (\nabla\varphi)_e, \quad \forall\, e\in E,\ 1\le p<2\\
\mu^*_e = |\sigma^*_e|^{p'-2} &= |(\nabla\varphi)_e|^{2-p}, \quad \forall\, e\in E,\ 1<p<2\\
|\sigma^*_e| &\le 1, \quad \forall\, e\in E,\ p=1\\
\mu^*_e|\sigma^*_e|^2 - \mu^*_e &= 0, \quad \forall\, e\in E,\ p=1\\
\mu^*_e &= |(\nabla\varphi)_e|, \quad \forall\, e\in E,\ p=1.
\end{aligned}$$

In addition, for the case $p=1$, it is possible to show that μ^* is the unique optimal density. It is now easy to see that it is possible to retrieve a posteriori the standard duality identity:

$$\mathtt{E}_{p,\omega=1}(\varphi) = \mathtt{L}^p_\varphi(\mu^*,\sigma^*) = \sup_{\sigma\in\mathcal{H}(E)} -\sum_{e\in E}\frac{1}{p'}|\sigma^*_e|^{p'} + \sigma^*\cdot\nabla\varphi \quad \varphi\in\mathcal{H}(V)\,.$$

This gives a strong motivation to consider also the variational formulation of the p-Poisson problem. Thus, as in Section 1.2, given a forcing term $f\in\mathcal{H}(V_I)$ and non-homogeneous Dirichlet boundary conditions on a subset $B\subset V$, $B\cap V_I=\emptyset$, $B\cup V_I = V$, the variational formulation of the p-Poisson can be written as:

$$\inf_{\varphi\in\mathcal{H}^B_0(V)}\sum_{e\in E}\frac{|(\nabla(\varphi+\bar\varphi))_e|^p}{p} - \sum_{v\in V_I} f_v\varphi_v\,, \tag{1.5.21}$$

where, again for simplicity, we use uniform edge weights, $\omega=1$, and we recall that $\mathcal{H}^B_0(V) := \{h\in\mathcal{H}(V)\mid h_v=0,\ \forall\, v\in B\}$. To accommodate non-homogeneous Dirichlet boundary condition we introduce the lifting function $\bar\varphi$ such that $\bar\varphi_v = g_v$ for all $v\in B$, and $\bar\varphi_v=0$ for all $v\in V_I$. Thus, eq. (1.5.21) can be re-written as:

$$\inf_{\varphi\in\mathcal{H}^B_0(V)}\mathtt{E}_{p,\omega=1}(\varphi+\bar\varphi) - \sum_{v\in V_I} f_v\varphi_v\,.$$

Using eq. (1.5.20) we find immediately that the previous problem is equivalent to the following saddle point problem:

$$\begin{matrix}\inf\\ \mu\in\mathcal{H}(E)^+\\ \varphi\in\mathcal{H}^B_0(V)\end{matrix}\ \begin{matrix}\sup\\ \sigma\in\mathcal{H}(E)\end{matrix} -\sum_{e\in E}\frac{1}{2}\mu_e|\sigma_e|^2 + \sigma\cdot\nabla(\varphi+\bar\varphi) - \sum_{v\in V_I} f_v\varphi_v + \frac{1}{2\gamma}\sum_{e\in E}\mu_e^\gamma, \tag{1.5.22}$$

where $\gamma := \frac{p}{2-p}$.
In the next Chapter, Theorem 2.9.1, we will show that for $1 < p < 2$ the saddle point $((\varphi^*, \mu^*), \sigma^*)$ is unique and satisfies the following extremality equations:

$$\begin{aligned} \mu_e^* \sigma_e^* &= (\nabla(\varphi^* + \bar{\varphi}))_e \quad \forall\, e \in E \\ -(\operatorname{div} \sigma^*)_v &= f_v \quad \forall\, v \in V_I \\ \varphi_v^* &= 0, \quad \forall\, v \in B \\ \mu_e^* = |\sigma_e^*|^{p'-2} &= |\,\nabla(\varphi^* + \bar{\varphi})_e|^{2-p} \quad \forall\, e \in E\,. \end{aligned}$$

From these conditions it follows that $\tilde{\varphi}^* := \varphi^* + \bar{\varphi}$ is the unique solution of the saddle point problem:

$$\begin{cases} |\sigma_e^*|^{p_e'-2}\sigma_e^* = (\nabla\, \tilde{\varphi}^*)_e \quad \forall\, e \in E \\ (\nabla^T\, \sigma^*)_v = f_v \quad \forall\, v \in V_I \\ \tilde{\varphi}_v^* = g_v \quad \forall\, v \in B, \end{cases} \tag{1.5.23}$$

or equivalently of the p-Poisson problem:

$$\begin{aligned} (\Delta_{p,\omega=1}\, \tilde{\varphi}^*)_v &= f_v \quad v \in V_I \\ \tilde{\varphi}_v^* &= g_v \quad v \in B. \end{aligned}$$

Now we introduce the Tikhononv regularized Lagrangian functional $\mathtt{L}^{p,\delta} : (\mathcal{H}_0^B(V) \times \mathcal{H}(E)^+ \times \mathcal{H}(E))$:

$$\mathtt{L}^{p,\delta}(\varphi, \mu, \sigma) := -\sum_{e\in E} \frac{1}{2}(\mu_e + \delta)|\sigma_e|^2 + \sigma \cdot \nabla(\varphi + \bar{\varphi}) - \sum_{v\in V_I} f_v\varphi_v + \frac{1}{2\gamma}\sum_{e\in E} {\mu_e}^{\gamma}\,, \tag{1.5.24}$$

where $\delta > 0$ is a small Tikhononv parameter, and define our regularized functional:

$$\mathcal{L}_\delta^p(\varphi, \mu) := \sup_{\sigma\in\mathcal{H}(E)} \mathtt{L}^{p,\delta}(\varphi, \mu, \sigma). \tag{1.5.25}$$

Since now $\mu + \delta > 0$, the supremum in σ in (1.5.25) is in fact a maximum (we have indeed strong concavity, differntiability and anti-coerciveness), and the maximizer σ^* satisfies

$$\sigma_e^* = \frac{\nabla(\varphi + \bar{\varphi})_e}{\mu_e + \delta} \quad \forall\, e \in E. \tag{1.5.26}$$

Thus, computing $\mathtt{L}^{p,\delta}(\varphi, \mu, \sigma)$ at the maximizer σ^*, the functional $\mathcal{L}_\delta^p(\varphi, \mu)$ simplifies as follows:

$$\mathcal{L}_\delta^p(\varphi, \mu) = \sum_{e\in E} \frac{1}{2}\frac{|\,\nabla(\varphi + \bar{\varphi})_e|^2}{(\mu_e + \delta)} - \sum_{v\in V_I} f_v\varphi_v + \frac{1}{2\gamma}\sum_{e\in E} \mu_e^{\gamma}\,, \tag{1.5.27}$$

which motivates the following double minimization problem in place of eq (1.5.22):

$$\inf_{\substack{\varphi\,\in\,\mathcal{H}_0^B(V) \\ \mu\,\in\,\mathcal{H}(E)^+}} \mathcal{L}_\delta^p(\varphi, \mu), \tag{1.5.28}$$

which is the Tikhonov regularization of the saddle point problem (1.5.22). It is possible to show (see Chapter 2 Section 2.9), that $\mathcal{L}^p_\delta(\varphi,\mu)$ is lower semi-continuous, stictly convex and norm coercive in the pair (φ,μ) thus the existence of a unique minimizer (φ^*,μ^*) is guaranteed.
Inspired by the DMK(Dynamic-Monge-Kantorovich) scheme in [55–57], we introduce the following minimizing dynamics for (1.5.28):

$$\begin{aligned}
\sigma_e(t) &= \frac{(\nabla(\varphi(t)+\bar{\varphi}))_e}{\mu_e(t)+\delta} \quad \forall\, e \in E \\
(\nabla^T \sigma(t))_v &= (\Delta_{\frac{1}{\mu(t)+\delta}}(\varphi(t)+\bar{\varphi}))_v = f_v \quad \forall\, v \in V_I \\
\varphi(t)_v &= 0 \quad \forall\, v \in B \\
\partial_t \mu_e(t) &= \mu_e(t)|\sigma_e(t)|^2 - \mu_e(t)^{\frac{p}{2-p}} \quad \mu_e(0) = \mu_{0_e} > 0, \quad \forall\, e \in E.
\end{aligned} \tag{1.5.29}$$

As in [56, 59], a solution (φ^*,μ^*) of (1.5.28) is sought via a gradient descent approach not applied directly to the functional $\mathcal{L}^p_\delta(\varphi,\mu)$ but rather to its composition with the change of variable $\mu(t) = \Psi(\xi(t)) := \xi(t)^2$ and performing then a pull-back of the descending dynamics on the original variable $\mu(t)$. It is possible to see that such a dynamics can be interpreted as a descent dynamics that preserves the positivity constraint on $\mu(t)$ (see Chapter 2, Section 2.7, Subsection 2.8.2 and Section 2.9 for full details).
We then propose an improved version ofthe dynamics in (1.5.29), which has been observed to converge faster in our numerical experiments. This is derived by composition with the map:

$$\mu_e = \Psi(\xi_e) := |\xi_e|^{\frac{2(2-p)}{p}}, \quad \forall\, e \in E,$$

leading to the following new dynamics for the density μ in (1.5.29):

$$\partial_t \mu_e(t) = \mu_e(t)^{\frac{4-3p}{2-p}} |\sigma_e(t)|^2 - \mu_e(t), \quad \forall\, e \in E. \tag{1.5.30}$$

The gradient descent approach applied to the computation of a minimizer has to be intended as a long time solution $(\varphi^*,\mu^*) = \lim_{t\to\infty}(\varphi(t),\mu(t))$ where $(\varphi(t),\mu(t))$ is a solution of the state-space initial value problem (1.5.29). Therefore, it is necessary to introduce an opportune time discretization scheme and an opportune stopping rule.
In Chapter 2, Section 2.7, three approaches of time discretization are presented: the explicit Euler (EE) approach, a semi-implicit (SI) improvement and the implicit Euler(or the Gradient Flow) approach.
We present here for completeness the first approach, i.e. the explicit one, which would be used also in our numerical examples. Given a sequence $\Delta t_k > 0$ of time steps, the approximation sequence $\left(\mu^k\right)_{k=1,\dots,k_{\max}}$ is given by the following set of

equations:

$$\begin{cases} (\Delta_{\frac{1}{\mu^k+\delta}}(\varphi^k+\bar{\varphi}))_v = 0, & \forall\, v \in V_I \\ \varphi_v^k = 0, & \forall\, v \in B \\ \sigma_e^k = \dfrac{(\nabla(\varphi^k+\bar{\varphi}))_e}{\mu_e^k+\delta}, & \forall\, e \in E \\ \mu_e^{k+1} = \mu_e^k + \Delta t_k \left((\mu_e^k)^{\frac{4-3p}{2-p}} |\sigma_e^k|^2 - \mu_e^k \right), & k = 0, \dots, k_{\max}, e \in E \\ \mu_e^0 = \mu_{0e} > 0, & \forall\, e \in E. \end{cases} \tag{1.5.31}$$

Hence at each time step, we only need to solve the lifted linear system

$$\begin{aligned} (\Delta_{\frac{1}{\mu^k+\delta}}(\varphi^k+\bar{\varphi}))_v = 0 \quad \forall\, v \in V_I \\ \varphi_v^k = 0 \quad \forall\, v \in B. \end{aligned} \tag{1.5.32}$$

Some geometric considerations can be done on the updating scheme defined in (1.5.31). Indeed, it is possible to interpret (1.5.31) as a type of projected gradient descent. Thus, heuristically, if we start from an initial $\mu^0 > 0$ and a sufficiently small initial time step, the positivity is preserved since we are moving in a descent direction projected tangentially to the exponential map. Hence we converge toward zero from a parallel direction to the axis $\mu_e = 0$(see 2 Subsection 2.8.2).
The explicit Euler scheme (1.5.31) is therefore a linear iterative solver for the p-Poisson problem. It has indeed several advantages. Observe that the variable μ has the main role to absorb the non linearity induced by the factor $|\sigma|^{p'-2}$ thus reducing the non linear system (1.5.23) to the weighted laplacian in (1.5.32).
Moreover, multiple experiments shows that the derived numerical scheme exhibits very good stability properties and can be placed somewhere in the middle between the augmented lagrangian approaches [13], [33], and the Newton method for the p-Poisson problem.
On the other hand, differently from the Newton method where we have to invert an Hassian matrix, here we only have to solve for a weighted laplacian linear system with Dirichlet boundary conditions and perfom an integration step for the dynamics of $\mu(t)$.
Aside from the very simple implementation of (1.5.31), having a structure which depends upon inverting a graph laplacian matrix, which is naturally sparse and symmetric, has the main advantage derived from the huge weaponry of the numerical linear algebra(e.g. multi grid methods, preconditioning strategies etc.).
Observe that differently from the standard augmented lagrangian approach where typically some variable substitutions are performed via Lagrange multipliers, here the formal substitution $\mu = |\sigma|^{p'-2}$ is naturally given by the Legendre transform(see Chapter 2 Sections 2.2, 2.5).
Furthermore, upon introducing the Tikhonov regularized Lagrangian (1.5.24) and

the functional (1.5.25), the original saddle point problem (1.5.22) is reduced to a differentiable and strictly convex double minimization problem, hence the second order method derived from the implicit Euler time discretization is well defined, improving drastically the performance of the numerical scheme. Moreover, differently from the Newton method which needs a sufficient accurate initial guess to converge, here we can benefit from the stability induced by (1.5.25) which acts as a Lyapunov functional for the dynamics. Thus, starting with a sufficiently small initial time step, the newton method applied to the implicit Euler time discretization of (1.5.29) is guaranteed to converge(see [59] for details).
Last but not least, note that having a double minimization problem instead of a saddle point problem, allows us to easily introduce further constraints on the variable φ.

Let us now return to Problem (1) and equations (1.5.5).
It is now evident the similarity between the Tikhonov regularized lagrangians (1.5.17), (1.5.24), the primal equations (1.5.5) and the first three equations in (1.5.29):

$$\begin{gathered}(\mu_e+\delta)\sigma_e=(\nabla(\varphi+\bar{\varphi}))_e,\quad \forall\, e\in E\\ (\nabla^T\sigma)_v=(\Delta_{\frac{1}{\mu+\delta}}(\varphi+\bar{\varphi}))_v=f_v,\quad \forall\, v\in V_I\\ \varphi_v=0,\quad \forall\, v\in B.\end{gathered}$$

We are indeed motivated to introduce the following Lagrangian $\mathtt{L}^{w,p,\delta_w,\delta_q}:(\mathcal{H}_0^B(V)\times\mathcal{H}(E)^+\times\mathcal{H}(E))\to\mathbb{R}$, $\forall\, j=1,\dots,M$:

$$\begin{aligned}&\mathtt{L}^{w,p,\delta_w,\delta_q}({h_0}^j,\mu^j,q^j):=\\ &-\sum_{e\in E}\frac{1}{2}\frac{\mu_e^j+\delta_q}{w_e+\delta_w}|q_e^j|^2-q^j\cdot\nabla({h_0}^j+\tilde{h}^j)-\sum_{v\in V}f_v^j{h_0}_v^j+\sum_{e\in E}\frac{2-p_e}{2p_e(w_e+\delta_w)}{\mu_e^j}^{\frac{p_e}{2-p_e}}.\end{aligned}$$

Note that here the variable $q^j\in\mathcal{H}(E)$ plays the role of $-\sigma$ in (1.5.24) while the variable ${h_0}^j\in\mathcal{H}_0^B(V)$ plays the role of φ. Thus, we consider the functional:

$$\mathcal{L}^{w,p}_{\delta_w,\delta_q}({h_0}^j,\mu^j):=\sup_{q^j\in\mathcal{H}(E)}\mathtt{L}^{w,p,\delta_w,\delta_q}({h_0}^j,\mu^j,q^j).$$

and with the same arguments as in (1.5.26)-(1.5.27) we have that there exists a maximizer ${q^*}^j$ given by:

$${q^*}_e^j=-\frac{(w_e+\delta_w)\,\nabla({h_0}^j+\tilde{h}^j)_e}{{\mu^j}_e+\delta_q},\quad \forall\, e\in E. \tag{1.5.33}$$

Thus, computing $\mathtt{L}^{w,p,\delta_w,\delta_q}({h_0}^j,\mu^j,q^j)$ in the maximizer ${q^*}^j$, the functional $\mathcal{L}^{w,p}_{\delta_w,\delta_q}({h_0}^j,\mu^j)$

simplifies as follows:

$$\mathcal{L}^{w,p}_{\delta_w,\delta_q}(h_0{}^j,\mu^j)=\sum_{e\in E}\frac{1}{2}\frac{(w_e+\delta_w)|\nabla(h_0{}^j+\tilde{h}^j)_e|^2}{(\mu_e+\delta_q)}-\sum_{v\in V}f_v^j h_{0v}^j+\sum_{e\in E}\frac{2-p_e}{2p_e(w_e+\delta_w)}{\mu_e^j}^{\frac{p_e}{2-p_e}},\tag{1.5.34}$$

Consider now the following double minimization problem:

$$\inf_{\substack{h_0{}^j\in\mathcal{H}_0^B(V)\\ \mu^j\in\mathcal{H}(E)^+}}\mathcal{L}^{w,p}_{\delta_w,\delta_q}(h_0{}^j,\mu^j).$$

The KKT conditions for the minimizer $(h_0^{*j},\mu^{*j})\in(\mathcal{H}_0^B(V)\times\mathcal{H}(E)^+)$ of $\mathcal{L}^{w,p}_{\delta_w,\delta_q}(h_0{}^j,\mu^j)$ satisfies:

$$\begin{cases} q^{*j}_e=-\frac{(w_e+\delta_w)\nabla(h_0^{*j}+\tilde{h}^j)_e}{{\mu^{*j}}_e+\delta_q}, & \forall\, e\in E\\ -|q^{*j}_e|^2+{\mu^{*j}}_e{}^{\frac{2}{p'_e-2}}-c_e(w_e+\delta_w)=0, & \forall\, e\in E\\ (\Delta_{\frac{(w+\delta_w)}{(\mu^{*j}+\delta_q)}}(h_0^{*j}+\tilde{h}^j))_v=f_v^j, & \forall\, v\in V_I\\ h_{0v}^{*j}=0, & \forall\, v\in B\\ c_e{\mu^{*j}}_e=0,\quad c_e\geq 0, & \forall\, e\in E, \end{cases}$$

Thus, ${\mu^{*j}}_{\bar{e}}=0$ on some edge $\bar{e}\in E$ if and only if

$$q^{*j}_{\bar{e}}=\nabla(h_0^{*j}+\tilde{h}^j)_{\bar{e}}=0,$$

and $c_{\bar{e}}=0$, there is no other possibility.
On the other hand, if ${\mu^{*j}}_{\bar{e}}>0$ we have that

$${\mu^{*j}}_{\bar{e}}=|q^{*j}_{\bar{e}}|^{p'_{\bar{e}}-2}.$$

As a consequence, if

$$(h_0^{*j},\mu^{*j})\text{ is a minimizer for }\mathcal{L}^{w,p}_{\delta_w,\delta_q}(h_0{}^j,\mu^j),$$

and q^{*j} is given by (1.5.33) then

$$(h_0^{*j}+\tilde{h}^j,q^{*j})$$

is a solution for the primal equations (1.5.5).
Therefore, defining:

$$h^j:=h_0^j+\tilde{h}^j,$$

we have

$$h_v^j=\bar{h}_v^j,\quad v\in B,$$

and we can recycle the EDMK scheme (1.5.29) as a converging dynamics to compute a solution of the primal equations (1.5.5).

The corresponding dynamical system of (1.5.29) and (1.5.30) for a solution of the primal equations, $\forall\, j = 1, \dots, M$, reads as follows:

$$\begin{aligned} q_e^j(t) &= -\frac{(w_e + \delta_w)\, \nabla (h^j(t))_e}{{\mu^j}_e(t) + \delta_q}, \quad \forall\, e \in E \\ (\operatorname{div} q^j(t))_v &= (\Delta_{\frac{w+\delta_w}{\mu^j(t)+\delta_q}} h^j(t))_v = f_v^j, \quad \forall\, v \in V_I \\ h^j(t)_v &= \bar{h}_v^j \quad \forall\, v \in B \end{aligned} \tag{1.5.35}$$

$$\partial_t \mu_e^j(t) = \mu_e^j(t)^{\frac{4-3p_e}{2-p_e}} |q_e^j(t)|^2 - \mu_e^j(t), \quad \mu_e^j(0) = \mu_{0_e}^j > 0, \quad \forall\, e \in E,$$

and the Explicit Euler scheme for (1.5.35) is given by:

$$\begin{cases} (\Delta_{\frac{w+\delta_w}{{\mu^j}^k+\delta_q}} {h^j}^k)_v = 0, \quad \forall\, v \in V_I \\ {h^j}^k = \bar{h}_v^j, \quad \forall\, v \in B \\ {q^j}_e^k = \dfrac{(\nabla {h^j}^k)_e}{{\mu^j}^k + \delta_q}, \quad \forall\, e \in E \\ {\mu^j}_e^{k+1} = {\mu^j}_e^k + \Delta t_k \left(({\mu^j}_e^k)^{\frac{4-3p_e}{2-p_e}} |{q^j}_e^k|^2 - {\mu^j}_e^k \right), \quad k = 0, \dots, k_{\max}, e \in E \\ {\mu^j}_e^0 = {\mu^j}_{0e} > 0, \quad \forall\, e \in E. \end{cases}$$

1.5.4 Total Variation Regularization

Since problem (1.5.2) is non convex, a regularization term is necessary in order to select opportune local minimizers. A common choice is to add to the Lagrangian $\mathcal{L}$ in (1.5.4) a Tikhonov penalty term. Typically, quadratic terms are added and have the effect to smooth out the solutions, thus gaining stability and regularity. A not common strategy is to add non differentiable term typically derived by the l_1 norm.
Among them a very important role is played by the total variation regularization. This naturally lead to locally constant optimal solutions, see [26], [142], [33] for an exhaustive treatment of total variation regularization.
The choice of this type of regularization fits well in the case of our problem since our optimal parameters (w, p') depends on the mechanical properties of the pipes, such as the diameters, material and age. Typically the pipes are posed in sequence with the same material and diameter, therefore, it is of central importance to find such a method which promotes locally constant solutions on sequence of pipes with the same properties.
Moreover, we can genuinely carry out the optimization procedure on less boundary/sampling nodes since the the design parameters are "hold together" by the regularization.

In graph theory we can take gradients only of functions defined on the nodes set while our parameters (w, p') are defined on the edges.
The common procedure is to consider a new graph obtained from the original graph by connecting the middle points of adjacent edges, the so called "Line-Graph". This is one of the most classical example of graph duality. Note that, by definition, only the nodes of topological degree greater or equal than two in the original graph, contributes to the construction of the line graph.
The gradient operator generated by the "Line-Graph" is a matrix from the original graph edges set to the "Line-Graph" edges set, which has constant functions on the original graph edges set as kernel see [121].
Therefore the strategy is to create a regularization defining the total variation of our edge weight and exponent using the gradient derived from the "Line-Graph".
In figure (1.3) we can see an example of comparison between original graph and "Line-Graph". Given a graph $\mathcal{G}(V, E)$ we denote as $L(\mathcal{G})(E, Y)$ the "Line-Graph"

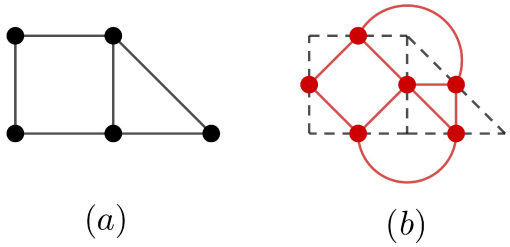

Figure 1.3: (a) original graph(black) vs (b) derived line graph(red).

of $\mathcal{G}$. Then $L(\mathcal{G})$ has by definition $m = |E|$ nodes, i.e. the number of original edges and it is easy to see that the number of edges is given by:

$$|Y| = \sum_{v \in V} \frac{k_v(k_v - 1)}{2},$$

where k_v is the topological degree of a node $v \in V$ in the original graph $\mathcal{G}$.
Thus, by construction, each node v of degree k_v of the original graph $\mathcal{G}$ corresponds to a k_v fully connected clique in $L(\mathcal{G})$.
Line graphs have been studied extensively and, among their well-known properties, Whitney's uniqueness theorem states that the structure of $\mathcal{G}$ can be recovered completely from its line graph $L(\mathcal{G})$, for any graph other than a triangle or a star network of four nodes [138]. Hence we don't loose any information on the topological structure of the original graph.
As already observed, a single node v in G leads to a connected clique of $\frac{k_v(k_v-1)}{2}$ links in the line graph $L(\mathcal{G})$). This seems to suggest that the line graph $L(\mathcal{G})$ gives too much prominence to the high degree nodes of the original graph G. In [53] an opportune topological weighting strategy is presented to overcome this issue. The main idea is to define a weighted line graph whose links are scaled by a factor of $\mathcal{O}(1/k_v)$. This is motivated by the fact that each vertex v in the

original graph $\mathcal{G}$ contributes $\frac{k_v(k_v-1)}{2}$ edges to $L(\mathcal{G})$ even though its importance in the original graph could be estimated to be just k_v. Thus, for any node $v \in V$ in the original graph $\mathcal{G}$ we define the adjacency of v as:

$$adj_v := \{e \in E \mid e = uv \text{ or } e = vu\}, \quad \forall\, v \in V.$$

With this definition we have that:

$$k_v = |adj_v|\,, \quad v \in V.$$

Then, we consider the weighted line graph $L(\mathcal{G})(E, Y, \omega^{LG})$ such that for any edge $y \in Y$:

$$\omega_y^{LG} := \frac{1}{k_v - 1}, \quad y = e_1e_2,\ (e_1, e_2) \in E,\ (e_1, e_2) \in adj_v,\ v \in V.$$

and it's weighted gradient matrix $\nabla_{LG} : \mathcal{H}(E) \longrightarrow \mathcal{H}(Y)$ is the $|Y| \times m$ matrix given by:

$$(\nabla_{LG})_{ij} = \begin{cases} -\omega_{y_i}^{LG} & \text{if } y_i = e_je_k, \\ \omega_{y_i}^{LG} & \text{if } y_i = e_ke_j, \\ 0 & \text{otherwise.} \end{cases}$$

As a motivating example, consider the case of collaboration networks. Every link(edge) in a collaboration network corresponds to a joint work between two authors. Thus, the $(k_v - 1)$ normalization is justified by the desire that two authors should be less connected if they wrote a joint paper with many co-authors than a paper with few authors.
In the WDS framework, this translate to enhancing the connection between pipes on the same topological line(i.e. in sequence of junctions with topological degree equal to two), which is typically composed of pipes with the same properties(diameters, materials etc.), while considering as less connected the pipes which lies in the adjacency of a cross junction(a junction between more than two pipes), where it is most probable to have a connection between pipes with different diameters and materials.
This kind of weighted gradient matrix fits well for our regularization purpose. We will consider therefore the following new Lagrangian:

$$\begin{aligned}\mathcal{L}_{TV}(H(V), Q(E), p', w, \Phi, \Psi, \Xi, Tk_{p'}, Tk_w, \delta_q, \delta_w) := \mathcal{L}(p', w, H(V), Q(E), \Phi, \Psi, \Xi, \delta_q, \delta_w) + \\ + Tk_{p'} \| \nabla_{LG}\, p' \|_{l_1} + Tk_w \| \nabla_{LG}\, w \|_{l_1}\end{aligned} \tag{1.5.36}$$

where $\mathcal{L}(p', w, H(V), Q(E), \Phi, \Psi, \Xi, \delta_q, \delta_w)$ is the Lagrangian defined in (1.5.4) and $(Tk_{p'}, Tk_w)$ are two positive small regularization parameters.
In Section 1.5.3 we have seen an equivalent saddle point formulation for the graph p-Dirichlet energy. In Chapter 2, Sections 2.4, 2.8, 2.11 we extensively treat the limit case $p = 1$, and we show that the same arguments as in Section 1.5.3 can

be applied to the general framework of TV and l_1-norm regularization. Thus as in (1.5.19), given a graph $\mathcal{G}(V,E)$ where we set for simplicity the edge weight fix to one, we introduce the Lagrangian $\mathtt{L}^1_\varphi : (\mathcal{H}(E)^+ \times \mathcal{H}(E)) \to \mathbb{R}$ as:

$$\mathtt{L}^1_\varphi(\mu,\sigma) := -\sum_{e\in E}\frac{1}{2}\mu_e|\sigma_e|^2 + \sigma\cdot\nabla\varphi + \frac{1}{2}\sum_{e\in E}\mu_e, \quad \varphi\in\mathcal{H}(V),$$

which is the Lagrangian in (1.5.19) for $p=1$. In Chapter 2(see Theorem 2.4.1) we show that the graph 1-Dirichlet energy or the graph Total Variation energy:

$$TV(\varphi) := \mathtt{E}_1(\varphi) = \|\nabla\varphi\|_{l_1}$$

admits the following equivalent formulation:

$$TV(\varphi) = \inf_{\mu\in\mathcal{H}(E)^+}\sup_{\sigma\in\mathcal{H}(E)}\mathtt{L}^1_\varphi(\mu,\sigma).$$

Moreover, there exists a saddle point (μ^*,σ^*) for $\mathtt{L}^1_\varphi$ and it satisfies the extremality relations:

$$\begin{aligned}
\mu^*_e\sigma^*_e &= (\nabla\varphi)_e, \quad \forall\, e\in E,\\
|\sigma^*_e| &\le 1, \quad \forall\, e\in E,\\
\mu^*_e|\sigma^*_e|^2 - \mu^*_e &= 0, \quad \forall\, e\in E,\\
\mu^*_e &= |(\nabla\varphi)_e|, \quad \forall\, e\in E.
\end{aligned}$$

We then introduce the Tikhononv regularized Lagrangian:

$$\mathtt{L}^{1,\delta}(\varphi,\mu,\sigma) := -\sum_{e\in E}\frac{1}{2}(\mu_e+\delta)|\sigma_e|^2 + \sigma\cdot\nabla\varphi + \frac{1}{2}\sum_{e\in E}\mu_e,$$

where $\delta>0$ is a small Tikhononv parameter, and the functional:

$$\mathcal{L}^1_\delta(\varphi,\mu) := \sup_{\sigma\in\mathcal{H}(E)}\mathtt{L}^{1,\delta}(\varphi,\mu,\sigma).$$

With the same arguments as in (1.5.26), $\mathcal{L}^1_\delta(\varphi,\mu)$ simplifies as follows:

$$\mathcal{L}^1_\delta(\varphi,\mu) = \sum_{e\in E}\frac{1}{2}\frac{|(\nabla\varphi)_e|^2}{(\mu_e+\delta)} + \frac{1}{2}\sum_{e\in E}\mu_e,$$

and we consider the following minimization problem:

$$\inf_{\mu\in\mathcal{H}(E)^+}\mathcal{L}^1_\delta(\varphi,\mu). \tag{1.5.37}$$

Again, as in Section 1.5.3, we have that the KKT conditions for a minimizer (μ^*) of (1.5.37) satisfies:

$$\begin{cases}
-\frac{|(\nabla\varphi)_e|^2}{(\mu^*_e+\delta)^2} + 1 - c_e = 0, & \forall\, e\in E\\
c_e\mu^*_e = 0, \quad c_e\ge 0, & \forall\, e\in E.
\end{cases}$$

Thus, ${\mu^*}_{\bar{e}} = 0$ on some edge $\bar{e} \in E$ if and only if:

$$|(\nabla \varphi)_{\bar{e}}| \leq \delta, \tag{1.5.38}$$

and if ${\mu^*}_{\bar{e}} > 0$ we have that

$$|(\nabla \varphi)_{\bar{e}}| = \mu^*_{\bar{e}} + \delta. \tag{1.5.39}$$

Hence defining:

$$TV_\delta(\varphi) := \inf_{\mu \in \mathcal{H}(E)^+} \mathcal{L}^1_\delta(\varphi, \mu), \tag{1.5.40}$$

from (1.5.38), (1.5.39) we have:

$$TV_\delta(\varphi) = TV(\varphi) + \mathcal{O}(\delta).$$

We are indeed motivated to consider the following approximated Lagrangian instead of the total variation regularized one in (1.5.36):

$$\begin{aligned}\mathcal{L}^\delta_{TV}(p', w, \mu_{p'}, \mu_w, H(V), Q(E), \Phi, \Psi, \Xi, Tk_{p'}, Tk_w, \delta_q, \delta_w, \delta_{\mu_{p'}}, \delta_{\mu_w}) := \\ = \mathcal{L}(p', w, H(V), Q(E), \Phi, \Psi, \Xi, \delta_q, \delta_w) + \\ + Tk_{p'} \sum_{y \in Y} \left(\frac{1}{2} \frac{|\nabla_{LG} p'|^2_y}{\mu_{p'y} + \delta_{\mu_{p'}}} + \frac{1}{2} \mu_{p'y} \right) + Tk_w \sum_{y \in Y} \left(\frac{1}{2} \frac{|\nabla_{LG} w|^2_y}{\mu_{wy} + \delta_{\mu_w}} + \frac{1}{2} \mu_{wy} \right),\end{aligned} \tag{1.5.41}$$

where Y is the edges set of the line graph $L(\mathcal{G})$ of the original graph $\mathcal{G}$. The main advantage of considering (1.5.41) instead of using directly the total variation of (p', w) comes from (1.5.40). Indeed, having introduced the new positive densities variables $\mu_{p'}$ and μ_w which depend only on (p', w), allows us to perform simultaneously the minimization in the quadruple $(p', w, \mu_{p'}, \mu_w)$. Moreover, introducing the regularization parameters $(\delta_{\mu_{p'}}, \delta_{\mu_w})$ we have the necessary differentiability to use our EDMK scheme for the total variation minimization. The algorithmic issue and numerical implementation will be presented in full detail in the following subsection.
Let us consider as an illustrative example the simplified problem:

$$\min_{\substack{w \in \mathcal{H}(E)^+ \\ \mu \in \mathcal{H}(Y)^+}} F(w) + Tk_w \sum_{y \in Y} \left(\frac{1}{2} \frac{|\nabla_{LG} w|^2_y}{\mu_{wy} + \delta_{\mu_w}} + \frac{1}{2} \mu_{wy} \right), \tag{1.5.42}$$

where $F : \mathcal{H}(E) \to \mathbb{R}$ is a sufficiently smooth map.
Observe that we are in the same situation as in (1.5.28). The only difference is that we have a double positivity constraint so that in general we can not directly compute a minimizer in the variable w(differently from (1.5.28) where w is substituted by φ without the positivity constraint). Nevertheless, since we have a double minimization problem, we can consider a double "gradient descent"

approach in the pair (μ_w, w).
With the same arguments as in (1.5.29), by composing with the change of variable $(\mu_w(t) = |\xi(t)|^2, w = |\varepsilon(t)|^2)$ to enforce the positivity and then performing a pull-back of the descending dynamics on the original variables $(\mu_w(t), w(t))$, we get the following descending dynamics(see Chapter 2 Sections 2.8, 2.11):

$$\sigma_{wy}(t) = \frac{(\nabla_{LG}\, w(t))_y}{\mu_{wy}(t) + \delta_{\mu_w}}, \quad \forall\, y \in Y,$$

$$\partial_t \mu_{wy}(t) = \mu_{wy}(t)|\sigma_{wy}(t)|^2 - \mu_{wy}(t), \quad \forall\, y \in Y,$$

$$\mu_{wy}(0) = \mu_{w0y} > 0, \quad \forall\, y \in Y,$$

$$\partial_t w_e(t) = w_e(t)\left(-\partial_{w_e} F(w(t)) - Tk_w(\Delta^{LG}_{\frac{1}{\mu_w(t)+\delta_{\mu_w}}} w(t))_e\right), \quad \forall\, e \in E,$$

$$w_e(0) = w_{0e} > 0, \quad \forall\, e \in E.$$

where:

$$\Delta^{LG}_{\frac{1}{\mu_w(t)+\delta_{\mu_w}}} := \nabla_{LG}^T \,\mathrm{Diag}\left(\frac{1}{\mu_w(t) + \delta_{\mu_w}}\right)\nabla_{LG}, \quad \forall\, t \geq 0. \tag{1.5.43}$$

We propose the following semi-implicit Proximal Forward-Backward Splitting scheme(see [13],[40] for an exhaustive treatment):

$$\begin{cases} \sigma_{wy}^{\,k} = \dfrac{(\nabla_{LG}\, w^k)_y}{\mu_{wy}^{\,k} + \delta_{\mu_w}}, & \forall\, y \in Y \\ \mu_{wy}^{\,k+1} = \mu_{wy}^{\,k} + \Delta t_k(\mu_{wy}^{\,k})\left(|\sigma_{wy}^{\,k}|^2 - 1\right), & k = 0, \ldots, k_{\max}, y \in Y \\ \mu_{wy}^{\,0} = \mu_{w0y} > 0, & \forall\, y \in Y \\ \tilde{w}_e^k = w_e^k - \Delta t_k\left([\mathrm{Diag}(w^k)]\partial_w F(w^k)\right)_e, & \forall\, e \in E \\ \left(\mathbb{1} + \Delta t_k T k_w [\mathrm{Diag}(w^k)]\Delta^{LG}_{\frac{1}{\mu_w{}^k+\delta_{\mu_w}}}\right) w^{k+1} = \tilde{w}^k, & k = 0, \ldots, k_{\max}, e \in E \\ w_e^0 = w_{0e} > 0, & \forall\, e \in E. \end{cases}$$

With similar arguments one can also consider the following problem:

$$\min_{\substack{p' \in \mathcal{H}(E) \\ a_e \leq p'_e \leq b_e,\ e \in E \\ \mu \in \mathcal{H}(Y)^+}} F(p') + Tk_{p'} \sum_{y \in Y}\left(\frac{1}{2}\frac{|\nabla_{LG}\, p'|_y^2}{\mu_{p'y} + \delta_{\mu_{p'}}} + \frac{1}{2}\mu_{p'y}\right), \tag{1.5.44}$$

where again, $F : \mathcal{H}(E) \to \mathbb{R}$ is a sufficiently smooth map.
In this example we have an interval constraint on the variable p' for any edge

$e \in E$. This kind of constraint can be treated in a similar way to the positivity constraint as in the previous example, composing with the flux generated by a sigmoidal vector field and considering the Lie derivative along that flux or equivalently by composing with the change of variable:

$$p'_e(t) = a_e + (b_e - a_e)\cos^2\left(\frac{\varepsilon_e(t)}{\sqrt{b_e - a_e}}\right), \quad e \in E,$$

and then performing a pull-back of the descending dynamics on the original variable p'. We refer to Chapter 2 Subsection 2.8.2 for full details on the heuristics behind this techniques.
The positivity constraint for the density $\mu_{p'}$ is treated as for (1.5.42) by composing with the quadratic map $\mu_{p'}(t) = |\xi(t)|^2$.
Thus we have the following descending dynamics for (1.5.44):

$$\begin{aligned}
\sigma_{{p'}_y}(t) &= \frac{(\nabla_{LG}\, p'(t))_y}{{\mu_{p'}}_y(t) + \delta_{\mu_{p'}}}, \quad \forall\, y \in Y,\\
\partial_t {\mu_{p'}}_y(t) &= {\mu_{p'}}_y(t)|{\sigma_{p'}}_y(t)|^2 - {\mu_{p'}}_y(t), \quad \forall\, y \in Y,\\
{\mu_{p'}}_y(0) &= {\mu_{p'}}_{0y} > 0, \quad \forall\, y \in Y,\\
\partial_t p'_e(t) &= \left(b_e - p'_e(t)\right)\left(p'_e(t) - a_e\right)\left(-\partial_{p'_e} F(p'(t)) - T k_{p'}(\Delta^{LG}_{\frac{1}{\mu_{p'}(t)+\delta_{\mu_{p'}}}} p'(t))_e\right), \quad \forall\, e \in E,\\
{p'}_e(0) &= {p'}_{0e} > 0,\ a_e < {p'}_{0e} < b_e, \quad \forall\, e \in E.
\end{aligned}$$

where as in (1.5.43):

$$\Delta^{LG}_{\frac{1}{\mu_{p'}(t)+\delta_{\mu_{p'}}}} := \nabla^T_{LG}\,\mathrm{Diag}\left(\frac{1}{\mu_{p'}(t) + \delta_{\mu_{p'}}}\right)\nabla_{LG}, \quad \forall\, t \geq 0.$$

Defining the vectors $\mathtt{a} \in \mathcal{H}(E)$ and $\mathtt{b} \in \mathcal{H}(E)$ as:

$$\mathtt{a}_e = a_e,\ \forall\, e \in E,$$

and

$$\mathtt{b}_e = b_e,\ \forall\, e \in E,$$

the corresponding semi-implicit Proximal Forward-Backward Splitting scheme reads as follows:

$$\begin{cases} {p'}_y^k = \dfrac{(\nabla_{LG}\, p'^k)_y}{{\mu_{p'}}_y^k + \delta_{\mu_{p'}}}, & \forall\, y \in Y \\ {\mu_{p'}}_y^{k+1} = {\mu_{p'}}_y^k + \Delta t_k({\mu_{p'}}_y^k)\left(|{\sigma_{p'}}_y^k|^2 - 1\right), & k = 0, \dots, k_{\max}, y \in Y \\ {\mu_{p'}}_y^0 = {\mu_{p'}}_{0y} > 0, & \forall\, y \in Y \\ \tilde{p'}_e^k = {p'}_e^k - \Delta t_k \left([\mathrm{Diag}((\mathtt{b} - p'^k) \odot (p'^k - \mathtt{a}))]\partial_{p'} F(p'^k)\right)_e, & \forall\, e \in E \\ \left(\mathbb{1} + \Delta t_k T k_{p'}[\mathrm{Diag}((\mathtt{b} - p'^k) \odot (p'^k - \mathtt{a}))]\Delta^{LG}_{\frac{1}{{\mu_{p'}}^k + \delta_{\mu_{p'}}}}\right) p'^{k+1} = \tilde{p'}^k, & k = 0, \dots, k_{\max}, e \in E \\ {p'}_e^0 = {p'}_{0e},\ a_e < {p'}_{0e} < b_e, & \forall\, e \in E. \end{cases}$$

1.5.5 The Algorithm

In the Subsection 1.5.3 we have seen how to integrate our EDMK scheme for the p-Poisson problem, after an opportune regularization, to the solution of the primal equations (1.5.5), which are necessary to be solved, along with the adjoints equations (1.5.6) in order to compute the derivative of the Lagrangian in (1.5.4) with respect to the design parameters (p', w).
In Subsection 1.5.4 we have seen how to use our EDMK scheme for the Total Variation regularization which allows us to easily integrate the physical constraints on our design parameters. Moreover, upon introducing another further small regularization parameter, we show how to transform a Total Variation regularized minimization problem into a simplified and well approximated problem. We then provide two illustrative examples in (1.5.42) and (1.5.44) which will be used in the construction of our minimizing scheme for Problem (1).
We now give some insights on the main tools, providing also a summary of the main results shown in the previous sections. The main idea is to construct a descending dynamics scheme by using the EDMK scheme as the main tool to solve the primal equations along with the Total Variation regularization. We then propose an "all-in-one" descending scheme which is essentially based upon observing that we can interlace the EDMK scheme to compute an approximated descending iteration, given by not directly solving the primal equations, but rather updating in synchronization both the EDMK and a gradient descent for the variables (p', w).
We propose moreover to scale the variable w by a factor $\mathcal{O}(\frac{D}{L})$ where L is the length of the pipe and D the internal diameter as in the original momentum and mass balance equations (1.3.1), (1.3.2). This is useful to make w independent from the length of the pipe. So that, as in Section 1.3, we define the hogenization

edge weight $l \in \mathcal{H}(E)^+$ as:

$$l_e := \frac{C_e D_e}{L_e}, \quad \forall\, e \in E$$

where C is the roughness coefficient.
We will consider the following extended variational problem:

$$\min_{[p',w,\mu_{p'},\mu_w]} \min_{[H(V)_{:,j},Q(E)_{:,j}]} \max_{[\phi^j,\psi^j,\xi^j]} \mathcal{L}^{\delta,l}_{TV}(p', w, \mu_{p'}, \mu_w, H(V), Q(E), \Phi, \Psi, \Xi, Tk_{p'}, Tk_w, \delta_q, \delta_w, \delta_{\mu_{p'}}, \delta_{\mu_w}),$$

$$s.t. \quad \begin{aligned} 3.5 \geq p' &\geq 2.25, \\ w &\geq 0, \\ \mu_{p'} &\geq 0, \\ \mu_w &\geq 0, \end{aligned}$$

where the Lagrangian $\mathcal{L}^{\delta,l}_{TV}$ is essentially the same as in (1.5.41), with the only difference that we introduce the homogenization weight l as a scaling factor for w:

$$\begin{aligned} &\mathcal{L}^{\delta,l}_{TV}(p', w, \mu_{p'}, \mu_w, H(V), Q(E), \Phi, \Psi, \Xi, Tk_{p'}, Tk_w, \delta_q, \delta_w, \delta_{\mu_{p'}}, \delta_{\mu_w}) := \\ &= \mathcal{L}(p', w \odot l, H(V), Q(E), \Phi, \Psi, \Xi, \delta_q, \delta_w) + \\ &+ Tk_{p'} \sum_{y \in Y} \left(\frac{1}{2} \frac{|\nabla_{LG}\, p'|^2_y}{\mu_{p'y} + \delta_{\mu_{p'}}} + \frac{1}{2} \mu_{p'y} \right) + Tk_w \sum_{y \in Y} \left(\frac{1}{2} \frac{|\nabla_{LG}\, w|^2_y}{\mu_{wy} + \delta_{\mu_w}} + \frac{1}{2} \mu_{wy} \right), \end{aligned} \tag{1.5.45}$$

where $\mathcal{L}$ is the original Lagrangian defined in (1.5.4) that we used for the computation of the primal equations, the adjoints equations and consequently the derivative with respect of the design parameters (p', w).
Observe that in (1.5.45) we don't scale the variable w in the regularization term. This is due by the fact that indeed having scaled w in $\mathcal{L}$, which determines the constraint equations(or the physics of the WDS) is enough to make it "independent" from the length of the pipe. As a consequence, the regularization has to be applied without the scaling factor in order to benefit from the homogenization. The variable p' is naturally a dimensionless variable, therefore it doesn't need to be scaled by the length.
We refer to (1) and Subsection 1.5.1 for the definition of the variables $Q(E)$, $\overline{Q}(E_S)$, $H(V)$, $\overline{H}(B)$, $F(V_I)$, $\overline{F}(B)$, Φ, Ψ, Ξ which will be involved in what follows, while $Tk_{p'}$, Tk_w are the positive regularization(Tikhonov) parameters for the approximated Total Variation regularization and δ_q, δ_w, $\delta_{\mu_{p'}}$, δ_{μ_w} are also small strictly positive regularization parameters.
Let $q^j := Q(E)_{:,j} \in \mathcal{H}(E)$, $\bar{q}^j := \overline{Q}(E_S)_{:,j} \in \mathcal{H}(E_S)$, $h^j := H(V)_{:,j} \in \mathcal{H}(V)$, $\bar{h}^j := \overline{H}(B)_{:,j} \in \mathcal{H}(B)$, $f^j := F(V_I)_{:,j} \in \mathcal{H}(V_I)$, $\bar{f}^j := \overline{F}(B)_{:,j} \in \mathcal{H}(B)$, $\forall\, j = 1, \ldots, M$.
With the same arguments(we only have multiplied w by l) as in Subsection 1.5.1, we have that the primal equations(or the p-Poisson constraint equations) are

given by:

$$\begin{cases} (|q_e^j|^{p'_e-2}+\delta_q)q_e^j = -(w_e l_e+\delta_w)(\nabla h^j)_e, & \forall\, e\in E \\ -(\nabla^T q^j)_v = f_v^j, & \forall\, v\in V_I \\ h_v^j = \bar{h}_v^j, & \forall\, v\in B, \end{cases} \tag{1.5.46}$$

while the adjoint equations(or the Lagrange multipliers equations) are given by:

$$\begin{cases} ((p'_e-1)|q_e^j|^{p'_e-2}+\delta_q)\phi_e^j + (\nabla\,\psi^j)_e = q_e^j - \bar{q}_e^j, & \forall\, e\in E_S \\ ((p'_e-1)|q_e^j|^{p'_e-2}+\delta_q)\phi_e^j + (\nabla\,\psi^j)_e = 0, & \forall\, e\in E_I \\ -(\nabla^T(\mathrm{Diag}(w\odot l)+\delta_w\mathbb{1})\phi^j)_v = 0, & \forall\, v\in V_I \\ \psi_v^j = -\bar{f}_v^j - (q^j\cdot\vec{\nu})_v, & \forall\, v\in B. \end{cases} \tag{1.5.47}$$

Again, with the same arguments as in Subsection 1.5.1 we have that, once the solutions q^j, h^j, ϕ^j, ψ^j of the primal and adjoints equation are computed for any sampling time $j=1,\dots,m$, the derivative of $\mathcal{L}$ with respect of (p',w) are given by:

$$\frac{d}{dw_e}\mathcal{L} = \partial_{w_e}\mathcal{L} = -\sum_{j=1}^{M}\phi_e^j l_e(\nabla h^j)_e, \quad \forall\, e\in E,$$

$$\frac{d}{dp'_e}\mathcal{L} = \partial_{p'_e}\mathcal{L} = -\sum_{j=1}^{M}\phi_e^j \log(|q_e^j|)|q_e^j|^{p'_e-2}q_e^j, \quad \forall\, e\in E.$$

In subsection 1.5.2 we have introduced the intermediate variable

$$\mu^j\in\mathcal{H}(E)^+, \quad \forall\, j=1,\dots,m,$$
$$\mu_e^j := |q_e^j|^{p'_e-2}, \quad \forall\, e\in E,$$

which has the important role to formally reduce the primal equation into a weighted laplacian system.
Indeed, introducing the variable μ^j we have that equations (1.5.46) becomes:

$$\begin{cases} (\mu_e^j+\delta_q)q_e^j = -(w_e l_e+\delta_w)(\nabla h^j)_e, & \forall\, e\in E \\ -(\nabla^T q^j)_v = f_v^j, & \forall\, v\in V_I \\ h_v^j = \bar{h}_v^j, & \forall\, v\in B. \end{cases}$$

Since

$$(\mu_e^j+\delta_q) > 0, \quad \forall\, e\in E,$$

we have that formally:

$$q_e^j = -\frac{w_e l_e+\delta_w}{\mu_e+\delta_q}(\nabla h^j)_e, \quad \forall\, e\in E,$$

so that (1.5.46) is equivalent to the following(still non-linear) weighted laplacian system:

$$\begin{cases} \left(\nabla^T \operatorname{Diag}\left(\dfrac{w \odot l + \delta_w}{\mu^j + \delta_q}\right) \nabla h^j\right)_v = f_v^j, & \forall\, v \in V_I \\ h_v^j = \bar{h}_v^j, & \forall\, v \in B. \end{cases}$$

Moreover, if we introduce the variable $\tilde{q}^j$ such that:

$$\begin{cases} \tilde{q}_e^j = q_e^j - \bar{q}_e^j, & \forall\, e \in E_S \\ \tilde{q}_e^j = 0, & \forall\, e \in E_I, \end{cases}$$

then, from the first two equations in (1.5.47), we have that:

$$\phi_e^j = -\frac{(\nabla \psi^j)_e}{(p'_e - 1)\mu_e^j + \delta_q} + \frac{\tilde{q}_e^j}{(p'_e - 1)\mu_e^j + \delta_q},$$

Thus, the system of adjoint equations (1.5.47) is equivalent as well to the following weighted laplacian system in the variable ψ^j:

$$\begin{cases} (\nabla^T \operatorname{Diag}\left(\dfrac{w \odot l + \delta_w}{(p'-1)\mu^j + \delta_q}\right) \nabla \psi^j)_v = (\nabla^T \operatorname{Diag}\left(\dfrac{w \odot l + \delta_w}{(p'-1)\mu^j + \delta_q}\right) \tilde{q}^j)_v, & \forall\, v \in V_I \\ \psi_v^j = -\bar{f}_v^j - (q^j \cdot \vec{\nu})_v, & \forall\, v \in B. \end{cases} \tag{1.5.48}$$

The variable μ^j also appears in the derivative of $\mathcal{L}$ with respect to p'. Indeed from (1.5.8) we have:

$$\frac{d}{dp'_e}\mathcal{L} = -\sum_{j=1}^{M} \phi_e^j \log(|q_e^j|)|q_e^j|^{p'_e - 2} q_e^j = -\sum_{j=1}^{M} \phi_e^j \log(|q_e^j|) q_e^j \mu_e^j, \quad \forall\, e \in E.$$

It is clear that the variable μ^j plays the fundamental role to simplify all the computations. It naturally appears in the primal equations, in the adjoint equations and in the computation of the gradient for the variable p'. Moreover, in Subsection 1.5.3 we have presented an EDMK based "Gradient Flow" like approach to the solution of the primal equations which naturally involves the variable μ^j as an iterative linear solver, once opportunely time discretized.
The strategy is therefore to perform an "all-in-one" descending dynamics. This is reasonable to think as a kind of Picard iteration.
Thus, the descending algorithm will be initialized with an initial distribution of exponents $p'_0 \in \mathcal{H}(E)$, $2.25 < p'_0 < 3.5$, an initial distribution of weights $w_0 \in \mathcal{H}(E)^+$ and the derived primal and adjoint solutions $q^{j\,0}$, $h^{j\,0}$, $\phi^{j\,0}$, $\psi^{j\,0}$ computed solving the non-linear equations (1.5.46), (1.5.47) with the given initial distributions (p'_0, w_0) and our EDMK scheme.
Once initialized, the algorithm will follows a pseudo-descent dynamics, where instead of solving at every iteration the non-linear primal-adjoint equations for

the computation of the derivative of the extended regularized Lagrangian $\mathcal{L}^{\delta}_{TV}$, we will rather perform one integration step of the dynamics given by the EDMK scheme for the primal equations in (1.5.35):

$$\begin{aligned} q^j_e(t) &= -\frac{(w_e l_e + \delta_w)(\nabla h^j(t))_e}{{\mu^j}_e(t) + \delta_q}, \quad \forall\, e \in E \\ (\Delta_{\frac{w \odot l + \delta_w}{\mu^j(t) + \delta_q}} h^j(t))_v &= f^j_v, \quad \forall\, v \in V_I \\ h^j(t)_v &= \bar{h}^j_v \quad \forall\, v \in B \\ \partial_t \mu^j_e(t) = \mu^j_e(t)^{\frac{4-3p_e}{2-p_e}} |q^j_e(t)|^2 - \mu^j_e(t), &\quad \mu^j_e(0) = \mu^j_{0e} > 0, \quad \forall\, e \in E, \end{aligned} \tag{1.5.49}$$

where the initial value for μ^j, for any $j = 1, \dots, M$ in (1.5.49), is set to be equal to:

$$\mu^j_{0e} = |{q^j}^0_e|^{p'_e - 2}, \quad \forall\, e \in E$$

and $q^{j\,0}$ is the flux solution of the primal equations given by the initial distributions (p'_0, w_0).

This type of pseudo-gradient descent method has some reminiscents of the one introduced in [140].

If the Explicit Euler time discretization is used for (1.5.49) we have the following iterative scheme for the solution of the primal equations:

$$\begin{cases} (\Delta_{\frac{w \odot l + \delta_w}{{\mu^j}^k + \delta_q}} {h^j}^k)_v = 0, \quad \forall\, v \in V_I \\ {h^j}^k = \bar{h}^j_v, \quad \forall\, v \in B \\ {q^j}^k_e = \dfrac{(w_e l_e + \delta_w)(\nabla {h^j}^k)_e}{{\mu^j}^k + \delta_q}, \quad \forall\, e \in E \\ {\mu^j}^{k+1}_e = {\mu^j}^k_e + \Delta t_k \left(({\mu^j}^k_e)^{\frac{4-3p_e}{2-p_e}} |{q^j}^k_e|^2 - {\mu^j}^k_e \right), \quad k = 0, \dots, k_{\max}, e \in E \\ {\mu^j}^0_e = {\mu^j}_{0e} > 0, \quad \forall\, e \in E. \end{cases} \tag{1.5.50}$$

Thus, instead to compute a full solution of the primal equations which corresponds to a steady state for (1.5.49), in the case where the explicit time discretization in (1.5.50) is used, we only need to solve for a weighted laplacian system to compute the new approximated density ${\mu^j}^{k+1}$.

With the same arguments, once the solution of the linear adjoint equations (1.5.48) given by the previous approximated density ${\mu^j}^k$ is computed, we can also compute an approximated descent direction(gradient) for the variables (p', w). In this way we have all the ingredients for an iterative(approximated) gradient descent approach to the computation of the minimizing weights and exponents distribution.

The reason behind this choice, a part from the numerical benefit to solve for a linear system instead of a non-linear equation, is essentially motivated by the fact

that the dynamics in (1.5.49) admits the strictly convex Lyapunov functional $\mathcal{L}^{w,p}_{\delta_w,\delta_q}$ defined in (1.5.34), hence the updating scheme converges to a solution independently from the initial guess(starting point). As a consequence, we are expecting that an iterative algorithm constructed in such a manner, will converge to a solution if a sufficiently small initial time step is provided. Thus, initially we still get a reasonably good approximation of the p-Poisson equation and the approximated descent direction is not affected so much by the error derived by not solving well the primal equations.
Once the minimization process starts to be near to a local minima, intuitively the changing velocity of the approximated candidate minimizer at iteration k, (p'^k, w^k), will slow down and the dynamics given by the EDMK scheme will synchronizes as well, converging to a good approximated solution of the primal equations.
For what concern the Total Variation regularization, observe that we are in the same situation of examples (1.5.42), (1.5.44). Summing up all together, the algorithm is composed by two parts:

- **Initialization**: Given an initial distribution of exponents and weights such that $2.25 < p'_{0e} < 3.5$, $w_{0e} \geq 0$, $\forall\, e \in E$, we compute a well approximated solution $(q^{j\,0}, h^{j\,0})$, of the primal equations (1.5.46) with the EDMK scheme (1.5.50) and a solution $(\phi^{j\,0}, \psi^{j\,0})$ of the adjoint equations (1.5.47), relative to the initial distribution (p'_0, w_0), for any $j = 1, \ldots, M$.
  A practical method to select an initial distribution of parameters is to fix the initial exponent
  $$p'_{0e} = 2.8524, \quad \forall\, e \in E,$$
  as a good empirical guess given by the Hazen-Williams formula(see [1]), and to fix a value $\tilde{w}_0 > 0$ such that:
  $$w_{0e} := \tilde{w}_0, \quad \forall\, e \in E, \tag{1.5.51}$$
  where the parameter $\tilde{w}_0$ is computed by performing a dichotomic search until we find the value which reasonable minimizes the relative error between the sampled boundary demand $\tilde{f}^j_v$ and the initial Dirichlet-to-Neumann map $-(q^j_0 \cdot \vec{\nu})_v$, for any $v \in B$.
  We observed experimentally that it is not important the precise value of $\tilde{w}_0 > 0$ but rather the order of magnitude.
  Since Problem (1) is not convex, we point out that this initialization process is of fundamental importance for the performances and the stability of the algorithm.
  Other two fundamental parameters to be carefully setted are the regularization parameters $(Tk_w, Tk_{p'})$. There are various techniques in order to proper determine the regularization parameters. For the interested reader we refer to [14, 26, 30, 69].

- **Minimizing flow**: The full descending "all-in-one" scheme reads as an opportune time discretization of the following dynamics:

$$
\begin{aligned}
&\text{——————— } \textbf{primal} \text{ ———————} \\
&\qquad\qquad \forall\, j = 1, \dots, M, \\
q_e^j(t) &= -\frac{(w_e l_e + \delta_w)(\nabla\, h^j(t))_e}{{\mu^j}_e(t) + \delta_q}, \quad \forall\, e \in E \\
\left(\nabla^T \operatorname{Diag}\left(\frac{w(t) \odot l + \delta_w}{\mu^j(t) + \delta_q}\right) \nabla\, h^j(t)\right)_v &= f_v^j, \quad \forall\, v \in V_I \\
h^j(t)_v &= \bar{h}_v^j \quad \forall\, v \in B \\
\partial_t \mu_e^j(t) &= \mu_e^j(t)^{\frac{4-3p_e(t)}{2-p_e(t)}} |q_e^j(t)|^2 - \mu_e^j(t), \quad \forall\, e \in E \\
\mu_e^j(0) &= \mu_{0e}^j > 0, \quad \forall\, e \in E \\
&\text{——————— } \textbf{adjoint} \text{ ———————} \\
&\qquad\qquad \forall\, j = 1, \dots, M, \\
\tilde{q}_e^j(t) &= q_e^j(t) - \bar{q}_e^j, \quad \forall\, e \in E_S \\
\tilde{q}_e^j(t) &= 0, \quad \forall\, e \in E_I \\
\phi_e^j(t) &= -\frac{(\nabla\, \psi^j(t))_e}{(p_e'(t) - 1)\mu_e^j(t) + \delta_q} + \frac{\tilde{q}_e^j(t)}{(p_e'(t) - 1)\mu_e^j(t) + \delta_q}, \quad \forall\, e \in E \\
&\begin{aligned}(\nabla^T \operatorname{Diag}\left(\frac{w(t) \odot l + \delta_w}{(p'(t) - 1)\mu^j(t) + \delta_q}\right) \nabla\, \psi^j(t))_v = \\ = (\nabla^T \operatorname{Diag}\left(\frac{w(t) \odot l + \delta_w}{(p'(t) - 1)\mu^j(t) + \delta_q}\right) \tilde{q}^j(t))_v\end{aligned}, \quad \forall\, v \in V_I \\
\psi_v^j(t) &= -\bar{f}_v^j - (q^j(t) \cdot \vec{\nu})_v, \quad \forall\, v \in B \\
&\text{——————— } \textbf{w: descent + } \mathbf{TV}_\delta \text{ ———————} \\
\sigma_{wy}(t) &= \frac{(\nabla_{LG}\, w(t))_y}{\mu_{wy}(t) + \delta_{\mu_w}}, \quad \forall\, y \in Y \\
\partial_t \mu_{wy}(t) &= \mu_{wy}(t)|\sigma_{wy}(t)|^2 - \mu_{wy}(t), \quad \forall\, y \in Y \\
\mu_{wy}(0) &= \mu_{w0y} > 0, \quad \forall\, y \in Y
\end{aligned}
\tag{1.5.52}
$$

$$\partial_t w_e(t) = w_e(t)\left(\sum_{j=1}^{M}\phi_e^j(t) l_e(\nabla h^j(t))_e - Tk_w(\Delta^{LG}_{\frac{1}{\mu_w(t)+\delta_{\mu_w}}} w(t))_e\right), \quad \forall\, e\in E$$

$$w_e(0) = w_{0e} > 0, \quad \forall\, e\in E$$

p': descent + TV$_\delta$

$$\sigma_{p'y}(t) = \frac{(\nabla_{LG}\, p'(t))_y}{\mu_{p'y}(t)+\delta_{\mu_{p'}}}, \quad \forall\, y\in Y,$$

$$\partial_t \mu_{p'y}(t) = \mu_{p'y}(t)|\sigma_{p'y}(t)|^2 - \mu_{p'y}(t), \quad \forall\, y\in Y,$$

$$\mu_{p'y}(0) = \mu_{p'0y} > 0, \quad \forall\, y\in Y,$$

$$\partial_t p'_e(t) = \left(3.5 - p'_e(t)\right)\left(p'_e(t) - 2.5\right)\left(\sum_{j=1}^{M}\phi_e^j(t)\log(|q_e^j(t)|)q_e^j(t)\mu_e^j(t) + -Tk_{p'}(\Delta^{LG}_{\frac{1}{\mu_{p'}(t)+\delta_{\mu_{p'}}}} p'(t))_e\right), \quad \forall\, e\in E,$$

$$p'_e(0) = p'_{0e} > 0,\ a_e < p'_{0e} < b_e, \quad \forall\, e\in E.$$

We propose the following semi implicit time discretization for (1.5.52), which is essentially the union of the schemes in (1.5.50) and examples (1.5.42), (1.5.44). Thus given a sequence of time steps Δt_k, $k = 0,\dots,k_{\max}$, the approximated sequence of solutions $(p'^k, w^k, \mu_w{}^k, \mu_{p'}{}^k, \mu^{jk}, q^{jk}, h^{jk}, \phi^{jk}, \psi^{jk})$, is computed with the following recurrent scheme:

(1.5.53)

primal

$$\forall\, j = 1,\dots,M,$$

$$q^{jk}_e = \frac{(w_e^k l_e + \delta_w)(\nabla h^{jk})_e}{\mu^{jk}+\delta_q}, \quad \forall\, e\in E$$

$$\left(\nabla^T \operatorname{Diag}\left(\frac{w^k\odot l + \delta_w}{\mu^{jk}+\delta_q}\right)\nabla h^{jk}\right)_v = 0, \quad \forall\, v\in V_I$$

$$h^{jk} = \bar{h}^j_v, \quad \forall\, v\in B$$

$$\mu^{jk+1}_e = \mu^{jk}_e + \Delta t_k\left((\mu^{jk}_e)^{\frac{4-3p_e^k}{2-p_e^k}}|q^{jk}_e|^2 - \mu^{jk}_e\right), \quad \forall\, e\in E$$

$$\mu^{j}{}_{e}^{0} = \mu^{j}{}_{0e} > 0, \quad \forall\, e \in E$$

adjoint

$$\forall\, j = 1, \dots, M,$$

$$\tilde{q}_e^{j\,k} = q_e^{j\,k} - \bar{q}_e^{j}, \quad \forall\, e \in E_S$$

$$\tilde{q}_e^{j\,k} = 0, \quad \forall\, e \in E_I$$

$$\phi_e^{j\,k} = -\frac{(\nabla\, \psi^{j\,k})_e}{(p'_e{}^{k} - 1)\mu_e^{j\,k} + \delta_q} + \frac{\tilde{q}_e^{j\,k}}{(p'_e{}^{k} - 1)\mu_e^{j\,k} + \delta_q}, \quad \forall\, e \in E$$

$$\begin{aligned}(\nabla^T \operatorname{Diag}\left(\frac{w^k \odot l + \delta_w}{(p'^{k} - 1)\mu^{j\,k} + \delta_q}\right) \nabla\, \psi^{j\,k})_v = \\ = (\nabla^T \operatorname{Diag}\left(\frac{w^k \odot l + \delta_w}{(p'^{k} - 1)\mu^{j\,k} + \delta_q}\right) \tilde{q}^{j\,k})_v\end{aligned}, \quad \forall\, v \in V_I$$

$$\psi_v^{j\,k} = -\bar{f}_v^{j} - (q^{j\,k} \cdot \vec{\nu})_v, \quad \forall\, v \in B$$

w: descent + TV$_\delta$

$$\sigma_{w\,y}^{\;k} = \frac{(\nabla_{LG}\, w^k)_y}{\mu_{w\,y}^{\;k} + \delta_{\mu_w}}, \quad \forall\, y \in Y$$

$$\mu_{w\,y}^{\;k+1} = \mu_{w\,y}^{\;k} + \Delta t_k(\mu_{w\,y}^{\;k}) \left(|\sigma_{w\,y}^{\;k}|^2 - 1\right), \quad \forall\, y \in Y$$

$$\mu_{w\,y}^{\;0} = \mu_{w0y} > 0, \quad \forall\, y \in Y$$

$$b_{w\,e}^{\;k} = w_e^k + \Delta t_k([\operatorname{Diag}(w^k)] \sum_{j=1}^{M} \phi^{j\,k} \odot l \odot \nabla\, h^{j\,k})_e, \quad \forall\, e \in E$$

$$\left(\mathbb{1} + \Delta t_k T k_w [\operatorname{Diag}(w^k)] \Delta \frac{LG}{\frac{1}{\mu_w{}^{k} + \delta_{\mu_w}}}\right) w^{k+1} = b_w{}^{k}, \quad \forall\, e \in E$$

$$w_e^0 = w_{0e} > 0, \quad \forall\, e \in E$$

p': descent + TV$_\delta$

$$\sigma_{p'\,y}^{\;k} = \frac{(\nabla_{LG}\, p'^{k})_y}{\mu_{p'\,y}^{\;k} + \delta_{\mu_{p'}}}, \quad \forall\, y \in Y$$

$$\mu_{p'\,y}^{\;k+1} = \mu_{p'\,y}^{\;k} + \Delta t_k(\mu_{p'\,y}^{\;k}) \left(|\sigma_{p'\,y}^{\;k}|^2 - 1\right), \quad \forall\, y \in Y$$

$$\mu_{p'\,y}^{\;0} = \mu_{p'0y} > 0, \quad \forall\, y \in Y$$

$$
\begin{aligned}
&{b_{p'}}_e^k = {p'}_e^k + \\
&- \Delta t_k \left(\left[\mathrm{Diag}((3.5 - p'^k) \odot (p'^k - 2.25)) \right] \sum_{j=1}^{M} \phi^{jk} \odot \log(|q^{jk}|) \odot q^{jk} \odot \mu^{jk} \right)_e, \quad \forall\, e \in E \\
&\left(\mathbb{1} + \Delta t_k T k_{p'} [\mathrm{Diag}((3.5 - p'^k) \odot (p'^k - 2.25))] \Delta \frac{LG}{\frac{1}{{\mu_{p'}}^k + \delta_{\mu_{p'}}}} \right) p'^{k+1} = {b_{p'}}^k, \quad \forall\, e \in E \\
&{p'}_e^0 = {p'}_{0e}, \quad \forall\, e \in E \\
&2.25 < {p'}_{0e} < 3.5, \quad \forall\, e \in E.
\end{aligned}
$$

A stopping criteria must be chosen to terminate the algorithm. In our numerical examples we will use the relative error stopping criteria. Indeed, when the **Initialization** process is done, we choose a stopping tolerance ε and let evolve the iterative scheme in (1.5.53) until:

$$
\max \left\{ \frac{\|\mu^{jk+1} - \mu^{jk}\|_{l_2}}{\Delta t_k \|\mu^{jk}\|_{l_2}}, \frac{\|\mu_w^{k+1} - \mu_w^k\|_{l_2}}{\Delta t_k \|\mu_w^k\|_{l_2}}, \frac{\|w^{k+1} - w^k\|_{l_2}}{\Delta t_k \|w^k\|_{l_2}}, \frac{\|\mu_{p'}^{k+1} - \mu_{p'}^k\|_{l_2}}{\Delta t_k \|\mu_{p'}^k\|_{l_2}}, \frac{\|p'^{k+1} - p'^k\|_{l_2}}{\Delta t_k \|p'^k\|_{l_2}} \right\} < \varepsilon. \tag{1.5.54}
$$

We point out that other far more performing numerical schemes can be developed for the time discretization of the flow in (1.5.52), for example the Nesterov/Beck and Teboulle's acceleration [13] and the Implicit Euler scheme. This will be surely a matter of future development. Nevertheless, good results can also be obtained with the proposed scheme(which is quite simple to implement), once a sufficiently small initial time step is provided. For example a good empirical time stepping method is the following:

$$
\begin{gathered}
0 < \Delta t_0 << 1, \\
0 < \alpha << 1, \\
\Delta t_{k+1} = (1 + \alpha) \Delta t_k, \quad k = 0, \ldots, k_{max}, \\
if \;\; \Delta t_{k+1} > \Delta_{max} \;\; then \;\; \Delta t_{k+1} = \Delta_{max},
\end{gathered}
$$

where the parameters $(\alpha, \Delta t_0, \Delta_{max})$ have to be carefully selected to avoid instabilities and possibly the failure of the convergence.

1.6 Numerical experiments

We conclude this chapter with some numerical experiments on a synthetic EPANET WDS which corresponds to the digitalization of a real world test case. In particular, the test case is given by a portion of the WDS which supplies the area near the city of Treviso, in North-East Italy. The model is composed by 204 nodes and 214 edges and it is depicted in Figure (1.4). All pipes in the network are

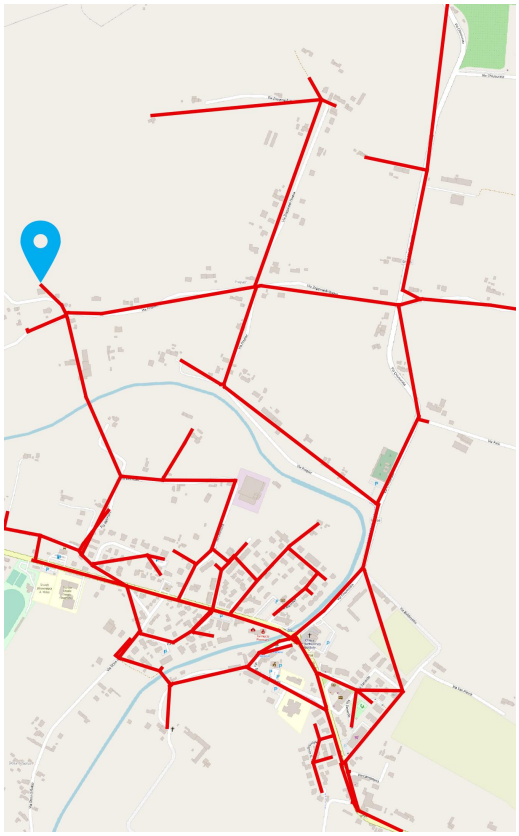

Figure 1.4: Test case WDS on the street map. The blue marker on the left highlights the tank position.

constructed using diverse materials such as steel, cast iron, concrete, or plastic and have varying diameters. The entire network is supplied by a single tank situated in the center left position (as identified by the blue marker in Figure 1.4). An EPANET model is used, which has a demand distribution that is calibrated by previous measurements to accurately reproduce the user's daily consumption. In our numerical experiments, we optimize the network with only one sampling measurement ($M = 1$). This is ultimately done for the purpose of achieving clear numerical results. When both parameters (p', w) are used in the minimization, using a single measurement may result in several local minimizers as there are many degrees of freedom. As such, we will present two separate results obtained through varying sampling strategies while keeping the exponent fixed and equal to

$$p'_e = 2.8524, \quad \forall\, e \in E,$$

as a good empirical found value(Hazen-Williams formula). Then we will present a third test case that is identical to the first one, where we also optimize the parameter p'. In all three tests, we calculate the optimal w using the method de-

scribed in equations (1.5.53). Despite having only one measurement, we observe the beneficial impact of TV regularization in selecting a locally constant distribution of weights (and exponents in the third test) that can accurately replicate the missing heads and fluxes data. Additionally, it is evident that the weight distribution remains consistent across all three test cases when utilizing various sampling strategies. As a result, it can be suggested that the TV regularization approach selects "good local minima".

- **Test case 1. house service meters bad scenario**:
  In this test case we consider an house service meters bad scenario where the demand on the sampling nodes is very small, in average 1 liter per minute. We suppose to have at disposal a single time measurement $M = 1$, and to get available data only on the external nodes of the WDS, i.e. on the 37 leaves of the graphs and on the source node, which is the only tank. Thus the boundary nodes B are composed by the leaves of the graph where we know as collected data the sampling demand and the piezometric head. No flux data are considered and no information is given on the internal nodes except for the calibrated user demand distribution. The initialization process is carried out by setting an initial fixed weight

  $$\tilde{w}_0 = 1e-2,$$

  as in (1.5.51).
  We then set a fixed time step

  $$\Delta t_k = 1e-1,\ k = 0, \dots, k_{max},$$

  and the regularization parameters δ

  $$\delta_q = \delta_w = \delta_{\mu_w} = 1e-8.$$

  We empirically find that a good compromise is to set the TV regularization parameter to

  $$Tk_w = 1e-5.$$

  Since we fix the exponent p' we don't need the regularization parameters $\delta_{\mu_{p'}}$ and $Tk_{p'}$.

  Finally we set a stopping tolerance $\varepsilon = 1e-6$ for the relative error stopping criteria in Equation (1.5.54).

  Surprisingly, even if the time measurement is only one and we don't have any internal node data, the Total Variation regularization works very well, choosing a suitable w that can reproduce the missing measurements quite well. As expected, since the demand data is proximal to be irrelevant, most of the error is committed in reproducing the internal fluxes, which are proximal to be zero, and nothing is known to synchronize the model on these edges.

In Figure 1.5 we can see the optimal weights distribution computed with our EDMK based scheme (1.5.53), where it is evident the regularizing (BV clustering) effect induced by the TV regularization. In Figures 1.6 and 1.7 we can see the comparison between the piezometric heads and fluxes computed with EPANET, considered the "real" reference values, and the simulated or reconstructed ones computed with our scheme for the given resulting optimal weight.

- **Test case 2. Divergence kernel avoiding scenario**:

  In this test case we consider the same demand distribution and sampling data as in Test case 1, with the same single time measurement $M = 1$. The difference is the sampling strategy. In this case we assume that we have the demand, the piezometric head, and the fluxes incident on the source node (the tank) and on each node with a topological degree greater than 2. As a result, the boundary sampling set B is composed of 54 nodes. As already observed in Subsection 1.5.2, this sampling strategy is optimal in the sense that it avoids in principle the lack of information on the loops of the graph (which corresponds to the kernel of the divergence matrix), thus inducing the optimality condition (1.5.15) to be satisfied. The initialization process is carried out as in Test case 1, with the same initial value distribution for the weight w, the same time step, the same regularization parameters "δ", Tk_w and the same stopping tolerance $\varepsilon = 1e-6$ for the relative error stopping criteria in (1.5.54).

  It is worth noting that we have more data in this test case. As a result, we have a much better reconstruction of the fluxes at the internal edges. In Figure 1.8 we can see the optimal weights distribution computed with our EDMK based scheme (1.5.53), where also in this case we can see the regularization effect induced by the TV regularization. In Figures 1.9, 1.10 we can see the comparison between the "real" piezometric heads and fluxes computed with EPANET and the simulated or reconstructed ones computed with our scheme for the given resulting optimal weight. In Figure 1.11 we can see the comparison between the optimal weights distribution for Test case 1 and Test case 2. We can also see the coherent increasing localization of the optimal weight given by Test case 2, where more data is available for solving the inverse problem.

- **Test case 3. Test case 1+ p'**:

  In this test case we consider the same exactly scenario and data of Test case 1, with the difference that we optimize also in the parameter p'. The initialization process is carried out exactly as in Test case 1, with the same time step, "δ" regularization parameters, initial weights distribution and initial exponents distribution, set as the fixed p' as in Test case 1, i.e.:

$$p'_{0e} = 2.8524, \quad \forall\, e \in E.$$

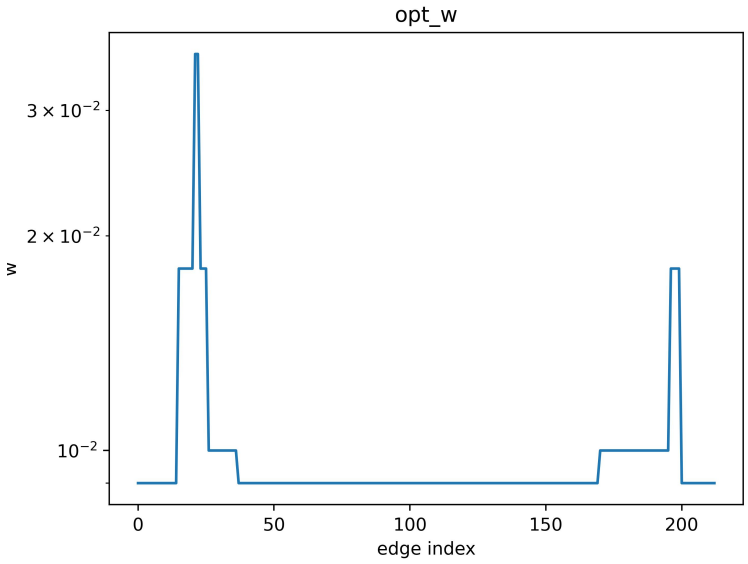

(a)

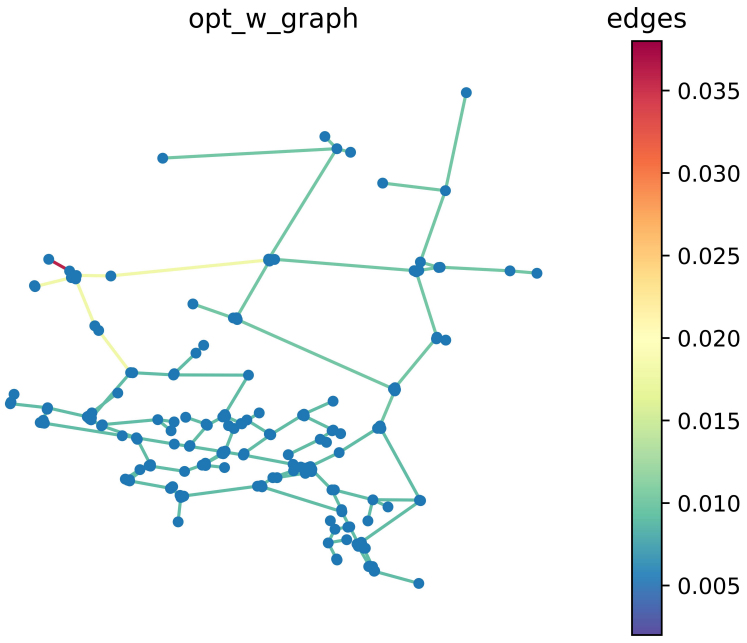

(b)

Figure 1.5: Test case 1, (a): optimal weight vs edge index (b) optimal weight distribution on the graph

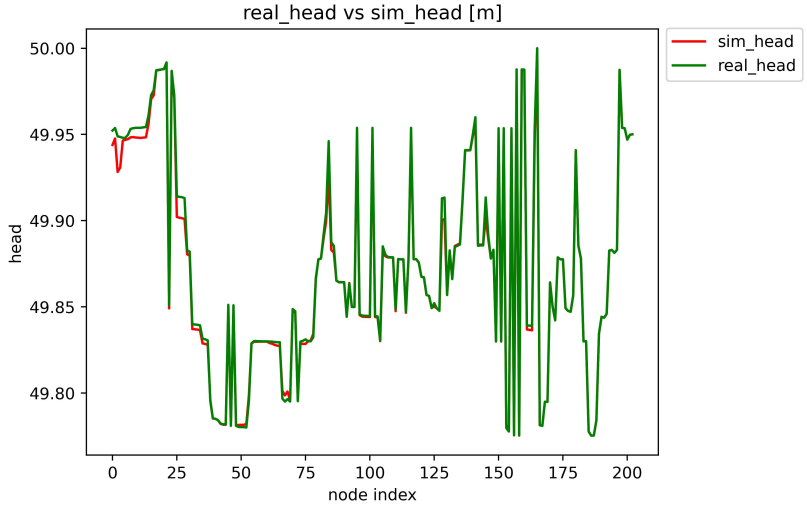

(a)

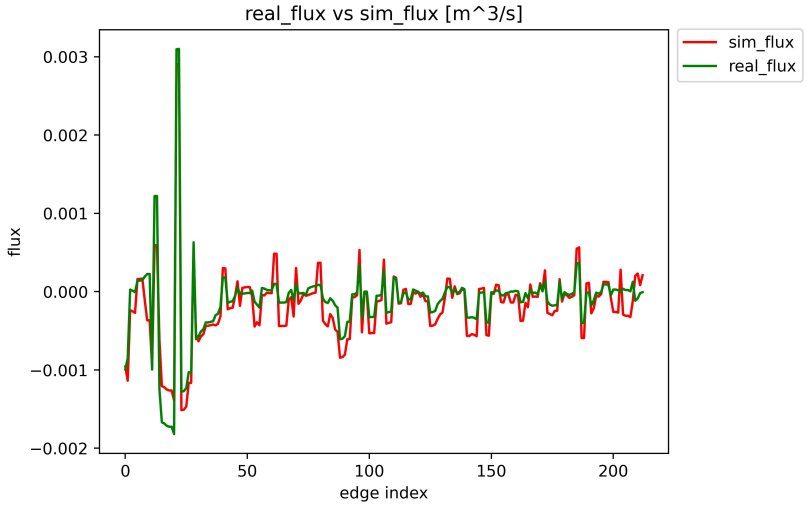

(b)

Figure 1.6: Test case 1, (a): real (EPANET) piezometric head(green) VS simulated piezometric head (red) (b) real (EPANET) flux(green) VS simulated flux (red)

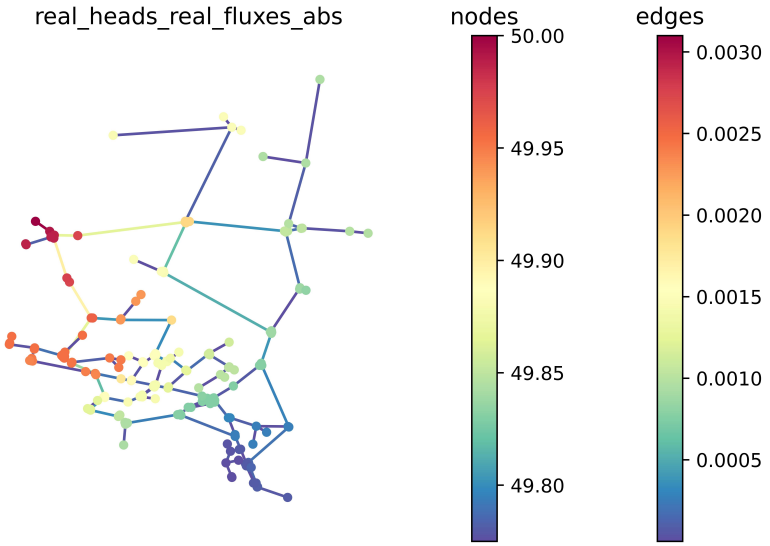

(a)

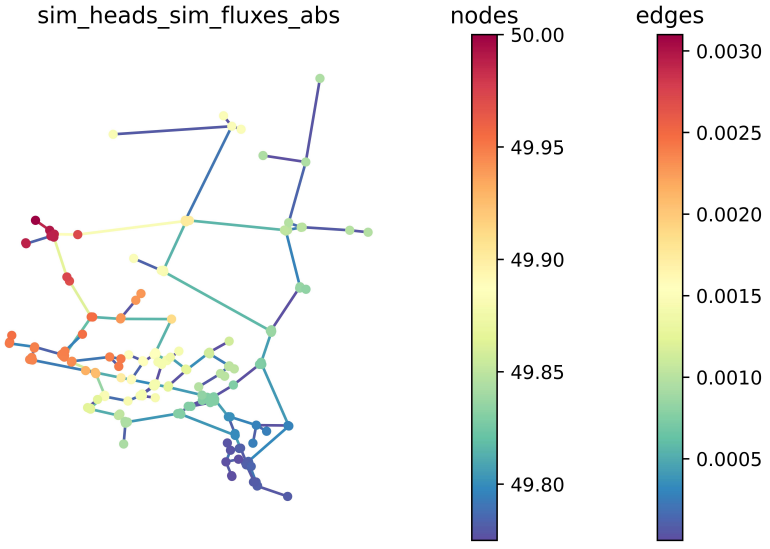

(b)

Figure 1.7: Test case 1, (a): real(EPANET) heads[m] and fluxes[m^3/s] in absolute value VS (b): simulated(reconstruction) heads[m] and fluxes[m^3/s] in absolute value

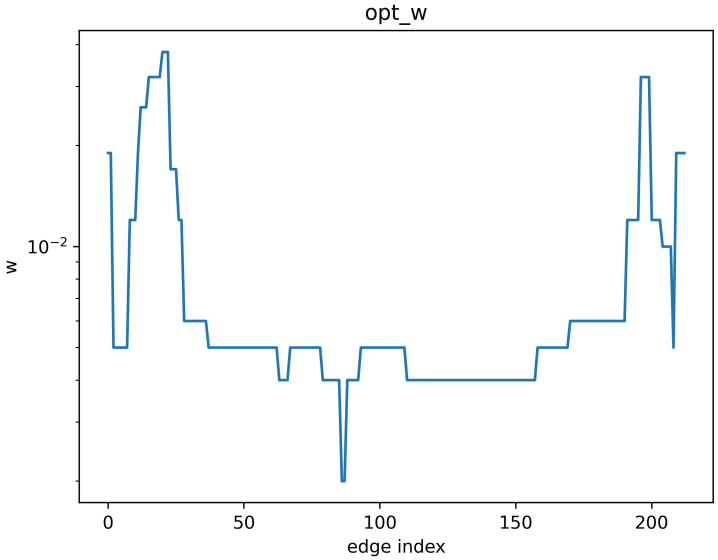

(a)

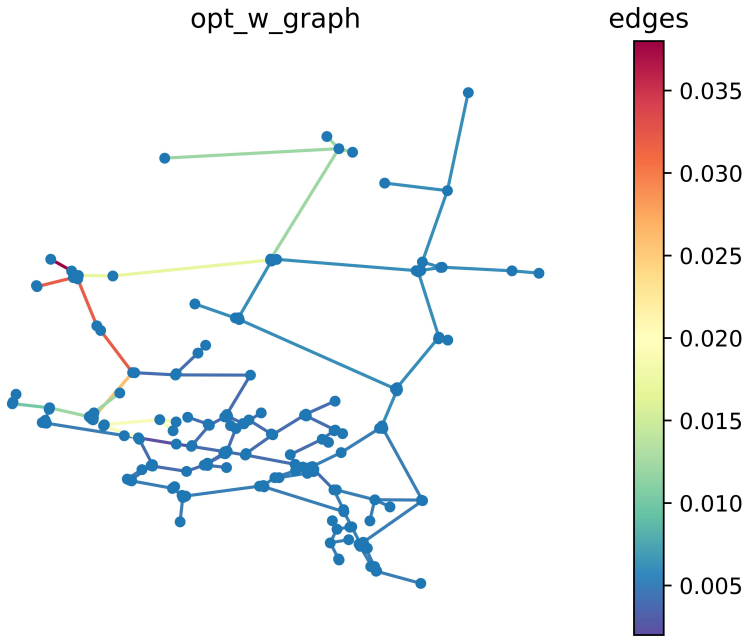

(b)

Figure 1.8: Test case 2, (a): optimal weight vs edge index (b) optimal weight distribution on the graph

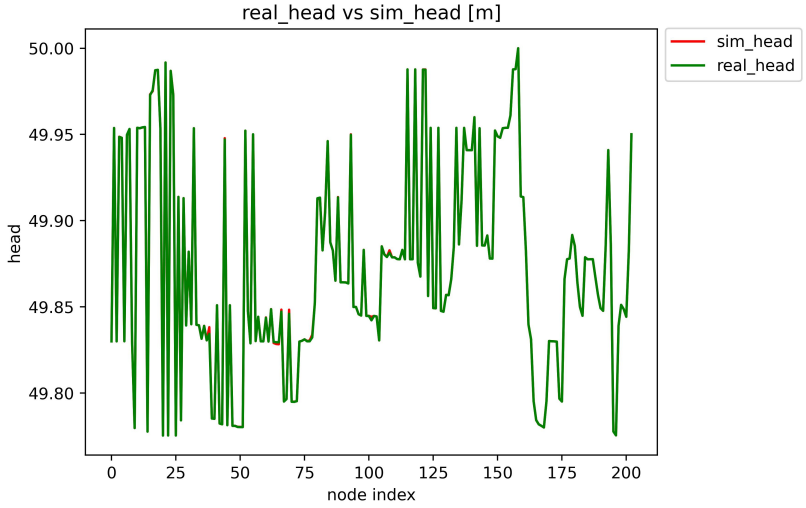

(a)

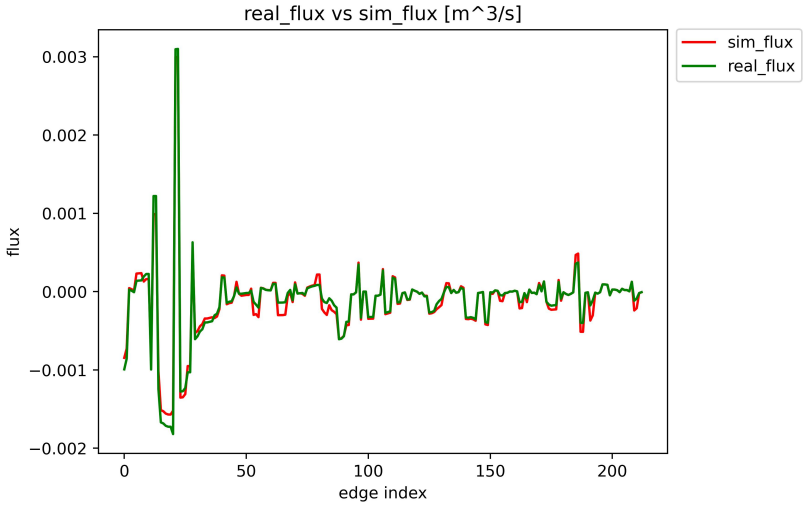

(b)

Figure 1.9: Test case 2, (a): real(EPANET) piezometric head(green) VS simulated piezometric head(red)
(b) real(EPANET) flux(green) VS simulated flux(red)

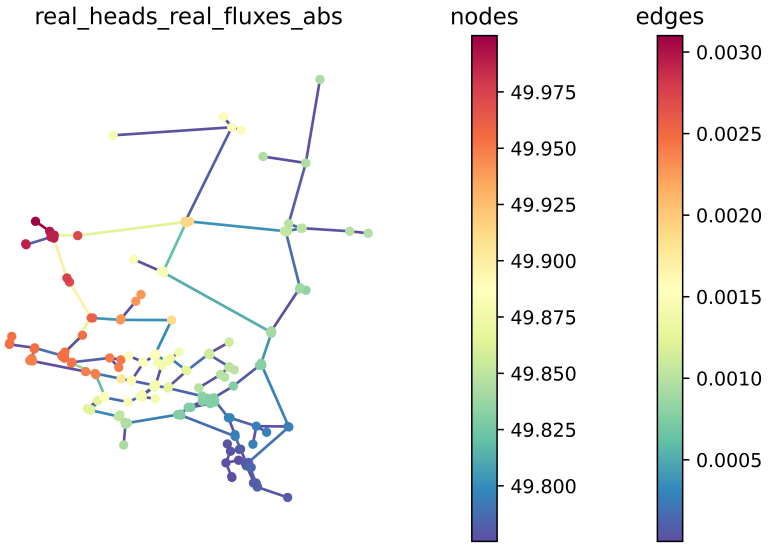

(a)

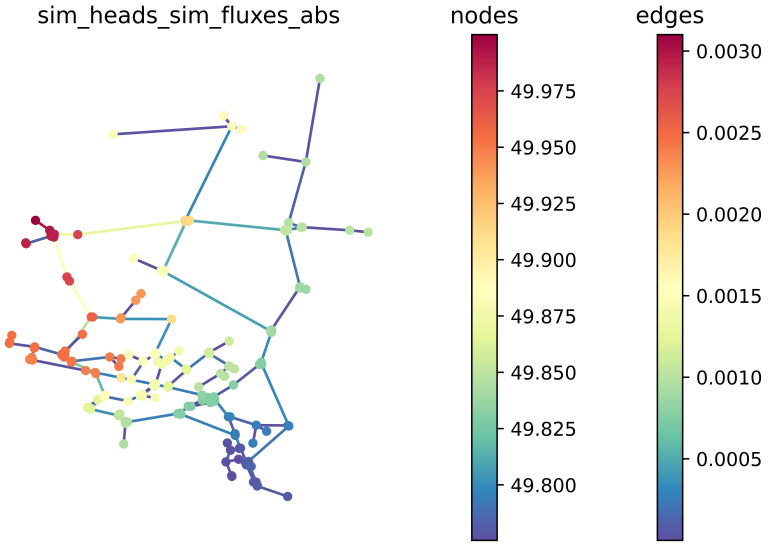

(b)

Figure 1.10: Test case 2, (a): real (EPANET) heads[m] and fluxes[m^3/s] in absolute value VS (b): simulated (reconstruction) heads[m] and fluxes [m^3/s] in absolute value

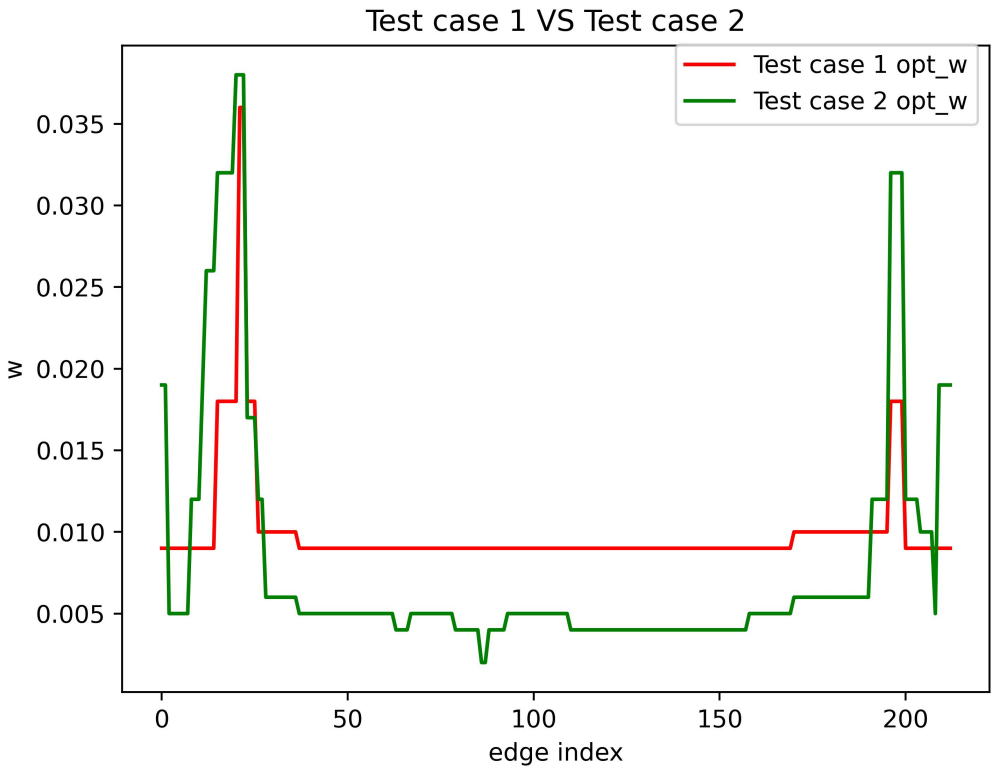

Figure 1.11: optimal weights distribution for Test case 1(red) vs Test case 2(green)

In order to make the optimization in the further parameter p' effective, we relaxed a bit the Tikhonov regularization parameters and we set

$$Tk_w = 5e - 6,$$

and

$$Tk_{p'} = 5e - 6.$$

This is necessary to ensure that the parameter p' can evolve far enough from the initial distribution p'_0 to achieve effective evolution, although the latter already provides a good approximation.

Finally we set a stopping tolerance $\varepsilon = 1e-6$ for the relative error stopping criteria in (1.5.54). Surprisingly, even with just one time measurement, we can accurately compute both the exponent and weight distributions, which reflect a spatial distribution similar to that of Test case 1. Additionally, the approximations of the missing internal fluxes are slightly better compared to Test case 1. With such limited data, it is not feasible to expect a significant increase in precision with the moving parameter p'.

In Figure 1.12 we can see the optimal weights distribution computed with our EDMK based scheme (1.5.53). The most remarkable difference with respect to Test case 1, is that this new computed optimal weights distribution exhibits a "peak" in the center, which corresponds to the edge with the smallest flux of the entire WDS. This result is notable, given that the edge in question is internal and there was no data on sampled heads and fluxes in its immediate proximal vicinity. In Figure 1.13 we can see the computed optimal exponents distribution. It is evident that the magnitude differences between the optimal weights of Test case 1 and Test case 3 are compensated by the distribution of the exponents p', which is "synchronized" with the distribution of the weights. In Figures 1.14 and 1.15 we can see the comparison between the "real" piezometric heads and fluxes computed with EPANET and the simulated or reconstructed ones computed with our scheme for the given resulting optimal weight and optimal exponent. Additionally, Figure 1.14 displays a comparison of the actual flux, the simulated flux in Test case 1, and the simulated flux in Test case 3. Figure 1.16 presents a comparison of the optimal weights for each test case. Additionally, Figure 1.17 depicts the spatial distribution of absolute errors (in both edges and nodes) between simulated and real fluxes (edges) as well as simulated and real heads (nodes) for each test case.

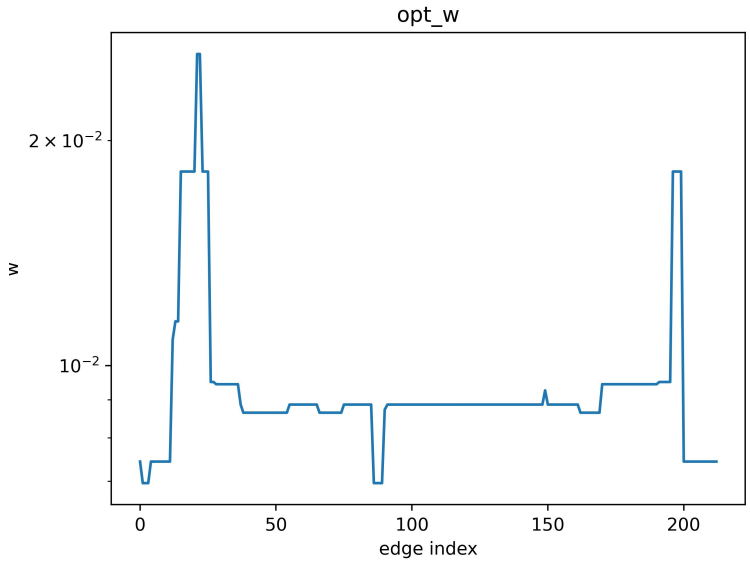

(a)

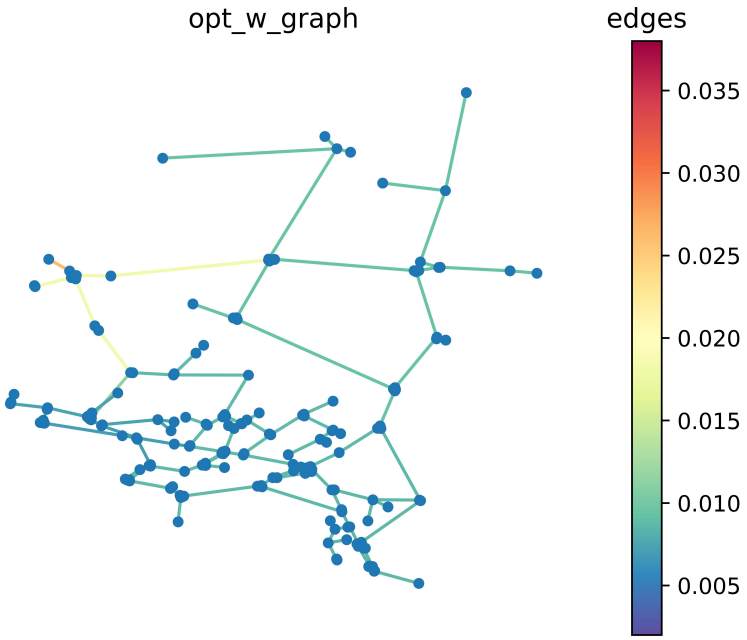

(b)

Figure 1.12: Test case 3, (a): optimal weight vs edge index (b) optimal weight distribution on the graph

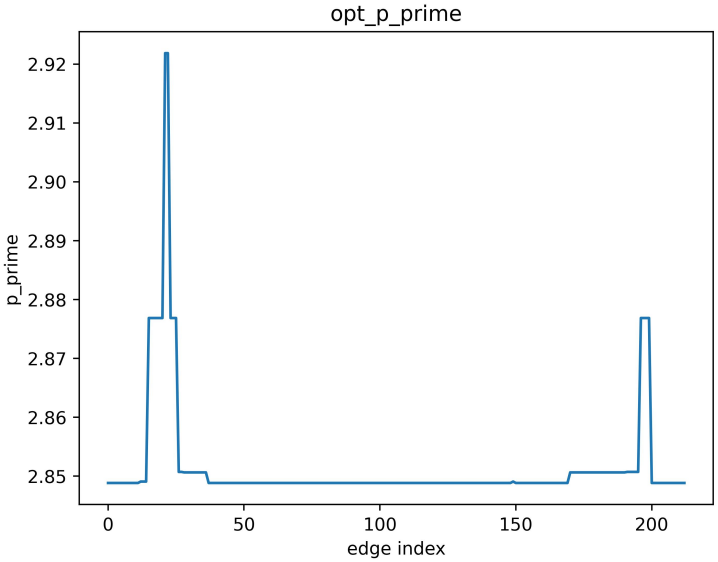

(a)

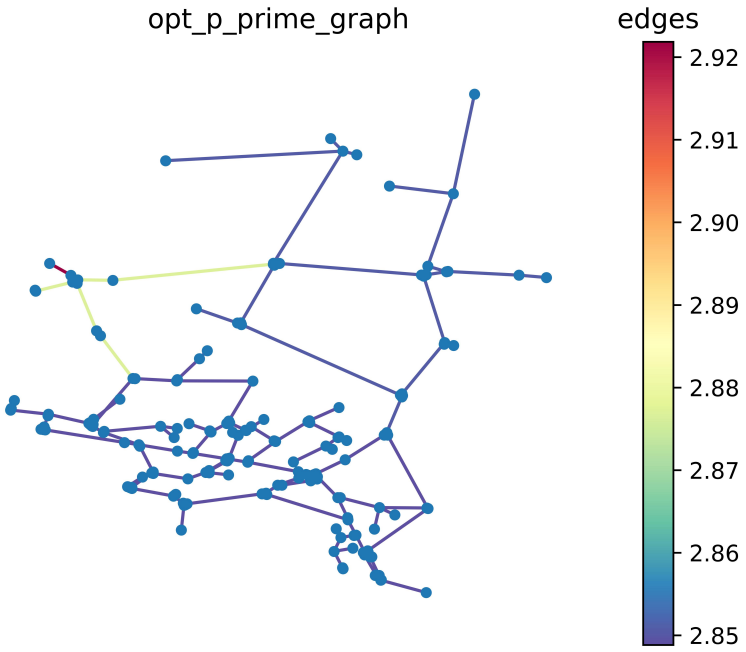

(b)

Figure 1.13: Test case 3, (a): optimal exponents vs edge index (b) optimal exponents distribution on the graph

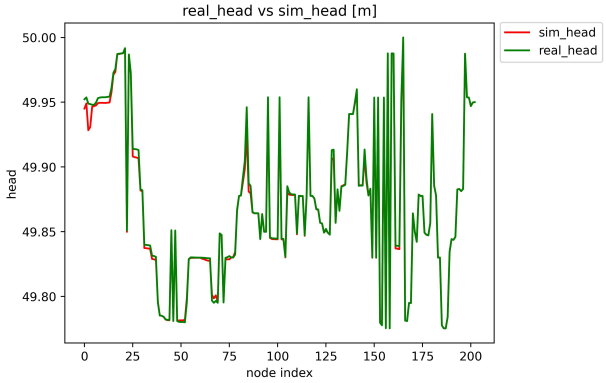

(a)

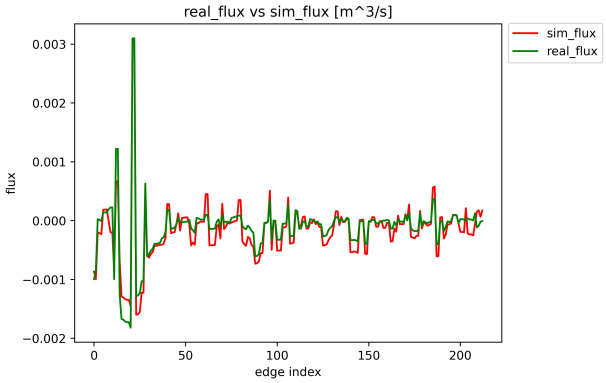

(b)

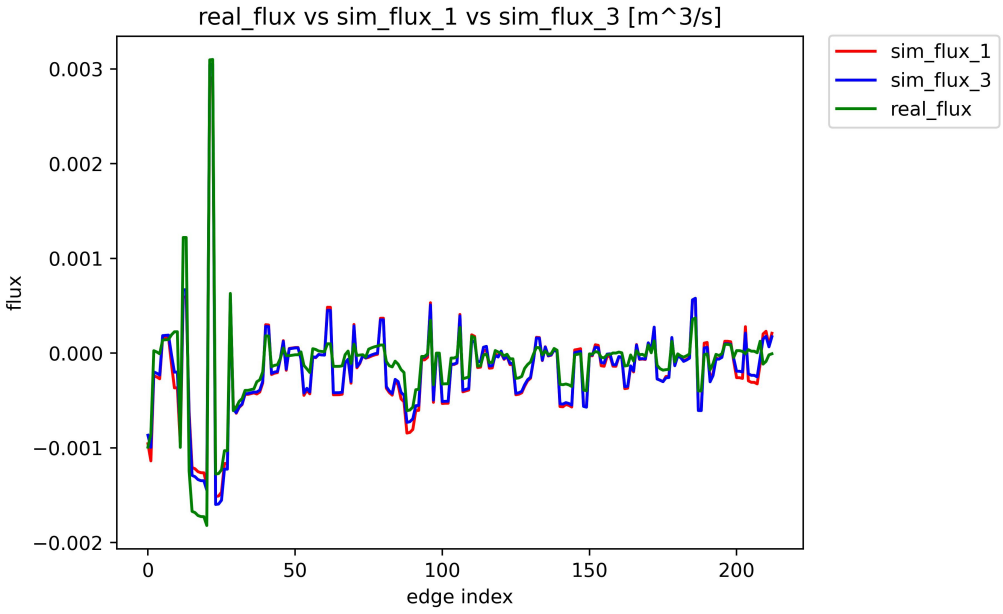

(c)

Figure 1.14: Test case 3, (a): real (EPANET) piezometric head(green) VS simulated piezometric head(red)
(b) real(EPANET) flux (green) VS simulated flux (red)
(c) real(EPANET) flux (green) VS Test case 1 simulated flux(red) VS Test case 3 simulated flux(blue)

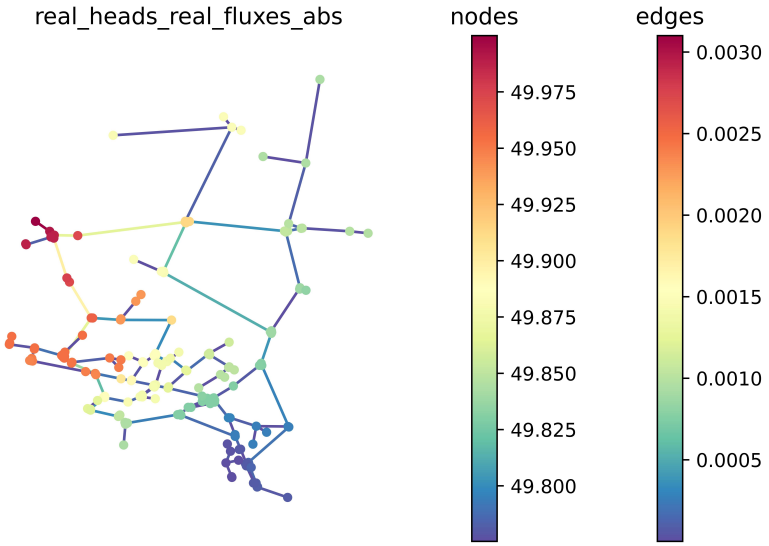

(a)

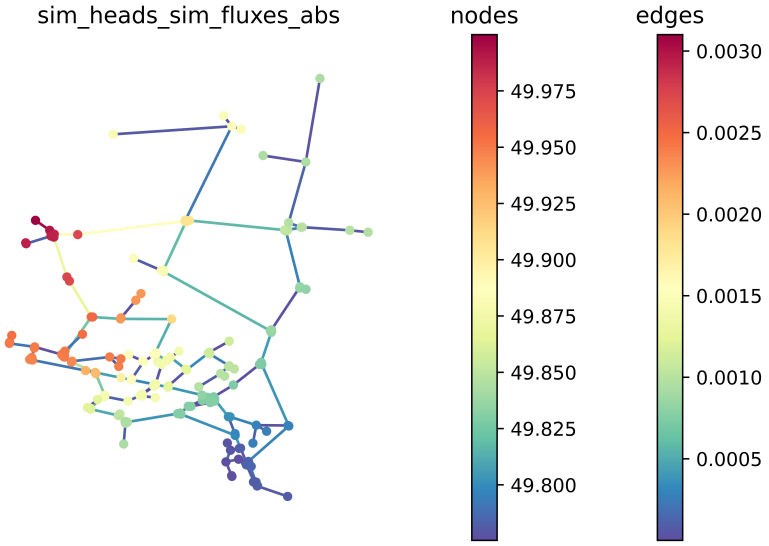

(b)

Figure 1.15: Test case 3, (a): real(EPANET) heads[m] and fluxes[m^3/s] in absolute value VS (b): simulated(reconstruction) heads[m] and fluxes[m^3/s] in absolute value

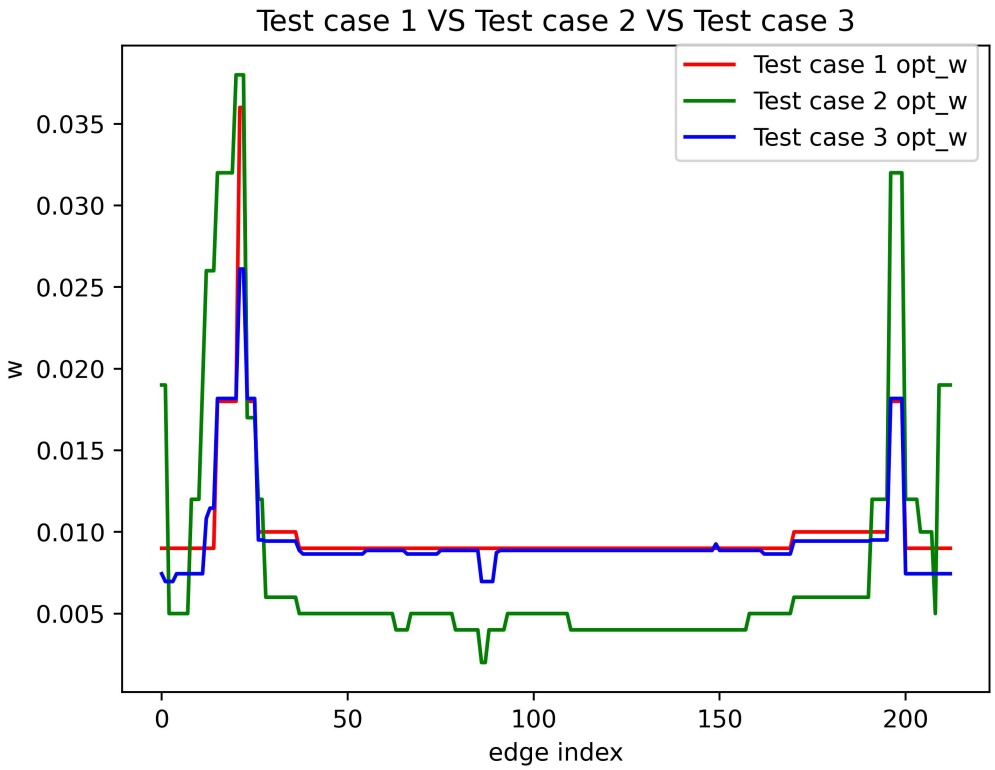

Figure 1.16: optimal weights distribution for Test case 1 (red) vs Test case 2 (green) vs Test case 3 (blue)

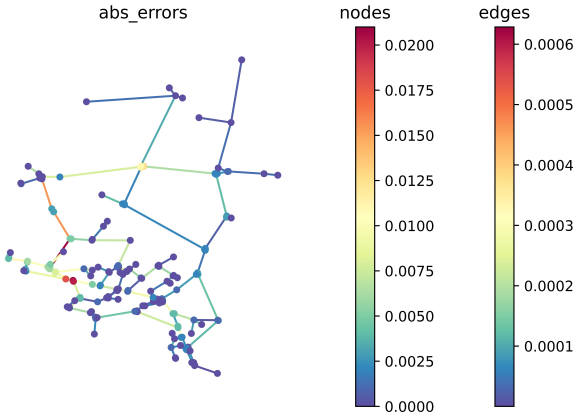

(a)

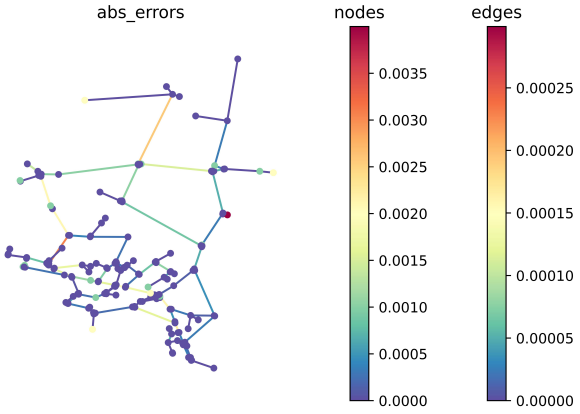

(b)

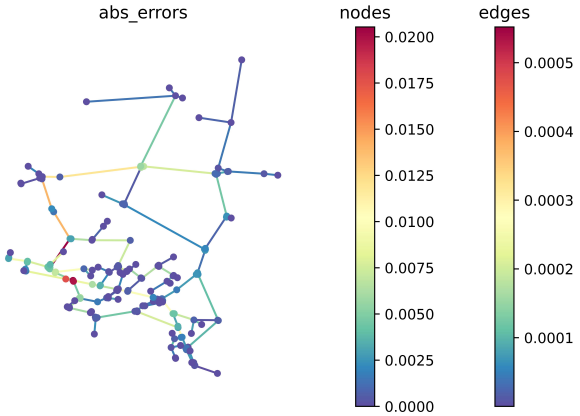

(c)

Figure 1.17: Test case 1 (a), Test case 2 (b), Test case 3 (c): absolute value error between real (EPANET) heads and simulated(reconstruction) heads on the nodes[m] and absolute value error between real (EPANET) fluxes and simulated(reconstruction) fluxes on the edges $[m^3/s]$

2 A duality based DMK approach to the Total Variation Energy, extensions and applications

2.1 Introduction

In this Chapter we discuss how to properly rewrite a convex energy functional into an equivalent saddle point formulation, to tackle the problem of finding it's minimizers from an alternative and more performing perspective.
We extensively study the case of the p-Dirichlet energy for $1 < p < 2$, and of the Total Variation energy as limit case for $p \to 1$, including it's application as a regularization term in various type of inverse problems.
These saddle points formulations are obtained by duality techniques carried out in two different frameworks: on directed graphs(or on $\mathbb{R}^{m=\#edges}$), and on a Lipschitz bounded domain of $\mathbb{R}^n$.
There are various reasons that suggest to transform a minimization problem into a saddle point problem. The most attracting feature of saddle point formulations is that the higher degree of freedom can be used to enforce qualitative features of the solution, even at a finite stage of discretization/approximation. This is the case of the mixed FEM formulation of divergence form elliptic PDEs introduced in [43], where the natural H_{div} regularity of the flux (i.e., the argument of the divergence operator) is explicitly enforced in the discretization space. This regularity property has a major importance in certain applications such as, e.g., when the PDE is coupled with a transport equation driven by the flux itself. Indeed, a discretization of the elliptic PDE not preserving at any finite stage such regularity property would lead to the presence of numerical sources and sinks in the coupled transport problem: the overall numerical scheme would become unstable.
In other cases, the second variable is introduced in the formulation of the problem because of its physical relevance, or even because it is the real quantity of interest in the particular application of the model. This is the case, for example, of linear elasticity mixed model [4, 43] , where the introduction of the stress tensor as a state variable may be used for the practical scope of checking the mechanical admissibility of the stress for a given material.
In other cases there are two natural independent variables and so, the mixed

formulation is the natural one. This is the case of the Stokes equations, where the two variables are the velocity and the pressure.
Another example of the advantage of transforming a minimization problem into a saddle point problem, is the case of non-linear inequality constraints optimization problems. This kind of non-linear inequality constraints are very difficult to handle, but, introducing an opportune positive Lagrange multiplier (see [46] p. 64 for full details), the initial minimization problem is transformed in a saddle point problem. The advantage here is given by considering the dual problem obtained by interchanging "inf" with "sup" that allows to transform the initial non-linear inequality constraint into a positivity constraint, which is easier to handle. This will be one of the reasons why we will introduce a saddle point formulation for the total variation energy, as observed in Remark 2.3.9.
Saddle points reformulations for convex minimization problems arise not only from Lagrange multipliers but also directly from iterating the Legendre transform, which is the classical method of duality based on Lagrangians introduced in [46], Chapter VI, Section 4.
All this techniques are at the basis of a large class of numerical algorithms for convex optimization problems. Among them, methods based on Lagrange multipliers and saddle points formulations are the well known augmented lagrangian approaches [33], [13] and the split Bregman iteration method [104], [142], [106], [64]. Another class of algorithms is the one based on Legendre duality, often referred to as the primal-dual algorithms or the Chambolle–Pock algorithms, which are mainly used for non differentiable problems such as the total variation denoising in image and signal processing [146], [49], [32], [71] and recently also for Reimannian manifolds optimization [15] and applications to deep learning and reinforcement learning [102], [111], [103].
Our interest for a saddle point reformulation of the p-Dirichlet energy and the Total Variation energy, is motivated also by a perhaps less noble justification, which is in turn extremely effective from a practical perspective. Indeed, the obtained saddle point problems closely resemble the one of the L^1 optimal transport [59]. As a matter of fact, this observation enables the use the techniques originally developed in the context of L^1 optimal transport, possibly after some required adaptations.

The derivation of these saddle point formulations is essentially based on the iteration of the Legendre transform combined with ad-hoc substitutions and transformations of the involved variables. Indeed, this is a classical technique in convex optimization theory extensively treated in, e.g., [46], and widely used in the variational formulation of partial differential equations, see e.g., [43].
Due to the centrality of this technique in what follows, we wish to provide here the most commonly encountered instance of this procedure. Consider a reflexive Banach space $(V, \|\cdot\|_V)$ and let $(V^*, \|\cdot\|_{V^*})$ it's dual space. Let $<\cdot,\cdot>_{V\times V^*}$ the duality pairing between V and V^*. Let $G : V \to \mathbb{R}$ be a convex and proper

function, then we define the Legendre transform $G^* : V^* \to \mathbb{R}$ as

$$G^*(\varphi^*) := \sup_{\varphi \in V} \langle \varphi, \varphi^* \rangle_{V \times V^*} - G(\varphi).$$

It is a standard fact that in such a setting we can recover G by iterating the Legendre transform:

$$G(\varphi) = G^{**}(\varphi) = \sup_{\varphi^* \in V^*} \langle \varphi^*, \varphi \rangle_{V^* \times V} - G^*(\varphi^*).$$

Consider now a problem of the form

$$\inf_{\varphi \in V} F(\varphi) + G(\varphi), \tag{2.1.1}$$

where $F : V \to \mathbb{R}$ and $G : V \to \mathbb{R}$ are proper, convex and lower semi-continuous functions. We can use the Legendre transform to rewrite it as follows:

$$\inf_{\varphi \in V} \left\{ F(\varphi) + \sup_{\varphi^* \in V^*} \left[\langle \varphi^*, \varphi \rangle_{V^* \times V} - G^*(\varphi^*) \right] \right\},$$

which is precisely the saddle-point problem:

$$\inf_{\varphi \in V} \sup_{\varphi^* \in V^*} F(\varphi) + \langle \varphi^*, \varphi \rangle_{V^* \times V} - G^*(\varphi^*). \tag{$\mathcal{P}$}$$

We may also consider the dual problem:

$$\sup_{\varphi^* \in V^*} \left\{ \inf_{\varphi \in V} F(\varphi) + \langle \varphi^*, \varphi \rangle_{V^* \times V} - G^*(\varphi^*) \right\}. \tag{$\mathcal{P}^*$}$$

and, possibly under some further regularity assumptions, try to show that the solution of $(\mathcal{P}^*)$ is indeed a solution of $(\mathcal{P})$.
Another commonly encountered problem is the following:

$$\inf_{\varphi \in V} \mathcal{F}(\varphi) + \mathcal{G}(\nabla \varphi), \tag{2.1.2}$$

where $\nabla : V \to E$ is a linear continuous operator between Banach spaces and $\mathcal{G} : E \to \mathbb{R}$, $\mathcal{F} : V \to \mathbb{R}$ are again proper, convex and lower semi-continuous functions. Also in this case, letting $< \cdot, \cdot >_{E^* \times E}$ be the duality pairing between E and E^*, we can use the Legendre transform to rewrite it as follows:

$$\inf_{\varphi \in V} \left\{ \mathcal{F}(\varphi) + \sup_{\sigma \in E^*} \left[\langle \sigma, \nabla \varphi \rangle_{E^* \times E} - \mathcal{G}^*(\sigma) \right] \right\},$$

which is called the Fenchel primal-dual saddle point formulation:

$$\inf_{\varphi \in V} \sup_{\sigma \in V^*} \mathcal{F}(\varphi) + \langle \sigma, \nabla \varphi \rangle_{E^* \times E} - \mathcal{G}^*(\sigma).$$

The dual problem, given by exchanging "inf" with "sup", is the famous Fenchel-Rockafellar duality formula:

$$\sup_{\sigma\in V^*}\left\{\inf_{\varphi\in V}\mathcal{F}(\varphi)+\langle\sigma,\nabla\varphi\rangle_{E^*\times E}-\mathcal{G}^*(\sigma)\right\}=$$
$$=\sup_{\sigma\in V^*}-\mathcal{F}^*(-\nabla^T\sigma)-\mathcal{G}^*(\sigma)\ .$$

If V is a reflexive Banach space, the equivalence between problem $(\mathcal{P})$ and $(\mathcal{P}^*)$ is ultimately related to the existence of a saddle point. On the contrary, if the reflexivity assumption is removed, the equivalence of $(\mathcal{P})$ with $(\mathcal{P}^*)$ may be drastically harder to be proven, or even not hold. This is the case for instance of the space of functions of bounded variation (BV, for short). Note that, despite the lack of reflexivity, BV functions play a pivotal role in many optimization problems and come in to the play rather naturally in certain inverse problems where the total variation is used as regularization term [26], [33], [64], [104], [115]. Various problems arise when dealing with BV functions rather than Sobolev functions. For instance, the characterization of the dual of the space of BV functions is still an open problem, with obvious difficulties arising when trying to perform the Gateaux differentiation or the Legendre transform of functionals defined on BV spaces. Indeed, fine techniques has been developed to generalize the standard objects and tools of classical functional analysis such as for example generalized differential operators, integration by parts formulas and traces operators. This ultimately ends up with the connection between Radon measures and BV functions, which is essentially based on the Riesz-Representation Theorem (Structure Theorem of BV functions, Anzellotti pairings, traces theorems, Dirichlet-to-Neumann maps etc., see [17], [34], [52], [70] for details). In order to overcome these problems, we will use a different strategy, which essentially relies upon the interconnection of the space of BV functions with the positive Radon measures. The main idea behind this approach comes directly from iterating the Legendre transform and using a sligtly different approah to the one used for problem (2.1.1) and problem (2.1.2). As an illustrative example of our proposed techniques, let $V:=\mathbb{R}^n$, $E:=\mathbb{R}^m$, $E^*:=E$, and, with abuse of notation, let $\nabla:V\to E$ be a linear operator. For a given $\varphi\in V$, $\varphi_i<\infty$, $i=1,...,n$, let $h:\mathbb{R}\to\mathbb{R}^+$ be a positive, lower semi-continuous, convex and even function and $f\in V$ a forcing or loading term.
Consider the following type of energy:

$$\mathtt{E}(\varphi):=\sum_{i=1}^{m}h((\nabla\varphi)_i)-f\cdot\varphi.$$

The function h can be in principle not differentiable, nevertheless, as for the Fenchel-Rockafellar duality formula (2.1.2), we can always compute the Legendre transform:

$$h^*(x^*)=\sup_{x\in\mathbb{R}}x^*x-h(x),$$

Is easy to see([46] p.62) that the Legendre transform for a function $\Gamma : E \to \mathbb{R}$ of the type $\Gamma(y) = \sum_{i=1}^{m} \gamma(y_i)$, $\gamma : \mathbb{R} \to \mathbb{R}$, is exactly the sum of the Legendre transforms for any single addendum, i.e. $\Gamma^*(y^*) = \sum_{i=1}^{m} \gamma^*(y_i^*)$.
Hence we have:

$$E(\varphi) = \sum_{i=1}^{m} h^{**}((\nabla\varphi)_i) - f\cdot\varphi = \sum_{i=1}^{m} \sup_{\sigma_i\in\mathbb{R}} \sigma_i(\nabla\varphi)_i - h^*(\sigma_i) - f\cdot\varphi =$$

$$= \sup_{\sigma\in E} \sigma\cdot\nabla\varphi - \sum_{i=1}^{m} h^*(\sigma_i) - f\cdot\varphi. \quad (2.1.3)$$

Since h is even, it is a known fact, see [87], that also h^* is even. Let us suppose that there exists a convex, lower semi-continuous function $H : \mathbb{R} \to \mathbb{R}$ such that:

$$h^*(x^*) = \frac{1}{2} H(|x^*|^2), \quad \forall\, x^* \in \mathbb{R},$$

thus setting

$$\frac{1}{2} H(\cdot) = h^* \circ \sqrt{|\cdot|},$$

we have that H is even, H^* is even and hence there exists a function $g : \mathbb{R} \to \mathbb{R}$ such that:

$$H^*(\cdot) = g \circ |\cdot|.$$

Iterating again the Legendre transform we get:

$$H(|x^*|^2) = H^{**}(|x^*|^2) = sup_{\mu\in\mathbb{R}}\, \mu|x^*|^2 - H^*(\mu) =$$

$$= sup_{\mu\in\mathbb{R}}\, \mu|x^*|^2 - g(|\mu|) = (g\circ|\cdot|)^*(|x^*|^2).$$

Observe now that, for any function $g : \mathbb{R} \to \mathbb{R}$ and $\forall\, y \geq 0$ we have that:

$$(g\circ|\cdot|)^*(y) = \sup_{\mu\geq 0} \mu y - g(\mu),$$

since:

$$\sup_{\mu\geq 0} \mu y - g(\mu) = \sup_{\mu\geq 0} \mu y - g(|\mu|) \leq (g\circ|\cdot|)^*(y) \leq$$

$$\overset{(y\geq 0)}{\leq} \sup_{\mu} |\mu| y - g(|\mu|) = \sup_{\mu\geq 0} \mu y - g(\mu).$$

Summing up all together, we have:

$$-\sum_{i=1}^{m} h^*(\sigma_i) = -\frac{1}{2}\sum_{i=1}^{m} H(|\sigma_i|^2),$$

and

$$-\sum_{i=1}^{m} h^*(\sigma_i) = -\sum_{i=1}^{m} \sup_{\mu_i \geq 0} \frac{1}{2}\mu_i|\sigma_i|^2 - \frac{1}{2}g(\mu_i) =$$

$$= \inf_{\mu \in E^+} \sum_{i=1}^{m} -\frac{1}{2}\mu_i|\sigma_i|^2 + \frac{1}{2}g(\mu_i). \quad (2.1.4)$$

Therefore, defining the Lagrangian $\mathtt{L}^{\mathtt{E}}_{\varphi} : (E^+ \times E) \to \mathbb{R}$ as

$$\mathtt{L}^{\mathtt{E}}_{\varphi}(\mu, \sigma) := -\frac{1}{2}\sum_{i=1}^{m} \mu_i|\sigma_i|^2 + \sigma \cdot \nabla \varphi + \frac{1}{2}\sum_{i=1}^{m} g(\mu_i),$$

from (2.1.3) and (2.1.4), we have that the original energy $\mathtt{E}(\varphi)$ is equivalent to the following saddle point problem:

$$\mathtt{E}(\varphi) = \sup_{\sigma \in E} \inf_{\mu \in E^+} \mathtt{L}^{\mathtt{E}}_{\varphi}(\mu, \sigma) - f \cdot \varphi, \quad \forall\, \varphi \in V. \quad (2.1.5)$$

If g is proper, convex and lower semi-continuous function, the saddle point problem in (2.1.5) is well defined.
Moreover, under some further regularity(coercivity) assumptions it is possible to show that the Lagrangian $\mathtt{L}^{\mathtt{E}}_{\varphi}$ admits at least a saddle point (μ^*, σ^*), for any $\varphi \in V$(see Section 2.6). The existence of a saddle point implies also that the dual problem:

$$\inf_{\mu \in E^+} \left\{ \sup_{\sigma \in E} \mathtt{L}^{\mathtt{E}}_{\varphi}(\mu, \sigma) \right\}, \quad \forall\, \varphi \in V.$$

is finite and that

$$\mathtt{E}(\varphi) = \inf_{\mu \in E^+} \sup_{\sigma \in E} \mathtt{L}^{\mathtt{E}}_{\varphi}(\mu, \sigma) - f \cdot \varphi, \quad \forall\, \varphi \in V. \quad (2.1.6)$$

This last saddle point formulation for $\mathtt{E}(\varphi)$ is far more convenient than (2.1.5). Indeed, if we define the extended Lagrangian $\mathtt{L}^{\mathtt{E}} : (V \times E^+ \times E) \to \mathbb{R}$ as

$$\mathtt{L}^{\mathtt{E}}(\varphi, \mu, \sigma) := \mathtt{L}^{\mathtt{E}}_{\varphi}(\mu, \sigma) - f \cdot \varphi,$$

by virtue of (2.1.6) the problem:

$$\inf_{\varphi \in V} \mathtt{E}(\varphi),$$

is equivalent to:

$$\inf_{\varphi \in V} \inf_{\mu \in E^+} \sup_{\sigma \in E} \mathtt{L}^{\mathtt{E}}(\varphi, \mu, \sigma). \quad (2.1.7)$$

Since we have a double minimization problem we can also minimize in the pair (φ, μ) or interchange the order of minimization. Observe that for any given positive μ the problem:

$$\inf_{\varphi \in V} \sup_{\sigma \in E} \mathtt{L}^{\mathtt{E}}(\varphi, \mu, \sigma) = \inf_{\varphi \in V} \sup_{\sigma \in E} -\frac{1}{2}\sum_{i=1}^{m} \mu_i|\sigma_i|^2 + \sigma \cdot \nabla \varphi - f \cdot \varphi, \quad (2.1.8)$$

has some reminiscent with the mixed FEM formulation for linear elliptic PDEs introduced in [43].
In the common case of variational problems, where typically boundary conditions are considered for the specific physical phenomena described by the energy $\mathtt{E}(\varphi)$, the Euler-Lagrange equations for (2.1.8) involve a classical linear saddle-point system of equations.
In some cases, the particular properties of the function $g(\mu)$ in $\mathtt{L}^{\mathtt{E}}(\varphi, \mu, \sigma)$, implies that an optimal μ^* for (2.1.7) has to be necessary strictly positive. In that case, assuming further regularity(strong convexity, norm coerciveness) of the map $\mu \mapsto \mathtt{L}^{\mathtt{E}}(\varphi, \mu, \sigma)$, we can show that there exists a $\delta > 0$ such that problem (2.1.7) is equivalent to:

$$\inf_{\varphi \in V} \inf_{\substack{\mu \in E^+ \\ \mu_i \geq \delta}} \sup_{\sigma \in E} \mathtt{L}^{\mathtt{E}}(\varphi, \mu, \sigma). \tag{2.1.9}$$

Thereofore, since μ is strictly positive, the "sup" in (2.1.9) is indeed a maximum $\forall\, \mu \geq \delta$(we have indeed strong concavity, differentiability and anti-coerciveness), and the maximizer σ^* is given by:

$$\sigma_i^* := \frac{(\nabla \varphi)_i}{\mu_i}, \quad i = 1, \ldots, m. \tag{2.1.10}$$

Introducing the functional:

$$\mathcal{L}^{\mathtt{E}}(\varphi, \mu) := \sup_{\sigma \in E} \mathtt{L}^{\mathtt{E}}(\varphi, \mu, \sigma),$$

and computing $\mathtt{L}^{\mathtt{E}}(\varphi, \mu, \sigma)$ in the maximizer $\sigma = \sigma^*$ we get:

$$\mathcal{L}^{\mathtt{E}}(\varphi, \mu) = \sum_{i=1}^{m} \frac{1}{2} \frac{|(\nabla \varphi)_i|^2}{\mu_i} - f \cdot \varphi + \frac{1}{2} \sum_{i=1}^{m} g(\mu_i).$$

Thus problem (2.1.7) is equivalent to the following simplified double minimization problem:

$$\inf_{\substack{\varphi \in V \\ \mu \in E^+}} \mathcal{L}^{\mathtt{E}}(\varphi, \mu), \tag{2.1.11}$$

In the general case, we can not expect that the optimal density μ^* is strictly detached from zero. Nevertheless, if the Lagrangian $\mathtt{L}^{\mathtt{E}}$ satisfies some convex(concave) and norm corciveness(anti norm coerciveness) hypothesis, we can prove the existence of at least a saddle point

$$((\varphi^*, \mu^*), \sigma^*) \in ((V \times E^+) \times E),$$

for $\mathtt{L}^{\mathtt{E}}$.
Thus, in the general case, it is not possible to have a direct formula for σ^* as in (2.1.10) and the equivalence to the simplified problem (2.1.11).

A possible solution to circumnavigate this issue is to introduce an "artificial lower bound" $0 < \delta << 1$ as a small Tikhononv regularization parameter. Indeed, instead of $\mathtt{L}^{\mathtt{E}}$, consider the following regularized Lagrangian:

$$\mathtt{L}^{\mathtt{E},\delta}(\varphi,\mu,\sigma) := -\frac{1}{2}\sum_{i=1}^{m}(\mu_i+\delta)|\sigma_i|^2 + \sigma\cdot\nabla\varphi - f\cdot\varphi + \frac{1}{2}\sum_{i=1}^{m} g(\mu_i), \qquad (2.1.12)$$

and the functional:

$$\mathcal{L}^{\mathtt{E}}_{\delta}(\varphi,\mu) := \sup_{\sigma\in E}\mathtt{L}^{\mathtt{E},\delta}(\varphi,\mu,\sigma). \qquad (2.1.13)$$

Since now $\mu+\delta > 0$, the supremum in σ in (2.1.13) is in fact a maximum $\forall\,\mu\in E^+$, and the maximizer σ^* is given by the analogous formula to (2.1.10):

$$\sigma_i^* = \frac{(\nabla\varphi)_i}{\mu_i+\delta}, \quad i=1,\dots,m.$$

Thus, computing $\mathtt{L}^{\mathtt{E},\delta}(\varphi,\mu,\sigma)$ in $\sigma=\sigma^*$, the functional $\mathcal{L}^{\mathtt{E}}_{\delta}(\varphi,\mu)$ simplifies as follows:

$$\mathcal{L}^{\mathtt{E}}_{\delta}(\varphi,\mu) = \sum_{i=1}^{m}\frac{1}{2}\frac{|(\nabla\varphi)_i|^2}{(\mu_i+\delta)} - f\cdot\varphi + \frac{1}{2}\sum_{i=1}^{m} g(\mu_i),$$

hence, if δ is sufficiently small, we are motivated to consider the following double minimization problem:

$$\inf_{\varphi\in V}\inf_{\mu\in E^+}\mathcal{L}^{\mathtt{E}}_{\delta}(\varphi,\mu), \qquad (2.1.14)$$

which is the Tikhonov regularization of the saddle point problem (2.1.7).
In either the cases, of the original saddle point problem (2.1.7) or the regularized double minimization problem (2.1.14), the strong advantage of this formulation is that we transform an original possibly non-linear and non differentiable problem, to a quadratic optimization problem in the original variable φ, which involves an elliptic structure of a weighted Laplacian-like operator.
The non-linearity is reabsorbed by introducing the density variable μ, the mass term $g(\mu)$ and a positivity constraint which is reasonable easy to handle.
This is in some sense an example of the well known augmented lagrangian approach [13], [33]. Observe that differently from the standard augmented lagrangian approach where typically some variable substitutions are performed via Lagrange multipliers, here the introduction of the variable μ is naturally given by the Legendre transform.
Relying upon these new formulations, and starting from the so-called Dynamic-Monge-Kantorovich(DMK) scheme for the L^1 optimal transport problem ([55], [58], [54], [59]), we develop a number of numerical methods for the solution of a rather large class of variational problems which can be traced back to the same framework as problem (2.1.7) for an opportune energy functional.
Among them, we developed numerical methods for problems including, e.g., 1-harmonic Dirichlet problem and the inhomogeneous Dirichlet problem for the

p-Laplacian on graphs. Also, we develop other applications in inverse problems based on the use of the total variation or the l_1 norm as Tikhonov regularization terms in certain discrete optimization problems such as the classical Rudin-Osher-Fatemi(ROF) problem, or the TV denoising [104], and the compressed modes for the graph Laplacian [106].
The derivation of these numerical schemes is based on rewriting a convex problem in a form that includes a term of the type (2.1.7) or the regularized version (2.1.14), for which the DMK scheme was appositevely designed, as the linear iterative solver derived by the time discretization of a dynamics of the type:

$$\begin{aligned}
(\mu(t)+\delta)\sigma_i(t) &= \nabla(\varphi(t))_i, \quad i=1,\dots,m \\
\nabla^T\sigma(t) &= \nabla^T \operatorname{Diag}\left(\frac{1}{\mu(t)+\delta}\right)\nabla\varphi(t) = f \\
\partial_t\mu_i(t) &= \mu_i(t)\left(|\sigma_i(t)|^2 - \partial_\mu g(\mu_i(t))\right), \quad \mu_i(0)=\mu_{0i}>0, \quad i=1,\dots,m,
\end{aligned} \tag{2.1.15}$$

where $\operatorname{Diag}(c)$ is the diagonal matrix which has the vector $c\in E$ as diagonal.
The DMK scheme, in all of it's variants, is essentially based on the numerical integration of a "Gradient-Flow like" minimizing scheme, which involves, at every iteration, the solution of a sparse, symmetric linear system and the updating of a descent dynamics for the variable μ.
Thus, for certain aspects, it is a variant of the Newton method. It is moreover quite easy to implement(if an explicit time discretization for the gradient flow is used) for many applications, and it exhibits good stability properties.
Aside from the simple numerical implementation, having a structure which depends upon inverting a symmetric and sparse matrix, has the main advantage derived from the huge weaponry of the numerical linear algebra(e.g. multi grid methods, preconditioning strategies etc.).
Furthermore, having introduced the Tikhonov regularized Lagrangian (2.1.12) and the functional (2.1.13), the original saddle point problem (2.1.7) is reduced to the differentiable and convex double minimization problem, hence the second order method derived from the implicit Euler time discretization for the DMK gradient flow like (2.1.15) is well defined, improving drastically the performance of the numerical scheme. Moreover, differently from the Newton method which needs a sufficient accurate initial guess to converge, here we can benefit from the stability induced by $\mathcal{L}_\delta^{\mathtt{E}}$ which acts as a Lyapunov functional for the dynamics. Thus, starting with a sufficiently small initial time step, we can consider the previous iteration as an initial guess, and the newton method applied to the implicit Euler time discretization of (2.1.15) is guaranteed to converge(see [59] for details).
Note that having a descending scheme such as (2.1.15) which is derived from a gradient descent approach for a double minimization problem of the type (2.1.14), allows us to easily introduce further constraints on the variable φ and also various type of boundary conditions.

2.1.1 Our study

For the reader's convenience, we start with a brief overview of the results that we prove in the next sections. This provides also the needed information on the organization of the chapter.
In Section 2.2 we first introduce the p-Dirichlet energy $\mathcal{E}_p$, $1 < p < 2$, in an open bounded Lipschitz domain $\Omega \subset \mathbb{R}^n$ by setting

$$\mathcal{E}_p(\varphi) := \int_\Omega \frac{1}{p} |\nabla \varphi|^p, \ \varphi \in W^{1,p}(\Omega).$$

Since the classical Sobolev space $W^{1,p}(\Omega)$ is reflexive for any $1 < p < \infty$, we can make repeated use of all standard tools of convex analysis. Indeed, iterating the Legendre transform upon different selections of the variables and conjugate variables we derive the following Lagrangian:

$$\mathcal{L}^p_\varphi(\mu, \sigma) := -\int_\Omega \frac{1}{2}\mu|\sigma|^2 + \int_\Omega \sigma \cdot \nabla \varphi + \frac{2-p}{2p} \int_\Omega \mu^{\frac{p}{2-p}},$$

and the following saddle point formulation for the p-Dirichlet energy of a function $\varphi \in W^{1,p}(\Omega)$

$$\mathcal{E}_p(\varphi) = \sup_{\sigma \in \left[W^{p'}(\mathrm{div},\Omega)\right]^n} \ \inf_{\substack{\mu \geq 0 \\ \mu \in L^\gamma(\Omega)}} \mathcal{L}^p_\varphi(\mu, \sigma),$$

where $\gamma = \frac{p}{2-p}$. The main result of Section 2.2 is Theorem 2.2.2, where we show the existence and characterization of a saddle point and the equivalence between the p-Dirichlet energy with its dual formulation, namely:

$$\mathcal{E}_p(\varphi) = \inf_{\substack{\mu \geq 0 \\ \mu \in L^\gamma(\Omega)}} \ \sup_{\sigma \in \left[W^{p'}(\mathrm{div},\Omega)\right]^n} \mathcal{L}^p_\varphi(\mu, \sigma).$$

This result would be the basis for our saddle point formulation for the p-Poisson energy minimization problem.
In Section 2.3 we extend the saddle point formulation for the p-Dirichlet energy to the limit case when $p = 1$ and the space $BV(\Omega)$.
The main idea behind this come from observing that fixing a density μ^* such that $\mathrm{supp}(\nabla \varphi) \subseteq \mathrm{supp}(\mu^*)$, then we can formally write

$$\sigma^* = \arg\max_\sigma -\int_\Omega \frac{1}{2}\mu^*|\sigma|^2 + \int_\Omega \sigma \cdot \nabla \varphi \implies \mu^*\sigma^* = \nabla \varphi,$$

while on the other hand:

$$\inf_{\mu \geq 0} \int_\Omega \mu(1 - |\sigma|^2) = \begin{cases} 0 & |\sigma(x)| \leq 1, \ \forall\, x \in \Omega \\ -\infty & \textit{otherwise.} \end{cases}$$

Thus, observing that by the structure theorem of BV functions, $\forall\, \varphi \in BV(\Omega)$ there exists a positive radon measure μ_φ and a μ_φ-measurable vector field σ_φ such that

$$\mu_\varphi \sigma_\varphi = \nabla\, \varphi,$$
$$|\sigma_\varphi(x)| = 1,$$

for $\mu_\varphi - a.e.\ x \in \Omega$ and

$$TV(\varphi) = \int_\Omega d\mu_\varphi,$$

taking inspiration from [17], we introduce the following Lagrangian $\mathcal{L}^1_\varphi : (\mathcal{M}^+(\Omega) \times \left[\mathcal{C}^1_c(\Omega)\right]^n) \to \mathbb{R}$:

$$\mathcal{L}^1_\varphi(\mu, \sigma) := -\int_\Omega \frac{1}{2}|\sigma|^2 d\mu + \int_\Omega \sigma \cdot d[\nabla\, \varphi] + \frac{1}{2}\int_\Omega d\mu,$$

and the following functional:

$$\mathcal{L}^*_1(\varphi) := \sup_{\sigma \in [\mathcal{C}^1_c(\Omega)]^n} \left\{ \inf_{\mu \in \mathcal{M}^+(\Omega)} \mathcal{L}^1_\varphi(\mu, \sigma) \right\}, \quad \varphi \in BV(\Omega),$$

where $\mathcal{M}^+(\Omega)$ is the space of positive Radon measures on Ω.
It is easy to show(see (2.3.6)) that

$$\mathcal{L}^*_1(\varphi) = TV(\varphi), \quad \forall\, \varphi \in BV(\Omega),$$

on the other hand, due to the lack of reflexivity we can not directly prove the existence of a saddle point for $\mathcal{L}^*_1(\varphi)$.
Nevertheless, in Theorem 2.3.10 we show that the dual functional:

$$\mathcal{L}_1(\varphi) := \inf_{\mu \in \mathcal{M}^+(\Omega)} \left\{ \sup_{\sigma \in [\mathcal{C}^1_c(\Omega)]^n} \mathcal{L}^1_\varphi(\mu, \sigma) \right\}, \quad \varphi \in BV(\Omega),$$

satisfies:

$$TV(\varphi) = \mathcal{L}_1(\varphi), \quad \varphi \in BV(\Omega),$$

and if we introduce the functional

$$E_\varphi(\mu) := \sup_{\sigma \in [\mathcal{C}^1_c(\Omega)]^n} \mathcal{L}^1_\varphi(\mu, \sigma),$$

the unique optimal measure

$$\mu^* = \arg\min_{\mu \in \mathcal{M}^+(\Omega)} E_\varphi(\mu),$$

is precisely the total variation measure:

$$\mu^* = |\, \nabla\, \varphi|,$$

and there exists a unique saddle point

$$(\mu^*, \sigma^*_{\mu^*}) \in (\mathcal{M}^+(\Omega), [L^2_{\mu^*}(\Omega)]^n),$$

for $\mathcal{L}^1_\varphi$, where the optimal vector field $\sigma^*_{\mu^*}$ is the one given by the Structure Theorem of BV functions.
The lack of a saddle point in the spaces $(\mathcal{M}^+(\Omega), \left[\mathcal{C}^1_c(\Omega)\right]^n)$ is ultimately do to the fact that we can not found a proper topology which guarantees that the Lagrangian $\mathcal{L}^1_\varphi$ has the necessary regularity to admits a maximizer(the supremum σ^* indeed does not belong to the space $\left[\mathcal{C}^1_c(\Omega)\right]^n$, hence it can not be a maximizer). Nevertheless, as soon as one introduce an opportune discretization everything is well defined and reflexive and continuous. That is the reason why, as a case of direct interest for this thesis, in Section 2.4 we state the finite dimension counterpart on graphs of the results of Section 2.2 and Section 2.3. The graph-based counterpart of the continuous gradient operator is given by the signed incidence matrix, where the variable μ becomes a positive weight on the edges while the variables σ and φ become functions on the edges and on the nodes respectively.
Let $\mathcal{G} = (E, V, \omega)$ be a weighted, directed(i.e. every edge has a prescribed direction) graph, where E is the set of $m = |E|$ edges, V the set of $n = |V|$ nodes and ω is a weight on the edges. We denote as $\mathcal{H}(V) = \mathbb{R}^n$ and $\mathcal{H}(E) = \mathbb{R}^m$ the Banach spaces of real-valued functions on V and E, respectively. The graph gradient operator $\nabla : \mathcal{H}(V) \longrightarrow \mathcal{H}(E)$ is the $m \times n$ matrix of the weighted signed differences i.e. for every $\varphi \in \mathcal{H}(V)$, $(\nabla\,\varphi)_e = \omega_e(\varphi_{v_k} - \varphi_{v_j})$ if $e \in E$ connects the node v_j to the node v_k. Observe that it is necessary to work with directed graph in order to define a gradient matrix.
The graph-based p-Dirichlet energy, $p \geq 1$ is defined as:

$$\mathtt{E}_p(\varphi) := \frac{\|\nabla\,\varphi\|^p_{l_p}}{p} = \sum_{e\in E} \frac{|(\nabla\,\varphi)_e|^p}{p},$$

as for the continuous case we introduce a family of Lagrangians $\mathtt{L}^p_\varphi : (\mathcal{H}(E)^+ \times \mathcal{H}(E)) \to \mathbb{R}$ for the graph p-Dirichlet energy, $1 \leq p < 2$:

$$\mathtt{L}^p_\varphi(\mu, \sigma) := -\sum_{e\in E} \frac{1}{2}\mu_e|\sigma_e|^2 + \sigma \cdot \nabla\,\varphi + \frac{2-p}{2p}\sum_{e\in E} \mu_e{}^{\frac{p}{2-p}}.$$

In Theorem 2.4.1 we show that:

$$\mathtt{E}_p(\varphi) = \inf_{\mu\in\mathcal{H}(E)^+} \sup_{\sigma\in\mathcal{H}(E)} \mathtt{L}^p_\varphi(\mu, \sigma), \quad \varphi \in \mathcal{H}(V),$$

where $\mathcal{H}(E)^+ := \{\mu \in \mathcal{H}(E) \mid \mu_e \geq 0,\ \forall\, e \in E\}$ and we can prove the existence of a saddle point (μ^*, σ^*) (unique in the case $p > 1$) which satisfies the following

extremality relations:

$$\begin{aligned} \mu_e^* \sigma_e^* &= (\nabla \varphi)_e, \quad \forall\, e \in E, \\ \mu_e^* &= |(\nabla \varphi)_e|^{2-p}, \quad \forall\, e \in E, \\ |\sigma_e^*| &\leq 1, \quad \forall\, e \in E,\ p = 1, \\ \mu_e^* |\sigma_e^*|^2 - \mu_e^* &= 0, \quad \forall\, e \in E,\ p = 1. \end{aligned}$$

As a direct generalization, in Section 2.6 we extend the same results for a general linear operator $\Lambda : V \to E$, $V := \mathbb{R}^n$, $E := \mathbb{R}^m$ instead of the graph gradient operator.
Thus we consider the following generalized p-Dirichlet energy:

$$\mathtt{E}_p^{\Lambda}(\varphi) := \frac{\|\Lambda\varphi\|_{l_p}^p}{p},$$

and we define the Lagrangian $\mathtt{L}_{\varphi}^{p,\Lambda} : (E^+ \times E) \to \mathbb{R}$:

$$\mathtt{L}_{\varphi}^{p,\Lambda}(\mu, \sigma) := -\sum_{i=1}^{m} \frac{1}{2} \mu_i |\sigma_i|^2 + \sigma \cdot \Lambda\varphi + \frac{2-p}{2p} \sum_{i=1}^{m} \mu_i^{\frac{p}{2-p}},$$

then we have that:

$$\mathtt{E}_p^{\Lambda}(\varphi) = \inf_{\mu \in E^+} \sup_{\sigma \in E} \mathtt{L}_{\varphi}^{p,\Lambda}(\mu, \sigma).$$

For example, in the case where $\Lambda := id$, is the identity operator, we have the following saddle point formulation of the discrete l_p norm, $1 \leq p < 2$, for a vector $\varphi \in V$:

$$\frac{1}{p} \|\varphi\|_{l_p}^p = \inf_{\nu \in V^+} \sup_{\sigma \in V} -\sum_{i=1}^{n} \frac{1}{2} \nu_i |\sigma_i|^2 + \sigma \cdot \varphi + \frac{2-p}{2p} \sum_{i=1}^{n} \nu_i^{\frac{p}{2-p}}.$$

where $V^+ := \{\nu \in V \mid \nu_i \geq 0,\ i = 1, ..., n\}$.
Also in this case, we have the existence of a saddle point (ν^*, σ^*) which exhibits analogous extremality relations, see Theorem 2.5.1.
We then introduce a regularized version for the generalized family of Lagrangians and saddle point formulations involving the operator Λ. In the framework of the Tikhonov regularization consider the regularized Lagrangian:

$$\mathtt{L}_{\varphi}^{p,\Lambda,\delta}(\mu, \sigma) := -\sum_{i=1}^{m} \frac{1}{2} (\mu_i + \delta) |\sigma_i|^2 + \sigma \cdot \Lambda\varphi + \frac{2-p}{2p} \sum_{i=1}^{m} \mu_i^{\frac{p}{2-p}},$$

and the following regularized saddle point formulation for the generalized p-Dirichlet energy $\mathtt{E}_p^{\Lambda}(\varphi)$:

$$\mathtt{L}_{p,\delta}^{\Lambda}(\varphi) := \inf_{\mu \in E^+} \sup_{\sigma \in E} \mathtt{L}_{\varphi}^{p,\Lambda,\delta}(\mu, \sigma). \tag{2.1.16}$$

where δ is a small positive regularization parameter.
If we introduce the functional

$$\mathcal{L}_{\delta}^{p,\Lambda}(\varphi,\mu) := \sup_{\sigma\in E} \mathtt{L}_{\varphi}^{p,\Lambda,\delta}(\mu,\sigma), \tag{2.1.17}$$

then (2.1.16) rewrites as:

$$\mathtt{L}_{p,\delta}^{\Lambda}(\varphi) = \inf_{\mu\in E^+} \mathcal{L}_{\delta}^{p,\Lambda}(\varphi,\mu).$$

The parameter δ has the important role to guarantees the coercivity and the differentiability of the map:

$$\sigma \mapsto \mathtt{L}_{\varphi}^{p,\Lambda,\delta}(\mu,\sigma), \quad \forall\, \varphi \in V,\ \forall\, \mu \in E^+,$$

with the aim to directly compute a maximizer σ^* for (2.1.17) and simplify (2.1.16), while retaining a good approximation of the original saddle point formulation for $\mathtt{E}_p^{\Lambda}(\varphi)$, if δ is sufficiently small.
Since $\mu+\delta>0$, the supremum in (2.1.17) is in fact a maximum(we have indeed strong concavity, differentiability and anti-coerciveness), and the maximizer σ^* is given by:

$$\sigma_i^* = \frac{(\Lambda\varphi)_i}{\mu_i+\delta}, \quad i=1,...,m.$$

.
Hence, computing $\mathtt{L}_{\varphi}^{p,\Lambda,\delta}(\mu,\sigma)$ for $\sigma=\sigma^*$, the functional defined in (2.1.17) is equal to:

$$\mathcal{L}_{\delta}^{p,\Lambda}(\varphi,\mu) = \sum_{i=1}^{m} \frac{1}{2}\frac{|(\Lambda\varphi)_i|^2}{(\mu_i+\delta)} + \frac{2-p}{2p}\sum_{i=1}^{m} \mu_i^{\frac{p}{2-p}},$$

and the regularized saddle point formulation in (2.1.16) simplifies as follows:

$$\mathtt{L}_{p,\delta}^{\Lambda}(\varphi) = \inf_{\mu\in E^+} \sum_{i=1}^{m} \frac{1}{2}\frac{|(\Lambda\varphi)_i|^2}{(\mu_i+\delta)} + \frac{2-p}{2p}\sum_{i=1}^{m} \mu_i^{\frac{p}{2-p}}. \tag{2.1.18}$$

The regularized problem makes evident that the existence of a minimizer μ^* in (2.1.18), depends only on the properties of the mass term

$$G(\mu) := \frac{2-p}{2p}\sum_{i=1}^{m} \mu_i^{\frac{p}{2-p}},$$

since, if G is convex, lower semi-continuous, and coercive, the existence of a minimizer μ^* for the function:

$$\varepsilon_{\varphi}(\mu) := \mathcal{L}_{\delta}^{p,\Lambda}(\varphi,\mu), \quad \forall\, \varphi \in V,$$

is guaranteed.
Based on this observation on the mass term G, in Section 2.6 we consider the case of a general discrete energy of the type:

$$\mathtt{E}(\varphi) := \sum_{i=1}^{m} h((\Lambda\varphi)_i),$$

where $h : \mathbb{R} \to \mathbb{R}^+$ is a positive, lower semi-continuous, convex, and even function. The goal of Section 2.6 is to extend our Legendre duality based approach, to the computation of the opportune mass function G, such that the energy $\mathtt{E}(\varphi)$ can be written in the form of a saddle point problem as we have done for the p-Dirichlet energy.
In Theorem 2.6.1 we state sufficient and necessary conditions for the existence of the following saddle point formulation:

$$\mathtt{E}(\varphi) = \inf_{\mu\in E^+} \sup_{\sigma\in E} -\frac{1}{2}\sum_{i=1}^{m} \mu_i|\sigma_i|^2 + \sigma\cdot\Lambda\varphi + \frac{1}{2}\sum_{i=1}^{m} g(\mu_i),$$

where $g : \mathbb{R} \to \mathbb{R}^+$ is a positive, convex and proper function. Moreover we can recover g from h by means of the following Legendre transform based formula:

$$\left(\frac{1}{2}(g\circ|\cdot|)^*\circ|\cdot|^2\right)^* = h.$$

We provide moreover illustrative examples to recover the graph based TV energy saddle point formulation of Section 2.4 and in Example 2.6.4 an application to the Minimal Surfaces discrete type energy:

$$\mathtt{E}(\varphi) := \sum_{i=1}^{m} \sqrt{1+|(\Lambda\varphi)_i|^2}.$$

In Section 2.7 we see a first example of application of our proposed techniques in the graph setting.
The main idea is the following. Roughly speaking, in the graph setting, consider an energy $\mathtt{E}(\varphi)$, $\varphi \in \mathcal{H}(V)$, and suppose that we are in the situation to be able to provide a Lagrangian $L^{\mathtt{E}}_{\varphi} : (\mathcal{H}(E)^+, \mathcal{H}(E)) \to \mathbb{R}$ such that we have the following saddle point formulation for $\mathtt{E}(\varphi)$:

$$\mathtt{E}(\varphi) := \inf_{\mu\in\mathcal{H}(E)^+} \sup_{\sigma\in\mathcal{H}(E)} L^{\mathtt{E}}_{\varphi}(\mu,\sigma), \quad \forall\,\varphi\in\mathcal{H}(V).$$

Then, introducing the extended Lagrangian: $\mathtt{L}^{\mathtt{E}} : (V\times E^+\times E) \to \mathbb{R}$ as

$$\mathtt{L}^{\mathtt{E}}(\varphi,\mu,\sigma) := \mathtt{L}^{\mathtt{E}}_{\varphi}(\mu,\sigma), \quad \forall\,\varphi\in\mathcal{H}(V),\ \mu\in\mathcal{H}(E)^+,\ \forall\,\sigma\in\mathcal{H}(E).$$

the problem:

$$\inf_{\varphi\in V} \mathtt{E}(\varphi),$$

is equivalent to:

$$\inf_{\varphi\in V}\inf_{\mu\in E^+}\sup_{\sigma\in E}\mathtt{L}^{\mathtt{E}}(\varphi,\mu,\sigma).$$

Moreover, introducing a small regularization parameter δ, as we have done in (2.1.18), we can possibly provide a simplified, convex and differentiable well approximated problem, by directly compute a maximizer σ^* and reducing to a double minimization of the type:

$$\inf_{\varphi\in V}\mathtt{E}(\varphi)\approx\inf_{\substack{\varphi\,\in\,V\\ \mu\,\in\,E^+}}\mathcal{L}^{\mathtt{E}}_{\delta}(\varphi,\mu).$$

This last double minimization problem in φ and μ has the further numerical advantage given by considering a minimization simultaneously in the pair (φ,μ) and can be easily integrated in other more complex optimization problems where the energy $\mathtt{E}(\varphi)$ appears, for example, as regularization term(e.g. TV denoise, Lasso problems) as we will see in what follows.
Thus, in Section 2.7 we first consider the problem of computing 1-Harmonic functions on graphs.
Thus, given a boundary Dirichlet nodes subset $B\subset V$ and a profile function $g\in\mathcal{H}(B)$, we consider the problem of minimizing the graph Total Variation energy with prescribed Dirichlet boundary conditions on B. Therefore, we consider the following optimization problem:

$$\begin{aligned}&\inf_{\varphi\in\mathcal{H}(V)}\sum_{e\in E}|(\nabla\varphi)_e|\\ &s.t.\ \varphi_v=g_v\quad v\in B.\end{aligned}\tag{2.1.19}$$

The Euler-Lagrange equation for (2.1.19) involves the famous 1-Laplacian operator:

$$\Delta_1(\varphi)=-\operatorname{div}\Big(\operatorname{sign}(\nabla\varphi)\Big)\quad\varphi\in\mathcal{H}(V),$$

Where $\operatorname{sign}(\nabla\varphi)$ is defined in (2.4.9).
In the last years this problem, and the related eigenproblem, has been exhaustively studied for it's optimal spectral clustering properties in Machine Learning [84], [72], [19], [35], [41], [44].
Then, we introduce an opportune lifting function:

$$\bar{\varphi}_v:=\begin{cases}0 & v\in V_I\\ g_v & v\in B\end{cases},\tag{2.1.20}$$

where $V=B\cup V_I$, $V_I\cap B=\emptyset$, and problem (2.1.19) simplifies as follows:

$$\inf_{\varphi\in\mathcal{H}_0^B(V)}\sum_{e\in E}|\,(\nabla(\varphi+\bar{\varphi}))_e\,|,$$

Where $\mathcal{H}_0^B(V) := \{\varphi \in \mathcal{H}(V) \mid \varphi_v = 0,\ \forall\, v \in B\}$.
In Proposition 2.7.1 and Proposition 2.7.3, we introduce two preliminaries results essentially based on extending two classical results in [46] which will leads us to show how to integrate our saddle point formulation to solve the 1-Harmonic problem and other related problem which will be consider in the following sections.
Making use of our equivalent saddle point formulation for the graph Total Variation energy, for any $\tilde{\varphi} \in \mathcal{H}(V)$ we define the Lagrangian $\mathtt{L}^1_{\tilde{\varphi}} : (\mathcal{H}(E)^+ \times \mathcal{H}(E)) \to \mathbb{R}$ as:

$$\mathtt{L}^1_{\tilde{\varphi}}(\mu, \sigma) := -\sum_{e\in E} \frac{1}{2}\mu_e|\sigma_e|^2 + \sigma \cdot \nabla\, \tilde{\varphi} + \frac{1}{2}\sum_{e\in E} \mu_e,$$

and the function:

$$\mathtt{L}_1(\tilde{\varphi}) := \inf_{\mu\in\mathcal{H}(E)^+} \sup_{\sigma\in\mathcal{H}(E)} \mathtt{L}^1_{\tilde{\varphi}}(\mu, \sigma).$$

Then we have the following equivalence:

$$\inf_{\varphi\in\mathcal{H}_0^B(V)} \sum_{e\in E} |\,(\nabla(\varphi + \bar{\varphi}))_e\,| = \inf_{\varphi\in\mathcal{H}_0^B(V)} \mathtt{L}_1(\varphi + \bar{\varphi}),$$

So that:

$$\inf_{\varphi\in\mathcal{H}_0^B(V)} \sum_{e\in E} |\,(\nabla(\varphi + \bar{\varphi}))_e\,| = \tag{2.1.21}$$

$$= \inf_{\substack{\mu\,\in\,\mathcal{H}(E)^+ \\ \varphi\,\in\,\mathcal{H}_0^B(V)}} \sup_{\sigma\in\mathcal{H}(E)} -\sum_{e\in E} \frac{1}{2}\mu_e|\sigma_e|^2 + \sigma \cdot \nabla(\varphi + \bar{\varphi}) + \frac{1}{2}\sum_{e\in E} \mu_e \tag{2.1.22}$$

In Theorem 2.7.4, by using Proposition 2.7.1 and Proposition 2.7.3, we are able to prove the equivalence between problem (2.1.21) and problem (2.1.22). Moreover, we can show that there exists at least a saddle point

$$((\varphi^*, \mu^*), \sigma^*) \in \left(\mathcal{H}_0^B(V) \times \mathcal{H}(E)^+\right) \times \mathcal{H}(E)\big),$$

for problem (2.1.22), which satisfies the following "Monge-Kantorovich" equations:

$$\begin{aligned}
\mu_e^*\sigma_e^* &= (\nabla(\varphi^* + \bar{\varphi}))_e\,, && \forall\, e \in E \\
(\operatorname{div}\sigma^*)_v &= 0, && \forall\, v \in V_I \\
\varphi_v^* &= 0, && \forall\, v \in B \\
|\sigma_e^*| &\le 1, && \forall\, e \in E \\
|\sigma_e^*| &= 1, && \forall\, e \in E \ s.t.\ \mu_e^* > 0 \\
\mu_e^* &= |\,\nabla(\varphi^* + \bar{\varphi})_e|, && \forall\, e \in E.
\end{aligned}$$

The existence of a saddle point and the corresponding "Monge-Kantorovich" equations motivated us to use the experience gained with the DMK scheme for the L^1 Optimal transport [54], [59] to tackle problem (2.1.22).

In Section 2.7 we then introduce the DMK scheme for the computation of 1-Harmonic functions underlying the analogies to the Optimal Transport problem on graphs [54]. The proposed scheme can be placed in the framework of the Gradient Flow approach [5] upon composing with the quadratic map:

$$\mu_e = \Psi(\xi)_e = \xi_e^2, \quad \forall\, e \in E.$$

thus the resulting scheme can be genuinely understood in the setting of the update preserving schemes for the positivity constraint.
Then, we introduce the Lyapunov candidate functional:

$$\mathcal{L}(\varphi, \mu) := \sup_{\sigma \in \mathcal{H}(E)} -\sum_{e \in E} \frac{1}{2}\mu_e |\sigma_e|^2 + \sigma \cdot \nabla(\varphi + \bar{\varphi}) + \frac{1}{2}\sum_{e \in E} \mu_e,$$

and we will seek for a minimum in the pair (φ, μ) of the functional

$$\inf_{\substack{\varphi \,\in\, \mathcal{H}_0^B(V) \\ \mu \,\in\, \mathcal{H}(E)^+}} \mathcal{L}(\varphi, \mu).$$

As in [54] a solution will be sought via a gradient descent approach, not applied directly to the functional $\mathcal{L}(\varphi, \mu)$, but rather to its composition with the change of variable $\mu = \Psi(\xi)$. The gradient descent approach applied to the computation of a minimizer (φ^*, ξ^*) of $\mathcal{L}(\varphi, \Psi(\xi))$ has to be intended as a long time solution $(\varphi^*, \xi^*) = \lim_{t\to\infty}(\varphi(t), \xi(t))$, where $(\varphi(t), \xi(t))$ is a solution of the following state-space initial value problem:

$$\begin{aligned}
\mu_e(t) = \Psi(\xi(t))_e, \quad \forall\, e \in E, \\
[\operatorname{Diag} \mu(t)]\, \sigma(t) - \nabla(\varphi(t) + \bar{\varphi}) = 0, \\
(\operatorname{div} \sigma(t))_v = 0, \quad \forall\, v \in V_I, \\
\varphi(t)_v = 0, \quad \forall\, v \in B, \\
\partial_t \xi_e(t) = -\left[\partial_\xi \mathcal{L}(\varphi(t), \Psi(\xi(t)))\right]_e = \xi_e(t)|\sigma_e(t)|^2 - \xi_e(t), \quad \forall\, e \in E, \\
\xi_e(0) = \xi_{0e} \neq 0, \quad \forall\, e \in E.
\end{aligned} \tag{2.1.23}$$

Moreover, if $\xi(t)$ is a solution of (2.1.23), the relation $\mu(t) = \Psi(\xi(t))$ implies that:

$$\partial_t \mu_e(t) = \partial_\xi \Psi(\xi(t))_e \partial_t \xi_e(t) = \xi_e(t) \partial_t \xi_e, \quad \forall\, e \in E,$$

thus $\mu(t)$ can be reinterpreted as a "classical Gradient Descent" dynamics :

$$\partial_t \mu_e(t) = \mu_e(t)|\sigma_e(t)|^2 - \mu_e(t), \quad \mu_e(0) = \mu_{0e} > 0 \quad \forall\, e \in E. \tag{2.1.24}$$

The dynamics in (2.1.23) involves the following saddle point linear system:

$$\begin{aligned}
&[\operatorname{Diag} \mu(t)]\, \sigma(t) - \nabla(\varphi(t) + \bar{\varphi}) = 0, \\
&(\operatorname{div} \sigma(t))_v = 0, \quad \forall\, v \in V_I, \\
&\varphi(t)_v = 0, \quad \forall\, v \in B,
\end{aligned}$$

and hence the following saddle point matrix:

$$\left(\begin{array}{c|c} \operatorname{Diag}\mu(t) & -\nabla \\ \hline \operatorname{div} & \mathbf{0} \end{array}\right).$$

since 1-Harmonic functions are flat solution by the improving sparsity on the gradient induced by the Total Variation energy and our optimal density μ^* satisfies $\mu^* = |\nabla(\varphi + \bar{\varphi})|$, the variable $\mu(t)$ will inevitably go toward zero along the descending dynamics, thus, this linear system will inevitably become very ill-conditioned during the minimization flow. The strategy is therefore to consider an appropriately small Tikhonov parameter $\delta > 0$ to circumvent the ill-conditioning but maintaining sufficient accuracy:

$$\left(\begin{array}{c|c} \operatorname{Diag}\mu(t) + \delta & -\nabla \\ \hline \operatorname{div} & \mathbf{0} \end{array}\right).$$

Hence the δ-regularized version of (2.8.5) becomes equivalent to the following reduced lifted linear system:

$$\begin{aligned} &\sigma_e(t) = \frac{(\nabla(\varphi(t) + \bar{\varphi}))_e}{\mu_e(t) + \delta}, \quad \forall\, e \in E, \\ &(\Delta_{\frac{1}{\mu(t)+\delta}}(\varphi(t) + \bar{\varphi}))_v = 0, \quad \forall\, v \in V_I, \\ &\varphi(t)_v = 0 \quad \forall\, v \in B. \end{aligned} \tag{2.1.25}$$

It turns out that the linear system in (2.1.25) is derived by considering the regularized functional:

$$\begin{aligned} \mathcal{L}_\delta(\varphi, \mu) :&= \sup_{\sigma \in \mathcal{H}(E)} -\sum_{e\in E} \frac{1}{2}(\mu_e + \delta)|\sigma_e|^2 + \sigma \cdot \nabla(\varphi + \bar{\varphi}) + \frac{1}{2}\sum_{e\in E}\mu_e \\ &= \sum_{e\in E} \frac{1}{2}\frac{|\nabla(\varphi + \bar{\varphi})_e|^2}{(\mu_e + \delta)} + \frac{1}{2}\sum_{e\in E}\mu_e, \end{aligned}$$

instead of $\mathcal{L}(\varphi, \mu)$ and the following approximated problem:

$$\inf_{\substack{\varphi \,\in\, \mathcal{H}_0^B(V) \\ \mu \,\in\, \mathcal{H}(E)^+}} \mathcal{L}_\delta(\varphi, \mu) = \inf_{\substack{\varphi \,\in\, \mathcal{H}_0^B(V) \\ \mu \,\in\, \mathcal{H}(E)^+}} \sum_{e\in E} \frac{1}{2}\frac{|\nabla(\varphi + \bar{\varphi})_e|^2}{(\mu_e + \delta)} + \frac{1}{2}\sum_{e\in E}\mu_e. \tag{2.1.26}$$

Using the KKT conditions is possible to show that a solution (φ^*, μ^*) for (2.1.26) satisfies:

$$\begin{aligned} |\nabla(\varphi^* + \bar{\varphi})_e| &= \mu_e^* + \delta, \quad e \in E,\ \mu_e^* > 0 \\ |\nabla(\varphi^* + \bar{\varphi})_e| &\le \delta, \quad e \in E,\ \mu_e^* = 0. \end{aligned}$$

Thus the parameter δ controls well the accuracy and we are expecting to have good approximations if δ is opportunely small.

The corresponding version of the dynamics in (2.1.23), (2.1.24) for problem (2.1.26) is:

$$\begin{aligned} \sigma_e(t) &= \frac{(\nabla(\varphi(t)+\bar{\varphi}))_e}{\mu_e(t)+\delta} \quad \forall\, e \in E \\ (\Delta_{\frac{1}{\mu(t)+\delta}}(\varphi(t)+\bar{\varphi}))_v &= 0 \quad \forall\, v \in V_I \\ \varphi(t)_v &= 0 \quad \forall\, v \in B \\ \partial_t \mu_e(t) = \mu_e(t)|\sigma_e(t)|^2 - \mu_e(t), &\quad \mu_e(0) = \mu_{0_e} > 0 \quad \forall\, e \in E. \end{aligned} \tag{2.1.27}$$

In [59] it was shown that a solution μ^* of the Optimal Transport counterpart of (2.1.27) Γ-converges to a solution of the original problem when $\delta \to 0$.
We propose moreover three time discretization approaches for the dynamics in (2.1.27) and some interesting numerical applications showing the convergence rate and the stability of our numerical scheme.
In Subsection 2.8.2 we show an heuristics based on Lie derivatives along ad-hoc chosen vector fields to reinterpret our update preserving scheme derived by composing with the quadratic map, as a type of projected gradient descent. We also propose a variant based on the logistic map to extend this technique to the case of an interval constraint of the form $a \leq \mu \leq b$.
The 1-Harmonic problem has to be considered as a starting point test problem for this thesis . As a result, in virtue of the analoguous saddle point formulation for the p-Dirichlet energy, in Section 2.9 we extend the DMK scheme for the numerical solution of the graph p-Poisson problem, $1 < p < 2$, with a given loading term and Dirichlet boundary conditions:

$$\begin{aligned} (\Delta_p\, \varphi)_v &= f_v \quad v \in V_I \\ \varphi_v &= g_v \quad v \in B. \end{aligned}$$

where $g \in \mathcal{H}(B)$ is the Dirichlet profile function and $f \in \mathcal{H}(V_I)$ is the loading or forcing term.
As for the case of 1-Harmonic functions we will seek for a solution of the p-Poisson problem by first introducing a lifting function $\bar{\varphi}$ and looking for a minimizer of the following problem:

$$\inf_{\varphi \in \mathcal{H}_0^B(V)} \sum_{e \in E} \frac{|\,(\nabla(\varphi+\bar{\varphi}))_e\,|^p}{p} - \sum_{v \in V_I} f_v \varphi_v. \tag{2.1.28}$$

Observing the similarity with the 1-Harmonic problem, we use our saddle point formulation for the p-Dirichlet Energy and we introduce the following problem:

$$\inf_{\substack{\mu \,\in\, \mathcal{H}(E)^+ \\ \varphi \,\in\, \mathcal{H}_0^B(V)}} \sup_{\sigma \in \mathcal{H}(E)} -\sum_{e \in E} \frac{1}{2}\mu_e|\sigma_e|^2 + \sigma \cdot \nabla(\varphi+\bar{\varphi}) - \sum_{v \in V_I} f_v \varphi_v + \frac{1}{2\gamma}\sum_{e \in E} \mu_e^{\gamma}, \tag{2.1.29}$$

where $\gamma = \frac{p}{2-p}$.
In Theorem 2.9.5 we show that problem (2.1.28) is equivalent to (2.1.29) and

that the exists a unique saddle point $((\varphi^*, \mu^*), \sigma^*)$ which satisfies the following equations:

$$\begin{aligned} \mu_e^* \sigma_e^* &= (\nabla(\varphi^* + \bar{\varphi}))_e\,, \quad \forall\, e \in E \\ -(\operatorname{div} \sigma^*)_v &= f_v, \quad \forall\, v \in V_I \\ \varphi_v^* &= 0, \quad \forall\, v \in B \\ \mu_e^* = |\sigma_e^*|^{p'-2} &= |\,\nabla(\varphi^* + \bar{\varphi})_e|^{2-p}, \quad \forall\, e \in E. \end{aligned}$$

As a consequence, φ^* is the unique solution of the p-Poisson problem.
Then, we consider the regularized functional:

$$\begin{aligned} &\mathcal{L}_\delta^p(\varphi, \mu) := \\ &= \sup_{\sigma \in \mathcal{H}(E)} -\sum_{e \in E} \frac{1}{2}(\mu_e + \delta)|\sigma_e|^2 + \sigma \cdot \nabla(\varphi + \bar{\varphi}) - \sum_{v \in V_I} f_v \varphi_v + \frac{1}{2\gamma} \sum_{e \in E} \mu_e^\gamma = \\ &= \sum_{e \in E} \frac{1}{2} \frac{|\,\nabla(\varphi + \bar{\varphi})_e|^2}{(\mu_e + \delta)} - \sum_{v \in V_I} f_v \varphi_v + \frac{1}{2\gamma} \sum_{e \in E} \mu_e^\gamma, \end{aligned}$$

and the following double minimization problem:

$$\inf_{\substack{\varphi \,\in\, \mathcal{H}_0^B(V) \\ \mu \,\in\, \mathcal{H}(E)^+}} \mathcal{L}_\delta^p(\varphi, \mu),$$

which is the Tikhonov regularization of problem (2.1.29).
The corresponding derived version of the dynamics in (2.1.27) reads as follows:

$$\begin{aligned} \sigma_e(t) &= \frac{(\nabla(\varphi(t) + \bar{\varphi}))_e}{\mu_e(t) + \delta} \quad \forall\, e \in E \\ (\Delta_{\frac{1}{\mu(t)+\delta}}(\varphi(t) + \bar{\varphi}))_v &= f_v \quad \forall\, v \in V_I \\ \varphi(t)_v &= 0 \quad \forall\, v \in B \\ \partial_t \mu_e(t) = \mu_e(t)|\sigma_e(t)|^2 - \mu_e(t)^{\frac{p}{2-p}}, &\quad \mu_e(0) = \mu_{0e} > 0 \quad \forall\, e \in E. \end{aligned} \tag{2.1.30}$$

We propose moreover, an improved version for the dynamics in (2.1.30) which has been observed to converge faster in our numerical experiments and is derived by composing with the map:

$$\mu_e = \Psi(\xi_e) := |\xi_e|^{\frac{2(2-p)}{p}}, \quad \forall\, e \in E,$$

leading to the following new dynamics for the density μ in (2.1.30):

$$\partial_t \mu_e(t) = \mu_e(t)^{\frac{4-3p}{2-p}} |\sigma_e(t)|^2 - \mu_e(t), \quad \forall\, e \in E.$$

In Section 2.10 we further extend our DMK scheme to the numerical computation of Minimal Surfaces on graphs with a given profile Dirichlet boundary conditions. Thus we consider the following problem:

$$\inf_{\varphi \in \mathcal{H}_0^B(V)} \sum_{e \in E} \sqrt{1 + |\,\nabla(\varphi + \bar{\varphi})_e|^2}. \tag{2.1.31}$$

Where we have selected a Dirichlet boundary subset $B \subset V$, a profile function $g \in \mathcal{H}(B)$ and an appropriate lifting function $\bar{\varphi}$ as in (2.1.20). We then briefly show how to extend the DMK scheme presented in (2.1.27) and (2.1.30) for the numerical solution of problem (2.1.31) providing moreover some numerical results. After that, we show a very interesting application of the proposed techniques to the numerical solution of the so called Obstacle Problem [92] which is one of the most famous problem involving the Minimal Surfaces Energy. In the graph setting, the Obstacle Problem is formulated as the problem to seek for the equilibrium position of the membrane such that it lies above the body represented by a function $\phi \in \mathcal{H}(V_I)$ with Dirichlet boundary conditions on a boundary subset $B \subset V$. The problem can be formulated adding the further constraint $\varphi_v \geq \phi_v$, $\forall\, v \in V_I$ to (2.1.31):

$$\inf_{\substack{\varphi \in \mathcal{H}_0^B(V) \\ \varphi_v \geq \phi_v,\ \forall\, v \in V_I}} \sum_{e \in E} \sqrt{1 + |\, \nabla(\varphi + \bar{\varphi})_e|^2}. \tag{2.1.32}$$

As done for the 1-Harmonic case, we recast problem (2.1.32) as a doubled minimization problem in the variable φ and a density $\mu \geq 0$. Also for this case, we propose a numerical scheme based on an extension of the DMK scheme in (2.1.27), where we introduce two minimizing flows, one for the variable μ and one for the variable φ, composing with the quadratic maps:

$$\begin{aligned} \mu_e &= \xi_e^2, \quad \forall\, e \in E \\ \varphi_v &= \phi_v + h_v^2, \quad \forall\, v \in V_I, \end{aligned}$$

in order to preserve the constraints given an initial $\mu(0) > 0$ and an initial $\varphi_v(0) > \phi_v$, $\forall\, v \in V_I$. Moreover, we show that introducing a semi implicit time discretization approach the problem can be easily implemented. Finally, we provide a numerical example showing the convergence rate of our scheme and the constraints preserving along the minimization flow.
In Section 2.11 we show an application of our techniques for the Total Variation and the l_1 norm regularization in optimization problems, with emphasis on the graph setting applications. We first introduce the generalized Tikhonov regularization approach in both the continuous and the discrete framework, showing also a brief review on the common techniques in literature(Spilt Forward Backward Proximal Map approach, Augmented Lagrangian approach, Bregman iteration approach).
Then, we show in detail how to extend the EDMK scheme for the Total Variation regularization on graphs.
The main idea is to consider the regularized functional introduced in Subsection 2.5.1, instead of the Total Variation energy. Thus we call:

$$TV_\delta(\varphi) := \inf_{\mu \in \mathcal{H}(E)^+} \sum_{e \in E} \frac{1}{2} \frac{|(\nabla\, \varphi)_e|^2}{(\mu_e + \delta)} + \frac{1}{2} \sum_{e \in E} \mu_e, \quad \varphi \in \mathcal{H}(V),$$

and we consider the following approximated general TV regularization problem:

$$\begin{aligned}&\min_{\varphi\in\mathcal{H}(V)} F(\varphi) + \lambda TV_\delta(\varphi) = \\ &= \min_{\substack{\varphi\,\in\,\mathcal{H}(V)\\ \mu\,\in\,\mathcal{H}(E)^+}} F(\varphi) + \lambda\left(\sum_{e\in E}\frac{1}{2}\frac{|(\nabla\varphi)_e|^2}{(\mu_e+\delta)} + \frac{1}{2}\sum_{e\in E}\mu_e\right).\end{aligned} \tag{2.1.33}$$

where $F : V \to \mathbb{R}$ is a differentiable function and λ is a positive Tikhonov regularization parameter.
We provide moreover illustrative examples on how to extend our EDMK scheme for the numerical solution of a problem of the type as (2.1.33) in the unconstrained case and in the case of positivity and interval constraints for the variable φ.
Then, we briefly show, as a direct extension, how to adapt these techniques on the case where the Total Variation is substituted with the l_1 norm as the regularization term.
As an application, we show how to recover an EDMK scheme formulation for the numerical solution of the 1-D signal TV denoising or the Rudin-Osher-Fatemi problem, showing also a numerical example for a very noisy digital signal reconstruction.
Finally, we show an application of the EDMK scheme for the l_1 norm regularization on a non common problem, namely the Compress Modes for the Graph Laplacian operator, or the graph-based Sparse PCA [106].

2.2 The case $1 < p < 2$

Consider an open Lipschitz domain $\Omega \in \mathbb{R}^n$. Given a parameter $p \in \mathbb{R}$ with $1 < p < 2$ we define the p-Dirichlet energy on $W^{1,p}(\Omega)$ as:

$$\mathcal{E}_p(\varphi) := \int_\Omega \frac{1}{p}|\nabla\varphi|^p. \tag{2.2.1}$$

We recall here the Legendre transform for a sufficiently regular function $G(x)$:

$$G^*(x^*) = \sup_x \int_\Omega x^* x - G(x).$$

In particular if G is proper, lower semi-continuous and convex then is possible to show that:

$$G(x) = \sup_{x^*} \int_\Omega x x^* - G^*(x^*).$$

Consider now the p-Dirichlet energy (2.2.1) and observe that we can rewrite it as:

$$\begin{aligned}&\mathcal{E}_p(\varphi) = G(\nabla\varphi)\\ &G(x) : x \mapsto \int_\Omega \frac{|x|^p}{p}.\end{aligned} \tag{2.2.2}$$

The Legendre transform $G^*(x^*)$ is easy to compute and reads as follows:

$$G^*(x^*) = \int_\Omega \frac{|x^*|^{p'}}{p'},$$

where $p' = \frac{p}{p-1}$ is the conjugate exponent.
The function G in (2.2.2) is clearly proper, lower semi-continuous and convex therefore we can apply twice the Legendre transform obtaining the dual definition of the p-Dirichlet energy :

$$\mathcal{E}^*_{p'}(\varphi) := G^{**}(\nabla\varphi) = \sup_\sigma -\int_\Omega \frac{|\sigma|^{p'}}{p'} + \int_\Omega \sigma\cdot\nabla\varphi,$$

where $\sigma \in \left[W^{p'}(\mathrm{div},\Omega)\right]^n := \{v \in [L^{p'}(\Omega)]^n | \,\mathrm{div}\, v \in L^{p'}(\Omega)\}$.
Observe now that:

$$\begin{aligned}\int_\Omega \frac{|\sigma|^{p'}}{p'} &= \frac{H(|\sigma|^2)}{2}\\ H(y) &= \frac{\int_\Omega |y|^{\frac{p'}{2}}}{\frac{p'}{2}}.\end{aligned} \tag{2.2.3}$$

Since $1 < p < 2$ we have that $p' > 2$ and the function H in (2.2.3) is proper, lower semi-continuous and convex. By applying twice the Legendre transform we obtain:

$$H(y) = H^{**}(y) = \sup_{y^*} < y, y^* > - \frac{\int_\Omega |y^*|^{\frac{p'}{p'-2}}}{\frac{p'}{p'-2}}. \tag{2.2.4}$$

Evaluating (2.2.4) in $y = |\sigma|^2$ and setting $y^* = \mu \in L^{\frac{p'}{p'-2}}(\Omega)$ we get:

$$\begin{aligned}H(|\sigma|^2) &= \sup_\mu < \mu, |\sigma|^2 > - \frac{\int_\Omega |\mu|^{\frac{p'}{p'-2}}}{\frac{p'}{p'-2}}\\ &= \sup_{\mu\geq 0} < \mu, |\sigma|^2 > - \frac{\int_\Omega \mu^{\frac{p'}{p'-2}}}{\frac{p'}{p'-2}},\end{aligned} \tag{2.2.5}$$

where the constraint $\mu \geq 0$ follows by observing that if we call:

$$\varepsilon(\mu,\sigma) := < \mu, |\sigma|^2 > - \frac{\int_\Omega |\mu|^{\frac{p'}{p'-2}}}{\frac{p'}{p'-2}},$$

then clearly a supremum in μ of $\varepsilon(\mu,\sigma)$ exists (proposition 1.2 p.35 of [46]), the functional $-\varepsilon(\mu,\sigma)$ is convex (strictly since $2 < p' < \infty$) and lower semi-continuous in μ moreover $\lim_{||\mu||\to\infty} -\varepsilon(\mu,\sigma) = \infty$. Obviously, the supremum in

$\mu \geq 0$ is less or equal the unconstrained one, therefore it suffices to prove the other inequality which is easy since :

$$\sup_{\mu} \varepsilon(\mu, \sigma) \leq \sup_{\mu} \varepsilon(|\mu|, \sigma) = \sup_{\mu \geq 0} \varepsilon(\mu, \sigma).$$

Using (2.2.5) we obtain the following duality based definition of $\mathcal{E}^*_{p'}(\varphi)$:

$$\begin{aligned} \mathcal{L}^*_p(\varphi) : &\overset{(2.2.5)}{=} \sup_{\sigma} \left[-\sup_{\mu \geq 0} \int_\Omega \frac{1}{2}\mu|\sigma|^2 - \frac{1}{2}\int_\Omega \frac{\mu^{\frac{p}{2-p}}}{\frac{p}{2-p}} \right] + \int_\Omega \sigma \cdot \nabla \varphi \\ &= \sup_{\sigma} \inf_{\mu \geq 0} - \int_\Omega \frac{1}{2}\mu|\sigma|^2 + \frac{1}{2}\int_\Omega \frac{\mu^{\frac{p}{2-p}}}{\frac{p}{2-p}} + \int_\Omega \sigma \cdot \nabla \varphi. \end{aligned} \tag{2.2.6}$$

As often happens in optimization theory, one can also consider the dual problem associated with $\mathcal{L}^*_p(\varphi)$. Since we are dealing with a saddle point problem, the standard theory of duality in these cases (see for example [43] and [46] for an exhaustive treatment) tells us that the dual problem is achieved by exchanging the "inf" with the "sup", therefore formally we define the following dual functional:

$$\mathcal{L}_p(\varphi) := \inf_{\mu \geq 0} \sup_{\sigma} - \int_\Omega \frac{1}{2}\mu|\sigma|^2 + \int_\Omega \sigma \cdot \nabla \varphi + \frac{2-p}{2p}\int_\Omega \mu^{\frac{p}{2-p}}. \tag{2.2.7}$$

For completeness we compute the dual of $\mathcal{L}^*_p(\varphi)$ with the standard techniques in [46].

Set $V = \left[W^{p'}(\mathrm{div}, \Omega)\right]^n$ and $Y = L^{\frac{p'}{2}}(\Omega)$. We remind also that $\sigma \in V$ and $\mu \in Y^*$.

From now on we will tacitly omit belonging to the Banach spaces inside the "inf" or the "sup" when confusion doesn't arise.

Consider now the functional $\mathcal{L}^*_p(\varphi)$, clearly we have:

$$\mathcal{L}^*_p(\varphi) = -\tilde{\mathcal{L}}^*_p(\varphi), \tag{2.2.8}$$

where:

$$\begin{aligned} \tilde{\mathcal{L}}^*_p(\varphi) &:= \inf_{\sigma \in V} \sup_{\mu \geq 0} \int_\Omega \frac{1}{2}\mu|\sigma|^2 - \frac{1}{2\gamma}\int_\Omega \mu^\gamma - \int_\Omega \sigma \cdot \nabla \varphi \\ &= \inf_{\sigma \in V} J_\varphi(\sigma), \end{aligned}$$

and

$$J_\varphi(\sigma) := \sup_{\mu \geq 0} \int_\Omega \frac{1}{2}\mu|\sigma|^2 - \frac{1}{2\gamma}\int_\Omega \mu^\gamma - \int_\Omega \sigma \cdot \nabla \varphi,$$

where we set for simplicity $\gamma = \frac{p}{2-p}$ as in (2.2.7).

We focus our attention to $\tilde{\mathcal{L}^*}_p(\varphi)$. Define now the perturbation function $\Phi : (V \times Y) \to \bar{\mathbb{R}}$ as:

$$\Phi(\sigma, \rho) := \sup_{\mu \geq 0} \int_\Omega \frac{\mu(|\sigma|^2 + 2\rho)}{2} - \frac{1}{2\gamma}\int_\Omega \mu^\gamma - \int_\Omega \sigma \cdot \nabla \varphi, \tag{2.2.9}$$

where $\rho \in Y$ is the perturbation parameter.
Clearly we have that:

$$\Phi(\sigma, 0) = J_\varphi(\sigma).$$

We introduce now the Lagrangian $L : (V \times Y^*) \to \bar{\mathbb{R}}$ as:

$$L(\sigma, \mu) := \int_\Omega \frac{1}{2}\mu|\sigma|^2 - \frac{1}{2\gamma}\int_\Omega \mu^\gamma - \int_\Omega \sigma \cdot \nabla\,\varphi - \chi_{\mu\geq 0}, \tag{2.2.10}$$

where $\chi_{\mu\geq 0}$ is the indicator function:

$$\chi_{\mu\geq 0} := \begin{cases} +\infty & \mu \in \{\mu \geq 0\}^C \\ 0 & \mu \in \{\mu \geq 0\}, \end{cases}$$

and the sets $\{\mu \geq 0\}$, $\{\mu \geq 0\}^C$, are defined as

$$\{\mu \geq 0\} = \{\mu \in Y^* \mid \mu \geq 0 \ a.e.\ in\ \Omega\}$$

$$\{\mu \geq 0\}^C = \{\mu \in Y^* \mid \exists\, A \subseteq \Omega,\ \mathcal{L}(A) > 0,\ \mu < 0 \ a.e.\ in\ A\}.$$

Observe that our perturbation function can be written in a more convenient way using the Lagrangian function as:

$$\begin{aligned} \Phi(\sigma, \rho) &= \sup_\mu < \rho, \mu > + L(\sigma, \mu) \\ &= (-L_\sigma)^*(\rho), \end{aligned} \tag{2.2.11}$$

where $(-L_\sigma)^*$ is the Legendre transform of the map $-L_\sigma : \mu \mapsto -L(\sigma, \mu)$.
Clearly the map $-L_\sigma$ is lower semi-continuous, convex and proper $\forall\, \sigma \in V$.
Again, iterating the Legendre transform in (2.2.11) and evaluating in μ we get:

$$\Phi^*_\sigma(\mu) = -L_\sigma(\mu) \quad \forall\, \sigma \in V, \tag{2.2.12}$$

and Φ^*_σ is the Legendre transform of the map $\Phi_\sigma : \rho \mapsto \Phi(\sigma, \rho)$. Consider the Legendre transform of $\Phi^*(\sigma^*, \rho^*)$, we have that:

$$\begin{aligned} \Phi^*(0, \mu) &= \sup_{\sigma\in V, \rho \in Y} < \mu, \rho > - \Phi(\sigma, \rho) \\ &= \sup_{\sigma \in V} \Phi^*_\sigma(\mu) = \sup_{\sigma \in V} -L_\sigma(\mu), \end{aligned} \tag{2.2.13}$$

where the last equality comes from (2.2.12).
Now, by definition, the dual problem of $\tilde{\mathcal{L}^*}_p(\varphi)$ is:

$$(\tilde{\mathcal{L}}_p(\varphi)) := (\tilde{\mathcal{L}}^*_p(\varphi))^* = \sup_{\mu \in Y^*} -\Phi^*(0, \mu) = \sup_{\mu \in Y^*} \inf_{\sigma \in V} L(\sigma, \mu), \tag{2.2.14}$$

whence the last equality in (2.2.14) comes from (2.2.13).
Observe that, by the definition of $\tilde{\mathcal{L}^*}_p(\varphi)$ in (2.2.8):

$$(\mathcal{L}^*_p(\varphi))^* = -(\tilde{\mathcal{L}}_p(\varphi)),$$

and finally:

$$\begin{aligned}(\mathcal{L}_p^*(\varphi))^* &= \inf_{\mu\in Y^*}\sup_{\sigma\in V} -L(\sigma,\mu)\\ &= \inf_{\substack{\mu\in Y^*\\ \mu\geq 0}}\sup_{\sigma\in V} -\int_\Omega \frac{1}{2}\mu|\sigma|^2 + \int_\Omega \sigma\cdot\nabla\varphi + \frac{1}{2\gamma}\int_\Omega \mu^\gamma, \end{aligned} \tag{2.2.15}$$

which is precisely $\mathcal{L}_p(\varphi)$ defined in (2.2.7).
We investigate now the properties of the perturbation function $\Phi(\sigma,\rho)$.
We denote as $\Gamma_0(V\times Y)$ the set of functions (other than the constants $+\infty$ and $-\infty$) from $V\times Y$ to $\bar{\mathbb{R}}$ which are pointwise supremum of a family of continuous affine functions. We have the following Lemma:

Lemma 2.2.1. $\Phi(\sigma,\rho)\in\Gamma_0(V\times Y)$.

Proof. Observe that $\Phi(\sigma,\rho)$ is proper, lower semi-continuous and clearly convex since it is a supremum of a family of convex functions, therefore $\Phi(\sigma,\rho)\in\Gamma_0(V\times Y)$ by [46] Proposition 3.1 p.14. □

Moving on, we define the following useful sets:

$$\begin{aligned}\Omega_{|\sigma|^2+2\rho\geq 0} &= \{x\in\Omega \mid |\sigma(x)|^2+2\rho(x)\geq 0\},\\ \Omega_{|\sigma|^2+2\rho< 0} &= \{x\in\Omega \mid |\sigma(x)|^2+2\rho(x)< 0\}.\end{aligned}$$

Consider now problem (2.2.9), by a simple direct computation we have:

$$\sup_{\mu\geq 0}\int_{\Omega_{|\sigma|^2+2\rho\geq 0}} \frac{\mu(|\sigma|^2+2\rho)}{2} - \frac{1}{2\gamma}\int_{\Omega_{|\sigma|^2+2\rho\geq 0}}\mu^\gamma = \frac{1}{2\gamma'}\int_{\Omega_{|\sigma|^2+2\rho\geq 0}}(|\sigma|^2+2\rho)^{\gamma'}, \tag{2.2.16}$$

where $\gamma' = \frac{\gamma}{\gamma-1}$.
Observe that defining:

$$\tilde{\Phi}(\sigma,\rho) := \sup_{\substack{\mu\geq 0\\ \mu(x)=0,\,\forall\, x\,\in\,\Omega_{|\sigma|^2+2\rho<0}}} \int_\Omega \frac{\mu(|\sigma|^2+2\rho)}{2} - \frac{1}{2\gamma}\int_\Omega \mu^\gamma - \int_\Omega \sigma\cdot\nabla\varphi,$$

then clearly we have:

$$\tilde{\Phi}(\sigma,\rho)\leq\Phi(\sigma,\rho). \tag{2.2.17}$$

Obviously:

$$\int_{\Omega_{|\sigma|^2+2\rho<0}} \frac{\bar{\mu}(|\sigma|^2+2\rho)}{2} - \frac{1}{2\gamma}\int_{\Omega_{|\sigma|^2+2<0}}\bar{\mu}^\gamma < 0\,,\quad \forall\,\bar{\mu}\geq 0,$$

hence by splitting $\Omega = \Omega_{|\sigma|^2+2\rho\geq 0} \cup \Omega_{|\sigma|^2+2\rho<0}$ we have:

$$\Phi(\sigma,\rho) \leq \sup_{\mu\geq 0} \int_{\Omega_{|\sigma|^2+2\rho\geq 0}} \frac{\mu(|\sigma|^2+2\rho)}{2} - \frac{1}{2\gamma}\int_{\Omega_{|\sigma|^2+2\rho\geq 0}} \mu^{\gamma} - \int_{\Omega} \sigma\cdot\nabla\,\varphi = \tilde{\Phi}(\sigma,\rho). \tag{2.2.18}$$

Therefore, by (2.2.17),(2.2.18) and (2.2.16) our perturbation function becomes:

$$\Phi(\sigma,\rho) = \frac{1}{2\gamma'}\int_{\Omega_{|\sigma|^2+2\rho\geq 0}} (|\sigma|^2+2\rho)^{\gamma'} - \int_{\Omega}\sigma\cdot\nabla\,\varphi. \tag{2.2.19}$$

Moreover, we have the following result.

Theorem 2.2.2. *Let $\Omega \in \mathbb{R}^n$ be an open Lipschitz domain and set $p \in \mathbb{R}$ with $1 < p < 2$. For a given $\varphi \in W^{1,p}(\Omega)$ we define the Lagrangian $\mathcal{L}^p_\varphi(\mu,\sigma) : (L^{\frac{p}{2-p}}(\Omega) \times \left[W^{p'}(\mathrm{div},\Omega)\right]^n) \to \mathbb{R}$ as:*

$$\mathcal{L}^p_\varphi(\mu,\sigma) := -\int_\Omega \frac{1}{2}\mu|\sigma|^2 + \int_\Omega \sigma\cdot\nabla\,\varphi + \frac{2-p}{2p}\int_\Omega \mu^{\frac{p}{2-p}}.$$

Then we have that:

$$\mathcal{E}_p(\varphi) = \inf_{\substack{\mu\,\in\, L^{\frac{p}{2-p}}(\Omega)\\ \mu\,\geq\,0}} \sup_{\sigma\in\left[W^{p'}(\mathrm{div},\Omega)\right]^n} \mathcal{L}^p_\varphi(\mu,\sigma),$$

and the unique saddle point (μ^*,σ^*) for $\mathcal{L}^p_\varphi(\mu,\sigma)$ satisfies the following extremality relations:

$$\begin{aligned} \mu^*\sigma^* &= \nabla\,\varphi \\ \mu^* &= |\sigma^*|^{p'-2} = |\nabla\,\varphi|^{2-p}. \end{aligned} \tag{2.2.20}$$

Proof. Consider the functionals $\mathcal{L}^*_p(\varphi)$ and $\mathcal{L}_p(\varphi)$, defined in (2.2.6) and in (2.2.7), respectively. We have already seen in (2.2.6) the equivalence between $\mathcal{L}^*_p(\varphi)$ and $\mathcal{E}_p(\varphi)$ whence the unique solution σ^* for (2.2.6) satisfies by construction:

$$|\sigma^*|^{p'-2}\sigma^* = \nabla\,\varphi. \tag{2.2.21}$$

It remains to show that $\mathcal{L}_p(\varphi) = \mathcal{L}^*_p(\varphi)$ and that there exist a unique saddle point for the Lagrangian $\mathcal{L}^p_\varphi(\mu,\sigma)$.
We point out that working with $\tilde{\mathcal{L}}^*_p(\varphi)$ as defined in (2.2.8), instead of $\mathcal{L}^*_p(\varphi)$ is the same a part from a change of sign. Therefore, we will call $(\mathcal{P})$, the primal problem:

$$\tilde{\mathcal{L}}^*_p(\varphi) = \inf_\sigma \left\{ \sup_{\mu\geq 0} -\mathcal{L}^p_\varphi(\mu,\sigma) \right\} \quad (\mathcal{P}),$$

and $(\mathcal{P}^*)$, the dual problem:

$$\tilde{\mathcal{L}}_p(\varphi) = \sup_{\mu\geq 0} \left\{ \inf_\sigma -\mathcal{L}^p_\varphi(\mu,\sigma) \right\} \quad (\mathcal{P}^*).$$

Consider now the perturbation function $\Phi(\sigma, \rho)$ in (2.2.9). In Lemma 2.2.1 we have already shown that $\Phi(\sigma, \rho) \in \Gamma_0(V \times Y)$ and we have already state that problem $(\mathcal{P})$ have a solution and that it is finite, therefore, by [46] Propositions 2.1 p.51 and Corollary 2.1 p.52 it suffices to show that problem $(\mathcal{P})$ is stable.
We will apply [46] proposition 2.3 p.52, all the hypothesis are satisfied, we only have to show that there exists a $\sigma_0 \in V$ such that $\rho \mapsto \Phi(\sigma_0, \rho)$ is finite and continuous at $0(\in Y)$.
Set:

$$\sigma_0 = |\nabla \varphi|^{p-1} \operatorname{sign}(\nabla \varphi).$$

Clearly $\sigma_0 \in V$ where $\operatorname{sign}(\nabla \varphi)$ is the vector field given by the standard convention:

$$\operatorname{sign}(\nabla \varphi)_i = \begin{cases} \frac{(\nabla \varphi(x))_i}{|\nabla \varphi(x)|} & x \in \Omega \ s.t. \ |\nabla \varphi(x)| > 0 \\ [-1, 1] & x \in \Omega \ s.t. \ |\nabla \varphi(x)| = 0 \end{cases} \quad i = 1, .., n.$$

Using (2.2.19), it is easy to see that:

$$\Phi(\sigma_0, 0) = -\mathcal{E}_p(\varphi),$$

which is finite by hypothesis since $\varphi \in W^{1,p}(\Omega)$ and clearly the map $\rho \mapsto \Phi(\sigma_0, \rho)$ is continuous at $\rho = 0$.
This shows that problem $(\mathcal{P})$ is stable, $\inf(\mathcal{P}) = \sup(\mathcal{P}^*)$, and $(\mathcal{P}^*)$ has at least one solution μ^*.
We will show now that the optimal couple (μ^*, σ^*) is a saddle point.
By [46] Proposition 2.4 p.53, the optimal couple (μ^*, σ^*) is linked by the extremality relation:

$$\Phi(\sigma^*, 0) + \Phi^*(0, \mu^*) = 0. \tag{2.2.22}$$

Using (2.2.10), (2.2.13) and (2.2.19), (2.2.22) becomes:

$$\frac{1}{2\gamma'} \int_\Omega |\sigma^*|^{2\gamma'} - \int_\Omega \sigma^* \cdot \nabla \varphi = \tag{2.2.23}$$

$$= \inf_\sigma \int_\Omega \frac{1}{2} \mu^* |\sigma|^2 - \frac{1}{2\gamma} \int_\Omega \mu^{*\gamma} - \int_\Omega \sigma \cdot \nabla \varphi \tag{2.2.24}$$

$$\leq \int_\Omega \frac{1}{2} \mu^* |\sigma^*|^2 - \frac{1}{2\gamma} \int_\Omega \mu^{*\gamma} - \int_\Omega \sigma^* \cdot \nabla \varphi. \tag{2.2.25}$$

Observe that if $\operatorname{supp}(|\nabla \varphi|) \subseteq \operatorname{supp}(\mu^*)$ then a solution for (2.2.24) exists and it satisfies (2.2.20), to see this it suffices to note that (2.2.24) is differentiable in σ and strictly convex so that the solution is a zero of the first derivative. Moreover, (2.2.20) is also a necessary condition, otherwise either $\operatorname{supp}(\mu^*) \cap \operatorname{supp}(|\nabla \varphi|) = \emptyset$ or $\operatorname{supp}(\mu^*) \cap \operatorname{supp}(|\nabla \varphi|) \subset \operatorname{supp}(|\nabla \varphi|)$, therefore if that happens, there exists an $A \subset \Omega$ such that $\mu^*(x) = 0$ and $|\nabla \varphi|(x) > 0 \ \forall x \in A$, moreover, $\forall M > 0$, $M \in \mathbb{R}$, there exists a $\sigma_t = t\bar{\sigma}$, $t > M$, with $\sigma_t(x) = 0$, $\forall x \in \Omega \setminus \overline{A}$ and

$\int_A \sigma_t \cdot \nabla \varphi = t$, implying that:

$$\begin{aligned}\inf_{\sigma} \int_\Omega \frac{1}{2}\mu^*|\sigma|^2 - \frac{1}{2\gamma}\int_\Omega \mu^{*\gamma} - \int_\Omega \sigma \cdot \nabla \varphi \leq \\ \leq \int_\Omega \frac{1}{2}\mu^*|\sigma_t|^2 - \frac{1}{2\gamma}\int_\Omega \mu^{*\gamma} - \int_\Omega \sigma_t \cdot \nabla \varphi \leq \\ \leq -\frac{1}{2\gamma}\int_\Omega \mu^{*\gamma} - \int_A \sigma_t \cdot \nabla \varphi \leq -t < -M, \quad \forall\, M > 0.\end{aligned}$$

Hence, (2.2.24) is equal to $-\infty$ which is a contradiction since (2.2.23) is finite. Finally, if we set $\mu^* = |\sigma^*|^{p'-2}$ we have that (2.2.25) becomes (2.2.23) and the inequality becomes an equality, thus μ^* is unique and σ^* is also a solution for (2.2.24), where the necessary compatibility condition (2.2.20) becomes exactly (2.2.21) showing also that $\mu^* = |\nabla \varphi|^{2-p}$.
This completes the proof. □

Remark 2.2.3. *It is clear that all the construction of the perturbation function $\Phi(\sigma, \rho)$ and the Lagrangian $L(\sigma, \mu)$ heavily requires the reflexivity of the Banach spaces involved, therefore all this arguments cannot be applied to the case $p = 1$.*

We will see in the next section that the dual problem (2.2.7) in the limit case when $p = 1$, once defined on opportune function spaces, has indeed some advantages and can be used to formulate a new definition for the total variation of a function in $BV(\Omega)$.

2.3 Equivalence between Total Variation Energy and $\mathcal{L}_p$ in the limit case $p = 1$

2.3.1 Introduction and structure of the proofs

As in Section 2.2 we have seen the equivalence between the p-Dirichlet energy and our dual definition $\mathcal{L}_p^*(\varphi)$ in the case where $1 < p < 2$, one may wonder what happens in the limit case where $p = 1$. Consider an open bounded Lipschitz domain $\Omega \in \mathbb{R}^n$, we define the Total Variation for a function $\varphi \in L^1(\Omega)$ as:

$$TV(\varphi) := \sup_{\substack{\sigma \in \left[\mathcal{C}_c^1(\Omega)\right]^n \\ |\sigma(x)| \leq 1 \,\forall\, x \in \Omega}} -\int_\Omega \varphi \operatorname{div} \sigma, \tag{2.3.1}$$

where we say that a function $\varphi \in L^1(\Omega)$ belongs to the space $BV(\Omega)$ of bounded variation functions if $TV(\varphi) < \infty$.
It is a known fact ([52] Structure Theorem of BV functions p.167) that if $\varphi \in$

$BV(\Omega)$ then:

$$\begin{gathered} \nabla \varphi \in [\mathcal{M}(\Omega)]^n \\ \nabla \varphi = \mu_\varphi \sigma_\varphi \\ \mu_\varphi \in \mathcal{M}^+(\Omega) \\ \sigma_\varphi : \Omega \to \mathbb{R}^n \quad \mu_\varphi - measurable \\ |\sigma_\varphi(x)| = 1 \quad for\ \ \mu_\varphi - a.e.\ \ x \in \Omega, \end{gathered} \tag{2.3.2}$$

where $\mathcal{M}(\Omega)$ is the set of the signed Radon measures in Ω and $\mathcal{M}^+(\Omega)$ is the set of the positive Radon measures in Ω.
As a consequence, the following formula by parts holds for the Total Variation of $\varphi \in BV(\Omega)$:

$$\begin{aligned} TV(\varphi) = & \sup_{\substack{\sigma \in \left[\mathcal{C}_c^1(\Omega)\right]^n \\ |\sigma(x)| \leq 1 \, \forall x \in \Omega}} \int_\Omega \sigma \cdot d[\nabla \varphi] \\ = & \sup_{\substack{\sigma \in \left[\mathcal{C}_c^1(\Omega)\right]^n \\ |\sigma(x)| \leq 1 \, \forall x \in \Omega}} \left\{ \int_\Omega \sigma \cdot \sigma_\varphi d\mu_\varphi \,, \quad \nabla \varphi = \mu_\varphi \sigma_\varphi \right\}, \end{aligned} \tag{2.3.3}$$

where in (2.3.3) we write $d[\nabla \varphi]$ to enforce the fact that $\nabla \varphi$ is a vector valued measure.
With abuse of notation we will write $\mu_\varphi := |\nabla \varphi|$, moreover, from the proof of the structure theorem which relies on the proof of the Riesz representation theorem (cf. [52] theorem 1 p.49) we call $|\nabla \varphi|$ the total variation measure of φ and :

$$TV(\varphi) = \int_\Omega d|\nabla \varphi|. \tag{2.3.4}$$

Motivated by these facts we introduce our candidate definition of the 1-Dirichlet Energy as:

$$\mathcal{L}_1^*(\varphi) := \sup_{\sigma \in [\mathcal{C}_c^1(\Omega)]^n} \left[\inf_{\mu \in \mathcal{M}^+(\Omega)} - \int_\Omega \frac{|\sigma|^2}{2} d\mu + \int_\Omega \frac{d\mu}{2} \right] + \int_\Omega \sigma \cdot d[\nabla \varphi]. \tag{2.3.5}$$

It is straightforward to see that:

$$\inf_{\mu \in \mathcal{M}^+(\Omega)} \int_\Omega \frac{1 - |\sigma|^2}{2} d\mu = \begin{cases} 0 & |\sigma(x)| \leq 1, \ \forall x \in \Omega \\ -\infty & \exists \ x^* \in \Omega \ \ s.t. \ \ |\sigma(x^*)| > 1, \end{cases} \tag{2.3.6}$$

it suffices to observe that by the Lebesgue decomposition theorem for any $\mu \in \mathcal{M}^+(\Omega)$ we can write $\mu = \mu_{ac} + \mu_s$, with $\mu_{ac} << \mathcal{L}^n$, $\mu_{ac} \geq 0$ and $\mu_s \perp \mathcal{L}^n$, $\mu_s \geq 0$, implying that:

$$\inf_{\mu \in \mathcal{M}^+(\Omega)} \int_\Omega \frac{1 - |\sigma|^2}{2} d\mu = \inf_{\substack{\mu_{ac} \geq 0 \\ \mu_s \geq 0}} \int_\Omega \frac{1 - |\sigma|^2}{2} \mu_{ac} dx + \int_\Omega \frac{1 - |\sigma|^2}{2} d\mu_s.$$

Hence, (2.3.6) follows by observing that, if there exists a single point $x^* \in \Omega \cap \{\mu_s > 0\}$ such that $|\sigma(x^*)| > 1$, then we can concentrate all the mass of μ_s on x^*, while the thesis is obvious on $\{\mu_{ac} > 0\}$.
In conclusion, since we are looking for a supremum in σ in (2.3.5), by (2.3.6) we have that:

$$\mathcal{L}_1^*(\varphi) = TV(\varphi). \tag{2.3.7}$$

Remark 2.3.1. *Observe that the choice of the spaces for σ and μ is not only motivated by the definition of the Total Variation of a function in $BV(\Omega)$. The rigorous explanation comes directly from the definition of μ as the conjugate variable of $|\sigma|^2$ via Legendre transform (see (2.2.4)). The choice $\sigma \in \left[\mathcal{C}_c^1(\Omega)\right]^n$ implies that $|\sigma|^2$ is a positive compact supported continuous scalar function. Since μ, as a conjugate variable, must to live in the dual space of $|\sigma|^2$ then by the Riesz-Markov-Kakutani representation theorem we have that $\mu \in \mathcal{M}^+(\Omega)$.*

Consider now the candidate dual problem:

$$\mathcal{L}_1(\varphi) := \inf_{\mu \in \mathcal{M}^+(\Omega)} \sup_{\sigma \in [\mathcal{C}_c^1(\Omega)]^n} -\int_\Omega \frac{1}{2}|\sigma|^2 d\mu + \int_\Omega \sigma \cdot d[\nabla \varphi] + \frac{1}{2}\int_\Omega d\mu. \tag{2.3.8}$$

The goal of this section is actually to prove that the dual problem defined in (2.3.8) is precisely the Total Variation of φ.
We will proceed at steps introducing first a surrogate problem taking inspirations from the results in [18] for the L_1-Optimal Transport problem and finally showing the equivalence selecting some ad hoc parameters. The proof of the equivalence between our saddle point formulation and the Total Variation for a function in $BV(\Omega)$ is based upon showing the equivalence between multiple variational problems. We first consider the problem in (2.3.8) without the mass term $\frac{1}{2}\int_\Omega d\mu$ defining the following functional:

$$\mathcal{L}_\varphi(\mu, \sigma) := -\int_\Omega \frac{1}{2}|\sigma|^2 d\mu + \int_\Omega \sigma \cdot d[\nabla \varphi].$$

We then show that the well-posedness of the problem:

$$\inf_{\mu \in \mathcal{M}^+(\Omega)} \sup_{\sigma \in [\mathcal{C}_c^1(\Omega)]^n} \mathcal{L}_\varphi(\mu, \sigma), \tag{2.3.9}$$

is ensured if we further constrain the measure μ to be such that $|\nabla \varphi| << \mu$. Moreover we will show that the "sup" becomes a "max" if $\sigma \in [L^2_\mu(\Omega)]^n$, this result is shown in Proposition 2.3.2. This is a crucial part of the proof, even if the relaxed problem where $\sigma \in [L^2_\mu(\Omega)]^n$ seems to be more complex since in that case the variable σ lives in a manifold which depends upon μ, it adds the properties to be a reflexive space and admits a candidate maximizer, thus leading us to state some bounds to the original problem. Next we show that problem (2.3.9) is equivalent to the problem without the further constraint $|\nabla \varphi| << \mu$, this is

a consequence of Lemma 2.3.3 and Lemma 2.3.4. As a result, from Proposition 2.3.2 we have the following equivalence between variational problems:

$$\inf_{\mu\in\mathcal{M}^+(\Omega)}\max_{\sigma\in[L^2{}_\mu(\Omega)]^n}\mathcal{L}_\varphi(\mu,\sigma)= \tag{2.3.10}$$

$$=\inf_{\substack{\mu\,\in\,\mathcal{M}^+(\Omega)\\ |\,\nabla\varphi|\,<<\,\mu}}\left\{\int_\Omega\frac{1}{2}|\sigma_\varphi|^2d\mu\,,\quad \mu\sigma_\varphi=\nabla\varphi\right\} \tag{2.3.11}$$

This result is shown in Corollary 2.3.5. After that, following the work in [18], we introduce the fixed mass surrogate problem:

$$T_m(\varphi)=\inf_{\substack{\mu\,\in\,\mathcal{M}^+(\Omega)\\ \int_\Omega d\mu\,=\,m}}\sup_{\sigma\in[\mathcal{C}^1_c(\Omega)]^n}-\int_\Omega\frac{1}{2}|\sigma|^2d\mu+\int_\Omega\sigma\cdot d[\nabla\varphi], \tag{2.3.12}$$

which is essentially problem (2.3.9) where we add the further constraint on the mass of the measure μ. From (2.3.10), (2.3.11) an homogeneity argument and the Structure Theorem of BV functions, we can state some bounds from above and below for (2.3.12) leading to the following equivalence:

$$T_m(\varphi)=\frac{(TV(\varphi))^2}{2m}.$$

This result is shown in Theorem 2.3.7. An immediate corollary is that we have an explicit formula which interconnects $TV(\varphi)$ with $T_m(\varphi)$ when the mass $m=TV(\varphi)$:

$$TV(\varphi)=2T_{TV(\varphi)}(\varphi).$$

This result is shown in Corollary 2.3.8.
This observation enables us to show the equivalence between $TV(\varphi)$ and $\mathcal{L}_1(\varphi)$. Thus, in Theorem 2.3.10 we state the main result of this Section:

$$TV(\varphi)=2T_{TV(\varphi)}(\varphi)=\mathcal{L}_1(\varphi).$$

Moreover we can show that the optimal measure μ^* for $\mathcal{L}_1(\varphi)$ is precisely the total variation measure, $\mu^*=|\,\nabla\varphi|$ and there exists a unique saddle point $(\mu^*,\sigma^*_{\mu^*})\in(\mathcal{M}^+(\Omega),[L^2_{\mu^*}(\Omega)]^n)$ which is precisely the measure and vector field given by the Structure Theorem of BV functions.

2.3.2 Main results and proofs

We now present the main results and proofs for this section.
Consider the following variational problem:

$$T_m(\varphi)=\inf_{\substack{\mu\,\in\,\mathcal{M}^+(\Omega)\\ \int_\Omega d\mu\,=\,m}}\sup_{\sigma\in[\mathcal{C}^1_c(\Omega)]^n}-\int_\Omega\frac{1}{2}|\sigma|^2d\mu+\int_\Omega\sigma\cdot d[\nabla\varphi]. \tag{2.3.13}$$

We have the following preparatory proposition:

Proposition 2.3.2. *Let Ω be a bounded open Lipschitz domain in $\mathbb{R}^n$, then $\forall\, \varphi \in BV(\Omega)$ we have that the problem:*

$$\inf_{\substack{\mu \,\in\, \mathcal{M}^+(\Omega) \\ |\,\nabla \varphi| \,<<\, \mu}} \frac{1}{2} \int_\Omega \left| \frac{d\, \nabla \varphi}{d\mu} \right|^2 d\mu, \tag{2.3.14}$$

is equivalent to:

$$\inf_{\substack{\mu \,\in\, \mathcal{M}^+(\Omega) \\ |\,\nabla \varphi| \,<<\, \mu}} \sup_{\sigma \in [\mathcal{C}^1_c(\Omega)]^n} - \int_\Omega \frac{1}{2} |\sigma|^2 d\mu + \int_\Omega \sigma \cdot d[\nabla \varphi]. \tag{2.3.15}$$

Moreover, problem (2.3.15) *is equivalent to the following:*

$$\inf_{\substack{\mu \,\in\, \mathcal{M}^+(\Omega) \\ |\,\nabla \varphi| \,<<\, \mu}} \max_{\sigma \in [L^2{}_\mu(\Omega)]^n} - \int_\Omega \frac{1}{2} |\sigma|^2 d\mu + \int_\Omega \sigma \cdot d[\nabla \varphi],$$

where $|\nabla \varphi| << \mu$ means that the measure $|\nabla \varphi|$ is absolutely continuous with respect to μ, i.e. that there exists a μ-measurable, $\sigma_\varphi : \Omega \to \mathbb{R}^n$, such that $\nabla \varphi = \mu \sigma_\varphi$.
Moreover, $\mu^* \in \mathcal{M}^+(\Omega)$ is a solution for (2.3.14) *iff it is a solution for* (2.3.15).

Proof. Let $\sigma \in \left[\mathcal{C}^1_c(\Omega)\right]^n$ and define $\sigma_t = t\sigma$, $\forall\, t \geq 0$, then the following inequality holds:

$$\int_\Omega \sigma_t \sigma_\varphi d\mu - \frac{1}{2} \int_\Omega |\sigma_t|^2 d\mu \leq \frac{1}{2} \left(\int_\Omega \frac{\sigma}{\|\sigma\|_{[L^2{}_\mu(\Omega)]^n}} \cdot \sigma_\varphi d\mu \right)^2,$$

and we have an equality for

$$t = t^* := \frac{\int_\Omega \sigma \cdot \sigma_\varphi}{\|\sigma\|^2_{[L^2{}_\mu(\Omega)]^n}}.$$

Hence:

$$\begin{aligned}
\sup_{\sigma \in [\mathcal{C}^1_c(\Omega)]^n} - \int_\Omega \frac{1}{2} |\sigma|^2 d\mu + \int_\Omega \sigma \cdot d[\nabla \varphi] = \\
= \sup_{\sigma \in [\mathcal{C}^1_c(\Omega)]^n} - \int_\Omega \frac{1}{2} |\sigma|^2 d\mu + \int_\Omega \sigma \cdot \sigma_\varphi d\mu = \\
= \frac{1}{2} \sup_{\sigma \in [\mathcal{C}^1_c(\Omega)]^n} \left(\int_\Omega \frac{\sigma}{\|\sigma\|_{[L^2{}_\mu(\Omega)]^n}} \cdot \sigma_\varphi d\mu \right)^2 = \\
= \frac{1}{2} \sup_{\substack{\sigma \,\in\, \left[\mathcal{C}^1_c(\Omega)\right]^n \\ \|\sigma\|_{[L^2{}_\mu(\Omega)]^n} \,=\, 1}} \left(\int_\Omega \sigma \cdot \sigma_\varphi d\mu \right)^2 = \frac{1}{2} \|\sigma_\varphi\|^2_{([L^2{}_\mu(\Omega)]^n)^*}.
\end{aligned} \tag{2.3.16}$$

Where the last equality in (2.3.16) follows by [61] Theorem 6.14. This shows that (2.3.14) is equivalent and has the same solution of (2.3.15) since $[L^2{}_\mu(\Omega)]^n = \big([L^2{}_\mu(\Omega)]^n\big)^*$.
Finally, observe that completing the squares we have:

$$\max_{\sigma\in[L^2{}_\mu(\Omega)]^n} -\int_\Omega \frac{1}{2}|\sigma|^2 d\mu + \int_\Omega \sigma\cdot d[\nabla\varphi] =$$
$$\max_{\sigma\in[L^2{}_\mu(\Omega)]^n} \frac{1}{2}\|\sigma_\varphi\|^2_{[L^2{}_\mu(\Omega)]^n} - \frac{1}{2}\|\sigma_\varphi-\sigma\|^2_{[L^2{}_\mu(\Omega)]^n} =$$
$$= \max_{\sigma\in[L^2{}_\mu(\Omega)]^n} \frac{1}{2}\|\sigma_\varphi\|^2_{[L^2{}_\mu(\Omega)]^n} - \frac{1}{2}\|\sigma_\varphi-\sigma\|^2_{[L^2{}_\mu(\Omega)]^n} = \frac{1}{2}\|\sigma_\varphi\|^2_{[L^2{}_\mu(\Omega)]^n}.$$

This shows the last assertion. □

The next technical lemma will be used:

Lemma 2.3.3. *Let Ω be a bounded open Lipschitz domain in $\mathbb{R}^n$, and set*

$$\mathcal{L}_\varphi(\mu,\sigma) := -\int_\Omega \frac{1}{2}|\sigma|^2 d\mu + \int_\Omega \sigma\cdot d[\nabla\varphi], \quad \forall\,\varphi\in BV(\Omega),$$

where $\mu\in\mathcal{M}^+(\Omega)$ and $\sigma\in Y$, $Y=\big[\mathcal{C}^1_c(\Omega)\big]^n$. If $|\nabla\varphi|$ is not absolutely continuous with respect to μ, then:

$$\sup_{\sigma\in Y}\mathcal{L}_\varphi(\mu,\sigma) = +\infty. \tag{2.3.17}$$

As a consequence, the same holds for $Y := [L^2{}_\mu(\Omega)]^n$.

Proof. Let $\mathcal{B}$ be the Borel σ-algebra of Ω and $\mathcal{M}^+_{|\nabla\varphi|} := \{\mu\in\mathcal{M}^+(\Omega)\mid |\nabla\varphi| << \mu\}$. For any $\bar\mu\notin\mathcal{M}^+_{|\nabla\varphi|}$ there exists an $N\subset\mathcal{B}$ such that $\bar\mu(N)=0$ and $|\nabla\varphi|(N)=m>0$.
Let $M>0$, then for all $\delta>0$ there exists an open $A_\delta\subset\Omega$ such that $N\subset A_\delta$ and $\bar\mu(A_\delta)=\delta$. As a consequence, the following chain of inequalities holds:

$$\sup_{\sigma\in[\mathcal{C}^1_c(\Omega)]^n}\mathcal{L}_\varphi(\mu,\sigma) \geq \sup_{\sigma\in[\mathcal{C}^1_c(A_\delta)]^n}\mathcal{L}_\varphi(\mu,\sigma) \geq \sup_{\substack{\sigma\,\in\,\left[\mathcal{C}^1_c(A_\delta)\right]^n\\ |\sigma(x)|\,\leq\,M\ \forall\,x\,\in\,\Omega}}\mathcal{L}_\varphi(\mu,\sigma) \geq$$
$$\geq -\frac{1}{2}\delta M^2 + \sup_{\substack{\sigma\,\in\,\left[\mathcal{C}^1_c(A_\delta))\right]^n\\ |\sigma(x)|\,\leq\,M\ \forall\,x\,\in\,\Omega}}\int_\Omega \sigma\cdot d[\nabla\varphi] =$$
$$= -\frac{1}{2}\delta M^2 + M|\nabla\varphi|(A_\delta) \geq -\frac{1}{2}\delta M^2 + M|\nabla\varphi|(N) =$$
$$= -\frac{1}{2}\delta M^2 + Mm.$$

Taking the limit for $\delta \to 0$ yields:

$$\sup_{\sigma \in [\mathcal{C}_c^1(\Omega)]^n} \mathcal{L}_\varphi(\mu, \sigma) \geq Mm \quad \forall\, M > 0,$$

which implies (2.3.17).
Finally, observe that:

$$\sup_{\sigma \in [L^2{}_\mu(\Omega)]^n} \mathcal{L}_\varphi(\mu, \sigma) \geq \sup_{\sigma \in [\mathcal{C}_c^1(\Omega)]^n} \mathcal{L}_\varphi(\mu, \sigma).$$

Therefore, the assertion also holds for $\sigma \in [L^2{}_\mu(\Omega)]^n$. □

We are now ready for the following Lemma.

Lemma 2.3.4. *With the same definitions of Lemma 2.3.3,* $\forall\, \varphi \in BV(\Omega)$, $\mu \in \mathcal{M}^+(\Omega)$ *and* $\sigma \in Y$, $Y := \left[\mathcal{C}_c^1(\Omega)\right]^n$, *we have that the problem:*

$$\inf_{\substack{\mu \,\in\, \mathcal{M}^+(\Omega) \\ |\,\nabla \varphi| \,<<\, \mu}} \sup_{\sigma \in Y} \mathcal{L}_\varphi(\mu, \sigma), \tag{2.3.18}$$

is equivalent to

$$\inf_{\mu \in \mathcal{M}^+(\Omega)} \sup_{\sigma \in Y} \mathcal{L}_\varphi(\mu, \sigma). \tag{2.3.19}$$

and $\mu^* \in \mathcal{M}^+(\Omega)$ *is a solution for* (2.3.18) *iff it is a solution for* (2.3.19).
Moreover, the same results hold if $Y := [L^2{}_\mu(\Omega)]^n$ *and the "sup" becomes a "max".*

Proof. By Lemma 2.3.3, we have that (2.3.19) is equivalent and has the same solutions to:

$$\inf_{\mu \in \mathcal{M}^+(\Omega)} \sup_{\sigma \in Y} \mathcal{L}_\varphi(\mu, \sigma) + \chi_{|\,\nabla \varphi| << \mu}, \tag{2.3.20}$$

where $\chi_{|\,\nabla \varphi| << \mu}$ is the indicator function of the set

$$\mathcal{M}^+_{|\nabla \varphi|} := \{\mu \in \mathcal{M}^+(\Omega) \mid |\,\nabla \varphi| << \mu\},$$

$$\chi_{|\,\nabla \varphi| << \mu} := \begin{cases} +\infty & \mu \notin \mathcal{M}^+_{|\nabla \varphi|} \\ 0 & \mu \in \mathcal{M}^+_{|\nabla \varphi|}. \end{cases}$$

Next, observe that (2.3.20) is precisely (2.3.18) since by the Structure Theorem of BV functions the set $\mathcal{M}^+_{|\nabla \varphi|}$ is non empty, therefore, $\mu^* \in \mathcal{M}^+(\Omega)$ is a solution for (2.3.18) iff it is a solution for (2.3.19).
Finally observe that Lemma 2.3.3 holds if $Y = [L^2{}_\mu(\Omega)]^n$ hence we can apply the same arguments. This complete the proof. □

From Proposition 2.3.2 and Lemma 2.3.4 we have an immediate corollary:

Corollary 2.3.5. *With the same hypothesis as Proposition 2.3.4 we have:*

$$\inf_{\mu\in\mathcal{M}^+(\Omega)}\max_{\sigma\in[L^2{}_\mu(\Omega)]^n}\mathcal{L}_\varphi(\mu,\sigma)= \tag{2.3.21}$$

$$=\inf_{\substack{\mu\,\in\,\mathcal{M}^+(\Omega)\\ |\,\nabla\varphi|\,<<\,\mu}}\left\{\int_\Omega\frac{1}{2}|\sigma_\varphi|^2d\mu\,,\quad \mu\sigma_\varphi=\nabla\varphi\right\} \tag{2.3.22}$$

and $\mu^*\in\mathcal{M}^+(\Omega)$ is a solution for (2.3.21) *iff it is a solution for* (2.3.22)*.*

Proof. The equivalence between the two problems is a simple consequence of Proposition 2.3.2 and Lemma 2.3.4 where we have seen the equivalence between problems (2.3.14), (2.3.15) and (2.3.19) for $Y=[L^2{}_\mu(\Omega)]^n$. □

Remark 2.3.6. *Observe that in the proofs of of Proposition 2.3.2 and Lemma 2.3.4 no restrictions were used on the mass of μ, therefore we also have the following equality:*

$$\inf_{\substack{\mu\,\in\,\mathcal{M}^+(\Omega)\\ \int_\Omega d\mu\,=\,m}}\max_{\sigma\in[L^2{}_\mu(\Omega)]^n}\mathcal{L}_\varphi(\mu,\sigma)=\inf_{\substack{\mu\,\in\,\mathcal{M}^+(\Omega)\\ |\,\nabla\varphi|\,<<\,\mu\\ \int_\Omega d\mu\,=\,m}}\left\{\int_\Omega\frac{1}{2}|\sigma_\varphi|^2d\mu\,,\quad \mu\sigma_\varphi=\nabla\varphi\right\}.$$

We are ready now to prove the following theorem:

Theorem 2.3.7. *Let Ω be a bounded open Lipschitz domain in $\mathbb{R}^n$ and consider the functional $T_m(\varphi)$ defined in* (2.3.13) *then, for any $\varphi\in BV(\Omega)$, we have that:*

$$T_m(\varphi)=\frac{(TV(\varphi))^2}{2m}. \tag{2.3.23}$$

Proof. The proof is a simple extension of the proof of Theorem 1 in [18].
For the sake of simplicity we define:

$$\varepsilon_\varphi(\mu):=\sup_{\sigma\in[\mathcal{C}^1_c(\Omega)]^n}-\int_\Omega\frac{1}{2}|\sigma|^2d\mu+\int_\Omega\sigma\cdot d[\nabla\varphi].$$

Thus, $T_m(\varphi)$ can be written as:

$$\begin{aligned}T_m(\varphi)&=\inf_{\substack{\mu\,\in\,\mathcal{M}^+(\Omega)\\ \int_\Omega d\mu\,=\,m}}\varepsilon_\varphi(\mu)\\ &=\inf_{\substack{\mu\,\in\,\mathcal{M}^+(\Omega)\\ \int_\Omega d\mu\,=\,m}}\sup_{\sigma\in[\mathcal{C}^1_c(\Omega)]^n}-\int_\Omega\frac{1}{2}|\sigma|^2d\mu+\int_\Omega\sigma\cdot d[\nabla\varphi].\end{aligned}$$

First observe that the infimum in $T_m(\varphi)$ is in fact a minimum since $\varepsilon_\varphi(\mu)$ is lower semi-continuous with respect to the *weak**-topology, convex and proper because

it is a supremum of a family of *weak**-continuous affine functionals in $\mathcal{M}^+(\Omega)$ which is a closed and convex subset of $\mathcal{M}(\Omega)$.
Moreover, the set $\{\mu \in \mathcal{M}^+(\Omega) \mid \int_\Omega d\mu = m\}$ is convex and compact in the *weak**-topology, therefore, a minimum exists from the direct method of the calculus of variations.
If $TV(\varphi) = 0$ then φ is constant a.e. and there is nothing to prove since $T_m(\varphi)$ is clearly zero.
In the more general case where $TV(\varphi) > 0$ we proceed as follows, first we show that $\frac{(TV(\varphi))^2}{2m}$ is a lower bound for $T_m(\varphi)$ and after that we will show that there exists a particular admissible pair $(\bar{\mu}, \bar{\sigma})$ such that $\frac{(TV(\varphi))^2}{2m}$ is also an upper bound for $T_m(\varphi)$.

- ($\geq$) By homogeneity, $\forall\, t \geq 0$, $t \in \mathbb{R}$ and $\forall\, \mu \in \mathcal{M}^+(\Omega)$, $\int_\Omega d\mu = m$, we have that:

$$\varepsilon_\varphi(\mu) \geq \sup_{\substack{t \geq 0 \\ t \in \mathbb{R}}} \sup_{\substack{\bar{\sigma} \in \left[\mathcal{C}_c^1(\Omega)\right]^n \\ |\bar{\sigma}(x)| \leq 1,\ \forall\, x \in \Omega}} -\frac{mt^2}{2} + t \int_\Omega \bar{\sigma} \cdot d[\nabla \varphi] =$$

$$= \sup_{\substack{t \geq 0 \\ t \in \mathbb{R}}} -\frac{mt^2}{2} + t\, TV(\varphi) := \sup_{\substack{t \geq 0 \\ t \in \mathbb{R}}} g(t).$$

  Finally, observe that the function $g(t)$ is strictly concave and increasing for $t \leq \frac{TV(\varphi)}{m}$, therefore, the supremum is attained at $t^* = \frac{TV(\varphi)}{m}$ and after evaluating at t^* we find that:

$$\varepsilon_\varphi(\mu) \geq \frac{(TV(\varphi))^2}{2m}, \quad \forall\, \mu \in \mathcal{M}^+(\Omega),\ \int_\Omega d\mu = m. \tag{2.3.24}$$

  Taking the infimum in μ on the left side of (2.3.24) we get:

$$T_m(\varphi) \geq \frac{(TV(\varphi))^2}{2m}.$$

- ($\leq$) From the structure theorem of BV functions (2.3.2) we have that $\forall\, \varphi \in BV(\Omega)$ there exists an opportune $\tilde{\mu} \in \mathcal{M}^+(\Omega)$ and a $\tilde{\mu}$-measurable $\tilde{\sigma} : \Omega \to \mathbb{R}^n$ such that $\nabla \varphi = \tilde{\mu}\tilde{\sigma}$, $|\sigma(x)| = 1$, $\tilde{\mu}$-a.e. in Ω and, by (2.3.4), $TV(\varphi) = \int_\Omega d\tilde{\mu}$.
  Define now

$$\bar{\mu} = \frac{m}{TV(\varphi)}\tilde{\mu},$$

  and

$$\bar{\sigma} = \frac{TV(\varphi)}{m}\tilde{\sigma}.$$

Observe that the space $\left[\mathcal{C}_c^1(\Omega)\right]^n \subset [L^2{}_\mu(\Omega)]^n$ for any $\mu \in \mathcal{M}^+(\Omega)$ and clearly $\bar{\sigma} \in [L^2{}_\mu(\Omega)]^n$, $|\nabla \varphi| << \bar{\mu}$, $\bar{\mu}\bar{\sigma} = \nabla \varphi$ and $\int_\Omega d\bar{\mu} = m$ then, by Remark 2.3.6, we have the following chain of inequalities:

$$T_m(\varphi) \leq \inf_{\substack{\mu \in \mathcal{M}^+(\Omega) \\ \int_\Omega d\mu = m}} \max_{\sigma \in [L^2{}_\mu(\Omega)]^n} \mathcal{L}_\varphi(\mu, \sigma) \leq \int_\Omega \frac{1}{2}|\bar{\sigma}|^2 d\bar{\mu} = \frac{(TV(\varphi))^2}{2m}.$$

□

From Theorem 2.3.7 we have an immediate corollary:

Corollary 2.3.8. *For any $\varphi \in BV(\Omega)$ we have that:*

$$TV(\varphi) = 2T_{TV(\varphi)}(\varphi). \tag{2.3.25}$$

Proof. We have already seen in the proof of theorem (2.3.7) that if $TV(\varphi) = 0$ then $T_m(\varphi) = 0$, $\forall\, m \geq 0$, while in the case where $TV(\varphi) > 0$ the results follows directly by (2.3.23). □

Remark 2.3.9. *Corollary 2.3.8 characterizes the Total Variation of a function in $BV(\Omega)$ reabsorbing the "difficult" part in the standard definition* (2.3.1)*, i.e. the constraint $|\sigma(x)| \leq 1$, $\forall\, x \in \Omega$, by introducing a new variable μ and a mass constraint. However, this does not make the problem tractable from the numerical point of view since* (2.3.25) *requires a priori the knowledge of $TV(\varphi)$. We will show next that it is possible to circumvent this obstacle by introducing an equivalent variational problem to* (2.3.25) *but without the mass constraint. This new equivalent variational problem turns out to be exactly our dual formulation functional $\mathcal{L}_1(\varphi)$ defined in* (2.3.8)*.*

We are now ready to state the main Theorem of this section:

Theorem 2.3.10. *Given a function $\varphi \in BV(\Omega)$, we have that:*

$$TV(\varphi) = 2T_{TV(\varphi)}(\varphi) = \mathcal{L}_1(\varphi). \tag{2.3.26}$$

Moreover, if we define the Lagrangian $\mathcal{L}_\varphi^1 : (\mathcal{M}^+(\Omega) \times \left[\mathcal{C}_c^1(\Omega)\right]^n) \to \mathbb{R}$:

$$\mathcal{L}_\varphi^1(\mu, \sigma) := -\int_\Omega \frac{1}{2}|\sigma|^2 d\mu + \int_\Omega \sigma \cdot d[\nabla \varphi] + \frac{1}{2}\int_\Omega d\mu,$$

and the functional

$$E_\varphi(\mu) := \sup_{\sigma \in [\mathcal{C}_c^1(\Omega)]^n} \mathcal{L}_\varphi^1(\mu, \sigma),$$

then the unique optimal measure

$$\mu^* = \arg\min_{\mu \in \mathcal{M}^+(\Omega)} E_\varphi(\mu),$$

is precisely the total variation measure:

$$\mu^* = |\nabla \varphi|,$$

and there exists a unique saddle point

$$(\mu^*, \sigma^*_{\mu^*}) \in (\mathcal{M}^+(\Omega), [L^2_{\mu^*}(\Omega)]^n),$$

for $\mathcal{L}^1_\varphi$, where the optimal vector field $\sigma^*_{\mu^*}$ is the one given by the Structure Theorem of BV functions.

Proof. The proof works as the proof of Theorem 2.3.7, indeed we will show that:

$$TV(\varphi) \leq \mathcal{L}_1(\varphi) \leq 2T_{TV(\varphi)}(\varphi).$$

- ($\geq$) It follows from (2.3.7) and observing that clearly $\mathcal{L}^*_1(\varphi) \leq \mathcal{L}_1(\varphi)$ since "supinf"$\leq$ "infsup", where $\mathcal{L}^*_1(\varphi)$ is defined in (2.3.5).
- ($\leq$) From Corollary 2.3.8 we know that:

$$T_{TV(\varphi)}(\varphi) = \frac{TV(\varphi)}{2}.$$

which implies that:

$$\begin{aligned}
\mathcal{L}_1(\varphi) &= \inf_{\mu\in\mathcal{M}^+(\Omega)} \sup_{\sigma\in[\mathcal{C}^1_c(\Omega)]^n} -\int_\Omega \frac{1}{2}|\sigma|^2 d\mu + \int_\Omega \sigma \cdot d[\nabla\varphi] + \frac{1}{2}\int_\Omega d\mu \leq \\
&\leq \inf_{\substack{\mu\,\in\,\mathcal{M}^+(\Omega) \\ \int_\Omega d\mu = TV(\varphi)}} \sup_{\sigma\in[\mathcal{C}^1_c(\Omega)]^n} -\int_\Omega \frac{1}{2}|\sigma|^2 d\mu + \int_\Omega \sigma \cdot d[\nabla\varphi] + \frac{1}{2}\int_\Omega d\mu = \\
&= T_{TV(\varphi)}(\varphi) + \frac{TV(\varphi)}{2} = TV(\varphi).
\end{aligned}$$

This completes the proof of the first part of the theorem.
We will now consider the characterization of the optimal measure μ^*.
We have:

$$\mathcal{L}_1(\varphi) = \inf_{\mu\in\mathcal{M}^+(\Omega)} E_\varphi(\mu) = \inf_{\mu\in\mathcal{M}^+(\Omega)} \sup_{\sigma\in[\mathcal{C}^1_c(\Omega)]^n} \mathcal{L}^1_\varphi(\mu,\sigma).$$

Observe that $E_\varphi(\mu)$ is lower semi-continuous with respect to the *weak**-topology, convex and proper because it is a supremum of a family of *weak**-continuous affine functionals in $\mathcal{M}^+(\Omega)$ which is a closed and convex subset of $\mathcal{M}(\Omega)$.
With the same arguments as in (2.3.24), $\forall\,\mu \in \mathcal{M}(\Omega)$, we have that:

$$E_\varphi(\mu) \geq \frac{(TV(\varphi))^2}{2\int_\Omega d\mu} + \frac{1}{2}\int_\Omega d\mu > \frac{1}{2}\int_\Omega d\mu \geq 0. \tag{2.3.27}$$

From (2.3.27) we have that $E_\varphi(\mu)$ is bounded from below and $\forall\, M > 0$, the set $\{\mu \mid E(\mu) < M\}$ is a subset of the *weak**-compact set $\{\mu \mid \int_\Omega d\mu \leq 2M\}$ which implies that $E(\mu)$ is coercive with respect to the *weak**-topology. As a consequence, a minimum exists by the direct method of the calculus of variation. Next, set $\mu_\varphi := |\nabla \varphi|$. From the structure theorem of BV functions (2.3.2) we have that there exists an opportune μ_φ-measurable $\sigma_\varphi : \Omega \to \mathbb{R}^n$ such that $\nabla \varphi = \mu_\varphi \sigma_\varphi$, $|\sigma_\varphi(x)| = 1$, μ_φ-a.e. in Ω and, by (2.3.4), $TV(\varphi) = \int_\Omega d\mu_\varphi$.
From these facts we have:

$$\begin{aligned} E_\varphi(\mu_\varphi) &= \sup_{\sigma \in [\mathcal{C}^1_c(\Omega)]^n} -\int_\Omega \frac{1}{2}|\sigma|^2 d\mu_\varphi + \int_\Omega \sigma \cdot \sigma_\varphi d\mu_\varphi + \frac{1}{2}\int_\Omega d\mu_\varphi \\ &= \sup_{\sigma \in [\mathcal{C}^1_c(\Omega)]^n} -\int_\Omega \frac{1}{2}|\sigma|^2 d\mu_\varphi + \int_\Omega \sigma \cdot \sigma_\varphi d\mu_\varphi + \frac{1}{2} TV(\varphi) = \qquad (2.3.28) \\ &= \frac{1}{2}\|\sigma_\varphi\|^2_{[L^2_{\mu_\varphi}(\Omega)]^n} + \frac{1}{2} TV(\varphi) = TV(\varphi), \end{aligned}$$

where the first and the second line of (2.3.28) follow by writing $d[\nabla \varphi] = \sigma_\varphi d\mu_\varphi$ and μ_φ being the Total Variation measure, while the third line of (2.3.28) follows by (2.3.16).
As a consequence, from (2.3.26) and (2.3.28), we have that

$$\mu^* := \mu_\varphi.$$

is a minimizer for $E_\varphi(\mu)$ and the pair:

$$(\mu^*, \sigma^*_{\mu^*} := \sigma_\varphi) \in (\mathcal{M}^+(\Omega), [L^2_{\mu^*}(\Omega)]^n),$$

given by the Structure Theorem of BV functions is a saddle point for $\mathcal{L}^1_\varphi(\mu, \sigma)$. It remains to show that μ^* is unique.
Suppose that there exists another minimizer for $E_\varphi(\mu)$ and call it $\bar{\mu}$. By Lemma 2.3.4, if $\bar{\mu}$ is a minimizer for $E_\varphi(\mu)$, then $|\nabla \varphi| << \bar{\mu}$ and hence there exists a $\bar{\mu}$-measurable $\bar{\sigma} : \Omega \to \mathbb{R}^n$ such that $\nabla \varphi = \bar{\mu}\bar{\sigma}$.
Now, with the same computations as in (2.3.28), and using the optimality condition for $\bar{\mu}$ given by (2.3.26), we have the following chain of equalities:

$$\begin{aligned} \int_\Omega |\bar{\sigma}| d\bar{\mu} = \sup_{\substack{\sigma \in \left[\mathcal{C}^1_c(\Omega)\right]^n \\ |\sigma(x)| \leq 1\ \forall\, x \in \Omega}} \int_\Omega \sigma \bar{\sigma} d\bar{\mu} = \sup_{\substack{\sigma \in \left[\mathcal{C}^1_c(\Omega)\right]^n \\ |\sigma(x)| \leq 1\ \forall\, x \in \Omega}} \int_\Omega \sigma \cdot d[\nabla \varphi] \\ = TV(\varphi) = E(\bar{\mu}) = \int_\Omega \frac{|\bar{\sigma}|^2 + 1}{2} d\bar{\mu}. \quad (2.3.29) \end{aligned}$$

Equating the first and the last term of (2.3.29) we have that $|\bar{\sigma}| = 1$, $\bar{\mu}$-a.e. and $TV(\varphi) = \int_\Omega d\bar{\mu}$. This implies that $\bar{\mu}$ have the same properties of the total variation measure μ_φ and therefore $\bar{\mu} = \mu_\varphi$, since by the Structure Theorem of BV functions there exists a unique total variation measure.
As a consequence, also the vector field $\sigma^*_{\mu^*}$ is unique.
This completes the proof. □

2.4 The Counterpart on Graphs

In this section, taking inspiration from the continuous case, we will consider the graph based discretized version of the p-Dirichlet Energy including the limit case where $p = 1$. We will further states the discrete version of the results in Section 2.2 and 2.3. We point out that in the discrete case everything is far more easier, nevertheless, our duality based approach leads to very efficient numerical algorithms based on the Dynmic Monge Kantorovich (DMK) scheme, originally developed in [55] for the L^1 Optimal Transport problem and in [54] for the graph based counterpart.
We define a weighted directed graph as a collection $\mathcal{G} = (E, V, \omega)$, where E is the set of $m = |E|$ edges, V the set of $n = |V|$ nodes and ω is a weight on the edges. Each edge $e_i \in E$ is characterized by the pair $e_i = v_j v_k$, with $v_j, v_k \in V$, and we write ω_i for the weight associated to the edge e_i. On a graph, we can define functions on nodes and functions on edges. We denote as $\mathcal{H}(V) = \mathbb{R}^n$ and $\mathcal{H}(E) = \mathbb{R}^m$ the Banach spaces of real-valued functions on V and E, respectively. We will write $\varphi_v = \varphi(v)$ for the value in a node $v \in V$ of the vector $\varphi = [\varphi_{v_1}, ..., \varphi_{v_n}] \in \mathcal{H}(V)$. With the same notation, we will write $\sigma_e = \sigma(e)$ for the value in an edge $e \in E$ of the vector $\sigma = [\sigma_{e_1}, ..., \sigma_{e_m}] \in \mathcal{H}(E)$.
We now introduce the graph gradient operator $\nabla : \mathcal{H}(V) \longrightarrow \mathcal{H}(E)$ as the $m \times n$ matrix whose (i, j)-element is:

$$(\nabla)_{ij} = \begin{cases} -\omega_i & e_i = v_j v_k,\ k \in \{1, \dots, n\} \\ \omega_i & e_i = v_k v_j,\ k \in \{1, \dots, n\} \\ 0 & \text{otherwise.} \end{cases}$$

Although the gradient matrix relies on a edge orientations, we point out that such orientation is arbitrary and does not affect the construction of the operator so that $\mathcal{G}$ can be still considered as undirected.
Next, we define the graph divergence operator $\text{div} : \mathcal{H}(E) \longrightarrow \mathcal{H}(V)$, which can be expressed as:

$$\text{div} = -\nabla^T,$$

i.e., as the negative transposed $n \times m$ matrix of ∇.
In analogy to the continuous case, we define the weighted graph laplacian operator for a function $\varphi \in \mathcal{H}(V)$ as:

$$\Delta_c \varphi := -\text{div}(c \odot \nabla\varphi) = \nabla^T Diag(c) \nabla\varphi,$$

where $c \in \mathcal{H}(E)$ is a weight functions on the edges set, $\odot$ is the Hadamard product:

$$\begin{aligned} u \odot v : \mathbb{R}^n \times \mathbb{R}^n &\to \mathbb{R}^n \\ (u \odot v)_i &\mapsto u_i \cdot v_i \qquad i = 1, \dots, n. \end{aligned}$$

and

$$\Delta_c = \nabla^T Diag(c) \nabla, \tag{2.4.1}$$

is the c-weighted graph laplacian matrix.
As a direct extension, we define p-Laplacian operator, $p > 1$, on graphs as:

$$\Delta_p \varphi := -\operatorname{div}(|\nabla \varphi|^{p-2} \odot \nabla \varphi) = \nabla^T Diag(|\nabla \varphi|^{p-2}) \nabla \varphi. \tag{2.4.2}$$

Moreover, for a given $\sigma \in \mathcal{H}(E)$ and $1 \leq p < \infty$ we define the discrete edges based p-norm as:

$$\|\sigma\|_{l_p} := \left(\sum_{e \in E} |\sigma_e|^p \right)^{\frac{1}{p}},$$

where in the limit case $p = \infty$ we define the l_∞-norm as:

$$\|\sigma\|_{l_\infty} := \sup_{e \in E} |\sigma_e|.$$

.
As in Section 2.2, we define the graph p-Dirichlet energy for a given $p \geq 1$ and a function $\varphi \in \mathcal{H}(V)$, $\varphi_v < \infty$, $\forall\, v \in V$ as:

$$\mathtt{E}_p(\varphi) := \frac{\|\nabla \varphi\|_{l_p}^p}{p} = \sum_{e \in E} \frac{|(\nabla \varphi)_e|^p}{p}. \tag{2.4.3}$$

From now on we will consider only finite functions $\varphi \in \mathcal{H}(V)$ i.e. $\varphi_v < \infty$, $\forall\, v \in V$.
In the limit case $p = 1$ we call the $\mathtt{E}_1(\varphi)$ as the graph Total Variation energy of φ.
Moving on, we define the edges based discrete counterpart of the Legendre transform for a function $\psi : \mathcal{H}(E) \to \bar{\mathbb{R}}$ as :

$$\begin{aligned} \psi^* &: \mathcal{H}(E) \to \bar{\mathbb{R}}, \\ \psi^*(g^*) :&= \sup_{g \in \mathcal{H}(E)} < g^*, g >_{\mathcal{H}(E) \times \mathcal{H}(E)} - \psi(g) \\ &= \sup_{g \in \mathcal{H}(E)} g^* \cdot g - \psi(g) \\ &= \sup_{g \in \mathcal{H}(E)} \sum_{e \in E} g_e^* g_e - \psi(g). \end{aligned}$$

In what follows we will tacitly omit belonging to the edges or nodes Banach spaces inside the "inf" or the "sup" when confusion doesn't arise.
With the same arguments as in Section 2.2, by applying twice the Legendre transform we obtain the dual definition of the graph p-Dirichlet energy in the case $1 < p < 2$:

$$\mathtt{E}^*_{p'}(\varphi) := \sup_{\sigma \in \mathcal{H}(E)} -\sum_{e \in E} \frac{|\sigma_e|^{p'}}{p'} + \sigma \cdot \nabla \varphi. \tag{2.4.4}$$

Since we have differentiability and strong concavity, the supremum in (2.4.4) is indeed a maximum and is attained for the unique σ^* such that:

$$|\sigma^*|^{p'-2} \odot \sigma^* = \nabla \varphi. \tag{2.4.5}$$

Again, with the same arguments as in (2.2.5)-(2.2.6) we obtain the following duality based saddle point reformulation of $\mathtt{E}^*_{p'}(\varphi)$ (in the case $1 < p < 2$ which implies $2 < p' < \infty$):

$$\mathtt{L}^*_p(\varphi) := \sup_{\sigma \in \mathcal{H}(E)} \inf_{\mu \in \mathcal{H}(E)^+} -\sum_{e \in E} \frac{1}{2}\mu_e |\sigma_e|^2 + \frac{2-p}{2p} \sum_{e \in E} \mu_e^{\frac{p}{2-p}} + \sigma \cdot \nabla \varphi, \tag{2.4.6}$$

where $\mathcal{H}(E)^+ := \{\mu \in \mathcal{H}(E) \mid \mu_e \geq 0,\ \forall\, e \in E\}$, $p := 2 - p$ and for simplicity we set $\gamma = \frac{p}{2-p}$.
By construction (see (2.2.5)-(2.2.6)), we have that $\bar{\sigma}$ is a solution of (2.4.6) iff it is a solution for (2.4.4) that is to say that it is unique and satisfies the extremality relation (2.4.5).
In the limit case where $p = 1$ we have $\gamma = 1$ and we define the functional:

$$\mathtt{L}^*_1(\varphi) := \sup_{\sigma \in \mathcal{H}(E)} \inf_{\mu \in \mathcal{H}(E)^+} -\sum_{e \in E} \frac{1}{2}\mu_e |\sigma_e|^2 + \frac{1}{2} \sum_{e \in E} \mu_e + \sigma \cdot \nabla \varphi. \tag{2.4.7}$$

Observe that the density μ plays the role of a Lagrange multiplier for the constraint $|\sigma_e|^2 \leq 1$, $\forall\, e \in E$ or equivalently $\|\sigma\|_{l_\infty} \leq 1$.
As a consequence, $\mathtt{L}^*_1(\varphi)$ is equivalent to the graph-based counterpart of (2.3.5)-(2.3.7) :

$$\mathtt{L}^*_1(\varphi) = \sup_{\substack{\sigma \in \mathcal{H}(E) \\ \|\sigma\|_{l_\infty} \leq 1}} \sigma \cdot \nabla \varphi = \| \nabla \varphi\|^*_{l_\infty} = \mathtt{E}_1(\varphi), \tag{2.4.8}$$

where the equality between $\mathtt{L}^*_1(\varphi)$ and $\mathtt{E}_1(\varphi)$ is given by observing that, since $\mathcal{H}(E) = \mathbb{R}^m$, the l_∞ norm is in duality with the l_1 norm.
A solution σ^* for (2.4.8) is one of the generalized signum functions for $\nabla \varphi$:

$$\sigma^* = \operatorname{sign}(\nabla \varphi) = \begin{cases} \frac{(\nabla \varphi)_e}{|(\nabla \varphi)_e|} & e \in E \ s.t.\ |(\nabla \varphi)_e| > 0 \\ [-1, 1] & e \in E \ s.t.\ |(\nabla \varphi)_e| = 0. \end{cases} \tag{2.4.9}$$

From (2.4.8) and (2.4.9), it makes sense to extend the definition of $\mathtt{L}^*_p(\varphi)$ to the case $1 \leq p < 2$.
Now, define the perturbation function $\Phi : (\mathcal{H}(E) \times \mathcal{H}(E)) \to \bar{\mathbb{R}}$ as:

$$\Phi(\sigma, \rho) := \sup_{\mu \in \mathcal{H}(E)^+} \sum_{e \in E} \frac{\mu_e(|\sigma_e|^2 + 2\rho_e)}{2} - \frac{1}{2\gamma} \sum_{e \in E} \mu_e^\gamma - \sigma \cdot \nabla \varphi,$$

where $\rho \in \mathcal{H}(E)$ is the perturbation parameter.
As in the continuous case, we introduce the Lagrangian $L : (\mathcal{H}(E) \times \mathcal{H}(E)) \to \bar{\mathbb{R}}$ as:

$$L(\sigma, \mu) := \sum_{e \in E} \frac{1}{2}\mu_e |\sigma_e|^2 - \frac{1}{2\gamma} \sum_{e \in E} \mu_e^\gamma - \sigma \cdot \nabla \varphi - \chi_{\mu \in \mathcal{H}(E)^+}, \tag{2.4.10}$$

where $\chi_{\mu\in\mathcal{H}(E)^+}$ is the indicator function:

$$\chi_{\mu\in\mathcal{H}(E)^+} := \begin{cases} +\infty & \mu \notin \mathcal{H}(E)^+ \\ 0 & \mu \in \mathcal{H}(E)^+. \end{cases}$$

Clearly we have that:

$$\mathtt{L}_p^*(\varphi) = \sup_{\sigma\in\mathcal{H}(E)} \inf_{\mu\in\mathcal{H}(E)^+} -L(\sigma,\mu), \tag{2.4.11}$$

moreover, it is useful to define:

$$\tilde{\mathtt{L}}_p^* := -\mathtt{L}_p^*(\varphi). \tag{2.4.12}$$

As in (2.2.11)-(2.2.15), the dual problem associated to $\mathtt{\Phi}$ is given by interchanging the "sup" with the "inf" in (2.4.11), so that we define:

$$\begin{aligned} \mathtt{L}_p(\varphi) &:= \inf_{\mu\in\mathcal{H}(E)^+} \sup_{\sigma\in\mathcal{H}_e} -L(\sigma,\mu) \\ &= \inf_{\mu\in\mathcal{H}(E)^+} \sup_{\sigma\in\mathcal{H}(E)} -\sum_{e\in E} \frac{1}{2}\mu_e|\sigma_e|^2 + \sigma\cdot\nabla\varphi + \frac{1}{2\gamma}\sum_{e\in E}{\mu_e}^{\gamma}, \end{aligned} \tag{2.4.13}$$

and

$$\tilde{\mathtt{L}}_p(\varphi) := -\mathtt{L}_p(\varphi).$$

We point out that differently from the continuous case, here we have all the reflexivity necessary in the Banach spaces involved, therefore, all the construction of the perturbation function, the Lagrangian and the dual problem $\mathtt{L}_p(\varphi)$ is well defined in the case $1 \le p < 2$.
Let's focus our attention on the perturbation function $\mathtt{\Phi}(\sigma,\rho)$, we have two cases:

- Case $1 < p < 2$: it is easy to see, with simple computations, that in this case we have the discrete counterpart of (2.2.19):

$$\mathtt{\Phi}(\sigma,\rho) = \frac{1}{2\gamma'} \sum_{e\in E_{|\sigma_e|^2+2\rho_e\ge 0}} (|\sigma_e|^2 + 2\rho_e)^{\gamma'} - \sigma\cdot\nabla\varphi, \tag{2.4.14}$$

  where:

$$E_{|\sigma_e|^2+2\rho_e\ge 0} = \{e\in E \mid |\sigma_e|^2 + 2\rho_e \ge 0\}.$$

- Case $p = 1$: In this case the density μ plays the role of a Lagrange multiplier for the constraint $|\sigma_e|^2 + 2\rho_e \le 1$, $\forall\, e\in E$, thus, the perturbation function becomes:

$$\mathtt{\Phi}(\sigma,\rho) = \begin{cases} -\sigma\cdot\nabla\varphi & |\sigma_e|^2 + 2\rho_e \le 1,\ \forall\, e\in E \\ +\infty & \textit{otherwise.} \end{cases} \tag{2.4.15}$$

As a consequence we have the following theorem.

Theorem 2.4.1. *Let $\mathcal{G} = (E, V, \omega)$ be a weighted directed graph and ∇ it's gradient matrix. Set $p \in \mathbb{R}$ with $1 \leq p < 2$. For a given $\varphi \in \mathcal{H}(V)$, $\varphi_v < \infty$, $\forall\, v \in V$, we define the Lagrangian $\mathtt{L}^p_\varphi : (\mathcal{H}(E)^+ \times \mathcal{H}(E)) \to \mathbb{R}$ as:*

$$\mathtt{L}^p_\varphi(\mu, \sigma) := -\sum_{e\in E} \frac{1}{2}\mu_e|\sigma_e|^2 + \sigma \cdot \nabla\, \varphi + \frac{2-p}{2p}\sum_{e\in E} \mu_e{}^{\frac{p}{2-p}}. \tag{2.4.16}$$

Then, we have that:

$$\mathtt{E}_p(\varphi) = \inf_{\mu\in\mathcal{H}(E)^+} \sup_{\sigma\in\mathcal{H}(E)} \mathtt{L}^p_\varphi(\mu, \sigma),$$

and a saddle point (μ^*, σ^*)(unique in the case $1 < p < 2$) for $\mathtt{L}^p_\varphi$ satisfies the extremality relations:

$$\mu^*_e\sigma^*_e = (\nabla\, \varphi)_e, \quad \forall\, e \in E,\ 1 \leq p < 2 \tag{2.4.17}$$

$$\mu^*_e = |\sigma^*_e|^{p'-2} = |(\nabla\, \varphi)_e|^{2-p}, \quad \forall\, e \in E,\ 1 < p < 2$$

$$|\sigma^*_e| \leq 1, \quad \forall\, e \in E,\ p = 1 \tag{2.4.18}$$

$$\mu^*_e|\sigma^*_e|^2 - \mu^*_e = 0, \quad \forall\, e \in E,\ p = 1 \tag{2.4.19}$$

$$\mu^*_e = |(\nabla\, \varphi)_e|, \quad \forall\, e \in E,\ p = 1. \tag{2.4.20}$$

Moreover, even in the case $p = 1$, μ^* is the unique optimal density.

Proof. First we point out that, with the same arguments as in Lemma 2.2.1, we have that $\Phi(\sigma, \rho) \in \Gamma_0(\mathcal{H}(E) \times \mathcal{H}(E))$.
In the case where $1 < p < 2$ the thesis follows with the same proof of Theorem 2.2.2 where it suffices to substitute integrals with sums over the edges.
As a consequence, we show only the case $p = 1$.
Consider now the functionals $\mathtt{L}^*_1(\varphi)$ and $\mathtt{L}_1(\varphi)$ defined in (2.4.7) and (2.4.13) for $p = 1$.
We have already seen in (2.4.8) the equivalence between $\mathtt{L}^*_1(\varphi)$ and $\mathtt{E}_1(\varphi)$ where a solution σ^* for (2.4.8) is given by (2.4.9), thus, $|\sigma^*_e| \leq 1$, $\forall\, e \in E$ which is (2.4.18).
We will show that $\mathtt{L}_1(\varphi) = \mathtt{L}^*_1(\varphi)$ and that there exist a saddle point for $\mathtt{L}^1_\varphi(\mu, \sigma)$.
As in the proof of Theorem 2.2.2, we will work with $\tilde{\mathtt{L}}^*_1(\varphi)$ as defined in (2.4.12) for $p = 1$ instead of $\mathtt{L}^*_1(\varphi)$, since it is clearly the same a part from a change of sign. Therefore, we will call $(\mathcal{P})$, the primal problem:

$$\tilde{\mathtt{L}}^*_1(\varphi) = \inf_\sigma \left\{ \sup_{\mu\geq 0} -\mathtt{L}^1_\varphi(\mu, \sigma) \right\} \quad (\mathcal{P}),$$

and $(\mathcal{P}^*)$, the dual problem:

$$\tilde{\mathtt{L}}_1(\varphi) = \sup_{\mu\geq 0} \left\{ \inf_\sigma -\mathtt{L}^1_\varphi(\mu, \sigma) \right\} \quad (\mathcal{P}^*).$$

From (2.4.8) and $\mathtt{L}_1^*(\varphi) = -\tilde{\mathtt{L}}_1^*(\varphi)$ we have that the primal problem is:

$$\begin{aligned} &\inf_{\substack{\sigma \in \mathcal{H}(E) \\ \|\sigma\|_{l_\infty} \leq 1}} -\sigma \cdot \nabla \varphi \qquad (\mathcal{P}). \end{aligned}$$

Again, by (2.4.8) and $\tilde{\mathtt{L}}_1^*(\varphi) = -\mathtt{L}_1^*(\varphi)$ we have that

$$\inf(\mathcal{P}) = -\mathtt{E}_1(\varphi).$$

For completeness we also write explicitly the dual problem:

$$\sup_{\mu \in \mathcal{H}(E)^+} \inf_{\sigma \in \mathcal{H}(E)} \sum_{e \in E} \frac{1}{2} \mu_e |\sigma_e|^2 - \frac{1}{2} \sum_{e \in E} \mu_e - \sigma \cdot \nabla \varphi \quad (\mathcal{P}^*).$$

Consider now the perturbation function $\mathtt{\Phi}(\sigma, \rho)$ in (2.4.15). We have already state that $\mathtt{\Phi}(\sigma, \rho) \in \Gamma_0(\mathcal{H}(E) \times \mathcal{H}(E))$ and that problem $(\mathcal{P})$ have a solution and it is finite, therefore, by [46] Propositions 2.1 p.51 and Corollary 2.1 p.52 it suffices to show that problem $(\mathcal{P})$ is stable.
First observe that $\mathtt{\Phi}(\sigma, \rho)$ is nothing that a classical perturbation function for a convex inequality constrained problem. By [46] Proposition 5.1 p.66, if there exists a $\sigma_0 \in \mathcal{H}(E)$ such that $|\sigma_{0e}|^2 < 1$, $\forall\, e \in E$ and $\mathtt{\Phi}(\sigma_0, 0)$ is finite, then problem $(\mathcal{P})$ is stable. Observe now that taking $\sigma_0 = \frac{1}{2}\operatorname{sign}(\nabla \varphi)$ as in (2.4.9), clearly $|\sigma_{0e}|^2 < 1$, $\forall\, e \in E$ and $\mathtt{\Phi}(\sigma_0, 0) = -\frac{1}{2}\mathtt{E}_1(\varphi)$ is finite.
This shows that problem $(\mathcal{P})$ is stable, $\inf(\mathcal{P}) = \sup(\mathcal{P}^*)$, and $(\mathcal{P}^*)$ has at least one solution μ^*.
We will show now that an optimal pair (μ^*, σ^*) is a saddle point for $\mathtt{L}_\varphi^1(\mu, \sigma)$.
By [46] Proposition 2.4 p.53, an optimal pair (μ^*, σ^*) is linked by the extremality relation:

$$\mathtt{\Phi}(\sigma^*, 0) + \mathtt{\Phi}^*(0, \mu^*) = 0. \tag{2.4.21}$$

Using (2.4.15) we have that:

$$\mathtt{\Phi}(\sigma^*, 0) = -\sigma^* \cdot \nabla \varphi.$$

On the other hand, in analogy to (2.2.13), we have:

$$\Phi^*(0, \mu) = \sup_{\sigma \in V} -L(\sigma, \mu), \tag{2.4.22}$$

where the Lagrangian L is defined in (2.4.10). Thus, from (2.4.22), we get:

$$-\Phi^*(0, \mu^*) = \inf_{\sigma \in V} L(\sigma, \mu^*) \overset{(2.4.10)}{=} \inf_{\sigma} \sum_{e \in E} \frac{1}{2} \mu_e^* |\sigma_e|^2 - \frac{1}{2} \sum_{e \in E} \mu_e^* - \sigma \cdot \nabla \varphi.$$

As a consequence, (2.4.21) implies that:

$$-\sigma^* \cdot \nabla \varphi = \tag{2.4.23}$$

$$= \inf_{\sigma} \sum_{e\in E} \frac{1}{2}\mu_e^*|\sigma_e|^2 - \frac{1}{2}\sum_{e\in E}\mu_e^* - \sigma \cdot \nabla \varphi \leq \tag{2.4.24}$$

$$\leq \sum_{e\in E} \frac{1}{2}\mu_e^*|\sigma_e^*|^2 - \frac{1}{2}\sum_{e\in E}\mu_e^* - \sigma^* \cdot \nabla \varphi. \tag{2.4.25}$$

Since σ^* is optimal for $(\mathcal{P})$ and μ^* is optimal for $(\mathcal{P}^*)$, we have that $|\sigma_e^*| \leq 1$, $\forall\, e \in E$ and $\mu^* \in \mathcal{H}(E)^+$, thus:

$$\mu_e^*|\sigma_e^*|^2 - \mu_e^* \leq 0, \quad \forall\, e \in E.$$

On the other hand, (2.4.23)$\leq$(2.4.25) implies that

$$\sum_{e\in E} \left[\mu_e^*|\sigma_e^*|^2 - \mu_e^*\right] \geq 0, \quad \forall\, e \in E,$$

thus, since the addendums are all negative, we have (2.4.19).
As a consequence, (2.4.23)=(2.4.24)=(2.4.25) and σ^* is a solution of (2.4.24) since (2.4.23) is finite.
With the same arguments as in the proof of Theorem 2.2.2, observe that if $\{e \in E \mid |\nabla\varphi|_e > 0\} := \operatorname{supp}(|\nabla\varphi|) \subseteq \operatorname{supp}(\mu^*) := \{e \in E \mid \mu_e^* > 0\}$ then a solution for (2.4.24) exists and it satisfies (2.4.17), to see this it suffices to note that (2.4.24) is differentiable in σ and strictly convex so that the solution is a zero of the first derivative. Moreover, (2.4.17) is also a necessary condition, otherwise either $\operatorname{supp}(\mu^*) \cap \operatorname{supp}(|\nabla\varphi|) = \emptyset$ or $\operatorname{supp}(\mu^*) \cap \operatorname{supp}(|\nabla\varphi|) \subset \operatorname{supp}(|\nabla\varphi|)$, therefore if that happens, there exists an $A \subset E$ such that $\mu_e^* = 0$ and $|\nabla\varphi|_e > 0$ $\forall\, e \in A$, moreover, $\forall\, M > 0$, $M \in \mathbb{R}$, there exists a $\sigma_t = t\bar{\sigma}$, $t > M$, with $\sigma_{te} = 0$, $\forall\, e \in E \setminus A$ and $\sum_{e\in A} \sigma_{te}(\nabla\varphi)_e = t$, implying that:

$$\inf_{\sigma} \sum_{e\in E} \frac{1}{2}\mu_e^*|\sigma_e|^2 - \frac{1}{2}\sum_{e\in E}\mu_e^* - \sigma \cdot \nabla \varphi \leq$$

$$\leq \sum_{e\in E} \frac{1}{2}\mu_e^*|\sigma_{te}|^2 - \frac{1}{2}\sum_{e\in E}\mu_e^* - \sum_{e\in E}\sigma_{te}(\nabla\varphi)_e \leq$$

$$\leq -\frac{1}{2}\sum_{e\in E}\mu_e^* - \sum_{e\in A}\sigma_{te}(\nabla\varphi)_e \leq -t < -M, \quad \forall\, M > 0.$$

hence, (2.4.24) is equal to $-\infty$ which is a contradiction since (2.4.23) is finite.
Setting

$$\mu_e^* = |(\nabla\varphi)_e|, \quad \forall\, e \in E,$$

for any generalized signum solution σ^* of $(\mathcal{P})$ we have clearly that

$$\mu^* \odot \sigma^* = \nabla\varphi,$$

and (2.4.19) is satisfied, therefore, the pair

$$(\mu^* = |\nabla \varphi|, \sigma^*),$$

is a saddle point for $\mathtt{L}^1_\varphi(\mu, \sigma)$.
Moreover, in virtue of (2.4.17) and (2.4.19) , $\mu^* = |\nabla \varphi|$ is the unique optimal density, there are no other possibilities, since $|\sigma^*_e| \leq 1$, $\forall\, e \in E$ and by (2.4.19), $|\sigma^*_e| = 1$, $\forall\, e \in E$ $s.t. \mu^*_e > 0$, so that:

$$|(\nabla \varphi)_e| = |\mu^*_e \sigma^*_e| = \mu^*_e |\sigma^*_e| \geq \mu^*_e \quad \forall\, e \in E,$$

hence μ^* is zero where $|\nabla \varphi|$ vanish and

$$|(\nabla \varphi)_e| = \mu^*_e \quad \forall\, e \in E \ s.t. \mu^*_e > 0.$$

This completes the proof. □

Remark 2.4.2. *The extremality relations* (2.4.17)-(2.4.20) *are nothing that the KKT conditions for the saddle points* (μ^*, σ^*) *of* $\mathtt{L}_p(\varphi)$, $1 \leq p < 2$, *which read as follows:*

$$\begin{cases} -|\sigma^*_e|^2 + {\mu^*_e}^{\frac{2(p-1)}{2-p}} - c_e = 0, & \forall\, e \in E \\ \mu^*_e \sigma^*_e = (\nabla \varphi)_e, & \forall\, e \in E \\ c_e \mu^*_e = 0, \quad c_e \geq 0, & \forall\, e \in E. \end{cases} \tag{2.4.26}$$

where $c \in \mathcal{H}(E)$ *is an opportune positive Lagrange multiplier.*
Observe that in the case $1 < p < 2$, *since* $c \geq 0$, *if* $\mu^*_{\bar e} = 0$ *on some edge* $\bar e$, *then the first equation in* (2.4.26) *implies that* $\sigma^*_{\bar e} = 0$ *and* $c_{\bar e} = 0$, *this is the unique possible solution. On the edges where* $\mu^*_e > 0$, *the third equation gives that* $c_e = 0$. *Therefore,* (2.4.26) *implies that*

$$\begin{cases} \mu^*_e = |\sigma^*_e|^{\frac{2-p}{p-1}} = |\sigma^*_e|^{p'-2} = |(\nabla \varphi)_e|^{2-p}, & \forall\, e \in E,\ 1 < p < 2 \\ \mu^*_e \sigma^*_e = (\nabla \varphi)_e. & \forall\, e \in E,\ 1 < p < 2. \end{cases}$$

In the case $p = 1$, *if* $\mu^*_{\bar e} = 0$ *on some edge* $\bar e$, *then the first equation in* (2.4.26) *admits a solution iff* $|\sigma^*_{\bar e}|^2 - 1 \leq 0$. *On the other hand, the third equation in* (2.4.26) *implies that if* $\mu^*_{\bar e} > 0$, *then* $c_{\bar e} = 0$ *and hence* $|\sigma^*_{\bar e}| = 1$. *At the end of the story,* (2.4.26) *recovers the remaining extremality relation of Theorem 2.4.1 in the case* $p = 1$*:*

$$\begin{cases} |\sigma^*_e| \leq 1, & \forall\, e \in E,\ p = 1 \\ |\sigma^*_e| = 1, & \forall\, e \in E \ s.t.\ \mu^*_e > 0,\ p = 1 \\ \mu^*_e \sigma^*_e = (\nabla \varphi)_e, & \forall\, e \in E,\ p = 1. \end{cases}$$

where the unique possible optimal density is $\mu^*_e = |(\nabla \varphi)_e|$, $\forall\, e \in E$.

2.5 Generalizations to different discrete operators

In Section 2.4 we have seen how the techniques presented in Section 2.3 interlaces with graph theory and more essentially with the natural differential structure on graphs given by the graph gradient operator.
From a mathematical point of view, working on graphs or working with a linear operator $\Lambda : \mathbb{R}^n \to \mathbb{R}^m$ is genuinely the same.
Motivated by this, we call $V := \mathbb{R}^n$ and $E := \mathbb{R}^m$ and we introduce the Λ based p-Dirichlet energy for $\varphi \in V$, $1 \leq p$, as:

$$\mathtt{E}_p^{\Lambda}(\varphi) := \frac{\|\Lambda\varphi\|_{l_p}^p}{p},$$

where for a $g \in \mathbb{R}^k$ we define $\|g\|_{l_p} := \left(\sum_{i=1}^k |g_i|^p\right)^{\frac{1}{p}}$, and in the limit case $p = \infty$ we define the l_∞-norm as $\|g\|_{l_\infty} := \sup_{i=1,..,k} |g_i|$.
As a consequence, for a finite $\varphi \in V$, $\varphi_i < \infty$, $i = 1, .., n$, all the arguments in Section 2.4 works and we introduce our duality based saddle point formulation of $\mathtt{E}_p^{\Lambda}(\varphi)$:

$$\mathtt{L}_p^{\Lambda^*}(\varphi) := \sup_{\sigma \in E} \inf_{\mu \in E^+} -\sum_{i=1}^m \frac{1}{2}\mu_i|\sigma_i|^2 + \sigma \cdot \Lambda\varphi + \frac{2-p}{2p}\sum_{i=1}^m \mu_i^{\frac{p}{2-p}}, \tag{2.5.1}$$

where $p := 2 - p$, and $E^+ := \{\mu \in E \mid \mu_i \geq 0,\ i = 1, ..., m\}$.
The dual definition of (2.5.1) reads as follows:

$$\mathtt{L}_p^{\Lambda}(\varphi) := \inf_{\mu \in E^+} \sup_{\sigma \in E} -\sum_{i=1}^m \frac{1}{2}\mu_i|\sigma_i|^2 + \sigma \cdot \Lambda\varphi + \frac{2-p}{2p}\sum_{i=1}^m \mu_i^{\frac{p}{2-p}}.$$

Theorem 2.4.1 rewrites as:

Theorem 2.5.1. *Let $V = \mathbb{R}^n$, $E = \mathbb{R}^m$ and $\Lambda : V \to E$ be a linear operator. Set $p \in \mathbb{R}$ with $1 \leq p < 2$. For a given $\varphi \in V$, $\varphi_i < \infty$, $i = 1, ..., n$, we define the Lagrangian $\mathtt{L}_\varphi^{p,\Lambda} : (E^+ \times E) \to \mathbb{R}$ as:*

$$\mathtt{L}_\varphi^{p,\Lambda}(\mu, \sigma) := -\sum_{i=1}^m \frac{1}{2}\mu_i|\sigma_i|^2 + \sigma \cdot \Lambda\varphi + \frac{2-p}{2p}\sum_{i=1}^m \mu_i^{\frac{p}{2-p}}.$$

Then, we have that

$$\mathtt{E}_p^{\Lambda}(\varphi) = \mathtt{L}_p^{\Lambda^*}(\varphi) = \mathtt{L}_p^{\Lambda}(\varphi) = \inf_{\mu \in E^+} \sup_{\sigma \in E} \mathtt{L}_\varphi^{p,\Lambda}(\mu, \sigma), \tag{2.5.2}$$

and a saddle point (μ^*, σ^*)(unique in the case $1 < p < 2$) for $\mathtt{L}_\varphi^{p,\Lambda}$ satisfies the

extremality relations:

$$\begin{aligned}
\mu_i^* \sigma_i^* &= (\Lambda\varphi)_i, \quad i = 1, ..., m,\ 1 \le p < 2 \\
\mu_i^* = |\sigma_i^*|^{p'-2} &= |(\Lambda\varphi)_i|^{2-p}, \quad i = 1, ..., m,\ 1 < p < 2 \\
|\sigma_i^*| &\le 1, \quad i = 1, ..., m,\ p = 1 \\
\mu_i^* |\sigma_i^*|^2 - \mu_i^* &= 0, \quad i = 1, ..., m,\ p = 1 \\
\mu_i^* &= |(\Lambda\varphi)_i|, \quad i = 1, ..., m,\ p = 1.
\end{aligned}$$

Moreover, even in the case $p = 1$, μ^* is the unique optimal density.

Proof. It suffices to observe that V plays the role of the nodes space, E plays the role of the edges space and Λ plays the role of the graph gradient operator. Thus, the proof is exactly the same of Theorem 2.4.1. □

We have an immediate corollary.

Corollary 2.5.2. *Let $V = \mathbb{R}^n$ and define the Lagrangian $\mathtt{l}_\varphi^p : (V^+ \times V) \to \mathbb{R}$ as:*

$$\mathtt{l}_\varphi^p(\nu, \sigma) := -\sum_{i=1}^n \frac{1}{2} \nu_i |\sigma_i|^2 + \sigma \cdot \varphi + \frac{2-p}{2p} \sum_{i=1}^n \nu_i^{\frac{p}{2-p}}.$$

Set

$$\begin{aligned}
\mathtt{l}_p{}^*(\varphi) &:= \sup_{\sigma \in V} \inf_{\nu \in V^+} \mathtt{l}_\varphi^p(\nu, \sigma), \\
\mathtt{l}_p(\varphi) &:= \inf_{\nu \in V^+} \sup_{\sigma \in V} \mathtt{l}_\varphi^p(\nu, \sigma),
\end{aligned} \tag{2.5.3}$$

where $1 \le p < 2$. For a given $\varphi \in V$, $\varphi_i < \infty$, $i = 1, ..., n$, we have that

$$\frac{1}{p} \|\varphi\|_{l_p}^p = \mathtt{l}_p{}^*(\varphi) = \mathtt{l}_p(\varphi) = \inf_{\nu \in V^+} \sup_{\sigma \in V} \mathtt{l}_\varphi^p(\nu, \sigma),$$

and a saddle point (ν^*, σ^*) (unique in the case $1 < p < 2$) for $\mathtt{l}_\varphi^p$ satisfies the extremality relations:

$$\begin{aligned}
\nu_i^* \sigma_i^* &= \varphi_i, \quad i = 1, ..., n,\ 1 \le p < 2 \\
\nu_i^* = |\sigma_i^*|^{p'-2} &= |\varphi_i|^{2-p}, \quad i = 1, ..., n,\ 1 < p < 2 \\
|\sigma_i^*| &\le 1, \quad i = 1, ..., n,\ p = 1 \\
\nu_i^* |\sigma_i^*|^2 - \nu_i^* &= 0, \quad i = 1, ..., n,\ p = 1 \\
\nu_i^* &= |\varphi_i|, \quad i = 1, ..., n,\ p = 1.
\end{aligned}$$

Moreover, even in the case $p = 1$, ν^* is the unique optimal density.

Proof. Set Λ equal to the identity operator in Theorem 2.5.1. □

2.5.1 The regularized problem

In order to avoid ill-conditioning still maintaining sufficient accuracy, it is useful, at least from the prospective of numerical applications, to consider a regularized version for the functional defined in (2.5). In the framework of the Tikhonov regularization, consider a small Tikhonov parameter $\delta > 0$, $\delta << 1$ and the regularized Lagrangian for $1 \leq p < 2$ as:

$$\mathtt{L}_{\varphi}^{p,\Lambda,\delta}(\mu,\sigma) := -\sum_{i=1}^{m} \frac{1}{2}(\mu_i+\delta)|\sigma_i|^2 + \sigma\cdot\Lambda\varphi + \frac{2-p}{2p}\sum_{i=1}^{m}\mu_i^{\frac{p}{2-p}}, \tag{2.5.4}$$

We define the regularized saddle point formulation of $\mathtt{E}_p^{\Lambda}$ as:

$$\mathtt{L}_{p,\delta}^{\Lambda}(\varphi) := \inf_{\mu\in E^+}\sup_{\sigma\in E}\mathtt{L}_{\varphi}^{p,\Lambda,\delta}(\mu,\sigma), \quad \forall\,\varphi\in V. \tag{2.5.5}$$

If we introduce the functional

$$\mathcal{L}_{\delta}^{p,\Lambda}(\varphi,\mu) := \sup_{\sigma\in E}\mathtt{L}_{\varphi}^{p,\Lambda,\delta}(\mu,\sigma), \tag{2.5.6}$$

then (2.5.5) rewrites as:

$$\mathtt{L}_{p,\delta}^{\Lambda}(\varphi) = \inf_{\mu\in E^+}\mathcal{L}_{\delta}^{p,\Lambda}(\varphi,\mu).$$

The parameter δ has the important role to guarantees the coercivity and the differentiability of the map:

$$\sigma \mapsto \mathtt{L}_{\varphi}^{p,\Lambda,\delta}(\mu,\sigma), \quad \forall\,\varphi\in V,\ \forall\,\mu\in E^+,$$

with the aim to directly compute a maximizer σ^* for (2.5.6) and simplify (2.5.5), while retaining a good approximation of the original saddle point formulation (2.5.2), if δ is sufficiently small.
Let's focus our attention on the functional $\mathtt{L}_{p,\delta}^{\Lambda}(\varphi)$.
Since $\mu+\delta > 0$, the supremum in (2.5.6) is in fact a maximum(we have indeed strong concavity, differentiability and anti-coerciveness), and the maximizer σ^* is given by:

$$\sigma_i^* = \frac{(\Lambda\varphi)_i}{\mu_i+\delta}, \quad i=1,...,m. \tag{2.5.7}$$

.
Hence, computing $\mathtt{L}_{\varphi}^{p,\Lambda,\delta}(\mu,\sigma)$ for $\sigma=\sigma^*$, the functional defined in (2.5.6) is equal to:

$$\mathcal{L}_{\delta}^{p,\Lambda}(\varphi,\mu) = \sum_{i=1}^{m}\frac{1}{2}\frac{|(\Lambda\varphi)_i|^2}{(\mu_i+\delta)} + \frac{2-p}{2p}\sum_{i=1}^{m}\mu_i^{\frac{p}{2-p}}, \tag{2.5.8}$$

and the regularized saddle point formulation in (2.5.5) simplifies as follows:

$$\mathtt{L}_{p,\delta}^{\Lambda}(\varphi) = \inf_{\mu\in E^+}\sum_{i=1}^{m}\frac{1}{2}\frac{|(\Lambda\varphi)_i|^2}{(\mu_i+\delta)} + \frac{2-p}{2p}\sum_{i=1}^{m}\mu_i^{\frac{p}{2-p}}. \tag{2.5.9}$$

Moreover, if we introduce the function:

$$\varepsilon_\varphi(\mu) := \mathcal{L}_\delta^{p,\Lambda}(\varphi,\mu), \quad \forall\, \varphi \in V,$$

we clearly have that:

$$\varepsilon_\varphi(\mu) \geq \sum_{i=1}^m \frac{1}{2}\frac{|(\Lambda\varphi)_i|^2}{\delta} + \frac{2-p}{2p}\sum_{i=1}^m \mu_i^{\frac{p}{2-p}}, \quad \forall\, \mu \in E^+. \tag{2.5.10}$$

Thus, $\varepsilon_\varphi(\mu)$ is convex, lower semi-continuous and coercive in μ, for any $\varphi \in V$. Therefore, the existence of a minimizer μ^* for (2.5.9) is guaranteed.
The same arguments can be applied for the graph based p-Dirichlet energy (2.4.13) and the discrete l_p-norm (2.5.3).
In particular, in the same setting of Theorem 2.4.1, the regularized functional of $\mathtt{L}_1(\varphi)$ becomes:

$$\mathtt{L}_{1,\delta}(\varphi) := \inf_{\mu\in\mathcal{H}(E)^+} \sum_{e\in E} \frac{1}{2}\frac{|(\nabla\varphi)_e|^2}{(\mu_e+\delta)} + \frac{1}{2}\sum_{e\in E}\mu_e, \tag{2.5.11}$$

and in the same setting of Corollary 2.5.2, the regularized version of $\mathtt{l}_1(\varphi)$ is:

$$\mathtt{l}_{1,\delta}(\varphi) := \inf_{\nu\in V^+} \sum_{i=1}^n \frac{1}{2}\frac{|\varphi_i|^2}{(\nu_i+\delta)} + \frac{1}{2}\sum_{i=1}^n \nu_i. \tag{2.5.12}$$

2.6 Extension to other types of discrete energies

In Section 2.5 we have seen how to generalize our saddle point formulation for l_p-norms type energies for general discrete linear operators.
In a similar fashion, one may wonder if the same techniques can be extended to more general types of convex discrete energies.
Let $V := \mathbb{R}^n$, $E := \mathbb{R}^m$ and $\Lambda : V \to E$ be a linear discrete operator. For a given $\varphi \in V$, $\varphi_i < \infty$, $i = 1, ..., n$, let $h : \mathbb{R} \to \mathbb{R}^+$ be a positive, lower semi-continuous, convex, even function and consider the following type of energy:

$$\mathtt{E}(\varphi) := \sum_{i=1}^m h((\Lambda\varphi)_i). \tag{2.6.1}$$

Our goal is to state a sufficient and necessary condition in order to provide a saddle point formulation for (2.6.1) as (2.4.6).
We have the following theorem.

Theorem 2.6.1. *Let $V := \mathbb{R}^n$, $E := \mathbb{R}^m$ and $\Lambda : V \to E$ be a linear discrete operator. For a given $\varphi \in V$, $\varphi_i < \infty$, $i = 1, ..., n$, consider the energy $\mathtt{E}(\varphi)$ as in (2.6.1). Define the Lagrangian $\mathtt{L}_\varphi^{E,\Lambda} : (E^+ \times E) \to \mathbb{R}$ as*

$$\mathtt{L}_\varphi^{\mathtt{E},\Lambda}(\mu,\sigma) := \sigma\cdot\Lambda\varphi - \frac{1}{2}\sum_{i=1}^m \mu_i|\sigma_i|^2 + \frac{1}{2}\sum_{i=1}^m g(\mu_i).$$

Then, we can write the following saddle point formulation:

$$\mathtt{E}(\varphi) = \sup_{\sigma\in E}\inf_{\mu\in E^+} \mathtt{L}_\varphi^{\mathtt{E},\Lambda}(\mu,\sigma), \tag{2.6.2}$$

iff there exists a convex, proper and lower semi-continuous function $g : \mathbb{R} \to \mathbb{R}$ such that the following Legendre duality relation holds:

$$\left(\frac{1}{2}(g\circ|\cdot|)^*\circ|\cdot|^2\right)^* = h, \tag{2.6.3}$$

where for a function $\gamma : \mathbb{R} \to \mathbb{R}$, $\gamma\circ|\cdot|(x) := \gamma(|x|)$ and $\gamma\circ|\cdot|^2(x) := \gamma(|x|^2)$ As a consequence:

$$\mathtt{E}(\varphi) = \sum_{i=1}^m \left(\frac{1}{2}(g\circ|\cdot|)^*\circ|\cdot|^2\right)^* ((\Lambda\varphi)_i)\,. \tag{2.6.4}$$

Moreover, if g implies that there exists a $\sigma_0 \in E$ and a discrete norm $\|\cdot\|$ such that:

$$\rho(\mu) := \sigma_0\cdot\Lambda\varphi - \frac{1}{2}\sum_{i=1}^m \mu_i|\sigma_{0i}|^2 + \frac{1}{2}\sum_{i=1}^m g(\mu_i), \tag{2.6.5}$$

is norm coercive i.e. $\lim_{\substack{\mu\in E^+\\ \|\mu\|\to\infty}} \rho(\mu) = +\infty$ and one of the following holds true:

- *(a)*
$$\varepsilon(\sigma) := \inf_{\mu\in E^+} \mathtt{L}_\varphi^{E,\Lambda}(\mu,\sigma),$$
is concave, upper semi-continuous and norm anti-coercive, i.e. there exists a discrete norm $\|\cdot\|$ such that $\lim_{\|\sigma\|\to\infty}\varepsilon(\sigma) = -\infty$

- *(b)*
$$\sup_{\sigma\in E}\varepsilon(\sigma) = \sup_{\sigma\in\mathcal{B}}\sigma\cdot\Lambda\varphi + J(\sigma),$$
where $\mathcal{B}\subset E$ is convex, closed, bounded, non empty and J is concave, upper semi-continuous

then there exists a saddle point (μ^*,σ^*) for $\mathtt{L}_\varphi^{\mathtt{E},\Lambda}$ and we can interchange "sup" with "inf" in (2.6.2):

$$\mathtt{E}(\varphi) = \inf_{\mu\in E^+}\sup_{\sigma\in E} \mathtt{L}_\varphi^{\mathtt{E},\Lambda}(\mu,\sigma). \tag{2.6.6}$$

If furthermore, g is differentiable with derivative g', a saddle point (μ^*,σ^*) for $\mathtt{L}_\varphi^{\mathtt{E},\Lambda}$ satisfies the following extremality relations:

$$\begin{aligned}
\mu_i^*\sigma_i^* &= (\Lambda\varphi)_i, \quad i = 1,...,m,\\
g'(\mu_i^*) &= |\sigma_i^*|^2, \quad i = 1,...,m,\ \mu_i^* > 0\\
-|\sigma_i^*|^2 + g'(0) &\geq 0, \quad i = 1,...,m,\ \mu_i^* = 0,\ g'(0) > 0\\
\sigma_i^* &= 0, \quad i = 1,...,m,\ \mu_i^* = 0,\ g'(0) = 0.
\end{aligned}$$

In the case where the particular structure of g implies this as a necessary condition and it is possible to know that g is differentiable on a convex and closed neighborhood $\mathcal{A} \subseteq E^+$ of a solution μ^*, or g is differentiable and $g'(0) < 0$, then $\mu_i^* > 0$, $i = 1, ..., m$.
In this case the extremality relations simplify to:

$$\mu_i^* > 0, \;\; \sigma_i^* = \frac{(\Lambda\varphi)_i}{\mu_i^*}, \;\; (\mu_i^*)^2 g'(\mu_i^*) = |(\Lambda\varphi)_i|^2 \quad i = 1, ..., m. \tag{2.6.7}$$

Proof. First we observe that the Legendre transform for a function $\Gamma : E \to \mathbb{R}$ of the type $\Gamma(y) = \sum_{i=1}^m \gamma(y_i)$, $\gamma : \mathbb{R} \to \mathbb{R}$, is exactly the sum of the Legendre transforms for any single addendum, i.e. $\Gamma^*(y^*) = \sum_{i=1}^m \gamma^*(y_i^*)$.
Moreover, observe that necessary the function h has to be convex and even since the Legendre transform of an even function is even [87], thus otherwise, formula (2.6.3) could not be satisfied for any mass function g.
Next, for any function $g : \mathbb{R} \to \mathbb{R}$ and $\forall\, x \geq 0$ we have that:

$$\sup_{\mu \geq 0} x\mu - g(\mu) = (g \circ |\cdot|)^*(x), \tag{2.6.8}$$

since:

$$\sup_{\mu \geq 0} x\mu - g(\mu) = \sup_{\mu \geq 0} x\mu - g(|\mu|) \leq (g \circ |\cdot|)^*(x) \leq$$
$$\overset{(x \geq 0)}{\leq} \sup_{\mu} x|\mu| - g(|\mu|) = \sup_{\mu \geq 0} x\mu - g(\mu).$$

Consider now the saddle point formulation (2.6.2). Summing up all together we have:

$$\sup_{\sigma \in E} \inf_{\mu \in E^+} \mathrm{L}_\varphi^{\mathrm{E},\Lambda}(\mu, \sigma) = \sup_{\sigma \in E} \inf_{\mu \in E^+} \sigma \cdot \Lambda\varphi - \frac{1}{2}\sum_{i=1}^m \mu_i |\sigma_i|^2 + \frac{1}{2}\sum_{i=1}^m g(\mu_i) =$$
$$= \sup_{\sigma \in E} \sigma \cdot \Lambda\varphi - \sup_{\mu \in E^+} \frac{1}{2}\sum_{i=1}^m \mu_i |\sigma_i|^2 - \frac{1}{2}\sum_{i=1}^m g(\mu_i) =$$
$$\overset{(2.6.8)}{=} \sup_{\sigma \in E} \sum_{i=1}^m \sigma_i (\Lambda\varphi)_i - \frac{1}{2}\sum_{i=1}^m (g \circ |\cdot|)^*(|\sigma_i|^2) =$$
$$= \sum_{i=1}^m \left(\frac{1}{2}(g \circ |\cdot|)^* \circ |\cdot|^2\right)^* ((\Lambda\varphi)_i)\,. \tag{2.6.9}$$

This shows that (2.6.2) holds true iff (2.6.3) holds and g, h are convex and proper, otherwise we can not recover g from h since this require to apply twice the Legendre transform to both of them. As a consequence, (2.6.4) follows directly from (2.6.3) and (2.6.9).

Now we treat the existence and characterization of a saddle point (μ^*, σ^*) for $\mathtt{L}_\varphi^{\mathtt{E},\Lambda}$.
If either (a) or (b) holds the problem

$$\sup_{\sigma\in E}\left\{\inf_{\mu\in E^+}\mathtt{L}_\varphi^{\mathtt{E},\Lambda}(\mu,\sigma)\right\},$$

admits a solution and the existence of a saddle point (μ^*, σ^*) follows directly from [46] Proposition 2.4 p.176.
This is essentially the stability of the primal problem $(\mathcal{P})$ in Theorems 2.4.1 and 2.5.1, since if we define the perturbation function:

$$\mathtt{\Phi}(\sigma,\psi) := \sup_{\mu\in E^+} -\sigma\cdot\Lambda\varphi + \sum_{i=1}^m \frac{\mu_i|\sigma_i|^2+2\psi_i}{2} - \frac{1}{2}\sum_{i=1}^m g(\mu_i).$$

where $\psi \in E$, clearly $\mathtt{\Phi}(\sigma,\psi)$ is well define (g is convex and lower semi-continuous) and $\mathtt{\Phi}(\sigma,\psi) \in \Gamma_0(E\times E)$ (as in Lemma 2.2.1) because it is a supremum of a family of convex functions, therefore, the existence of a $\sigma_0 \in E$ which makes $\rho(\mu)$ norm coercive is exactly equivalent to the continuity of $\psi \mapsto \mathtt{\Phi}(\sigma_0,\psi)$ in 0 (cf.[46] Lemma 4.3 p. 183).
As a consequence, problem (2.6.2) is equivalent to (2.6.6), i.e. they have the same optimal value $\mathtt{E}(\varphi)$, we can interchange "inf" with "sup" and there exists a saddle point (μ^*, σ^*) for $\mathtt{L}_\varphi^{\mathtt{E},\Lambda}$.
Finally if g is differentiable, the KKT conditions for problem (2.6.6) reads as follows:

$$\begin{cases} -|\sigma_i^*|^2 + g'(\mu_i) - c_i = 0, & i = 1,..,m \\ \mu_i^*\sigma_i^* = (\Lambda\varphi)_i, & i = 1,...,m \\ c_i\mu_i^* = 0, \quad c_i \geq 0, & i = 1,...,m. \end{cases} \tag{2.6.10}$$

where $c \in E$ is an opportune positive Lagrange multiplier.
In the case where $\mu_j^* > 0$ for an index $1 \leq j \leq m$, the third equation gives that $c_j = 0$ and therefore the extremality relations are satisfied iff $g'(\mu_j^*) = |\sigma_j^*|^2$.
On the other hand, since $c \geq 0$, if $\mu_j^* = 0$ on some index $1 \leq j \leq m$ and $g'(0) > 0$, (2.6.10) has a solutions iff $-|\sigma_j^*|^2 + g'(0) \geq 0$. If $g'(0) = 0$, the only possible solution is $\sigma_j^* = 0$ and $c_j = 0$ which holds iff $(\Lambda\varphi)_j = 0$. If $g'(0) < 0$, the first equation in (2.6.10) has no solutions, thus necessary $\mu^* > 0$ and the extremality relations simplify to (2.6.7). In the case where g implies that necessary a solution μ^* is such that $\mu_i^* > 0$, $i = 1,..,m$ and there exists a convex and closed neighborhood $\mathcal{A} \subseteq E^+$ of μ^* where g is differentiable, possibly restricting (2.6.6) on $\mathcal{A}$, μ^* becomes an interior critical point therefore the extremality relations simplify to (2.6.7). □

Remark 2.6.2. *In virtue of the symmetrical role played by μ and σ, (a) and (b) in Theorem 2.6.1 can be interchanged by the following:*

- *(I) there exists a* $\mu_0 \in E^+$ *and a discrete norm* $\|\cdot\|$ *such that:*

$$\rho(\sigma) := \sigma \cdot \Lambda\varphi - \frac{1}{2}\sum_{i=1}^{m} \mu_{0i}|\sigma_i|^2 + \frac{1}{2}\sum_{i=1}^{m} g(\mu_{0_i}),$$

is norm anti-coercive i.e. $\lim_{\|\sigma\|\to\infty} \rho(\sigma) = -\infty$

- *(II)* $g(\mu)$ *is norm coercive in* E^+*, i.e. there exists a discrete norm* $\|\cdot\|$ *such that*

$$\lim_{\substack{\mu \in E^+ \\ \|\mu\| \to \infty}} g(\mu) = +\infty.$$

Note that if (II) *holds, by the same homogeneity arguments as in* (2.3.27) *we have:*

$$\varepsilon(\mu) := \sup_{\sigma\in E} \sigma \cdot \Lambda\varphi - \frac{1}{2}\sum_{i=1}^{m} \mu_i|\sigma_i|^2 + \frac{1}{2}\sum_{i=1}^{m} g(\mu_i),$$

$$\varepsilon(\mu) \geq \frac{(\|\Lambda\varphi\|_{l_1})^2}{2\sum_{i=1}^{m}\mu_i} + \frac{1}{2}\sum_{i=1}^{m} g(\mu_i) > \frac{1}{2}\sum_{i=1}^{m} g(\mu_i) \geq 0.$$

Therefore,if g *is norm coercive, also* ε *is norm coercive and the hypothesis of [46] Porposition 2.4 p.176 are satisfied in the interchanged circumstances (see [46] Remark 2.4 p.177).*

We will now see two illustrative examples on how to use (2.6.3) to construct an equivalent saddle point formulation.

Example 2.6.3 (Recovering the graph Total Variation Energy saddle point formulation)**.** *Let* $\mathcal{G}$ *be a weighted directed graph and* ∇ *it's gradient matrix. Our spaces are therefore* $E = \mathbb{R}^m$ *and* $V = \mathbb{R}^n$ *where* $m = \#edges$*,* $n = \#nodes$ *and* $\Lambda = \nabla$*.*
The graph 1*-Dirichlet energy or the graph Total Variation energy is:*

$$\mathtt{E}(\varphi) := \|\nabla\varphi\|_{l_1} = \sum_{i=1}^{m} |(\nabla\varphi)_i|,$$

whence $h = |\cdot|$ *which is convex,proper, and even.*
Formula (2.6.3) *reads as follows:*

$$\left(\frac{1}{2}(g \circ |\cdot|)^* \circ |\cdot|^2\right)^* (x) = |x|.$$

The Legendre transform of h *is:*

$$h^*(x^*) = \chi_{|x^*|\leq 1} = \chi_{|x^*|^2\leq 1} = \begin{cases} 0 & |x^*|^2 \leq 1 \\ +\infty & |x^*|^2 > 1. \end{cases} \tag{2.6.11}$$

So that, using (2.6.11) *we have:*

$$\frac{1}{2}(g\circ|\cdot|)^*(|x^*|^2)=h^*(x^*)=\chi_{|x^*|^2\leq 1},$$

which implies that:

$$(g\circ|\cdot|)^*(y)=2\chi_{y\leq 1}=\chi_{y\leq 1}. \tag{2.6.12}$$

Applying again the Legendre transform and evaluating in $\mu\geq 0$ we have:

$$\begin{aligned} g(\mu)=(g\circ|\cdot|)(\mu)=(g\circ|\cdot|)^{**}(\mu)\overset{(2.6.12)}{=}(\chi_{(\cdot)\leq 1})^*(\mu)=\\ =\sup_y \mu y-\chi_{y\leq 1}=\sup_q \mu(1-q)-\chi_{q\geq 0}=\\ =\mu+\sup_{q\geq 0}-\mu q=\mu,\quad \forall\,\mu\geq 0. \end{aligned}$$

Hypothesis (2.6.5) *and (b) of Theorem 2.6.1 are satisfied (see the proof of Theorem 2.4.1,it suffices to take $\sigma_0=\frac{1}{2}\operatorname{sign}(\nabla\varphi)$). Observe that taking μ_0 such that $\mu_{0_i}=1$, $i=1,...,m$, having g clearly norm coercive, also hypothesis (I)-(II) of Remark 2.6.2 are satisfied.*
As a consequence we obtain that:

$$\|\nabla\varphi\|_{l_1}=\inf_{\mu\in E^+}\sup_{\sigma\in E}-\frac{1}{2}\sum_{i=1}^m\mu_i|\sigma_i|^2+\sigma\cdot\nabla\varphi+\frac{1}{2}\sum_{i=1}^m\mu_i,$$

which is exactly (2.4.13) *for $p=1$.*
Moreover the extremality relations from Theorem 2.4.1 are the same of that from Theorem 2.6.1.

Example 2.6.4 (Minimal Surfaces type energy)**.** *Let $V=\mathbb{R}^n$, $E=\mathbb{R}^m$ and $\Lambda:V\to E$ be a linear discrete operator. Consider now an energy of the type:*

$$\mathtt{E}(\varphi):=\sum_{i=1}^m\sqrt{1+|(\Lambda\varphi)_i|^2}.$$

This kind of energy is derived as a discrete counterpart for the continuous minimal surfaces energy where in the continuous case Λ is replaced by the gradient operator.
In this case we have $h=\sqrt{1+|\cdot|^2}$ which is convex and proper.
Formula (2.6.3) *reads as follows:*

$$\left(\frac{1}{2}(g\circ|\cdot|)^*\circ|\cdot|^2\right)^*(x)=\sqrt{1+|x|^2}.$$

The Legendre transform of h is easy to compute and is given by:

$$h^*(x^*)=\begin{cases}-\sqrt{1-|x^*|^2} & |x^*|^2\leq 1\\ +\infty & |x^*|^2>1.\end{cases} \tag{2.6.13}$$

Using (2.6.13) *we have:*

$$\frac{1}{2}(g\circ|\cdot|)^*(|x^*|^2)=h^*(x^*)=\begin{cases}-\sqrt{1-|x^*|^2} & |x^*|^2\leq 1\\ +\infty & |x^*|^2>1,\end{cases}$$

which implies that:

$$(g\circ|\cdot|)^*(y)=\gamma(y):=\begin{cases}-2\sqrt{1-y} & y\leq 1\\ +\infty & y>1.\end{cases} \tag{2.6.14}$$

Applying again the Legendre transform and evaluating in $\mu\geq 0$ *we have:*

$$\begin{aligned}g(\mu)=(g\circ|\cdot|)(\mu)=(g\circ|\cdot|)^{**}(\mu)\overset{(2.6.14)}{=}\gamma^*(\mu)=\\ =\sup_y \mu y-\gamma(y)=\sup_{y\leq 1}\mu y+2\sqrt{1-y}=\\ =\begin{cases}\frac{1}{\mu}+\mu & \mu>0\\ +\infty & \mu=0\end{cases},\quad \forall\,\mu\geq 0.\end{aligned}$$

Consider now the function:

$$\rho(\mu)=\sigma_0\cdot\Lambda\varphi-\frac{1}{2}\sum_{i=1}^m\mu_i|\sigma_{0i}|^2+\frac{1}{2}\sum_{i=1}^m(\frac{1}{\mu_i}+\mu_i).$$

Taking σ_0 *such that* $\sigma_{0i}=\frac{1}{\sqrt{2}}\frac{(\Lambda\varphi)_i}{\sqrt{1+|(\Lambda\varphi)_i|^2}}$, $i=1,...,m$ *we have:*

$$\begin{aligned}\rho(\mu)=&\frac{1}{\sqrt{2}}\sum_{i=1}^m\frac{|(\Lambda\varphi)_i|^2}{\sqrt{1+|(\Lambda\varphi)_i|^2}}-\frac{1}{4}\sum_{i=1}^m\mu_i\frac{|(\Lambda\varphi)_i|^2}{1+|\Lambda\varphi|^2}+\frac{1}{2}\sum_{i=1}^m(\frac{1}{\mu_i}+\mu_i)\\ \geq&\frac{1}{\sqrt{2}}\sum_{i=1}^m\frac{|(\Lambda\varphi)_i|^2}{\sqrt{1+|(\Lambda\varphi)_i|^2}}+\frac{1}{4}\sum_{i=1}^m\mu_i+\frac{1}{2}\sum_{i=1}^m\frac{1}{\mu_i}.\end{aligned}$$

Hence, $\rho(\mu)$ *is positive, bounded from below and taking as norm the infinity discrete norm* l_∞ *we have clearly that* $\rho(\mu)\to+\infty$ *if* $\|\mu\|_{l_\infty}\to\infty$.
Next, observe that:

$$\begin{aligned}\inf_{\mu\in E^+}-\frac{1}{2}\sum_{i=1}^m\mu_i|\sigma_i|^2+\frac{1}{2}\sum_{i=1}^m(\frac{1}{\mu_i}+\mu_i)=\\ =\begin{cases}\sum_{i=1}^m\sqrt{1-|\sigma_i|^2} & |\sigma_i|^2\leq 1,\ i=1,...,m\\ -\infty & otherwise,\end{cases}\end{aligned}$$

so that defining $\mathcal{B}_{l_\infty}:=\{\sigma\in E\mid|\sigma_i|\leq 1,\ i=1,...,m\}$ *we get:*

$$\begin{aligned}\sup_{\sigma\in E}\inf_{\mu\in E^+}-\frac{1}{2}\sum_{i=1}^m\mu_i|\sigma_i|^2+\sigma\cdot\Lambda\varphi+\frac{1}{2}\sum_{i=1}^m(\frac{1}{\mu_i}+\mu_i)=\\ =\sup_{\sigma\in\mathcal{B}_{l_\infty}}\sigma\cdot\Lambda\varphi+\sum_{i=1}^m\sqrt{1-|\sigma_i|^2}.\end{aligned}$$

Therefore, hypothesis (2.6.5) *and (b) of Theorem 2.6.1 are satisfied.*
The effective domain of g is $\{\mu \in E^+ \mid \mu_i > 0,\ i = 1, ..., m\}$ *but since we are looking for an infimum in* μ*, by [120] Theorem 36.3 p.382, we obtain that:*

$$\mathtt{E}(\varphi) = \inf_{\mu \in E^+} \sup_{\sigma \in E} -\frac{1}{2}\sum_{i=1}^{m} \mu_i |\sigma_i|^2 + \sigma \cdot \Lambda\varphi + \frac{1}{2}\sum_{i=1}^{m}(\frac{1}{\mu_i} + \mu_i). \tag{2.6.15}$$

Observe that μ^* *is necessary strictly greater then zero and g is differentiable in a convex and closed neighborhood of* μ^**, therefore the extremality relations reduce to* (2.6.7) *and we have:*

$$\begin{aligned} |(\Lambda\varphi)_i|^2 = (\mu_i^*)^2 g'(\mu_i^*) = (\mu_i^*)^2 - 1, \quad & i = 1, ..., m \\ \sigma_i^* = \frac{(\Lambda\varphi)_i}{\mu_i^*}, \quad & i = 1, ..., m, \end{aligned}$$

which implies that the optimal pair (μ^*, σ^*) *is unique and is given by:*

$$\begin{aligned} \mu_i^* &= \sqrt{1 + |(\Lambda\varphi)_i|^2}, \quad i = 1, ..., m \\ \sigma_i^* &= \frac{(\Lambda\varphi)_i}{\sqrt{1 + |(\Lambda\varphi)_i|^2}}, \quad i = 1, ..., m. \end{aligned}$$

Moreover, since the optimal density μ^* *is strictly greater then 1, possibly restricting* (2.6.15) *on the set* $\{\mu \in E \mid \mu_i \geq \delta > 0,\ \delta < 1, i = 1, ..., m\}$*, the minimizer* μ^* *remains the global minimizer, the "sup" in* σ *becomes a "max" and thus, evaluating in* $\sigma_i = \frac{(\Lambda\varphi)_i}{\mu_i}$*, we have the reduced formulation:*

$$\mathtt{E}(\varphi) = \inf_{\mu \in E^+} \frac{1}{2}\sum_{i=1}^{m} \frac{|(\Lambda\varphi)_i|^2}{\mu_i} + \frac{1}{2}\sum_{i=1}^{m}(\frac{1}{\mu_i} + \mu_i).$$

2.7 A saddle point approach for 1-Harmonic functions with given profile boundary data on Graphs

In this Section we will consider the problem of finding minimizers for the graph Total Variation energy. As in Section 2.4, let $\mathcal{G} = (E, V, \omega)$ be a weighted directed graph, ∇ it's gradient matrix and $\mathrm{div} = -\nabla^T$ it's divergence matrix. We denote as $\mathcal{H}(V) = \mathbb{R}^n$ and $\mathcal{H}(E) = \mathbb{R}^m$ the Banach spaces of real-valued functions on V, the nodes set, and E, the edges set, respectively.
Consider the graph p-Dirichlet energy, $1 \leq p < 2$, defined in (2.4.3).
The Euler-Lagrange equation for the p-Dirichle energy involves the graph p-Laplacian operator defined in (2.4.2). In the limit case where $p = 1$ we define the graph 1-Laplacian as:

$$\Delta_1(\varphi) = -\operatorname{div}\Big(\operatorname{sign}(\nabla\varphi)\Big) \quad \varphi \in \mathcal{H}(V),$$

where $\text{sign}(\nabla\varphi)$ is defined in (2.4.9). There is a wide literature about the graph 1-Laplacian operator mostly correlated to the graph 1-Laplacian eigenproblem and the particular properties of the eigenvctors nodal domains (optimal cuts, Cheeger constants) and their applications to machine learning for spectral clustering [84], [72], [19], [35], [41], [44].
Here we will approach a different problem, namely we are interested to compute graph 1-Harmonic functions with a given prescribed profile on a Dirichlet boundary nodes subset $B \subset V$, $V = B \cup V_I$, $V_I \cap B = \emptyset$, where we denote as V_I the internal nodes.
We envisage that the same techniques can possibly be extended to the computation of 1-Laplacian eigenpairs.
Note that, since the graph Total Variation energy is not differentiable, subgradients need to be used, making its numerical minimization highly nontrivial. The standard technique to circumnavigate this problem is to minimize the Total Variation energy using the Osher-Bregman Split iteration method [104], [64], [33]. We can use the experience gained with the DMK scheme, see [59], to tackle this problem in a different way with the aim to develop alternative and more performing numerical minimization strategies.
We are ready to state our problem. Given a boundary nodes subset $B \subset V$ with $|B| = d < n$ and a profile function $g \in \mathcal{H}(B) = \mathbb{R}^d$ we look at the following variational problem:

$$\begin{aligned} &\inf_{\varphi\in\mathcal{H}(V)} \sum_{e\in E} |(\nabla\varphi)_e| \\ &s.t.\ \varphi_v = g_v, \quad v \in B. \end{aligned} \tag{2.7.1}$$

Introducing an appropriate lifting function $\bar{\varphi}$ such that $\bar{\varphi}_v = g_v$ for all $v \in B$ and $\bar{\varphi}_v = 0$ for all $v \in V_I$, problem (2.7.1) simplifies to:

$$\inf_{\varphi\in\mathcal{H}_0^B(V)} \sum_{e\in E} |\,(\nabla(\varphi+\bar{\varphi}))_e\,|, \tag{2.7.2}$$

where $\mathcal{H}_0^B(V) := \{\varphi \in \mathcal{H}(V) \mid \varphi_v = 0,\ \forall\, v \in B\}$.
In the general case where $\bar{\varphi}$ is not identically zero, we observe that a solution φ^* of problem (2.7.2) exists by standard arguments because the objective function is convex, lower semi-continuous and coercive, whence the coercivity is given by observe that a discrete counterpart of the Poincaré inequality holds for the graph p-Dirichlet energy, $p \geq 1$, even for infinite graphs [91].
Before proceeding we need two preparatory propositions.

Proposition 2.7.1. *Let $(V, \|\cdot\|_V)$, $(Y, \|\cdot\|_Y)$ be two reflexive Banach spaces. Consider the Lagrangian $\mathtt{L}(u,\sigma) : (V \times Y) \to \bar{\mathbb{R}}$ such that, $\forall\, u \in V$, the map $\sigma \mapsto \mathtt{L}(u,\sigma)$ is concave, upper semi-continuous and, $\forall\, \sigma \in Y$, the map $u \mapsto \mathtt{L}(u,\sigma)$ is convex and lower semi-continuous.*
Let $\mathcal{A} \subseteq V$ and $\mathcal{B} \subseteq Y$ be two convex and closed subsets and consider the saddle

point problem:

$$\inf_{u\in\mathcal{A}}\sup_{\sigma\in\mathcal{B}}\mathtt{L}(u,\sigma).$$

Suppose moreover that there exists a bounded map $u\mapsto\bar{\sigma}(u)\in\mathcal{B}$, $\|\bar{\sigma}(u)\|_Y\leq C_1$, $0<C_1<+\infty$, $\forall\, u\in\mathcal{A}$ *and a bounded map* $\sigma\mapsto\bar{u}(\sigma)\in\mathcal{A}$, $\|\bar{u}(\sigma)\|_V\leq C_2$, $0<C_2<+\infty$, $\forall\,\sigma\in\mathcal{B}$, *such that the following holds:*

$$\rho(u):=\mathtt{L}(u,\bar{\sigma}(u)),$$

is bounded from below and norm coercive on $\mathcal{A}$*:*

$$\lim_{\substack{u\,\in\,\mathcal{A}\\ \|u\|_V\,\to\,\infty}}\rho(u)=+\infty, \tag{2.7.3}$$

and

$$\psi(\sigma):=\mathtt{L}(\bar{u}(\sigma),\sigma),$$

is bounded from above and norm anti-coercive on $\mathcal{B}$*:*

$$\lim_{\substack{\sigma\,\in\,\mathcal{B}\\ \|\sigma\|_Y\,\to\,\infty}}\psi(\sigma)=-\infty. \tag{2.7.4}$$

Then, L *admits at least a saddle point* $(u^*,\sigma^*)\in(\mathcal{A}\times\mathcal{B})$.

Proof. The proof is essentially an extension of the proof in [46] Proposition 2.2 p.173.
For a fixed $\delta>0$ let:

$$\mathcal{A}_\delta:=\{u\in\mathcal{A}\mid\|u\|_V\leq\delta\},$$
$$\mathcal{B}_\delta:=\{\sigma\in\mathcal{B}\mid\|\sigma\|_Y\leq\delta\}.$$

The sets $\mathcal{A}_\delta$ and $\mathcal{B}_\delta$ are closed convex and bounded, therefore, by [46] Proposition 2.1 p.171, there exists a saddle point $(u^*_\delta,\sigma^*_\delta)\in(\mathcal{A}_\delta\times\mathcal{B}_\delta)$ for L:

$$\mathtt{L}(u^*_\delta,\sigma)\leq\mathtt{L}(u^*_\delta,\sigma^*_\delta)\leq\mathtt{L}(u,\sigma^*_\delta),\quad\forall\, u\in\mathcal{A}_\delta,\ \forall\,\sigma\in\mathcal{B}_\delta. \tag{2.7.5}$$

Since $\|\bar{\sigma}(u)\|_Y\leq C_1,\forall\, u\in\mathcal{A}$ and $\|\bar{u}(\sigma)\|_V\leq C_2,\forall\,\sigma\in\mathcal{B}$, taking $\delta=\max\{C_1,C_2\}$ so that $\bar{\sigma}(u)\in\mathcal{B}_\delta$, $\forall\, u\in\mathcal{A}_\delta$ and $\bar{u}(\sigma)\in\mathcal{A}_\delta$, $\forall\,\sigma\in\mathcal{B}_\delta$, we also have:

$$\mathtt{L}(u^*_\delta,\bar{\sigma}(u^*_\delta))\leq\mathtt{L}(u^*_\delta,\sigma^*_\delta)\leq\mathtt{L}(\bar{u}(\sigma^*_\delta),\sigma^*_\delta). \tag{2.7.6}$$

Now, the map $\rho(u)$ is bounded from below on $\mathcal{A}$, hence there exists a constant $\alpha>-\infty$ such that:

$$\alpha\leq\rho(u^*_\delta)=\mathtt{L}(u^*_\delta,\bar{\sigma}(u^*_\delta)). \tag{2.7.7}$$

On the other hand, since the map $\psi(\sigma)$ is bounded from above on $\mathcal{B}$, there exists a constant $\beta<+\infty$ such that:

$$\mathtt{L}(\bar{u}(\sigma^*_\delta),\sigma^*_\delta)=\psi(\sigma^*_\delta)\leq\beta. \tag{2.7.8}$$

Thus, (2.7.6), (2.7.7), (2.7.8) implies also that:

$$\rho(u_\delta^*) = \mathtt{L}(u_\delta^*, \bar{\sigma}(u_\delta^*)) \leq \beta < +\infty \tag{2.7.9}$$

$$\psi(\sigma_\delta^*) = \mathtt{L}(\bar{u}(\sigma_\delta^*), \sigma_\delta^*) \geq \alpha > -\infty \tag{2.7.10}$$

$$-\infty < \alpha \leq \mathtt{L}(u_\delta^*, \sigma_\delta^*) \leq \beta < +\infty \tag{2.7.11}$$

whence, in virtue (2.7.3) and (2.7.9), the family u_δ^* is bounded independently of δ, while from (2.7.4) and (2.7.10) the family σ_δ^* is bounded independently of δ. From (2.7.11) the numbers $\mathtt{L}(u_\delta^*, \sigma_\delta^*)$ are also bounded, therefore, there exists a sequence $\delta_j \to \infty$ such that:

$$\mathtt{L}(u_{\delta_j}^*, \sigma_{\delta_j}^*) \to \gamma,$$

$$u_{\delta_j}^* \to u^* \textit{ weakly in } \mathcal{A},$$

$$\sigma_{\delta_j}^* \to \sigma^* \textit{ weakly in } \mathcal{B}.$$

Thus, from (2.7.5), we have:

$$\mathtt{L}(u^*, \sigma) \leq \liminf_{\delta_j \to \infty} \mathtt{L}(u_{\delta_j}^*, \sigma) \leq \liminf_{\delta_j \to \infty} \mathtt{L}(u_{\delta_j}^*, \sigma_{\delta_j}^*) \leq \gamma, \quad \forall\, \sigma \in \mathcal{B},$$

and

$$\mathtt{L}(u, \sigma^*) \geq \limsup_{\delta_j \to \infty} \mathtt{L}(u, \sigma_{\delta_j}^*) \geq \limsup_{\delta_j \to \infty} \mathtt{L}(u_{\delta_j}^*, \sigma_{\delta_j}^*) \geq \gamma, \quad \forall\, u \in \mathcal{A}.$$

So that:

$$\mathtt{L}(u^*, \sigma) \leq \gamma \leq \mathtt{L}(u, \sigma^*) \quad \forall\, u \in \mathcal{A}, \forall\, \sigma \in \mathcal{B},$$

which implies that $(u^*, \sigma^*) \in (\mathcal{A} \times \mathcal{B})$ is a saddle point of $\mathtt{L}$. □

Remark 2.7.2. *In Proposition 2.7.1, we can relax the hypothesis on the boundedness of the maps $u \mapsto \bar{\sigma}(u)$ and $\sigma \mapsto \bar{u}(\sigma)$ supposing that there exists two convex, lower semi-continuous, coercive functions $f : \mathcal{B} \to \bar{R}$ and $g : \mathcal{A} \to \bar{\mathbb{R}}$ such that $f(\bar{\sigma}(u)) \leq C_1$, $0 < C_1 < +\infty$, $\forall\, u \in \mathcal{A}$ and $g(\bar{u}(\sigma)) \leq C_2$, $0 < C_2 < +\infty$, $\forall\, \sigma \in \mathcal{B}$ since in this case for any fixed $\delta > 0$ the sets:*

$$\mathcal{A}_\delta := \{u \in \mathcal{A} \mid g(u) \leq \delta\},$$
$$\mathcal{B}_\delta := \{\sigma \in \mathcal{B} \mid f(\sigma) \leq \delta\},$$

are closed, convex and bounded, thus the proof is still valid with the same arguments. For example, this is the case where instead of using the p-norm one choose to use $\|\cdot\|_p^p$ to enforce the boundedness of $\bar{\sigma}(u)$ or $\bar{u}(\sigma)$.
Moreover, Proposition 2.7.1 is clearly still valid if (2.7.3) *holds and there exists a $u_0 \in \mathcal{A}$ such that:*

$$\lim_{\substack{\sigma \in \mathcal{B} \\ \|\sigma\|_Y \to \infty}} \mathtt{L}(u_0, \sigma) = -\infty,$$

or (2.7.4) *holds and there exists a* $\sigma_0 \in \mathcal{B}$ *such that:*

$$\lim_{\substack{u \in \mathcal{A} \\ \|u\|_V \to \infty}} \mathtt{L}(u, \sigma_0) = +\infty$$

, since $\psi(\sigma) := \mathtt{L}(u_0, \sigma)$*(respectively* $\rho(u, \sigma_0) := \mathtt{L}(u, \sigma_0)$ *) is concave, upper semi-continuous and anti-coercive(respectively convex, lower semi-continuous and norm coercive) so that it attains a maximum(minimum) on* $\mathcal{B}$*(* $\mathcal{A}$ *) and hence it is bounded from above(below).*

The following result is a consequence of Proposition 2.7.1.

Proposition 2.7.3. *Let* $(V, \|\cdot\|_V)$*,* $(Y, \|\cdot\|_Y)$ *be two reflexive Banach spaces. Consider the Lagrangian* $\mathtt{L}(u, \sigma) : (V \times Y) \to \bar{\mathbb{R}}$ *such that the map* $\sigma \mapsto \mathtt{L}(u, \sigma)$ *is concave, upper semi-continuous* $\forall\, u \in V$ *and the map* $u \mapsto \mathtt{L}(u, \sigma)$ *is convex and lower semi-continuous* $\forall\, \sigma \in Y$*.*
Let $\mathcal{A} \subseteq V$ *and* $\mathcal{B} \subseteq Y$ *be two convex and closed subsets and consider the saddle point problem:*

$$\inf_{u \in \mathcal{A}} \sup_{\sigma \in \mathcal{B}} \mathtt{L}(u, \sigma).$$

Suppose that there exists a bounded map $u \mapsto \bar{\sigma}(u) \in \mathcal{B}$*,* $\|\bar{\sigma}(u)\|_Y \leq C_1$*,* $0 < C_1 < +\infty$*,* $\forall\, u \in \mathcal{A}$ *such that:*

$$\rho(u) := \mathtt{L}(u, \bar{\sigma}(u)),$$

is bounded from below and norm coercive on $\mathcal{A}$*:*

$$\lim_{\substack{u \in \mathcal{A} \\ \|u\|_V \to \infty}} \rho(u) = +\infty.$$

If the dual problem:

$$\sup_{\sigma \in \mathcal{B}} F(\sigma) := \sup_{\sigma \in \mathcal{B}} \inf_{u \in \mathcal{A}} \mathtt{L}(u, \sigma) \quad (\mathcal{P}^*),$$

admits a solution σ^**, then* $\mathtt{L}$ *admits at least a saddle point* $(u^*, \sigma^*) \in (\mathcal{A} \times \mathcal{B})$*.*

Proof. For any $\epsilon \geq 0$ consider the following perturbed Lagrangian:

$$\mathtt{L}_\epsilon(u, \sigma) := \mathtt{L}(u, \sigma) - \epsilon \|\sigma\|_Y.$$

From [46] Proposition 2.3 p.175, we have that there exists $u_0 \in \mathcal{A}$ such that

$$\lim_{\substack{\sigma \in \mathcal{B} \\ \|\sigma\|_Y \to \infty}} \mathtt{L}_\epsilon(u_0, \sigma) = -\infty,$$

all the hypothesis of Proposition 2.7.1 are satisfied (if necessary, see Remark 2.7.2), we thus have that there exists a saddle point $(\hat{u}_\epsilon, \hat{\sigma}_\epsilon) \in (\mathcal{A} \times \mathcal{B})$ for $\mathtt{L}_\epsilon$. In particular we have:

$$\mathtt{L}(\hat{u}_\epsilon, \sigma) - \epsilon \|\sigma\|_Y \leq \mathtt{L}_\epsilon(\hat{u}_\epsilon, \hat{\sigma}_\epsilon) \leq \mathtt{L}(u, \hat{\sigma}_\epsilon) - \epsilon \|\hat{\sigma}_\epsilon\|_Y, \tag{2.7.12}$$

hence:

$$\mathtt{L}(\hat{u}_\epsilon, \hat{\sigma}_\epsilon) \leq \max_{\sigma\in\mathcal{B}} \inf_{u\in\mathcal{A}} \mathtt{L}(u,\sigma) := \alpha < +\infty, \quad \forall\, \epsilon \geq 0, \tag{2.7.13}$$

since by hypothesis there exists a solution of the dual problem $(\mathcal{P}^*)$.
On the other hand (2.7.12) and (2.7.13) imply that:

$$\mathtt{L}(\hat{u}_\epsilon, \sigma) \leq \mathtt{L}(\hat{u}_\epsilon, \hat{\sigma}_\epsilon) + \epsilon\|\sigma\|_Y \leq \alpha + \epsilon\|\sigma\|_Y, \quad \forall\, \sigma \in \mathcal{B}. \tag{2.7.14}$$

By computing (2.7.14) in $\bar{\sigma}_{\hat{u}_\epsilon}$ and observing that by definition $\|\bar{\sigma}_{\hat{u}_\epsilon}\|_Y \leq C_1$ we get:

$$\rho(\hat{u}_\epsilon) \leq \alpha + \epsilon C_1.$$

This means that $\rho(\hat{u}_\epsilon)$ is bounded from above when $\epsilon \to 0$ and, since by (2.7.3) $\rho(u)$ is norm coercive, we have that:

$$\hat{u}_\epsilon \; is\; bounded\; for\; \epsilon \to 0.$$

Thus, there exists a sequence $\epsilon_j \to 0$ and $\hat{u} \in V$ such that:

$$\hat{u}_{\epsilon_j} \to \hat{u} \quad weakly\; in\; V.$$

From (2.7.12) and (2.7.13) we have that for any fixed $\sigma \in \mathcal{B}$:

$$\mathtt{L}(\hat{u}, \sigma) \leq \liminf_{\epsilon_j\to 0} \mathtt{L}(\hat{u}_{\epsilon_j}, \sigma) \leq \liminf_{\epsilon_j\to 0} \mathtt{L}(\hat{u}_{\epsilon_j}, \hat{\sigma}_{\epsilon_j}) \leq \alpha.$$

This implies that:

$$\inf_{u\in\mathcal{A}} \sup_{\sigma\in\mathcal{B}} \mathtt{L}(u,\sigma) \leq \sup_{\sigma\in\mathcal{B}} \mathtt{L}(\hat{u},\sigma) \leq \alpha = \max_{\sigma\in\mathcal{B}} \inf_{u\in\mathcal{A}} \mathtt{L}(u,\sigma), \tag{2.7.15}$$

hence, since "maxinf"≤"infsup", all the inequalities in (2.7.15) are in fact equalities, $\hat{u}$ is a minimizer and we have:

$$\min_{u\in\mathcal{A}} \sup_{\sigma\in\mathcal{B}} \mathtt{L}(u,\sigma) = \max_{\sigma\in\mathcal{B}} \inf_{u\in\mathcal{A}} \mathtt{L}(u,\sigma).$$

Thus, the existence of a saddle point $(u^*, \sigma^*) \in (\mathcal{A}\times\mathcal{B})$ follows from [46] Proposition 1.2 p.167. □

We are now ready to state the main result of this section.
In Section 2.4 we have seen an equivalent saddle point formulation for the graph Total Variation energy, therefore, from Theorem 2.4.1 we have the following result:

Theorem 2.7.4. *For any $\tilde{\varphi} \in \mathcal{H}(V)$ define the Lagrangian $\mathtt{L}^1_{\tilde{\varphi}} : (\mathcal{H}(E)^+ \times \mathcal{H}(E)) \to \mathbb{R}$ as:*

$$\mathtt{L}^1_{\tilde{\varphi}}(\mu,\sigma) := -\sum_{e\in E} \frac{1}{2}\mu_e|\sigma_e|^2 + \sigma\cdot\nabla\,\tilde{\varphi} + \frac{1}{2}\sum_{e\in E}\mu_e,$$

and the function:

$$\mathtt{L}_1(\tilde{\varphi}) := \inf_{\mu\in\mathcal{H}(E)^+}\sup_{\sigma\in\mathcal{H}(E)} \mathtt{L}^1_{\tilde{\varphi}}(\mu,\sigma).$$

For a given Dirichlet boundary subset $B \subset V$ and a profile function $g \in \mathcal{H}(B)$ define the lifting function $\bar{\varphi} \in \mathcal{H}(V)$:

$$\bar{\varphi}_v := \begin{cases} 0 & v \in V_I \\ g_v & v \in B. \end{cases}$$

Then, we have the following equivalence:

$$\inf_{\varphi\in\mathcal{H}_0^B(V)} \sum_{e\in E} |\left(\nabla(\varphi+\bar{\varphi})\right)_e| = \inf_{\varphi\in\mathcal{H}_0^B(V)} \mathtt{L}_1(\varphi+\bar{\varphi}). \tag{2.7.16}$$

So that:

$$\inf_{\varphi\in\mathcal{H}_0^B(V)} \sum_{e\in E} |\left(\nabla(\varphi+\bar{\varphi})\right)_e| = \tag{2.7.17}$$

$$= \inf_{\substack{\mu\,\in\,\mathcal{H}(E)^+ \\ \varphi\,\in\,\mathcal{H}_0^B(V)}} \sup_{\sigma\in\mathcal{H}(E)} -\sum_{e\in E}\frac{1}{2}\mu_e|\sigma_e|^2 + \sigma\cdot\nabla(\varphi+\bar{\varphi}) + \frac{1}{2}\sum_{e\in E}\mu_e. \tag{2.7.18}$$

Moreover there exists at least a saddle point

$$((\varphi^*,\mu^*),\sigma^*) \in \left(\mathcal{H}_0^B(V)\times\mathcal{H}(E)^+)\times\mathcal{H}(E)\right),$$

and it satisfies the following "Monge-Kantorovich" type equations:

$$\begin{aligned} \mu_e^*\sigma_e^* &= \left(\nabla(\varphi^*+\bar{\varphi})\right)_e, && \forall\, e\in E \\ (\operatorname{div}\sigma^*)_v &= 0, && \forall\, v\in V_I \\ \varphi_v^* &= 0, && \forall\, v\in B \\ |\sigma_e^*| &\le 1, && \forall\, e\in E \\ |\sigma_e^*| &= 1, && \forall\, e\in E \text{ s.t. } \mu_e^*>0 \end{aligned} \tag{2.7.19}$$

$$\mu_e^* = |\nabla(\varphi^*+\bar{\varphi})_e|, \quad \forall\, e\in E. \tag{2.7.20}$$

and φ^* is a minimizer for (2.7.17).

Proof. The equivalence in (2.7.16) is a direct consequence of Theorem 2.4.1 where we have shown that for any $\tilde{\varphi}\in\mathcal{H}(V)$, $\mathtt{E}_1(\tilde{\varphi}) = \|\nabla\tilde{\varphi}\|_{l_1} = \mathtt{L}_1(\tilde{\varphi})$, thus it suffices to show that problem (2.7.18) admits a saddle point $((\varphi^*,\mu^*),\sigma^*)$ and automatically φ^* is a minimizer for (2.7.17).
We will proceed at steps, first we will show the existence of a saddle point in the space $\left(\mathcal{H}_0^B(V)\times\mathcal{H}(E)^+)\times\mathcal{H}(E)\right)$, then we will show that the KKT conditions for a saddle point of problem (2.7.18) are precisely (2.7.19)-(2.7.20).
In the case where $\bar{\varphi}_v = 0$, $\forall\, v\in B$ there is nothing to prove and the solution is

clearly $\varphi^* = 0$, $\mu^* = 0$ and $\sigma^* = 0$.
In the general case where $\bar{\varphi}$ is not identically zero, the existence of a saddle point for problem (2.7.18) is essentially based on showing that the hypothesis of Proposition 2.7.3 are satisfied.
Define the following Lagrangian:

$$\mathtt{L}(\varphi, \mu, \sigma) := -\sum_{e\in E} \frac{1}{2}\mu_e|\sigma_e|^2 + \sigma \cdot \nabla(\varphi + \bar{\varphi}) + \frac{1}{2}\sum_{e\in E}\mu_e. \tag{2.7.21}$$

So that the primal problem $(\mathcal{P})$ in (2.7.18) is equivalent to:

$$\inf_{\substack{\mu\,\in\,\mathcal{H}(E)^+\\ \varphi\,\in\,\mathcal{H}_0^B(V)}} \sup_{\sigma\in\mathcal{H}(E)} \mathtt{L}(\varphi, \mu, \sigma) \qquad (\mathcal{P}).$$

Consider the dual problem:

$$\sup_{\sigma\in\mathcal{H}(E)} \inf_{\substack{\mu\,\in\,\mathcal{H}(E)^+\\ \varphi\,\in\,\mathcal{H}_0^B(V)}} \mathtt{L}(\varphi, \mu, \sigma) \qquad (\mathcal{P}^*). \tag{2.7.22}$$

Note that the density μ plays the role of a Lagrange multiplier for the constraint $|\sigma|_e \le 1$, $\forall\, e \in E$ and taking a variation $\xi \in \mathcal{H}_0^B$, we have that for any $\varepsilon \ge 0$:

$$\sigma \cdot \nabla(\varphi + \varepsilon\xi + \bar{\varphi}) = -\sum_{v\in V_I} (\operatorname{div}\sigma)_v(\varphi_v + \varepsilon\xi_v) - \sum_{v\in B}(\operatorname{div}\sigma)_v\bar{\varphi}_v. \tag{2.7.23}$$

Therefore, we obtain that:

$$\inf_{\substack{\mu\,\in\,\mathcal{H}(E)^+\\ \varphi\,\in\,\mathcal{H}_0^B(V)}} \mathtt{L}(\varphi, \mu, \sigma) = \begin{cases} -\sum_{v\in B}(\operatorname{div}\sigma)_v\bar{\varphi}_v & |\sigma|_e \le 1\ \forall\, e \in E \\ & (\operatorname{div}\sigma)_v = 0\ \forall\, v \in V_I \\ -\infty & \textit{otherwise}, \end{cases}$$

and the dual problem (2.7.22) is equivalent to the following constrained problem:

$$\begin{aligned} \sup_{\sigma\,\in\,\mathcal{H}(E)} \quad & -\sum_{v\in B}(\operatorname{div}\sigma)_v\bar{\varphi}_v \qquad (\mathcal{P}^*), \\ (\operatorname{div}\sigma)_v = 0, \forall\, v \in V_I & \\ \|\sigma\|_{l_\infty} \le 1 & \end{aligned}$$

which has a solution since the set $\mathcal{B} := \{\sigma \in \mathcal{H}(E) \mid (\operatorname{div}\sigma)_v = 0, \forall\, v \in V_I,\ \|\sigma\|_{l_\infty} \le 1\}$ is non empty, convex, closed, bounded and the function $g(\sigma) := -\sum_{v\in B}(\operatorname{div}\sigma)_v\bar{\varphi}_v$ is linear.
Next, consider the map

$$\varphi \mapsto \bar{\sigma}(\varphi) := \frac{1}{\sqrt{2}}\operatorname{sign}(\nabla(\varphi + \bar{\varphi})),$$

with the standard convention as in (2.4.9) and the function:

$$\rho(\varphi,\mu) := \mathtt{L}(\varphi,\mu,\bar{\sigma}(\varphi)).$$

Clearly $\forall\,\varphi \in \mathcal{H}_0^B(V)$ we have that

$$\|\bar{\sigma}(\varphi)\|_{l_\infty} \leq \frac{1}{\sqrt{2}},$$

and

$$\bar{\sigma}(\varphi)\cdot\nabla(\varphi+\bar{\varphi}) = \frac{1}{\sqrt{2}}\|\nabla(\varphi+\bar{\varphi})\|_{l_1}.$$

So that:

$$\bar{\sigma}(\varphi) \textit{ is bounded } \forall\,\varphi \in \mathcal{H}_0^B(V).$$

It is therefore easy to see that:

$$\begin{aligned}\rho(\varphi,\mu) &= -\sum_{e\in E}\frac{1}{2}\mu_e|\bar{\sigma}(\varphi)_e|^2 + \bar{\sigma}(\varphi)\cdot\nabla(\varphi+\bar{\varphi}) + \frac{1}{2}\sum_{e\in E}\mu_e \geq \\ &\geq \frac{1}{\sqrt{2}}\|\nabla(\varphi+\bar{\varphi})\|_{l_1} + \frac{1}{4}\sum_{e\in E}\mu_e \geq \frac{c_1}{\sqrt{2}}\|\varphi+\bar{\varphi}\|_{l_1} + \frac{1}{4}\sum_{e\in E}\mu_e \geq \\ &\geq \frac{c_1}{\sqrt{2}}(\|\varphi\|_{l_1} - \|\bar{\varphi}\|_{l_1}) + \frac{1}{4}\sum_{e\in E}\mu_e,\end{aligned}$$

where $c_1 > 0$ is the Poincaré constant.
This implies that

$$\rho(\varphi,\mu) \textit{ is positive and norm coercive},$$

in the product space $(\mathcal{H}_0^B(V)\times\mathcal{H}(E)^+)$ equipped with the norm

$$\|(\varphi,\mu)\|_{(\mathcal{H}_0^B(V)\times\mathcal{H}(E)^+)} = \|\varphi\|_{l_1} + \|\mu\|_{l_1}.$$

Thus, all the hypothesis of Proposition 2.7.3 are satisfied and there exists a saddle point

$$((\varphi^*,\mu^*),\sigma^*) \in \left((\mathcal{H}_0^B(V)\times\mathcal{H}(E)^+)\times\mathcal{H}(E)\right).$$

The KKT conditions for the saddle points $((\varphi^*,\mu^*),\sigma^*)$ of (2.7.21), read as follows:

$$\begin{cases} -|\sigma_e^*|^2 + 1 - c_e = 0, & \forall\, e\in E \\ \mu_e^*\sigma_e^* = \nabla(\varphi^*+\bar{\varphi})_e, & \forall\, e\in E \\ (\operatorname{div}\sigma^*)_v = 0, & \forall\, v\in V_I \\ \varphi_v^* = 0, & \forall\, v\in B \\ c_e\mu_e^* = 0, \quad c_e\geq 0, & \forall\, e\in E. \end{cases} \tag{2.7.24}$$

where $c \in \mathcal{H}(E)$ is an opportune positive Lagrange multiplier.
As in Remark 2.4.2, from (2.7.24) we further have that:

$$\begin{cases} |\sigma_e^*| \leq 1, & \forall\, e \in E \\ |\sigma_e^*| = 1, & \forall\, e \in E \ s.t.\ \mu_e^* > 0, \end{cases}$$

where the unique possible optimal density is

$$\mu_e^* = |\nabla(\varphi^* + \bar{\varphi})_e|, \quad \forall\, e \in E.$$

This completes the proof. □

2.8 The DMK scheme: from Optimal Transport to 1-Harmonic functions

In this section we will see how to use the Dynamic-Monge-Kantorovich(DMK) scheme to tackle the problem of computing 1-Harmonic functions on graphs, using the saddle point formulation developed in Section 2.7 for the 1-Dirichlet energy. We will refer to the same Section 2.7 for the definitions of the graph-based framework involved in what follows.
The existence of a saddle point

$$((\varphi^*, \mu^*), \sigma^*) \in \left(\mathcal{H}_0^B(V) \times \mathcal{H}(E)^+) \times \mathcal{H}(E)\right),$$

for (2.7.18) characterized by the "Monge-Kantorovich" like equations (2.7.19)-(2.7.20) leads to very efficient numerical schemes which takes inspiration from the Dynamic-Monge-Kantorovich Gradient Flow like scheme introduced in [54].
The connection between the Optimal Transport problem is evident from Section 2.3 and the analogies between (2.7.19)-(2.7.20) and the L^1 optimal transport relaxed Monge-Kantorovich equations in [18].
In [54] a numerical solution of the L^1 optimal transport on graphs is given as a minimization problem for an energy functional $\mathcal{L}(\mu) : \mathcal{H}(E)^+ \to \mathbb{R}$, where the variable μ can be interpreted as a conductivity associated to the edges of the graph. In our case, the energy functional $\mathcal{L}$ will be substituted by the saddle point formulation defined in (2.7.18), more precisely we will consider the following problem:

$$\mathcal{L}(\varphi, \mu) := \sup_{\sigma \in \mathcal{H}(E)} -\sum_{e \in E} \frac{1}{2}\mu_e |\sigma_e|^2 + \sigma \cdot \nabla(\varphi + \bar{\varphi}) + \frac{1}{2}\sum_{e \in E} \mu_e. \tag{2.8.1}$$

and we will seek for a minimum in the pair (φ, μ) with homogeneous Dirichlet boundary conditions for φ on some nodes boundary Dirichlet subset $B \subset V$ and $\bar{\varphi}$ is an opportune lifting function as in (2.7.2). In this case, differently from the problem in [54], the variable μ will play the reciprocal role of a conductivity, so

that it is essentially a resistivity on the edges.
If φ^* is a solution of (2.7.2) then by Theorem 2.7.4 the function:

$$\tilde{\varphi} := \varphi^* + \bar{\varphi}, \tag{2.8.2}$$

is a 1-harmonic solution with prescribed profile function $g \in \mathcal{H}(B)$, $g_v = \bar{\varphi}_v$, $\forall\, v \in B$ and hence is a solution of the original problem (2.7.1).
As in [54] a solution will be sought via a gradient descent approach, not applied directly to the functional $\mathcal{L}(\varphi, \mu)$, but rather to its composition with the change of variable $\Psi : \mathcal{H}(E) \to \mathcal{H}(E)^+$ given component-wise as $\mu_e = \Psi(\xi)_e = \xi_e^2$, $\forall\, e \in E$. The gradient descent approach applied to the computation of a minimizer (φ^*, ξ^*) of $\mathcal{L}(\varphi, \Psi(\xi))$ has to be intended as a long time solution

$$(\varphi^*, \xi^*) = \lim_{t\to\infty} (\varphi(t), \xi(t)),$$

where $(\varphi(t), \xi(t))$ is a solution of the following state-space initial value problem:

$$\begin{gathered}
\mu_e(t) = \Psi(\xi(t))_e, \quad \forall\, e \in E, \\
[\operatorname{Diag} \mu(t)]\, \sigma(t) - \nabla(\varphi(t) + \bar{\varphi}) = 0, \\
(\operatorname{div} \sigma(t))_v = 0, \quad \forall\, v \in V_I, \\
\varphi(t)_v = 0, \quad \forall\, v \in B, \\
\partial_t \xi_e(t) = -\left[\partial_\xi \mathcal{L}(\varphi(t), \Psi(\xi(t)))\right]_e = \xi_e(t)|\sigma_e(t)|^2 - \xi_e(t), \quad \forall\, e \in E, \\
\xi_e(0) = \xi_{0e} \neq 0, \quad \forall\, e \in E.
\end{gathered} \tag{2.8.3}$$

Moreover, if $\xi(t)$ is a solution of (2.8.3), the relation $\mu(t) = \Psi(\xi(t))$ implies that:

$$\partial_t \mu_e(t) = \partial_\xi \Psi(\xi(t))_e \partial_t \xi_e(t) = \xi_e(t) \partial_t \xi_e, \quad \forall\, e \in E,$$

and remembering that $\forall\, e \in E$, $\mu_e(t) = \xi_e(t)^2$, we get that $\mu(t)$ can be reinterpreted as a "classical Gradient Descent" dynamics:

$$\partial_t \mu_e(t) = \mu_e(t)|\sigma_e(t)|^2 - \mu_e(t), \quad \mu_e(0) = \mu_{0e} > 0 \quad \forall\, e \in E. \tag{2.8.4}$$

Even if the dynamics in (2.8.3) is not proven yet to effectively converge to a minimizer, we point out that our conjecture is supported by several numerical experiments.
In virtue of (2.7.19)-(2.7.20), a saddle point $((\varphi^*, \mu^*), \sigma^*)$ for (2.7.18) is a stationary point of the dynamics in (2.8.3).
It is evident that the second, the third and the fourth equations in (2.8.3) are the Euler Lagrange equations for the saddle point:

$$\begin{aligned}
&\inf_{\varphi \in \mathcal{H}_0^B(V)} \mathcal{L}(\varphi, \mu) = \\
&\qquad = \inf_{\varphi \in \mathcal{H}_0^B(V)} \sup_{\sigma \in \mathcal{H}(E)} -\sum_{e\in E} \frac{1}{2} \mu_e |\sigma_e|^2 + \sigma \cdot \nabla(\varphi + \bar{\varphi}) + \frac{1}{2} \sum_{e \in E} \mu_e,
\end{aligned}$$

and are genuinely a linear saddle point system.
The last two equations in (2.8.3) define the descent direction dynamics for the variable ξ and therefore for the density $\mu = \Psi(\xi)$, where we have absorbed a factor 2 by a time scaling.
It is clear that, in virtue of (2.7.19)-(2.7.20), a saddle point for (2.7.18) is a stationary point for (2.8.3), while the map Ψ has the effect of multiplying the original gradient descent by $\xi(t)$(or by $\mu(t)$ if (2.8.4) is used). This further introduce a fake stationary point when $\mu(t)$ touches zero in some edge thus preserving the positivity of $\mu(t)$ if we start from an initial $\mu(0)$ sufficiently detached from zero. We will see in subsection 2.8.2 the heuristics behind the choice of Ψ as an update preserving scheme for the positivity constraint and extend this technique to the case of an interval components-wise constraint.
Let's focus our attention on the saddle point linear system in (2.8.3):

$$\begin{aligned} &[\operatorname{Diag}\mu(t)]\,\sigma(t) - \nabla(\varphi(t)+\bar{\varphi}) = 0,\\ &(\operatorname{div}\sigma(t))_v = 0, \quad \forall\, v \in V_I,\\ &\varphi(t)_v = 0, \quad \forall\, v \in B. \end{aligned} \tag{2.8.5}$$

Equation (2.8.5) is the Dirichlet lifted matrix system of the following saddle point matrix:

$$\left(\begin{array}{c|c} \operatorname{Diag}\mu(t) & -\nabla \\ \hline \operatorname{div} & \mathbf{0} \end{array}\right),$$

which becomes singular if $\mu_{\bar{e}}(t) = 0$ on some edge $\bar{e} \in E$.
Since 1-Harmonic functions are naturally flat solutions by the sparsity enhancing properties of the Total Variation energy on the gradient, our optimal density $\mu^* = \lim_{t\to\infty}\mu(t)$ will inevitably goes to zero in some edges, leading to very ill conditioned linear systems. The strategy is therefore to consider an appropriately small Tikhonov parameter $\delta > 0$ to circumvent the ill-conditioning but maintaining sufficient accuracy:

$$\left(\begin{array}{c|c} \operatorname{Diag}\mu(t)+\delta & -\nabla \\ \hline \operatorname{div} & \mathbf{0} \end{array}\right).$$

Hence, the Tikhonov regularized version of (2.8.5) becomes equivalent to the following reduced lifted linear system:

$$\begin{aligned} &\sigma_e(t) = \frac{(\nabla(\varphi(t)+\bar{\varphi}))_e}{\mu_e(t)+\delta}, \quad \forall\, e \in E,\\ &(\Delta_{\frac{1}{\mu(t)+\delta}}(\varphi(t)+\bar{\varphi}))_v = 0, \quad \forall\, v \in V_I,\\ &\varphi(t)_v = 0, \quad \forall\, v \in B. \end{aligned} \tag{2.8.6}$$

This a posteriori considerations will make clear the role of the Tikhonov regularized version of our saddle point formulation introduced in (2.5.11), indeed, taking

inspiration by [59, 60], we consider the following approximation of the functional defined in (2.8.1):

$$\mathcal{L}_\delta(\varphi,\mu) := \sup_{\sigma\in\mathcal{H}(E)} -\sum_{e\in E}\frac{1}{2}(\mu_e+\delta)|\sigma_e|^2 + \sigma\cdot\nabla(\varphi+\bar{\varphi}) + \frac{1}{2}\sum_{e\in E}\mu_e.$$

With the same arguments as in (2.5.7)-(2.5.8), $\mathcal{L}_\delta(\varphi,\mu)$ simplifies as:

$$\mathcal{L}_\delta(\varphi,\mu) = \sum_{e\in E}\frac{1}{2}\frac{|\nabla(\varphi+\bar{\varphi})_e|^2}{(\mu_e+\delta)} + \frac{1}{2}\sum_{e\in E}\mu_e.$$

and we consider the following double minimization problem:

$$\inf_{\substack{\varphi\in\mathcal{H}_0^B(V)\\ \mu\in\mathcal{H}(E)^+}} \mathcal{L}_\delta(\varphi,\mu). \tag{2.8.7}$$

With the same arguments as in (2.5.10), we have that $\mathcal{L}_\delta(\varphi,\mu)$ is convex, lower semi-continuous and coercive in the pair (φ,μ). Thus, the existence of a minimizer (φ^*,μ^*) is guaranteed. Moreover, $\mathcal{L}_\delta(\varphi,\mu)$ is differentiable in $(\mathcal{H}_0^B(V)\times\mathcal{H}(E)^+)$ but is not strictly convex (the Hessian is zero), hence is not possible to state the existence of a unique minimum couple. The KKT conditions for the minimizers of $\mathcal{L}_\delta(\varphi,\mu)$ reads as follows:

$$\begin{cases} -\frac{|\nabla(\varphi^*+\bar{\varphi})_e|^2}{(\mu_e^*+\delta)^2} + 1 - c_e = 0, & \forall\, e\in E\\ (\Delta_{\frac{1}{\mu^*+\delta}}(\varphi^*+\bar{\varphi}))_v = 0, & \forall\, v\in V_I\\ \varphi_v^* = 0, & \forall\, v\in B\\ c_e\mu_e^* = 0, \quad c_e\geq 0, & \forall\, e\in E. \end{cases} \tag{2.8.8}$$

The second and the third equations in (2.8.8) are exactly the reduced system (2.8.6). If $\mu_{\bar{e}}^* = 0$ on some edge $\bar{e}$, then the first equation in (2.8.8) admits a solution iff:

$$|\nabla(\varphi^*+\bar{\varphi})_{\bar{e}}| \leq \delta.$$

On the other hand, the last equation in (2.8.8) implies that if $\mu_{\bar{e}}^* > 0$, then $c_{\bar{e}} = 0$ and hence:

$$|\nabla(\varphi^*+\bar{\varphi})_{\bar{e}}| = \mu_{\bar{e}}^* + \delta.$$

Thus, the parameter δ controls the accuracy from above, and we can expect to have a good approximation if δ is sufficiently small.
The reduced system (2.8.6) is equivalent to the Euler-Lagrange equations for the saddle point problem:

$$\begin{aligned}\inf_{\varphi\in\mathcal{H}_0^B(V)} \mathcal{L}_\delta(\varphi,\mu) &= \\ &= \inf_{\varphi\in\mathcal{H}_0^B(V)}\sup_{\sigma\in\mathcal{H}(E)} -\sum_{e\in E}\frac{1}{2}(\mu_e+\delta)|\sigma_e|^2 + \sigma\cdot\nabla(\varphi+\bar{\varphi}) + \frac{1}{2}\sum_{e\in E}\mu_e,\end{aligned}$$

and the corresponding version of the dynamics in (2.8.3), (2.8.4) for problem (2.8.7) is the following **Extended-Dynamic-Monge-Kantorovich(EDMK)**:

$$\begin{aligned}
(\Delta_{\frac{1}{\mu(t)+\delta}}(\varphi(t)+\bar{\varphi}))_v &= 0, \quad \forall\, v \in V_I, \\
\varphi(t)_v &= 0, \quad \forall\, v \in B, \\
\sigma_e(t) &= \frac{(\nabla(\varphi(t)+\bar{\varphi}))_e}{\mu_e(t)+\delta}, \quad \forall\, e \in E, \\
\partial_t \mu_e(t) = \mu_e(t)|\sigma_e(t)|^2 - \mu_e(t), &\quad \mu_e(0) = \mu_{0e} > 0, \quad \forall\, e \in E.
\end{aligned} \tag{EDMK}$$

(2.8.9)

This dynamics would be the one that we will use in our numerical experiments. In [59] it was shown that a solution μ^* of the Optimal Transport counterpart of (2.8.9) Γ-converges to a solution of the original problem when $\delta \to 0$.
We now describe three approaches for the time-discretization of (2.8.9):

- **Explicit Euler [EE]**:
  The first approach is the explicit or forward Euler time-stepping where, given a sequence $\Delta t_k > 0$, the approximation sequence $\left(\mu^k\right)_{k=1,\dots,k_{\max}}$ is given by the following set of equations:

$$\begin{cases}
(\Delta_{\frac{1}{\mu^k+\delta}}(\varphi^k+\bar{\varphi}))_v = 0, \quad \forall\, v \in V_I \\
\varphi^k_v = 0, \quad \forall\, v \in B \\
\sigma^k_e = \dfrac{(\nabla(\varphi^k+\bar{\varphi}))_e}{\mu^k_e+\delta}, \quad \forall\, e \in E \\
\mu^{k+1}_e = \mu^k_e + \Delta t_k \mu^k_e \left(|\sigma^k_e|^2 - 1\right), \quad k = 0, \dots, k_{\max},\ e \in E \\
\mu^0_e = \mu_{0e} > 0, \quad \forall\, e \in E.
\end{cases} \tag{2.8.10}$$

  Hence at each time step, we only need to solve the lifted linear system

$$\begin{aligned}
(\Delta_{\frac{1}{\mu^k+\delta}}(\varphi^k+\bar{\varphi}))_v &= 0, \quad \forall\, v \in V_I, \\
\varphi^k_v &= 0, \quad \forall\, v \in B.
\end{aligned}$$

  A similar discretization scheme has been successfully adopted in [16, 54, 55].

- **Semi Implicit Euler [SE]**:
  The second approach is the semi implicit Euler time-stepping where the approximation sequence $\left(\mu^k\right)_{k=1,\dots,k_{\max}}$ is given by using an implicit time discretization for the variable μ considering it as indipendent from the vari-

able σ:

$$\begin{cases} (\Delta_{\frac{1}{\mu^k+\delta}}(\varphi^k+\bar{\varphi}))_v = 0, & \forall\, v \in V_I \\ \varphi_v^k = 0, & \forall\, v \in B \\ \sigma_e^k = \dfrac{(\nabla(\varphi^k+\bar{\varphi}))_e}{\mu_e^k+\delta}, & \forall\, e \in E \\ \mu_e^{k+1} = \dfrac{\mu_e^k}{(1-\Delta t_k\,(|\sigma_e^k|^2-1))}, & k=0,\dots,k_{\max},\ e\in E \\ \mu_e^0 = \mu_{0e} > 0, & \forall\, e \in E \end{cases} \tag{2.8.11}$$

This discretization scheme remains still an explicit scheme but exhibits better stability properties than the forward Euler scheme.

- **Implicit Euler [IE]**:
  The third approach is the implicit or backward Euler time-stepping where the approximation sequence $\left(\mu^k = \Psi(\xi^k), \varphi^k\right)_{k=1,\dots,k_{\max}}$ is given by looking for a solution of the following problem:

$$\begin{cases} (\xi^{k+1}, \varphi^{k+1}) = \underset{\xi\in\mathcal{H}(E)}{\arg\min}\ \underset{\varphi\in\mathcal{H}_0^B(V)}{\arg\min}\ \mathcal{L}_\delta(\varphi, \Psi(\xi)) + \dfrac{\|\xi-\xi^k\|_{l_2}^2}{2\Delta t_k} \\ \xi_e^0 = \xi_{0e} \neq 0, \quad \forall\, e \in E \end{cases} \tag{2.8.12}$$

  or equivalently:

$$\begin{cases} (\Delta_{\frac{1}{(\xi^{k+1})^2+\delta}}(\varphi^{k+1}+\bar{\varphi}))_v = 0, & \forall\, v \in V_I \\ \varphi_v^{k+1} = 0, & \forall\, v \in B \\ \sigma_e^{k+1} = \dfrac{(\nabla(\varphi^{k+1}+\bar{\varphi}))_e}{(\xi_e^{k+1})^2+\delta}, & \forall\, e \in E \\ (1-\Delta t_k\left(|\sigma_e^{k+1}|^2-1\right))\xi_e^{k+1} = \xi_e^k, & k=0,\dots,k_{\max},\ e\in E \\ \xi_e^0 = \xi_{0e} \neq 0, & \forall\, e \in E \\ \mu_e^{k+1} = (\xi_e^{k+1})^2, & \forall\, e \in E \end{cases}$$

  This discretization scheme requires the solution of nonlinear problems at every time step thus it needs more computational effort respect the other two approaches, but this is compensated by gaining stability and much faster convergence rate, we refer to [54] for full details.

After choosing a time discretization for (2.8.9), we introduce a target tolerance ϵ_μ and let evolve the dynamics until a prescribed stopping error is greater than

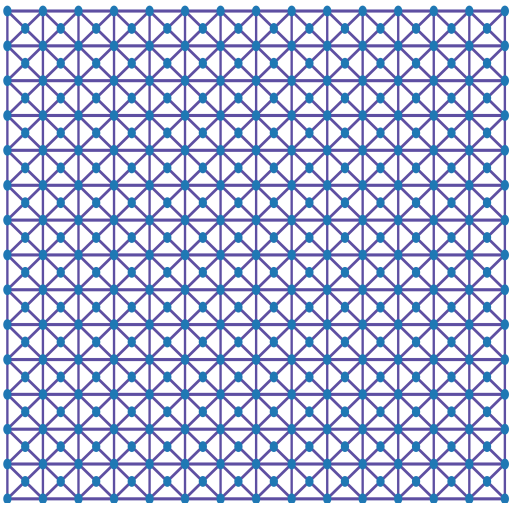

Figure 2.1: Test case graph

the target tolerance. For example, a possible choice is the relative error stopping rule:

$$err_{\mu^k}(\mu^{k+1}) := \frac{\|\mu^{k+1} - \mu^k\|_{l_2}}{\Delta t_k \|\mu^k\|_{l_2}} \leq \epsilon_\mu \tag{2.8.13}$$

we will see now some applications of our numerical scheme

2.8.1 Numerical examples

In our numerical examples we consider the graph generated by connecting the points of a $2d$-grid. In particular, we take the square $[0,1] \times [0,1]$, subdivide each side in 15 points and connect every point to form a grid. After that, we add a new point on every pixel center for increasing the precision as in figure 2.1. The graph constructed in this way has a total number 421 nodes and 1204 edges. We take as edge weight the reciprocal of the edge length, for any edge in the graph. Working with a graph which can be interpreted as a discretization of a two dimensional domain, leads us to make some a priori heuristc considerations.
Following [50], we can relate 1-Harmonic functions on a domain $\Omega \subset \mathbb{R}^n$ to the problem of finding surfaces with minimal mean-curvature and naturally, since the sparsity of the gradient is promoted by the L^1 norm, are flat solutions. Consider for example a parametric surface on $\mathbb{R}^3$:

$$S(x,y) := \begin{pmatrix} x \\ y \\ z = u(x,y) \end{pmatrix},$$

where $u : \Omega \subset \mathbb{R}^2 \to \mathbb{R}$. Consider now the level set:

$$\Gamma_c := \{\vec{x} \in \Omega | u(\vec{x}) = c\}.$$

Then, by classical differential geometry arguments, the unit normal to Γ_c is nothing that $\nu = \frac{\nabla u}{|\nabla u|}$ and the mean curvature is $H = \text{div}(\nu) = -\Delta_1(u)$, therefore, 1-Harmonic functions are locally zero mean curvature hypersurfaces.
As a consequence we are expecting to find numerical solutions which are a compounds of locally flat hyperplanes.
We select as Dirichlet boundary set the subset of the nodes that lie on each side of the squares:

$$B := \{v \in V \mid v_x = 0 \; or \; v_x = 1 \; or \; v_y = 0 \; or \; v_y = 1\},$$

where the symbols v_x and v_y state for the "x" and the "y" coordinate of the node v. We then consider four different profile functions $g \in \mathcal{H}(B)$:

- Test Case 1:(Cross Vault)

$$\begin{cases} g_v = \sqrt{0.25 - (v_x - 0.5)^2}, & v_y = 0 \; or \; v_y = 1 \\ g_v = \sqrt{0.25 - (v_y - 0.5)^2}, & v_x = 0 \; or \; v_x = 1. \end{cases}$$

- Test Case 2:(Tensile Structure)

$$\begin{cases} g_v = (v_x - 0.5)\,\text{sign}(v_x - 0.5), & v_y = 0 \; or \; v_y = 1 \\ g_v = (v_y - 0.5)\,\text{sign}(v_y - 0.5), & v_x = 0 \; or \; v_x = 1. \end{cases}$$

- Test Case 3:(Separation of sets)

$$\begin{cases} g_v = 1, & v_x = 0 \; and \; v_y \geq 0.3 \; or \; v_x \leq 0.7 \; and \; v_y = 1 \\ & \\ g_v = 0, & (v_x = 0 \; and \; v_y < 0.3) \; or \\ & (\; v_y = 0 \; or \; v_x = 1) \; or \\ & (v_x > 0.7 \; and \; v_y = 1). \end{cases}$$

Introducing the lifting function $\bar{\varphi}$ such that:

$$\bar{\varphi}_v := \begin{cases} 0 & v \in V_I \\ g_v & v \in B, \end{cases}$$

we have all the ingredient for our DMK scheme.
In figures 2.2,2.3,2.4 we can see the comparison between the Harmonic solution (left) and 1-Harmonic solution (right) computed with our regularized DMK scheme (2.8.9), using (2.8.10) Explicit Euler time discretization for test case 1

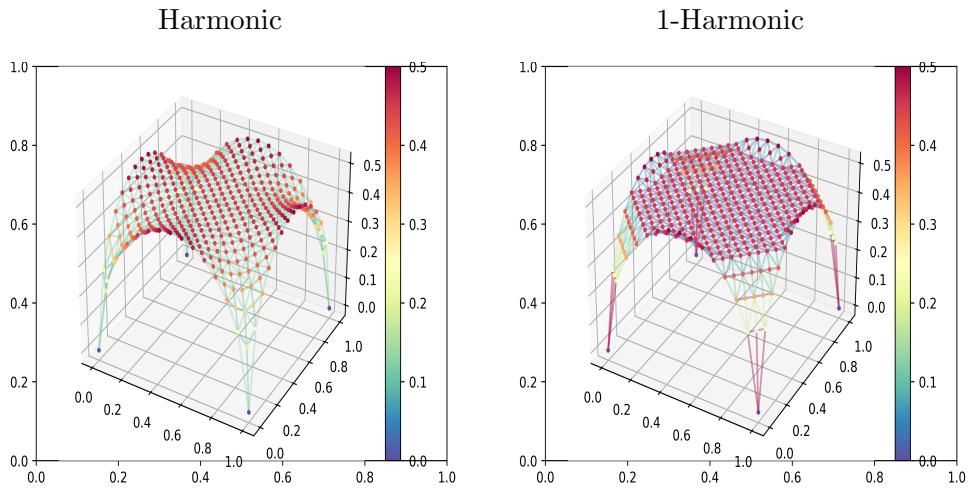

Figure 2.2: Test case 1, Harmonic vs 1-Harmonic, Potential (nodes) μ (edges)

,2 and 3 respectively. We have decided to plot the figures in three dimensions in order to enphasize the minimizing mean curvature properties of our solutions. Test case 3 is particularly interesting since it shows the optimal cuts property induced by the Total Variation minimization. The 1-Harmonic approximated solution obtain with our DMK scheme is, as already observed in (2.8.2), given by the sum:

$$\tilde{\varphi} := \varphi^* + \bar{\varphi},$$

where the pair (μ^*, φ^*) is a numerical solution obtained with (2.8.9). Thus we plot on the nodes the value of the function $\tilde{\varphi}$, which in these figures is represented by the third coordinate "z", and we give different colors to the edges depending on the value of the variable μ^*, following the heat colour bar on the right side. Finally, in figure 2.5 we show the convergence behaviour of our numerical algorithm for test case 1 (the same results was observed for test case 2) . We plot in the vertical axis the relative error as in (2.8.13) vs the number of iterations(horizontal axis). We point out that the no time stepping rule were adopted, so that we fixed a relative large time step $\Delta t = 0.5$ and a small regularization parameter $\delta = 1e-10$, in order to verify the robustness of our scheme. Thus, we choose an initial $\mu_0 > 0$, and we let evolve the dynamics until $err_{\mu^k}(\mu^{k+1}) \leq 1e-8$. As a result we can observe a linear convergence rate without any oscillations. We will further test the other time discretization approach (2.8.11), (2.8.12) as a matter of future development.

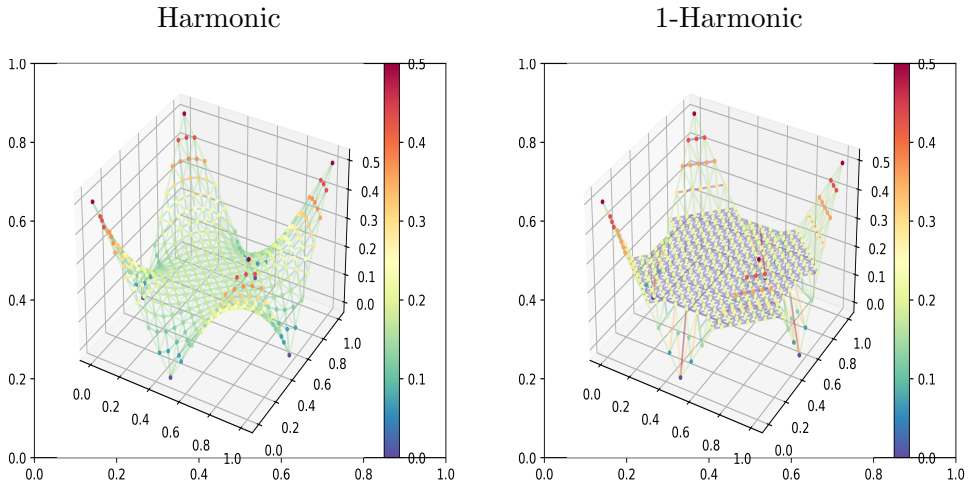

Figure 2.3: Test Case 2, Harmonic vs 1-Harmonic, Potential (nodes) μ (edges)

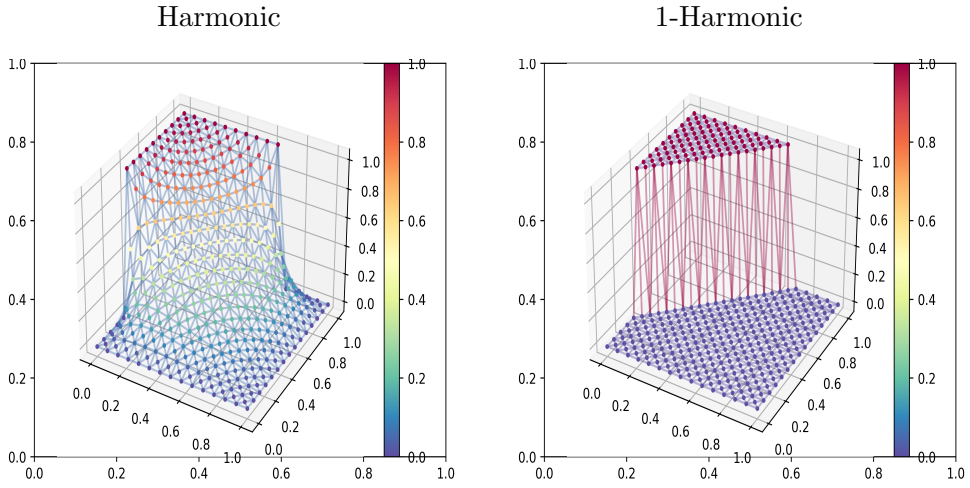

Figure 2.4: Test case 3, Harmonic vs 1-Harmonic, Potential (nodes) μ (edges)

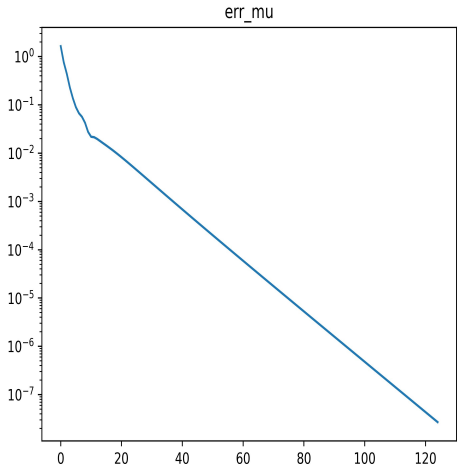

Figure 2.5: $err_{\mu^k}(\mu^{k+1})$ vs number of iterations

2.8.2 An Heuristic approach to a feasible update preserving descent dynamics for the positivity and interval constraints

In (2.8.3) and (2.8.4) we have introduced a dynamics which can be interpreted as an update preserving descent dynamics for the positivity constraint.
From a practical point of view, considering the dynamics (2.8.4), it is clear that it is equivalent to:

$$\partial_t \mu_e(t) = -\mu_e(t)\partial_{\mu_e}\mathcal{L}(\varphi(t), \mu(t)), \quad \forall\, e \in E. \tag{2.8.14}$$

The ones who have familiarity with Lie derivatives and dynamical systems can recognize that (2.8.14) is the descent direction computed along the flow of the identity map:

$$\begin{cases} \dfrac{d}{ds}\Phi^s_{id}(\mu_e(t)) = \Phi^s_{id}(\mu_e(t)) \\ \quad \Phi^0_{id}(\mu_e(t)) = \mu_e(t) \end{cases} \implies \Phi^s_{id}(\mu_e(t)) = \mu_e(t)\mathsf{e}^s \quad \forall\, e \in E.$$

and setting $\Phi^s_{id}(\mu(t)) \in \mathcal{H}(E)$ such that $\Phi^s_{id}(\mu(t))_e = \Phi^s_{id}(\mu_e(t))$ we have:

$$\begin{aligned} -\frac{d}{ds}\big|_{s=0}\mathcal{L}(\varphi(t), \Phi^s_{id}(\mu(t))) = \\ = -\left[\partial_{\mu_e}\mathcal{L}(\varphi(t), \Phi^s_{id}(\mu(t)))\right]\Phi^s_{id}(\mu_e(t))\big|_{s=0} = \\ = -\mu_e(t)\partial_{\mu_e}\mathcal{L}(\varphi(t), \mu(t)) = \partial_t\mu_e(t), \quad \forall\, e \in E. \end{aligned}$$

Thus heuristically if we start from an initial $\mu(0) > 0$ the positivity is preserved since we are moving in a descent direction projected tangentially to the exponential map so that we converge toward zero from a parallel direction to the axis

$\mu_e = 0$.
It is obvious that the same arguments can be applied more generally to a problem of the type:

$$\inf_{\substack{\mu \in \mathbb{R}^m \\ \mu \geq 0}} \sum_{i=1}^{m} L(\mu_i),$$

where $L : \mathbb{R} \to \mathbb{R}$ is a sufficiently smooth map. The induced minimizing scheme reads as the following dynamics:

$$\partial_t \mu_i(t) = -\mu_i(t) \partial_{\mu_i} L(\mu_i(t)), \quad i = 1, ..., m.$$

Furthermore, we can extend the idea of projecting along the flow of a map $X : \mathbb{R} \to \mathbb{R}$ as follows:

$$\begin{cases} \dfrac{d}{ds} \Phi_X^s(\mu_i(t)) = X(\Phi_X^s(\mu_i(t))) \\ \Phi_X^0(\mu_i(t)) = \mu_i(t) \end{cases} \quad i = 1, .., m,$$

and setting $\Phi_X^s(\mu(t))_i = \Phi_X^s(\mu_i(t))$ we define:

$$\partial_t \mu_i(t) := -\frac{d}{ds}\big|_{s=0} L(\Phi_X^s(\mu(t))) = \\ = -X(\mu_i(t)) \partial_{\mu_i} L(\mu(t)), \quad i = 1, .., m. \quad (2.8.15)$$

On the other hand, we can also try to reverse the process of finding what is the opportune transformation $\mu_i(t) = \Psi(\xi_i(t))$ such that:

$$\partial_t \xi_i(t) = -\partial_{\xi_i} L(\Psi(\xi_i(t)),$$

and:

$$- X(\mu_i(t)) \partial_{\mu_i} L(\mu(t)) = \\ = \partial_t \mu_i(t) = \partial_{\xi_i} \Psi(\xi_i(t)) \partial_t \xi_i(t) = \\ = -\partial_{\xi_i} \Psi(\xi_i(t)) \partial_{\xi_i} L(\Psi(\xi_i(t)).$$

Observe that if Ψ and L are sufficiently smooth we have the following identities:

$$\mu_i = \Psi(\xi_i),$$

$$\partial_{\xi_i} \mu_i = \partial_{\xi_i} \Psi(\xi_i),$$
$$\partial_{\xi_i} L(\Psi(\xi_i)) = \partial_{\xi_i} \mu_i \partial_{\mu_i} L(\mu_i). \quad (2.8.16)$$

Thus, dropping for simplicity the time dependence, 2.8.2 becomes:

$$X(\mu_i) \partial_{\mu_i} L(\mu_i) \overset{(2.8.16)}{=} (\partial_{\xi_i} \mu_i)^2 \, \partial_{\mu_i} L(\mu_i).$$

Hence, we can retrieve the map Ψ by solving the following separable ODE:

$$\frac{d\mu_i}{d\xi_i} = \sqrt{X(\mu_i)}.$$

Since the constants doesn't play a role in (2.8.16), a solution is given by computing a primitive of the following integral:

$$\xi_i = \Psi^{-1}(\mu_i) := \int \frac{1}{\sqrt{X(\mu_i)}} d\mu_i. \tag{2.8.17}$$

For example, in the case of the map $\mu_i = \xi_i^2$ introduced in (2.8.4), from (2.8.14) we have:

$$X(\mu_i) = \mu_i,$$

and (2.8.17) becomes:

$$\xi_i = \int \frac{1}{\sqrt{\mu_i}} d\mu_i = 2\sqrt{\mu_i},$$

thus dropping the scaling factor which can be eventually reabsorbed by a temporal scaling we get:

$$\mu_i(t) = \Psi(\xi_i(t)) = \xi_i^2(t).$$

This opens for multiple applications. A descending dynamics for the positivity constraint $\mu \geq 0$ which will be used in our numerical experiments is the one given by:

$$\partial_t \mu_i(t) := -\mu_i(t)^{\frac{4-3p}{2-p}} \partial_{\mu_i} L(\mu_i(t)), \quad i = 1, .., m,\ 1 \leq p < 2,$$

and it is easy to see from (2.8.17) that 2.8.2 is the dynamics derived by composing with the map

$$\mu_i(t) = \Psi(\xi_i(t)) := |\xi_i(t)|^{\frac{2(2-p)}{p}}. \tag{2.8.18}$$

.

Another case of direct interest is the following optimization problem:

$$\begin{aligned} \inf_{\mu \in \mathbb{R}^m} \quad & \sum_{i=1}^{m} L(\mu_i). \\ a_i \leq \mu_i \leq b_i & \\ i = 1, .., m & \end{aligned}$$

Taking inspiration from (2.8.14), we consider the the flow generated by a logistic map

$$X(y_i) = \frac{(b_i - y_i)(y_i - a_i)}{b_i - a_i},$$

$$\begin{cases} \dfrac{d}{ds}\Phi_X^s(\mu_i(t)) = \dfrac{(b_i - \Phi_X^s(\mu_i(t)))(\Phi_X^s(\mu_i(t)) - a_i)}{b_i - a_i} \\ \Phi_X^0(\mu_i(t)) = \mu_i(t) \end{cases} \quad i = 1, .., m. \tag{2.8.19}$$

the solution of (2.8.19) is the following sigmoidal function:

$$\Phi_X^s(\mu_i(t)) = \frac{b_i - a_i \mathsf{e}^{\gamma_i(t)-s}}{1 - \mathsf{e}^{\gamma_i(t)-s}},$$

where:

$$\gamma_i(t) := \log\left(\frac{\mu_i(t) - b_i}{\mu_i(t) - a_i}\right).$$

It is easy to see that, $\forall\, i = 1, .., m$, we have:

$$\begin{gathered} a_i \leq \mu_i(t) \leq b_i \implies a_i \leq \Phi_X^s(\mu_i(t)) \leq b_i, \\ \lim_{s\to+\infty} \Phi_X^s(\mu_i(t)) = b_i, \\ \lim_{s\to-\infty} \Phi_X^s(\mu_i(t)) = a_i. \end{gathered}$$

The sigmoid function is well known in the framework of Deep Learning and is often used as an activation function when some interval constraints needs to be satisfied.
The derived projected descent dynamics as in (2.8.15) is the following:

$$\partial_t \mu_i(t) = -\frac{(b_i - \mu_i)(\mu_i - a_i)}{b_i - a_i} \partial_{\mu_i} L(\mu_i), \quad i = 1, ..., m, \tag{2.8.20}$$

which is clearly a descent dynamics if $a_i \leq \mu_i(t) \leq b_i$. Differently from the case of the positivity constraint, we suggest to not scale the time by reabsorbing the factor $\frac{1}{b_i - a_i}$, since it helps to improve the stability of the dynamics if an explicit time discretization scheme is adopted.
Even in this case, the same heuristic geometric considerations can be done, since if we start from a $a_i < \mu_i(0) < b_i$ the dynamics is projected tangentially to the sigmoid function so that it will approach the asymptotes a_i and b_i from a parallel direction to the axis $\mu_i = b_i$ or $\mu_i = a_i$. Observe that the sigmoid function, and especially it's tangent map, acts as a barrier function for the dynamics.
We point out that multiple numerical experiments confirm our conjecture that the dynamics in (2.8.20) can be interpreted as an update preserving scheme providing a sufficiently small initial time step in the time discretization.
Finally, using (2.8.17), we can retrieve the composition map which generates (2.8.20):

$$\xi_i = \int \sqrt{\frac{b_i - a_i}{(b_i - \mu_i)(\mu_i - a_i)}} d\mu_i,$$

and easy computations show that:

$$\mu_i(t) = \Psi(\xi_i(t)) := a_i + (b_i - a_i)\cos^2\left(\frac{\xi_i(t)}{\sqrt{b_i - a_i}}\right), \quad i = 1, ..., m.$$

We point out that all these techniques have an analogy to the Multiplicative Weights Update Method introduced in [7] which is often used in Machine Learning and Online Optimization.

2.9 Extended DMK(EDMK) scheme for the graph p-Poisson problem in the case $1 < p < 2$

In this section we extend the dynamics in (2.8.9) for the problem of solving a p-Poisson equation on graphs, $1 < p < 2$.
As in Section 2.4, let $\mathcal{G} = (E, V, \omega)$ be a weighted directed graph, ∇ it's gradient matrix and div $= -\nabla^T$ it's divergence matrix. We denote as $\mathcal{H}(V) = \mathbb{R}^n$ and $\mathcal{H}(E) = \mathbb{R}^m$ the Banach spaces of real-valued functions on V, the nodes set, and E, the edges set, respectively.
As for the case of 1-Harmonic functions in Section 2.7, we will consider the equivalent problem of minimizing the p-Dirichlet energy in the case $1 < p < 2$. Thus, given a non homogeneous Dirichlet boundary conditions on a boundary subset $B \subset V$, $B \cap V_I = \emptyset$, $B \cup V_I = V$, some non homogeneous Dirichlet boundary data $g \in \mathcal{H}(B) = \mathbb{R}^d$, and a loading term $f \in \mathcal{H}(V_I)$, we look at the following variational problem:

$$\begin{gathered} \inf_{\varphi \in \mathcal{H}(V)} \sum_{e \in E} \frac{|(\nabla \varphi)_e|^p}{p} - \sum_{v \in V_I} f_v \varphi_v \\ s.t.\ \varphi_v = g_v, \quad v \in B. \end{gathered} \tag{2.9.1}$$

The Euler Lagrange equation for (2.9.1) is the graph p-Poisson problem:

$$\begin{gathered} (\Delta_p \varphi)_v = f_v, \quad v \in V_I \\ \varphi_v = g_v, \quad v \in B. \end{gathered} \tag{2.9.2}$$

Moreover, in virtue of the Poincaré inequality, problem (2.9.1) is strictly convex and coercive, therefore, it admits a unique minimizer.
Introducing an appropriate lifting function $\bar{\varphi}$ such that $\bar{\varphi}_v = g_v$ for all $v \in B$ and $\bar{\varphi}_v = 0$ for all $v \in V_I$, problem (2.9.1) simplifies to:

$$\inf_{\varphi \in \mathcal{H}_0^B(V)} \sum_{e \in E} \frac{|\,(\nabla(\varphi + \bar{\varphi}))_e\,|^p}{p} - \sum_{v \in V_I} f_v \varphi_v,$$

where $\mathcal{H}_0^B(V) := \{\varphi \in \mathcal{H}(V) \mid \varphi_v = 0,\ \forall\, v \in B\}$.
As for 1-Harmonic functions, in Section 2.4 we have seen an equivalent saddle point formulation for the graph p-Dirichlet energy when $1 \leq p < 2$, therefore, from Theorem 2.4.1 we have the following result:

Theorem 2.9.1. *For any $\tilde{\varphi} \in \mathcal{H}(V)$ define the Lagrangian $\mathtt{L}^p_{\tilde{\varphi}} : (\mathcal{H}(E)^+ \times \mathcal{H}(E)) \to \mathbb{R}$ as:*

$$\mathtt{L}^p_{\tilde{\varphi}}(\mu, \sigma) := -\sum_{e \in E} \frac{1}{2} \mu_e |\sigma_e|^2 + \sigma \cdot \nabla \tilde{\varphi} + \frac{2-p}{2p} \sum_{e \in E} \mu_e^{\frac{p}{2-p}},$$

and the following function:

$$\mathtt{L}_p(\tilde{\varphi}) := \inf_{\mu\in\mathcal{H}(E)^+}\sup_{\sigma\in\mathcal{H}(E)} \mathtt{L}^p_{\tilde{\varphi}}(\mu,\sigma).$$

For a given Dirichlet boundary subset $B \subset V$ and Dirichlet boundary data $g \in \mathcal{H}(B)$ define the lifting function $\bar{\varphi} \in \mathcal{H}(V)$:

$$\bar{\varphi}_v := \begin{cases} 0, & v \in V_I \\ g_v, & v \in B. \end{cases}$$

Then, we have the following equivalence:

$$\inf_{\varphi\in\mathcal{H}^B_0(V)} \sum_{e\in E} \frac{|\left(\nabla(\varphi+\bar{\varphi})\right)_e|^p}{p} - \sum_{v\in V_I} f_v\varphi_v = \inf_{\varphi\in\mathcal{H}^B_0(V)} \mathtt{L}_p(\varphi+\bar{\varphi}) - \sum_{v\in V_I} f_v\varphi_v. \quad (2.9.3)$$

So that:

$$\inf_{\varphi\in\mathcal{H}^B_0(V)} \sum_{e\in E} \frac{|\left(\nabla(\varphi+\bar{\varphi})\right)_e|^p}{p} - \sum_{v\in V_I} f_v\varphi_v = \quad (2.9.4)$$

$$= \inf_{\substack{\mu\,\in\,\mathcal{H}(E)^+ \\ \varphi\,\in\,\mathcal{H}^B_0(V)}} \sup_{\sigma\in\mathcal{H}(E)} -\sum_{e\in E}\frac{1}{2}\mu_e|\sigma_e|^2 + \sigma\cdot\nabla(\varphi+\bar{\varphi}) - \sum_{v\in V_I} f_v\varphi_v + \frac{1}{2\gamma}\sum_{e\in E}\mu_e, \quad (2.9.5)$$

where $1 < p < 2$ and $\gamma := \frac{p}{2-p}$.
Moreover there exists a unique saddle point

$$((\varphi^*,\mu^*),\sigma^*) \in \left(\mathcal{H}^B_0(V)\times\mathcal{H}(E)^+\right)\times\mathcal{H}(E)\big)$$

and it satisfies the following extremality equations:

$$\begin{aligned} \mu^*_e\sigma^*_e &= \left(\nabla(\varphi^*+\bar{\varphi})\right)_e, && \forall\, e\in E \quad (2.9.6)\\ -(\operatorname{div}\sigma^*)_v &= f_v, && \forall\, v\in V_I \\ \varphi^*_v &= 0, && \forall\, v\in B \\ \mu^*_e = |\sigma^*_e|^{p'-2} &= |\,\nabla(\varphi^*+\bar{\varphi})_e|^{2-p}, && \forall\, e\in E. \quad (2.9.7) \end{aligned}$$

whence $\tilde{\varphi}^* := \varphi^* + \bar{\varphi}$ is the unique solution of the p-Poisson problem (2.9.2).

Proof. The proof is essentially an extension of the proof for Theorem 2.7.4.
The equivalence (2.9.3) is a direct consequence of Theorem 2.4.1 where we have shown that for any $\tilde{\varphi} \in \mathcal{H}(V)$, $\mathtt{E}_p(\tilde{\varphi}) = \mathtt{L}_p(\tilde{\varphi})$, thus it suffices to show that problem (2.9.5) admits a saddle point $((\varphi^*,\mu^*),\sigma^*)$ and automatically φ^* is a minimizer for (2.9.4).
First we will show the existence of a saddle point, then we will show that the KKT conditions for a saddle point of problem (2.9.5) are precisely (2.9.6)-(2.9.7).
The existence of a saddle point for problem (2.9.5) is based on showing that the

hypothesis of Proposition 2.7.3 are satisfied.
For simplicity define the following Lagrangian:

$$\mathtt{L}(\varphi,\mu,\sigma) := -\sum_{e\in E}\frac{1}{2}\mu_e|\sigma_e|^2 + \sigma\cdot\nabla(\varphi+\bar{\varphi}) - \sum_{v\in V_I} f_v\varphi_v + \frac{1}{2\gamma}\sum_{e\in E}\mu_e^{\gamma}. \quad (2.9.8)$$

So that the primal problem $(\mathcal{P})$ in (2.9.5) is equivalent to:

$$\inf_{\substack{\mu\,\in\,\mathcal{H}(E)^+\\ \varphi\,\in\,\mathcal{H}_0^B(V)}}\ \sup_{\sigma\in\mathcal{H}(E)}\ \mathtt{L}(\varphi,\mu,\sigma) \qquad (\mathcal{P}).$$

Consider the dual problem:

$$\sup_{\sigma\in\mathcal{H}(E)}\ \inf_{\substack{\mu\,\in\,\mathcal{H}(E)^+\\ \varphi\,\in\,\mathcal{H}_0^B(V)}}\ \mathtt{L}(\varphi,\mu,\sigma) \qquad (\mathcal{P}^*). \quad (2.9.9)$$

With the same arguments as in (2.4.14) and (2.7.23) we have that:

$$\inf_{\substack{\mu\,\in\,\mathcal{H}(E)^+\\ \varphi\,\in\,\mathcal{H}_0^B(V)}}\ \mathtt{L}(\varphi,\mu,\sigma) =$$
$$= \begin{cases} -\frac{1}{2\gamma'}\sum_{e\in E}|\sigma_e|^{2\gamma'} - \sum_{v\in B}(\operatorname{div}\sigma)_v\bar{\varphi}_v & -(\operatorname{div}\sigma)_v = f_v\ \forall\, v\in V_I \\ -\infty & \textit{otherwise}, \end{cases}$$

and the dual problem (2.9.9) is equivalent to the following constrained problem:

$$\sup_{\substack{\sigma\,\in\,\mathcal{H}(E)\\ -(\operatorname{div}\sigma)_v = f_v,\forall\, v\in V_I}} -\frac{1}{2\gamma'}\sum_{e\in E}|\sigma_e|^{2\gamma'} - \sum_{v\in B}(\operatorname{div}\sigma)_v\bar{\varphi}_v \qquad (\mathcal{P}^*),$$

which has a unique solution since the set $\mathcal{B} := \{\sigma\in\mathcal{H}(E)\mid -(\operatorname{div}\sigma)_v = f_v, \forall\, v\in V_I\}$ is non empty, convex and closed and $2\gamma' = p' > 2$ if $1 < p < 2$, hence we have strict concavity, upper semi-continuity and norm anti-coerciveness.
Next, consider the map:

$$\varphi\mapsto\bar{\sigma}(\varphi) := \frac{|\nabla(\varphi+\bar{\varphi})|^{p-1}\odot\operatorname{sign}(\nabla(\varphi+\bar{\varphi}))}{\alpha\|\nabla(\varphi+\bar{\varphi})\|_{l_p}^{p-1}}, \quad 0<\alpha<+\infty,$$

with the standard convention as in (2.4.9) and the function:

$$\rho(\varphi,\mu) := \mathtt{L}(\varphi,\mu,\bar{\sigma}(\varphi)).$$

It is immediate to see that $\forall\,\varphi\in\mathcal{H}_0^B(V)$:

$$\|\bar{\sigma}(\varphi)\|_{l_{2\gamma'}} = \|\bar{\sigma}(\varphi)\|_{l_{p'}} = \frac{1}{\alpha},$$

and:

$$\bar{\sigma}(\varphi)\cdot\nabla(\varphi+\bar{\varphi})=\frac{\|\nabla(\varphi+\bar{\varphi})\|_{l_p}}{\alpha}.$$

Thus:

$$\bar{\sigma}(\varphi)\ is\ bounded\ \forall\,\varphi\in\mathcal{H}_0^B(V).$$

equipped with the $l_{2\gamma'}=l_{p'}$ norm and:

$$\begin{aligned}\rho(\varphi,\mu)&=-\sum_{e\in E}\frac{1}{2}\mu_e|\bar{\sigma}(\varphi)_e|^2+\bar{\sigma}(\varphi)\cdot\nabla(\varphi+\bar{\varphi})-\sum_{v\in V_I}f_v\varphi_v+\frac{1}{2\gamma}\|\mu\|_{l_\gamma}^{\gamma}\overset{Hölder}{\geq}\\&\geq\frac{\|\nabla(\varphi+\bar{\varphi})\|_{l_p}}{\alpha}-\|f\|_{l_{p'}}\|\varphi\|_{l_p}-\frac{1}{2\alpha^2}\|\mu\|_{l_\gamma}+\frac{1}{2\gamma}\|\mu\|_{l_\gamma}^{\gamma}\geq\\&\geq\left(\frac{1}{c_p\alpha}-\|f\|_{l_{p'}}\right)\|\varphi\|_{l_p}-\frac{\|\bar{\varphi}\|_{l_p}}{c_p\alpha}-\frac{1}{2\alpha^2}\|\mu\|_{l_\gamma}+\frac{1}{2\gamma}\|\mu\|_{l_\gamma}^{\gamma},\end{aligned}$$

where $c_p>0$ is the Poincaré constant.
Now, supposing that $\|f\|_{l_{p'}}\neq 0$, taking α such that:

$$\alpha<\frac{1}{c_p\|f\|_{l_{p'}}},$$

we have:

$$\left(\frac{1}{c_p\alpha}-\|f\|_{l_{p'}}\right)\|\varphi\|_{l_p}\geq 0,$$

and

$$\lim_{\|\varphi\|_{l_p}\to\infty}\left(\frac{1}{c_p\alpha}-\|f\|_{l_{p'}}\right)\|\varphi\|_{l_p}=+\infty.$$

If $\|f\|_{l_{p'}}=0$ the same is true $\forall\,\alpha>0$.
Observing that $\gamma>1$ if $1<p<2$ we also have that:

$$\begin{aligned}\lim_{\|\mu\|_{l_\gamma}\to\infty}&-\frac{1}{2\alpha^2}\|\mu\|_{l_\gamma}+\frac{1}{2\gamma}\|\mu\|_{l_\gamma}^{\gamma}=\\&=\lim_{\|\mu\|_{l_\gamma}\to\infty}\left(\frac{1}{2\gamma}-\frac{1}{2\alpha^2\|\mu\|_{l_\gamma}^{\gamma-1}}\right)\|\mu\|_{l_\gamma}^{\gamma}=+\infty.\end{aligned}$$

As a consequence, $\rho(\varphi,\mu)$ is norm coercive in the product space $(\mathcal{H}_0^B(V)\times\mathcal{H}(E)^+)$ equipped with the norm

$$\|(\varphi,\mu)\|_{(\mathcal{H}_0^B(V)\times\mathcal{H}(E)^+)}=\sup\{\|\varphi\|_{l_p},\|\mu\|_{l_\gamma}\}.$$

Moreover the function $g:\mathbb{R}\to\mathbb{R}$ defined as:

$$g(t):=\frac{1}{2\gamma}t^{\gamma}-\frac{1}{2\alpha^2}t,$$

admits the unique positive minimizer:

$$t^* = \left(\frac{1}{\alpha^2}\right)^{\frac{1}{\gamma-1}} > 0, \quad \forall\, \alpha \neq 0.$$

Summing up all together, we have found that:

$$\rho(\varphi, \mu) \textit{ is bounded from below and norm coercive.}$$

Thus, all the hypothesis of Proposition 2.7.3 are satisfied and there exists a saddle point $((\varphi^*, \mu^*), \sigma^*) \in \big((\mathcal{H}_0^B(V) \times \mathcal{H}(E)^+) \times \mathcal{H}(E)\big)$.
The KKT conditions for the saddle points $((\varphi^*, \mu^*), \sigma^*)$ of (2.9.8), read as follows:

$$\begin{cases} -|\sigma_e^*|^2 + {\mu_e^*}^{\frac{2(p-1)}{2-p}} - c_e = 0, & \forall\, e \in E \\ \mu_e^* \sigma_e^* = \nabla(\varphi^* + \bar{\varphi})_e, & \forall\, e \in E \\ -(\operatorname{div} \sigma^*)_v = f_v, & \forall\, v \in V_I \\ \varphi_v^* = 0, & \forall\, v \in B \\ c_e \mu_e^* = 0, \quad c_e \geq 0, & \forall\, e \in E. \end{cases} \tag{2.9.10}$$

where $c \in \mathcal{H}(E)$ is an opportune positive Lagrange multiplier.
Observe that if $\mu_{\bar{e}}^* = 0$ on some edge $\bar{e}$, then the first equation in (2.9.10) implies that $\sigma_{\bar{e}}^* = 0$ and $c_{\bar{e}} = 0$, this is the unique possible solution. On the edges where $\mu_e^* > 0$, the last equation gives that $c_e = 0$.
Therefore, (2.9.10) implies that

$$\begin{cases} \mu_e^* = |\sigma_e^*|^{\frac{2-p}{p-1}} = |\sigma_e^*|^{p'-2} = |\nabla(\varphi^* + \bar{\varphi})_e|^{2-p}, & \forall\, e \in E \\ \mu_e^* \sigma_e^* = (\nabla \varphi)_e, & \forall\, e \in E. \end{cases}$$

This last two equations imply also that:

$$\sigma_e^* = |\nabla(\varphi + \bar{\varphi})_e|^{p-1} \operatorname{sign}(\nabla(\varphi + \bar{\varphi}))_e, \quad \forall\, e \in E.$$

So that the remaining equations in (2.9.10):

$$\begin{cases} -(\operatorname{div} \sigma^*)_v = f_v, & \forall\, v \in V_I \\ \varphi_v^* = 0, & \forall\, v \in B, \end{cases}$$

are equivalent to the p-Poisson problem for $\tilde{\varphi}^* := \varphi^* + \bar{\varphi}$:

$$\begin{aligned} (\Delta_p \tilde{\varphi}^*)_v = f_v, \quad v \in V_I \\ \tilde{\varphi}_v^* = \gamma_v, \quad v \in B, \end{aligned}$$

which, by virtue of the Poincaré inequality, admits a unique solution.
This shows that the optimal triplet $((\varphi^*, \mu^*), \sigma^*)$ is unique, it satisfies the extremality relations (2.9.6)-(2.9.7) and $\tilde{\varphi}^* := \varphi^* + \bar{\varphi}$ is the unique solution of the p-Poisson problem (2.9.2).

□

Remark 2.9.2. *Observe that, exchanging sums we integrals, the proof of Theorem 2.9.1 works also in the continuous case, with the same arguments.*

We have now all the ingredients to extend our regularized DMK scheme (2.8.9). Consider the regularized functional:

$$\begin{aligned}\mathcal{L}^p_\delta(\varphi,\mu) :=& \\ = \sup_{\sigma\in\mathcal{H}(E)} &-\sum_{e\in E}\frac{1}{2}(\mu_e+\delta)|\sigma_e|^2+\sigma\cdot\nabla(\varphi+\bar\varphi)-\sum_{v\in V_I}f_v\varphi_v+\frac{1}{2\gamma}\sum_{e\in E}\mu_e^\gamma = \\ &= \sum_{e\in E}\frac{1}{2}\frac{|\nabla(\varphi+\bar\varphi)_e|^2}{(\mu_e+\delta)}-\sum_{v\in V_I}f_v\varphi_v+\frac{1}{2\gamma}\sum_{e\in E}\mu_e^\gamma,\end{aligned}$$

where $\gamma=\frac{p}{2-p}$, $1<p<2$, and consider the following double minimization problem:

$$\inf_{\substack{\varphi\,\in\,\mathcal{H}^B_0(V)\\ \mu\,\in\,\mathcal{H}(E)^+}}\mathcal{L}^p_\delta(\varphi,\mu). \tag{2.9.11}$$

With the same arguments as in (2.5.10) we have that $\mathcal{L}^p_\delta(\varphi,\mu)$ is convex, lower semi-continuous and coercive in the pair (φ,μ). Moreover, since $\gamma>1$ if $1<p<2$, the function $\mathcal{L}^p_\delta(\varphi,\mu)$ is strictly convex in $(\mathcal{H}^B_0(V)\times\mathcal{H}(E)^+)$ and the existence of a unique minimizer (φ^*,μ^*) for (2.9.11) is guaranteed.
The KKT conditions for the minimizers of $\mathcal{L}^p_\delta(\varphi,\mu)$ reads as follows:

$$\begin{cases}-\frac{|\nabla(\varphi^*+\bar\varphi)_e|^2}{(\mu^*_e+\delta)^2}+\mu^{\gamma-1}-c_e=0, & \forall\, e\in E\\ (\Delta_{\frac{1}{\mu^*+\delta}}(\varphi^*+\bar\varphi))_v=f_v, & \forall\, v\in V_I\\ \varphi^*_v=0, & \forall\, v\in B\\ c_e\mu^*_e=0,\quad c_e\geq 0, & \forall\, e\in E\end{cases} \tag{2.9.12}$$

The second and the third equations in (2.9.12) are exactly the reduced system as in (2.8.6). since $c\geq 0$, if

$$\mu^*_{\bar e}=0,$$

on some edge $\bar e$, then the first equation in (2.9.12) implies that

$$\nabla(\varphi^*+\bar\varphi)_{\bar e}=0,$$

and $c_{\bar e}=0$, this is the unique possible solution.
On the other hand, the last equation in (2.9.12) implies that if

$$\mu^*_{\bar e}>0,$$

then $c_{\bar e}=0$ and hence

$$|\nabla(\varphi^*+\bar\varphi)|^2_{\bar e}=(\mu^*_{\bar e}+\delta)^2{\mu^*_{\bar e}}^{\frac{2(p-1)}{2-p}},$$

which also implies that $\mu_{\bar{e}}^* \approx |\nabla(\varphi^* + \bar{\varphi})|_{\bar{e}}^{2-p} + \mathcal{O}(\delta)$.
We are indeed motivated to introduce the corresponding version of the dynamics in (2.8.9) as a good approximation:

$$\begin{aligned}
(\Delta_{\frac{1}{\mu(t)+\delta}}(\varphi(t)+\bar{\varphi}))_v &= f_v, \quad \forall\, v \in V_I, \\
\varphi(t)_v &= 0 \quad \forall\, v \in B, \\
\sigma_e(t) &= \frac{(\nabla(\varphi(t)+\bar{\varphi}))_e}{\mu_e(t)+\delta}, \quad \forall\, e \in E,
\end{aligned} \tag{EDMK}$$

$$\partial_t \mu_e(t) = \mu_e(t)|\sigma_e(t)|^2 - \mu_e(t)^{\frac{p}{2-p}}, \quad \mu_e(0) = \mu_{0_e} > 0, \quad \forall\, e \in E. \tag{2.9.13}$$

where as in (2.8.9), the dynamics in (2.9.13) is derived by composing with the quadratic map $\mu_e(t) = \xi_e(t)^2$, $\forall\, e \in E$ and we refer to Section 2.8 for the time discretization approaches.
As for the 1-Harmonic case, multiple experiments where done providing good stability and convergence properties. Another converging dynamics which exhibits faster convergence rate and improved stability in our numerical experiments is the one given in (2.8.18) derived by composing with the map:

$$\mu_e(t) = \Psi(\xi_e(t)) := |\xi_e(t)|^{\frac{2(2-p)}{p}}, \quad \forall\, e \in E,$$

which leads to the following new dynamics for μ:

$$\partial_t \mu_e(t) = \mu_e(t)^{\frac{4-3p}{2-p}} |\sigma_e(t)|^2 - \mu_e(t), \quad \forall\, e \in E.$$

This kind of dynamics, in the Optimal Transport case, was observed experimentally as describing the time evolution growing for some types of bacteria [55].

2.10 Generalized DMK(GDMK) scheme for the Minimal Surfaces problem

In this section we briefly describe how the DMK scheme (2.8.4) can be used to tackle the particular case of the Minimal Surfaces problem. We have already shown in Example 2.6.4 how to construct an equivalent formulation in the discrete setting of the minimial surfaces type energy. We will first introduce the problem in the continuous case and then state the discrete counterpart on graphs.
Consider an open bounded Lipschitz domain $\Omega \in \mathbb{R}^n$ and set $\Gamma = \partial\Omega$. Given a profile function $g(x) : \Gamma \mapsto \mathbb{R}$ we look at the following variational problem:

$$\begin{aligned}
&\inf_{\varphi \in \mathcal{C}^\infty(\Omega)} \int_\Omega \sqrt{1 + |\nabla \varphi|^2} \\
&s.t.\ \varphi(x) = g(x), \quad x \in \Gamma.
\end{aligned} \tag{2.10.1}$$

Problem (2.10.1) can be simplified by introducing the lifting function $\bar{\varphi}$ such that $\bar{\varphi}(x) = g(x)$ for all $x \in \Gamma$ and considering the problem:

$$\inf_{\varphi \in \mathcal{C}_c^\infty(\Omega)} \int_\Omega |\sqrt{1 + |\nabla(\varphi + \bar{\varphi})|^2}. \tag{2.10.2}$$

The Euler-Lagrange equation for problem (2.10.1) is the well known Minimal Surfaces PDE with fixed profile g:

$$\begin{aligned} -\operatorname{div}\Big(\frac{\nabla \varphi}{\sqrt{1 + |\nabla \varphi|^2}}\Big) = 0, \quad x \in \Omega \\ \varphi(x) = g(x), \quad x \in \Gamma. \end{aligned}$$

The discrete graph-based counterpart of (2.10.2) is the following problem:

$$\inf_{\varphi \in \mathcal{H}_0^B(V)} \sum_{e \in E} \sqrt{1 + |\nabla(\varphi + \bar{\varphi})_e|^2}, \tag{2.10.3}$$

where we have selected a Dirichlet boundary subset $B \subset V$, a profile function $g \in \mathcal{H}(B)$, an appropriate lifting function $\bar{\varphi}$ such that $\bar{\varphi}_v = g_v$ for all $v \in B$ and $\bar{\varphi}_v = 0$ for all $v \in V_I$ and considered a $\varphi \in \mathcal{H}_0^B(V)$ where $\mathcal{H}_0^B(V) := \{\varphi \in \mathcal{H}(V) \mid \varphi_v = 0,\ \forall\, v \in B\}$.
In Example 2.6.4 we have seen an equivalent saddle point formulation for the discrete Minimal Surfaces energy, hence in the graph framework, $\forall\, \varphi \in \mathcal{H}_0^B(V)$, we have that:

$$\mathtt{E}(\varphi) := \sum_{e \in E} \sqrt{1 + |\nabla(\varphi + \bar{\varphi})_e|^2}, \tag{2.10.4}$$

$$\begin{aligned} L_\varphi(\mu, \sigma) := -\frac{1}{2} \sum_{e \in E} \mu_e |\sigma_e|^2 + \sigma \cdot \nabla(\varphi + \bar{\varphi}) + \frac{1}{2} \sum_{e \in E} (\frac{1}{\mu_e} + \mu_e), \\ \mathtt{L}_{MS}(\varphi) = \inf_{\mu \in \mathcal{H}(E)^+} \sup_{\sigma \in \mathcal{H}(E)} L_\varphi(\mu, \sigma), \end{aligned}$$

and

$$\mathtt{E}(\varphi) = \mathtt{L}_{MS}(\varphi), \quad \forall\, \varphi \in \mathcal{H}_0^B(V).$$

moreover, as in Example 2.6.4, the unique saddle point (μ^*, σ^*) for $L_\varphi(\mu, \sigma)$ is given by:

$$\begin{aligned} \mu_e^* = \sqrt{1 + |\nabla(\varphi + \bar{\varphi})_e|^2}, \quad e \in E, \\ \sigma_e^* = \frac{\nabla(\varphi + \bar{\varphi})_e}{\sqrt{1 + |\nabla(\varphi + \bar{\varphi})_e|^2}}, \quad e \in E. \end{aligned}$$

With the same arguments as in Theorems 2.7.4, 2.9.1 is possible to show that problem (2.10.3) is equivalent to:

$$\begin{aligned} &\inf_{\varphi \in \mathcal{H}_0^B(V)} \mathtt{L}_{MS}(\varphi) = \\ &= \inf_{\substack{\varphi \,\in\, \mathcal{H}_0^B(V) \\ \mu \,\in\, \mathcal{H}(E)^+}} \sup_{\sigma \in \mathcal{H}(E)} -\frac{1}{2} \sum_{e \in E} \mu_e |\sigma_e|^2 + \sigma \cdot \nabla(\varphi + \bar{\varphi}) + \frac{1}{2} \sum_{e \in E} (\frac{1}{\mu_e} + \mu_e). \end{aligned} \tag{2.10.5}$$

and there exists a unique optimal triplet $(\varphi^*, \mu^*, \sigma^*)$ for (2.10.5) which satisfies the following extremality relations:

$$\begin{aligned} \mu_e^* \sigma_e^* &= (\nabla(\varphi^* + \bar{\varphi}))_e, \quad \forall\, e \in E \\ -(\operatorname{div} \sigma^*)_v &= 0, \quad \forall\, v \in V_I \\ \varphi_v^* &= 0, \quad \forall\, v \in B \\ \mu_e^* &= \sqrt{1 + |\nabla(\varphi + \bar{\varphi})_e|^2}, \quad \forall\, e \in E. \end{aligned}$$

As a consequence

$$\tilde{\varphi} := \varphi^* + \bar{\varphi},$$

is the unique solution of the graph Minimal Surfaces problem:

$$\begin{aligned} (\Delta_{\frac{1}{\sqrt{1+|\nabla(\tilde{\varphi}|^2}}} \tilde{\varphi})_v &= 0, \quad v \in V_I \\ \tilde{\varphi}_v &= g_v \quad v \in B. \end{aligned} \tag{2.10.6}$$

Moreover, since the optimal density μ^* is strictly greater then 1, possibly restricting (2.10.5) on the set $\{\mu \in \mathcal{H}(E)^+ \mid \mu_i \geq \delta,\, \delta < 1, i = 1, ..., m\}$, the minimizer μ^* remains the global minimizer, the "sup" in σ becomes a "max" and thus, evaluating (2.10.4) in

$$\sigma_e = \frac{\nabla(\varphi + \bar{\varphi})_e}{\mu_e}, \quad \forall\, e \in E,$$

we have:

$$\mathcal{L}_{MS}(\varphi, \mu) := \sum_{e \in E} \frac{1}{2} \frac{|\nabla(\varphi + \bar{\varphi})_e|^2}{\mu_e} + \frac{1}{2} \sum_{e \in E} (\frac{1}{\mu_e} + \mu_e),$$

and (2.10.5) is equivalent to the reduced formulation::

$$\begin{aligned} \inf_{\varphi \in \mathcal{H}_0^B(V)} \mathtt{L}_{MS}(\varphi) &= \inf_{\substack{\mu \,\in\, \mathcal{H}(E)^+ \\ \varphi \,\in\, \mathcal{H}_0^B(V)}} \mathcal{L}_{MS}(\varphi, \mu) = \\ &= \inf_{\substack{\mu \,\in\, \mathcal{H}(E)^+ \\ \varphi \,\in\, \mathcal{H}_0^B(V)}} \sum_{e \in E} \frac{1}{2} \frac{|\nabla(\varphi + \bar{\varphi})_e|^2}{\mu_e} + \frac{1}{2} \sum_{e \in E} (\frac{1}{\mu_e} + \mu_e). \end{aligned} \tag{2.10.7}$$

The function $\mathcal{L}_{MS}(\varphi, \mu)$ is strictly convex and differentiable in the interior of $(\mathcal{H}_0^B(V) \times \mathcal{H}(E)^+)$ thus, since the optimal densitity $\mu^* > 0$, the existence of a unique minimizer (φ^*, μ^*) for (2.10.7) is guaranteed.
We are indeed motivated to introduce the corresponding version of the dynamics in (2.8.9):

$$\begin{aligned} (\Delta_{\frac{1}{\mu(t)}} (\varphi(t) + \bar{\varphi}))_v &= 0, \quad \forall\, v \in V_I, \\ \varphi(t)_v &= 0, \quad \forall\, v \in B, \\ \partial_t \mu_e(t) &= \frac{|\nabla(\varphi(t) + \bar{\varphi})_e|^2 + 1}{\mu_e(t)} - \mu_e(t), \quad \mu_e(0) = 1, \quad \forall\, e \in E. \end{aligned} \tag{GDMK}$$

(2.10.8)

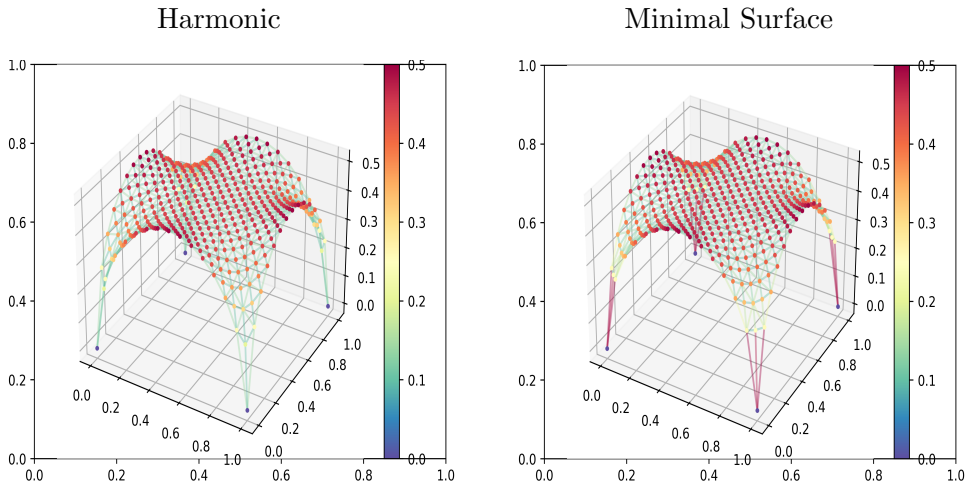

Figure 2.6: Test Case 1, Harmonic vs Minimal Surface, Potential (nodes) μ (edges)

where as in (2.8.9), the dynamics in (2.10.8) is derived by composing with the quadratic map $\mu_e(t) = \xi_e(t)^2$, $\forall\, e \in E$ and we refer to Section 2.8 for the time discretization approaches. Moreover, as we have already observed, the optimal density μ^* is strictly greater then 1, so that we propose to take as initial guess $\mu_e(0) = 1$, $\forall\, e \in E$.
We now present some numerical experiments in the same first two test cases as for the Total Variation Energy minimization(figures 2.2, 2.3). As for the 1-Harmonic case, we have decided to plot the figures in three dimensions where on the nodes we have the value of the function $\tilde{\varphi} = \varphi^* + \bar{\varphi}$, which in these figures is represented by the third coordinate "z", and we give different colors to the edges depending on the value of the variable μ^*, following the heat colour bar on the right side.
In figures 2.6,2.7 we can see the comparison between the Harmonic solution (left) and Minimal Surfaces solution(right) computed with our Generalized DMK(GDMK) scheme (2.10.8) and Explicit Euler time discretization scheme(see Section 2.8 for details) for test case 1 and 2 respectively. Finally, in figure 2.8 we show the convergence behaviour of our numerical algorithm for test case 1 (the same results was observed for test case 2). We plot in the vertical axis the relative error as in (2.8.13) vs the number of iterations(horizontal axis). We point out that the no time stepping rule were adopted, so that we fixed a relative large time step $\Delta t = 0.5$, an initial $\mu_0 > 0$, and we let evolve the dynamics until $err_{\mu^k}(\mu^{k+1}) \leq 1e-8$(as in (2.8.13). As a result, a greater convergence speed was observed with respect to the 1-Harmonic case.

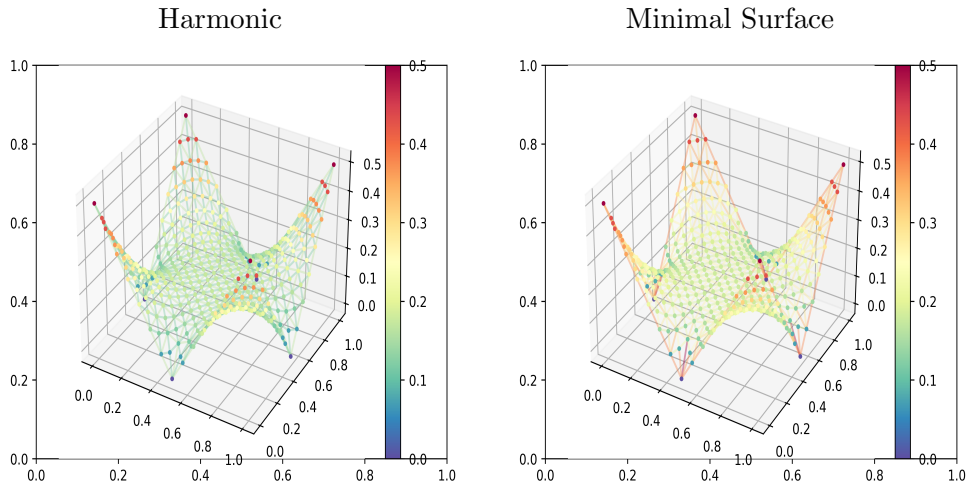

Figure 2.7: Test case 2, Harmonic vs Minimal Surface, Potential (nodes) μ (edges)

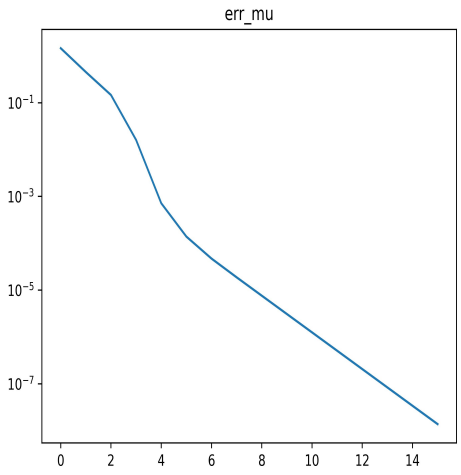

Figure 2.8: $err_{\mu^k}(\mu^{k+1})$ vs number of iterations

2.10.1 Application to the Obstacle Problem

One of the most famous application related to the Minimal Surfaces energy minimization is the Obstacle Problem, first introduced By Lions and Stampacchia in [92]. The problem reads as follows. Consider an open bounded Lipschitz domain $\Omega \in \mathbb{R}^2$ and set $\Gamma = \partial\Omega$. Consider moreover a body represented by

$$\left\{(x, y, z) \in \mathbb{R}^3 : z \leq \phi(x, y)\right\}.$$

As for the Minimal Surfaces energy minimization, let $g(x) : \Gamma \mapsto \mathbb{R}$ be a Dirichlet profile function. The Obstacle Problem is formulated as the problem to seek for the equilibrium position of the membrane such that it lies above the body represented by ϕ with Dirichlet boundary conditions on Γ. Namely, we look at the following variational problem:

$$\begin{aligned} &\inf_{\varphi \in \mathcal{C}^\infty(\Omega)} \int_\Omega \sqrt{1 + |\nabla \varphi|^2} \\ &s.t.\ \varphi(x) = g(x), \quad x \in \Gamma \\ &\qquad \varphi(x) \geq \phi(x), \quad x \in \Omega \end{aligned} \tag{2.10.9}$$

This kind problem and it's variants have multiple applications in Finance, Optimal Control Theory and non-linear Elasticity Theory (see for example [89]).
The Euler-Lagrange equations for (2.10.9) reads as follows [2], [89]:

$$\begin{aligned} -\operatorname{div}\Big(\frac{\nabla \varphi}{\sqrt{1 + |\nabla \varphi|^2}}\Big) \geq 0, \quad x \in \Omega \\ \varphi \geq \phi, \quad x \in \Omega \\ -(\varphi - \phi)\operatorname{div}\Big(\frac{\nabla \varphi}{\sqrt{1 + |\nabla \varphi|^2}}\Big) = 0, \quad x \in \Omega \\ \varphi(x) = g(x), \quad x \in \Gamma \end{aligned}$$

The graph-based counterpart of (2.10.9) is the following problem:

$$\begin{aligned} &\inf_{\varphi \in \mathcal{H}_0^B(V)} \quad \sum_{e \in E} \sqrt{1 + |\nabla(\varphi + \bar{\varphi})_e|^2} \\ &\varphi_v \geq \phi_v,\ \forall\, v \in V_I \end{aligned} \tag{2.10.10}$$

where as in (2.10.3) we have introduced a lifting function $\bar{\varphi}_v = g_v$, $\forall\, v \in B$, $\bar{\varphi}_v = 0$, $\forall\, v \in V_I$, $g \in \mathcal{H}(B)$ is the profile function and we imposed the further constraint on the obstacle function $\phi \in \mathcal{H}(V_I)$.
In analogy to the continuous case, the Euler-Lagrange equations for (2.10.10) are:

$$\begin{aligned} (\Delta_{\frac{1}{\sqrt{1+|\nabla(\varphi+\bar{\varphi})|^2}}}(\varphi + \bar{\varphi}))_v \geq 0, \quad v \in V_I \\ \varphi_v \geq \phi_v, \quad v \in V_I \\ (\varphi_v - \phi_v)(\Delta_{\frac{1}{\sqrt{1+|\nabla(\varphi+\bar{\varphi})|^2}}}(\varphi + \bar{\varphi}))_v = 0, \quad v \in V_I \\ \varphi_v = 0, \quad v \in B. \end{aligned} \tag{2.10.11}$$

We then consider our equivalent formulation of the Minimal Surfaces energy minimization as in (2.10.7) and look at the following problem:

$$\begin{aligned}\inf_{\substack{\mu\,\in\,\mathcal{H}(E)^+\\ \varphi\,\in\,\mathcal{H}_0^B(V)\\ \varphi_v\,\geq\,\phi_v,\ \forall\, v\,\in\,V_I}} \quad & \mathcal{L}_{MS}(\varphi,\mu) := \\ &= \inf_{\substack{\mu\,\in\,\mathcal{H}(E)^+\\ \varphi\,\in\,\mathcal{H}_0^B(V)\\ \varphi_v\,\geq\,\phi_v,\ \forall\, v\,\in\,V_I}} \sum_{e\in E}\frac{1}{2}\frac{|\,\nabla(\varphi+\bar\varphi)_e|^2}{\mu_e}+\frac{1}{2}\sum_{e\in E}(\frac{1}{\mu_e}+\mu_e). \quad (2.10.12)\end{aligned}$$

Motivated by (2.10.6) and the doubled minimization problem of (2.10.12) , we introduce the following GDMK minimization flow:

$$\begin{aligned}\partial_t\varphi_v(t) &= -(\varphi_v(t)+\bar\varphi_v-\phi_v)(\Delta_{\frac{1}{\mu(t)}}(\varphi(t)+\bar\varphi))_v, \quad \forall\, v\in V_I,\\ \varphi_v(0) &= \varphi_{0v}>\phi_v, \quad \forall\, v\in V_I,\\ \varphi_v(t) &= 0, \quad \forall\, v\in B,\\ \partial_t\mu_e(t) &= \frac{|\,\nabla(\varphi(t)+\bar\varphi)_e|^2+1}{\mu_e(t)}-\mu_e(t), \quad \mu_e(0)=1, \quad \forall\, e\in E.\end{aligned} \qquad \textbf{(GDMK)} \quad (2.10.13)$$

or equivalently:

$$\begin{aligned}\partial_t\tilde\varphi_v(t) &= -(\tilde\varphi_v(t)-\phi_v)(\Delta_{\frac{1}{\mu(t)}}(\tilde\varphi(t)))_v, \quad \forall\, v\in V_I,\\ \tilde\varphi_v(0) &= \tilde\varphi_{v0}>\phi_v, \quad \forall\, v\in V_I,\\ \tilde\varphi_v(t) &= g_v, \quad \forall\, v\in B,\\ \partial_t\mu_e(t) &= \frac{|(\nabla\,\tilde\varphi(t))_e|^2+1}{\mu_e(t)}-\mu_e(t), \quad \mu_e(0)=1, \quad \forall\, e\in E.\end{aligned} \quad (2.10.14)$$

where $g\in\mathcal{H}(B)$ is the profile function. As in (2.8.9), the dynamics in (2.10.13) and (2.10.14) are derived by composing with the quadratic maps

$$\tilde\varphi_v(t)=\varphi_v(t)+\bar\varphi=\phi_v+h_v(t)^2, \quad \forall\, v\in V_I,$$

and

$$\mu_e(t)=\xi_e(t)^2, \quad \forall\, e\in E.$$

Observe that a stationary point for (2.10.13) or (2.10.14) is a solution of the original Euler-Lagrange equations (2.10.11).
As for the time discretization approach, we propose the following semi implicit scheme for (2.10.14) which is quite easy to implement but it shows a relative

slow convergence rate. Given a sequence $\Delta t_k > 0$, the approximation sequence $\left(\mu^k\right)_{k=1,...,k_{\max}}$, $\left(\tilde{\varphi}^k\right)_{k=1,...,k_{\max}}$ is given by the following set of equations:

$$\begin{cases} \left(\mathbb{1} + \Delta t_k[\mathrm{Diag}(\tilde{\varphi}^k - \phi)]\Delta_{\frac{1}{\mu^k}}\right)\tilde{\varphi}^{k+1} = \tilde{\varphi}^k, & \forall\, v \in V_I \\ \tilde{\varphi}^{k+1} = g_v, & \forall\, v \in B \\ {\tilde{\varphi}_v}^0 > \phi_v, & \forall\, v \in V_I \\ {\tilde{\varphi}_v}^0 = g_v, & \forall\, v \in B \\ \mu_e^{k+1} = \mu_e^k + \Delta t_k\left(\dfrac{|(\nabla\,\tilde{\varphi}^k)_e|^2 + 1}{\mu_e^k} - \mu_e^k\right), & \forall\, e \in E \\ \mu_e^0 = 1, & \forall\, e \in E \\ k = 0, ..., k_{\max}. \end{cases} \tag{2.10.15}$$

Hence at each time step, we only need to solve the linear system

$$\begin{aligned} \left(\mathbb{1} + \Delta t_k[\mathrm{Diag}(\tilde{\varphi}_v^k - \phi)]\Delta_{\frac{1}{\mu^k}}\right)\tilde{\varphi}^{k+1} = \tilde{\varphi}^k, & \quad \forall\, v \in V_I \\ \tilde{\varphi}^{k+1} = g_v, & \quad \forall\, v \in B. \end{aligned}$$

We will now see an application of our proposed scheme in (2.10.15). We consider the same test case graph as in figure 2.1. We then impose null homogeneous Dirichlet boundary conditions on each side of the square and we considered the following obstacle function ϕ:

$$\begin{cases} \phi_v = 0.8, & 0.2 \leq v_x \leq 0.4 \; and \; 0.2 \leq v_y \leq 0.4 \\ \phi_v = 1.0, & 0.6 \leq v_x \leq 0.8 \; and \; 0.6 \leq v_y \leq 0.8 \\ \phi_v = 0, & otherwise. \end{cases}$$

In figure 2.9 we can see the comparison between the obstacle function ϕ(left) and the numerical solution $\tilde{\varphi}$(right) computed with our semi implicit DMK scheme (2.10.15). In figure 2.10 we can see the convergence behaviour of our numerical algorithm for the proposed test case. We plot in the vertical axis the relative error for the variable μ as in (2.8.13) vs the number of iterations(horizontal axis). In the numerical simulation we used a fixed time step $\Delta t = 1e-2$, an initial $\mu_0 > 0$, $\tilde{\varphi}_0 > \phi$, and we let evolve the dynamics until $err_{\mu^k}(\mu^{k+1}) \leq 1e-4$(as in (2.8.13)). Is clearly visible from figure 2.10 that two different linear convergence rates can be observed. This convergence behaviour correspond to the synchronization along the flow of the solution $\tilde{\varphi}$ on the two different peaks of the obstacle function ϕ. Unfortunately, the algorithm is quite slow, nevertheless it exhibits a good stability. We will further investigate the behaviour of the minimization flow in (2.10.14) with other more efficient numerical schemes such as the Implicit Euler scheme. Finally, in figure 2.11 we can see the value of the potential function $\tilde{\varphi}$ and the obstacle function ϕ corresponding to the same node index in the graph showing that the constraint $\tilde{\varphi} \geq \phi$ is preserved during the minimization.

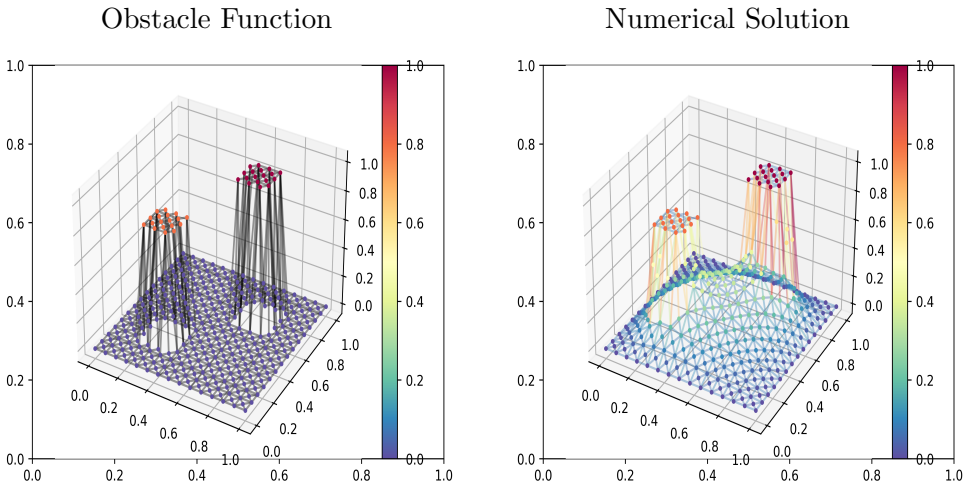

Figure 2.9: Obstacle vs Computed Solution, Potential (nodes) μ (edges)

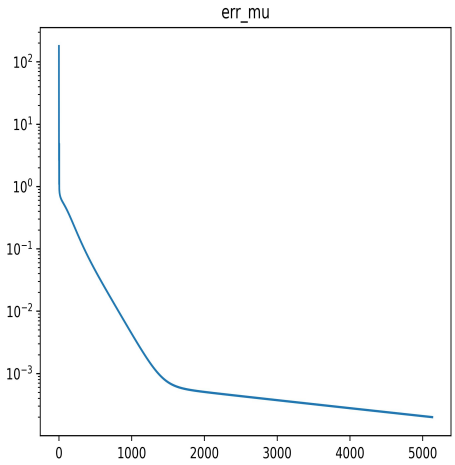

Figure 2.10: $err_{\mu^k}(\mu^{k+1})$ vs number of iterations

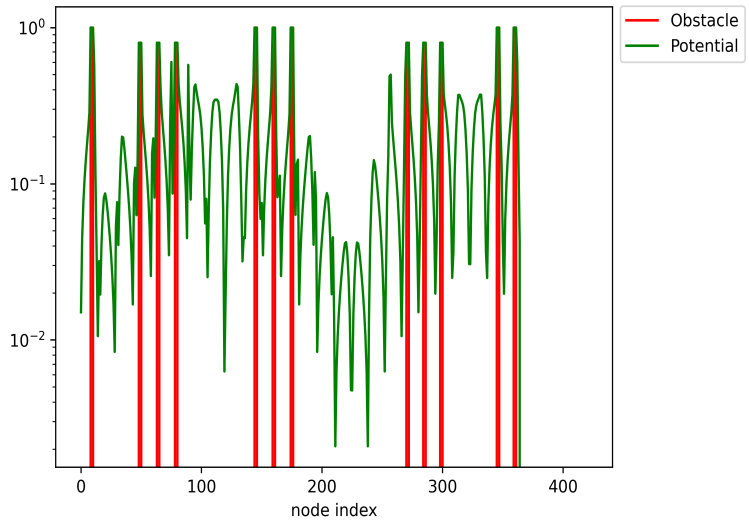

Figure 2.11: $\tilde{\varphi}$(green) vs ϕ(red)

2.11 Application to the general framework of TV and l_1-norm regularization

Optimization Problems and Inverse Problems are nowadays very popular with several applications in engineering and data analysis. Typically, inverse problems are ill-posed and admit infinite solutions. Analogously, non convex objective functions may admit multiple local extremal points drastically making their identification difficult or even impossible.
A common strategy to overcome this problem is to add regularization terms to the objective function. The aim of the regularization term is to gain convexity to improve the identifiability of local minimizers and improving the well-conditioning of the problem.
A very effective and challenging choice of regularizers are based on l_1-norms (compressed sensing, LASSO) or Total Variation of the optimization design parameters. The use of such regularization strategies is hampered by the difficulty in finding efficient and robust numerical solution algorithms. In this Section we will first introduce the problem of regularization in a very broad sense and describe how to incorporate our techniques based on the DMK scheme for the TV and l_1-norm Tikhonov regularization. The reasons and motivations for this section come not only from a case of direct interest for this thesis, but also as an introduction for future developments with multiple applications in different fields, for example Machine Learning and Deep Learning.
We will show moreover few interesting applications such as the classical problem of 1-D signal TV-Denoising and the more particular problem of the compressed sensing for the graph Laplacian partial eigenproblem, remarking the advantages

of our proposed numerical algorithms with respect to the standard techniques such as the Bregman-Split iteration [104], [64], [33], [115].

2.11.1 Introduction: Generalized Tikhonov Regularization in Variational Problems

Consider an open Lipschitz domain $\Omega \in \mathbb{R}^n$ and a Banach space $\mathcal{H}(\Omega)$ defined on Ω. In the most general case, the Generalized Tikhonov Regularization for a Variational Problem is the following optimization problem:

$$\begin{aligned} \min_{\varphi \in \mathcal{H}(\Omega)} \int_\Omega c(\varphi, \epsilon(\varphi)) + \int_\Gamma N(\varphi, \epsilon(\varphi)) + \lambda \int_\Omega R(\epsilon(\varphi)) \\ s.t. \quad g(\varphi) \geq 0, \quad in\ \Omega \\ b(\varphi) = 0, \quad in\ \Gamma = \partial\Omega. \end{aligned}$$

Where c is a cost function defined on Ω, N is a cost function defined on $\Gamma = \partial\Omega$, g is a linear or nonlinear constraint function, b define some boundary conditions, ϵ is a linear operator between Banach spaces, R is a positive convex function (the regularizer function) and λ is a positive parameter which controls the amount of regularization desired.
It is clear that one can define any discrete optimization problem by opportunely discretize a continuous variational problem.
For example, one can consider the following discrete kernel regression regularized problem, which is clearly derived from a continuous one where the integrals have become summations over a discrete samples set:

$$\begin{aligned} \min_f \sum_{i=1}^n \frac{|\, y_i - f(x_i)\,|^2}{2} + \lambda \sum_{i=1}^n \frac{|\, f(x_i)\,|^2}{2} \\ s.t. \quad f(x) = \sum_{i=1}^n c_i k(x, x_i), \\ x_i \in \mathbb{R}^2,\ i = 1, ..., n, \\ \lambda \geq 0. \end{aligned} \tag{2.11.1}$$

In this example the regularization term is nothing that the l_2-norm squared of the regression function f and is modulated by it's Tikhonov parameter λ.
In figure 2.12 we can see the effect of the Tikhonov regularization for problem (2.11.1) where we can clearly see that the regularization avoids the overfitting.
In this section we will focus our attention on a class of non common regularizers derived from the l_1-norm, namely the l_1-norm of the design parameters which is sometimes called the *compressed sensing* regularization and the Total Variation (TV) regularizer.
These choices of regularization functionals have the nice property to improve the sparsity (*compressed sensing*) or to improve the local flatness (TV) of the optimal solutions.

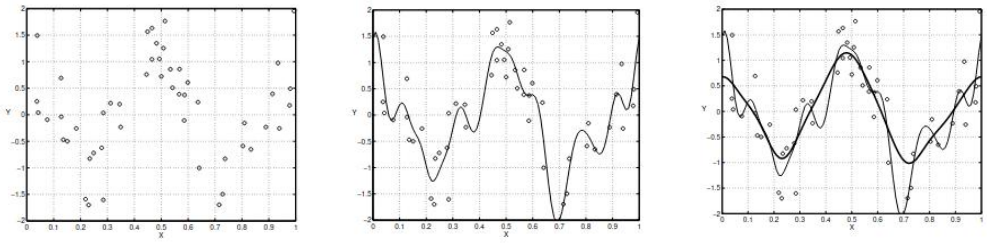

Figure 2.12: Samples (left), Overfitting (center), Regularized (right)

2.11.2 The classical framework in the discrete setting and the Proximal Forward-Backward Splitting scheme

In this subsection we will first see probably the most common situation in the framework of the Tichononv regularization for discrete problems and an overview of a very interesting application of the proximal map operator.
We follow the work in [33] and [13].
Let $V := \mathbb{R}^n$ and consider the following optimization problem:

$$\inf_{\varphi \in V} F(\varphi) + G(\varphi),$$

where $F : V \to \mathbb{R}$ is differentiable and $G : V \to \mathbb{R}$ is "simple" i.e. giving a certain $\Delta t > 0$ it is easy to compute the proximal map operator:

$$prox(G) := (\mathbb{1} + \Delta t \partial G)^{-1}$$

where G is possibly not differentiable and ∂G is the subdifferential of G. It is immediate to see that:

$$(\mathbb{1} + \Delta t \partial G)^{-1}(\varphi) = \arg\min_q \frac{\|q - \varphi\|_{l_2}^2}{2\Delta t} + G(q),$$

which is nothing that the update scheme given by the Implicit Euler time discretization.
A typical example of "simple" map, already encountered in Section 2.4 is the indicator function of the l_∞ unit ball:

$$\chi_{l_\infty}(\varphi) := \begin{cases} 0, & |\varphi_i| \leq 1,\ i = 1, ..., n \\ +\infty, & otherwise. \end{cases}$$

and it is easy to see [33] that the proximal map is given by:

$$(\mathbb{1} + \Delta t \partial \chi_{l_\infty})^{-1}(\varphi) = \Pi_C(\varphi), \quad \varphi \in V, \tag{2.11.2}$$

where $\Pi_C(\varphi)$ is the orthogonal projection on the l_∞ unit ball

$$\mathtt{B}_{l_\infty} := \{\varphi \in V \mid |\varphi_i| \leq 1,\ i = 1, ..., n\}.$$

which is straightforward to compute and is given by:

$$\Pi_C(\varphi)_i = \frac{\varphi_i}{\max\{1, |\varphi_i|\}}, \quad i = 1, \dots, n.$$

In the case where, as in the previous example, G is such that the proximal map $prox(G)$ is easy to invert, it is a common strategy to solves successively one step of the gradient descent of F(in an explicit way), and one step of the gradient descent of G(in an implicit way), in order to obtain a "full" gradient descent of $F + G$. This is the reason why the term "forward-backwards" splitting was introduced in [40]. Given a sequence Δt_k, the approximation sequence $\left(\varphi^k\right)_{k=1,\dots,k_{max}}$ is hence given by the following recurrent scheme:

$$\begin{cases} \varphi_i^0 = \varphi_{i0}, \quad i = 1, ..., n & \textbf{(SPLIT-} \\ \varphi^{k+1} = (\mathbb{1} + \Delta t_k \partial G)^{-1} \left(\varphi^k - \Delta t_k \nabla F(\varphi^k)\right), \quad k = 0, ..., k_{max}. & \textbf{FW-BW)} \end{cases} \tag{2.11.3}$$

It is interesting to understand the intuitive idea behind it. Consider the following quadratic map:

$$\psi \mapsto Q_L(\psi, \varphi) = F(\varphi) + \langle \nabla F(\varphi), \psi - \varphi \rangle + \frac{1}{2L} \|\psi - \varphi\|_{l_2}^2.$$

Since F is differentiable, for any fixed $\varphi \in V$, we have that [33]:

$$F(\psi) \leq Q_L(\psi, \varphi), \quad \forall\, \psi \in V. \tag{2.11.4}$$

Thus the parabola $Q_L(\psi, \varphi)$ approximates from above $F(\psi)$. Now, let $\varphi = \varphi^k$ and replace the minimization of F, at step k, with the minimization of $Q_L(\psi, \varphi^k)$ with respect to q:

$$\varphi^{k+1} := \arg\min_{\psi} Q_L(\psi, \varphi^k),$$

which implies that:

$$\varphi^{k+1} = \varphi^k - L \nabla F(\varphi^k), \tag{2.11.5}$$

that is a step of the gradient descent algorithm with step L. This is a way to interpret the "forward-backward" scheme, and provides a natural way to extend it to the minimization of $F + G$. Indeed, we can now let:

$$H_{\Delta t_k}(\psi, \varphi) = F(\varphi) + \langle \nabla F(\varphi), \psi - \varphi \rangle + \frac{1}{2\Delta t_k} \|\psi - \varphi\|_{l_2}^2 + G(\psi),$$

and. by virtue of (2.11.4):

$$F(\psi) + G(\psi) \leq H_{\Delta t_k}(\psi, \varphi), \quad \forall\, \varphi \in V,\ \Delta t_k > 0.$$

So that letting $\varphi = \varphi^k$ we consider the following updating scheme:

$$\varphi^{k+1} = \arg\min_{\psi} H_{\Delta t_k}(\psi, \varphi^k), \tag{2.11.6}$$

and by (2.11.2) and (2.11.5) we find that (2.11.6) is precisely the "forward-backward" splitting scheme (2.11.3).
In [33] Theorem 3.12 p.45 and in [13] it is shown that the scheme in (2.11.6) converges to a minimizer of $F+G$ with essentially the same convergent rate of the classical gradient descent algorithm. Nevertheless, it has improved stability properties and we will make extensive use of this kind of techniques in our proposed numerical algorithm based on the DMK scheme. Moreover, this scheme is quite easy to implement and has the necessary flexibility to be adapted for the solution of multiple problems. As a consequence, several acceleration techniques have been proposed during the years, where among them we remark the famous Nesterov/Beck and Teboulle's acceleration [13] which reads as the following scheme for the approximation sequence $\left(\varphi^k\right)_{k=1,\dots,k_{max}}$:

$$\begin{cases} \varphi^0 = \varphi_0 \\ y^1 = \varphi^0 \\ h^1 = 1 \\ \varphi^k = (\mathbb{1} + \Delta t \partial G)^{-1}\left(y^k - \Delta t \nabla F(y^k)\right) \\ h^{k+1} = \dfrac{1+\sqrt{1+4(h^k)^2}}{2} \\ y^{k+1} = \varphi^k + \dfrac{h^k - 1}{h^{k+1}}\left(\varphi^k - \varphi^{k-1}\right) \\ k = 1, \dots, k_{max}. \end{cases} \qquad \textbf{(Beck-Teboulle)} \qquad (2.11.7)$$

furthermore, we have the following convergence rate result:

Theorem 2.11.1. *[Beck and Teboulle [13], Theorem. 4.1]*
For any minimizer φ^* of $F+G$ we have that the sequence $\left(\varphi^k\right)_{k=1,\dots,k_{max}}$ generated by (2.11.7) *satisfies:*

$$F(\varphi^k) + G\varphi^k) - \left(F\left(\varphi^*\right) + G\left(\varphi^*\right)\right) \leq \frac{2\left\|\varphi^0 - \varphi^*\right\|^2}{\Delta t (k+1)^2}.$$

2.11.3 The Split-Bregman iteration for the Total Variation Denoising problem

In this subsection we will see another famous algorithm which that can be placed in the framework of the Augmented Lagrangian methods [33], the so called Begman-Split iteration. This kind of algorithms, especially for the problem of the Total Variation denoising, are typically employed in image restoration [104]. Nevertheless, we can consider the general framework based on graphs once observed that we can always associate to every image the graph generated by connecting a pixel with it's nearest ones upon selecting a neighborhood rule(for example by connecting every pixel to the 4 nearest ones).

Thus, let $V = \mathbb{R}^n$, $E = \mathbb{R}^m$ and $\nabla : V \to E$ be a linear operator(for example the graph gradient matrix if V is the nodes set and E the edges set). We then consider the following constrained problem:

$$\min_{\substack{p = \nabla \varphi \\ \varphi \in V}} \lambda \|p\|_{l_1} + \frac{1}{2}\|\varphi - b\|_{l_2}^2. \tag{2.11.8}$$

where b represents a collection of noisy samples and λ is the Tychonov parameter. Then, to enforce the constraint, we use an augmented Lagrangian approach, which consists in introducing

$$L(p, \varphi, \mu) = \lambda \|p\|_{l_1} + \frac{1}{2}\|\varphi - b\|_{l_2}^2 + \langle \mu, p - \nabla \varphi \rangle + \frac{\alpha}{2}\|p - \nabla \varphi\|_{l_2}^2,$$

where $\alpha > 0$ and $\mu \in E$ is a Lagrange multiplier for the constraint $p = \nabla v$. The method consists then in minimizing alternatively L with respect to p, φ, and maximizing with respect to μ :

$$\begin{cases} \varphi^{k+1} = \arg\min_{\varphi} L(p^k, \varphi, \mu^k), \\ p^{k+1} = \arg\min_{p} L(p, \varphi^{k+1}, \mu^k), \\ \mu^{k+1} = \mu^k + \Delta t_k (p^{k+1} - \nabla \varphi^{k+1}). \end{cases} \qquad \textbf{(ALM)}$$

the minimization in the variable p, which involves the l_1 norm decouples and has a closed form as a vectorial shrinkage [104], [142], [64]:

$$p_i^{k+1} = \frac{\alpha(\nabla \varphi)_i - \mu_i}{|\alpha(\nabla \varphi)_i - \mu_i|} \max\left\{ \frac{|\alpha(\nabla \varphi)_i - \mu_i| - \lambda}{\alpha}, 0 \right\}, \quad i = 1, ..., m. \tag{2.11.9}$$

In this case the change of variable $p = \nabla \varphi$ has the clear effect to simplify the problem, removing the difficulties derived by the non differentiability of the l_1 norm. A variant of the previous algorithm is the Bregman-Split iteration which is based on the Bregman Distance. Consider the following optimization problem:

$$\min_{\varphi \in V} F(\varphi)$$
$$s.t. H(\varphi) = 0,$$

where $F : V \to \mathbb{R}$ and $H : V \to \mathbb{R}$ are two convex possibly not differentiable functions and $(V, \|\cdot\|_V)$ is a Banach space. We define the Bregman distance as:

$$D_F^p(\varphi, \psi) := F(\varphi) - F(\psi) - \langle \rho, \varphi - \psi \rangle, \quad \rho \in \partial F(\psi),$$

where $\partial F(\psi)$ is the subgradient:

$$\partial F(\psi) := \{\rho : F(\varphi) \geq F(\psi) + \langle \rho, \varphi - \psi \rangle, \ \forall \varphi \in V\}.$$

The Bregman distance is not a distance in the usual sense because it is not symmetric. However, it does satisfy other distance-like properties following from it's definition and the convexity of F [64]:

- $D_F^p(\varphi, \varphi) = 0$
- $D_F^p(\varphi, \psi) \geq 0$
- $D_F^p(\varphi, \psi) + D_F^{\tilde{p}}(\psi, \tilde{\psi}) - D_F^{\tilde{p}}(\varphi, \tilde{\psi}) = \langle \rho - \tilde{p}, \psi - \varphi \rangle$.

Given a starting point v^0 and a parameter $\gamma > 0$, the Bregman iteration algorithm is given formally by the following iterative scheme:

$$\varphi^{k+1} = \arg\min_{\varphi} D_F^{p^k}(\varphi, \varphi^k) + \gamma H(\varphi), \quad \rho^k \in \partial F(\varphi^k) \tag{2.11.10}$$

In the case where H is differentiable, the sub-differential of H is it's gradient ∇H, and the sub-differential of the Lagrangian

$$L(\varphi) := D_F^{p^k}(\varphi, \varphi^k) + \gamma H(\varphi)$$

is given by

$$\partial_\varphi L(\varphi) = \partial_\varphi \left(F(\varphi) - F(\varphi^k) - \left\langle \rho^k, \varphi - \varphi^k \right\rangle + \gamma H(\varphi) \right) = \\ = \partial F - \rho^k + \gamma \nabla H.$$

Since from (2.11.10) φ^{k+1} minimizes $L(\varphi)$, the optimality condition for φ^{k+1} is given by:

$$\begin{aligned} & 0 \in \partial F(\varphi^{k+1}) - \rho^k + \gamma \nabla H(\varphi^{k+1}) \\ \Leftrightarrow \quad & \rho^k - \gamma \nabla H(\varphi^{k+1}) \in \partial F(\varphi^{k+1}). \end{aligned}$$

Therefore, $\rho^{k+1} \in \partial J(\varphi^{k+1})$ can be selected as

$$\rho^{k+1} = \rho^k - \gamma \nabla H(\varphi^{k+1}), \tag{2.11.11}$$

and the Bregman iteration (2.11.10) with this selecting rule for ρ^{k+1} becomes:

$$\begin{cases} \varphi^{k+1} = \arg\min_{\varphi} D_F^{\rho^k}(\varphi, \varphi^k) + \gamma H(\varphi), & \\ \rho^{k+1} = \rho^k - \gamma \nabla H(\varphi^{k+1}), & \textbf{(Bregman-} \\ \varphi^0 = \varphi_0, & \textbf{iteration)} \\ \rho^0 \in \partial J(\varphi^0), & \\ k = 0, \ldots, k_{max}. & \end{cases}$$

In the particular case where $V = \mathbb{R}^n$ and H is the residual of a linear system involving the matrix $A \in \mathbb{R}^{n \times n}$ and a known term $f \in V$:

$$H(\varphi) = \frac{1}{2} \|A\varphi - f\|_{l_2}^2,$$

then, the Bregman iteration simplifies and is equivalent to the Augmented Lagrangian method [104], [142]:

$$\begin{cases} \varphi^{k+1} = \arg\min_{\varphi} F(\varphi) + \frac{\gamma}{2}\left\|A\varphi - f + \rho^k\right\|_{l_2}^2 \\ \rho^{k+1} = \rho^k + A\varphi^{k+1} - f, \\ \varphi^0 = \varphi_0, \\ \rho^0 = 0, \\ k = 0, \ldots, k_{max}. \end{cases} \tag{2.11.12}$$

A variant of the Bregman iteration is the so called split Bregman iteration. Consider again problem (2.11.8):

$$\min_{\substack{p = \nabla\varphi \\ \varphi \in V}} \lambda\|p\|_{l_1} + \frac{1}{2}\|\varphi - b\|_{l_2}^2.$$

the idea is to apply the Bregman iteration (2.11.12) with the quadratic residual function given by:

$$H(\varphi) = \frac{1}{2}\|\nabla\varphi - p\|_{l_2}^2,$$

and the corresponding Bregman iteration as in (2.11.12) is given by:

$$\begin{cases} (\varphi^{k+1}, p^{k+1}) = \arg\min_{(\varphi,p)} \lambda\|p\|_{l_1} + \frac{1}{2}\|\varphi - b\|_{l_2}^2 + \frac{\gamma}{2}\left\|\nabla\varphi - p + \rho^k\right\|_{l_2}^2 \\ \rho^{k+1} = \rho^k + \nabla\varphi^{k+1} - p^{k+1}, \\ \varphi^0 = \varphi_0, \\ \rho^0 = 0, \\ k = 0, \ldots, k_{max}. \end{cases} \tag{2.11.13}$$

This updating scheme is fully implicit, but, since it involves the non differentiable term given by the l_1-norm of p, we can not apply the Newton method to compute the new iterates (φ^{k+1}, p^{k+1}). To circumnavigate this problem, Osher et.al. [104] proposed to "split" the original implicit scheme (2.11.13) to the following semi-implicit alternating sub-problems scheme:

- (p sub-problem): Given a fixed φ compute p^{k+1} by solving

$$p^{k+1} = \arg\min_{p} \lambda\|p\|_{l_1} + \frac{\gamma}{2}\left\|\nabla\varphi - p + \rho^k\right\|_{l_2}^2,$$

  as in (2.11.9), this problem as the closed solution as a vectorial shrinkage:

$$p_i^{k+1} = \frac{(\nabla\varphi)_i - \rho_i^k}{|(\nabla\varphi)_i - \rho_i^k|} \max\left\{|(\nabla\varphi)_i - \rho_i^k| - \frac{\lambda}{\gamma}, 0\right\}, \quad i = 1, ..., m.$$

- (φ sub-problem): Given a fixed p compute φ^{k+1} by solving:

$$\varphi^{k+1} = \arg\min_{\varphi} \frac{1}{2}\|\varphi - b\|_{l_2}^2 + \frac{\gamma}{2}\left\|\nabla\varphi - p + \rho^k\right\|_{l_2}^2,$$

  the solution is given by solving a Laplacian system:

$$(\mathbb{1} + \gamma\Delta)\,\varphi^{k+1} = b + \nabla^T(p - \rho^k).$$

- (ρ update): Given a fixed φ and p we update the variable ρ as in (2.11.13):

$$\rho^{k+1} = \rho^k + \nabla\varphi - p.$$

Summing up all together, the split Osher-Bregman iteration for the TV denoise reads as the following alternating iteration:

$$\begin{cases} p_i^{k+1} = \dfrac{(\nabla\varphi^k)_i - \rho_i^k}{|(\nabla\varphi^k)_i - \rho_i^k|}\max\left\{|(\nabla\varphi^k)_i - \rho_i^k| - \dfrac{\lambda}{\gamma}, 0\right\}, \\ \qquad\qquad i = 1, \dots, m, \\ (\mathbb{1} + \gamma\Delta)\,\varphi^{k+1} = b + \nabla^T(p^{k+1} - \rho^k), \\ \rho^{k+1} = \rho^k + \nabla\varphi^{k+1} - p^{k+1}, \\ p^0 = 0, \\ \varphi^0 = 0, \\ \rho^0 = 0, \\ k = 0, \dots, k_{max}. \end{cases} \quad \begin{matrix} \\ \\ \textbf{(TV-Osher-} \\ \textbf{Bregman-} \\ \textbf{iteration)} \\ \\ \\ \\ \\ \end{matrix} \tag{2.11.14}$$

For what concern the choice of the parameter γ, which strongly influence the good behaviour of the algorithm, we refer to [64] for an exhaustive treatment. This algorithm is quite fast, easy to implement and exhibits good stability properties. It is worthless to say that it is become the benchmark algorithm for TV denoising in image processing. Moreover, since it is not a gradient based method, it exhibits a lack of memory of the previous iterations, which is actually an advantage when it is used for example in non-convex optimization when multiple local minima are present, since it naturally penalizes "bad" local minima [106]. Unfortunely there are also several limitations. For instance, the update of the parameter ρ given by the selecting rule (2.11.11), requires to be able to solve the p sub-problem and the φ sub-problem, thus, this algorithm applies only on simple cases. Moreover, this also implies that this algorithm can not be applied in general if further inequality constraints on φ are considered, it can handle very well only equality constraints(e.g. linear and non-linear equations constraints involving the variable φ which have at least a direct method to compute a solution). Finally, since the fully implicit scheme (2.11.13) can not be applied, we can never expect to have a quadratic convergence rate given by a second order

method, that's the reason why we will introduce our EDMK scheme for the Total Variation denoising problem.

2.11.4 The EDMK scheme for the Total Variation and l_1 norm regularization in the graph setting

In this subsection we will show how to integrate our EDMK scheme for the Total Variation regularization for a general optimization problem on graphs, without constraints and in particular case of the positivity constraint and the interval constriant on the design variable. Moreover, we briefly show, as a direct extension, that the same techniques can be applied for l_1 norm regularization.
As in Section 2.4, let $\mathcal{G} = (E, V, \omega)$ be a weighted directed graph, ∇ it's gradient matrix and div $= -\nabla^T$ it's divergence matrix. We denote as $\mathcal{H}(V) = \mathbb{R}^n$ and $\mathcal{H}(E) = \mathbb{R}^m$ the Banach spaces of real-valued functions on V, the nodes set, and E, the edges set, respectively.
In Section 2.4 we have seen an equivalent saddle point formulation for the graph Total Variation energy or the 1-Dirichlet energy.
Thus, we recall the Lagrangian $\mathtt{L}^1_\varphi : (\mathcal{H}(E)^+ \times \mathcal{H}(E)) \to \mathbb{R}$ defined in (2.4.16) for $p = 1$ as:

$$\mathtt{L}^1_\varphi(\mu, \sigma) := -\sum_{e\in E} \frac{1}{2}\mu_e|\sigma_e|^2 + \sigma \cdot \nabla \varphi + \frac{1}{2}\sum_{e\in E} \mu_e, \quad \varphi \in \mathcal{H}(V),$$

In Theorem 2.4.1 we have shown that the graph 1-Dirichlet energy or the graph Total Variation energy:

$$TV(\varphi) := \mathtt{E}_1(\varphi) = \| \nabla \varphi\|_{l_1}$$

admits the following equivalent saddle point formulation:

$$TV(\varphi) = \inf_{\mu\in\mathcal{H}(E)^+} \sup_{\sigma\in\mathcal{H}(E)} \mathtt{L}^1_\varphi(\mu, \sigma). \tag{2.11.15}$$

Moreover, there exists a saddle point (μ^*, σ^*) for $\mathtt{L}^1_\varphi$ and it satisfies the extremality relations:

$$\begin{aligned} \mu^*_e\sigma^*_e &= (\nabla \varphi)_e, \quad \forall\, e \in E,\\ |\sigma^*_e| &\le 1, \quad \forall\, e \in E,\\ \mu^*_e|\sigma^*_e|^2 - \mu^*_e &= 0, \quad \forall\, e \in E,\\ \mu^*_e &= |(\nabla \varphi)_e|, \quad \forall\, e \in E. \end{aligned}$$

In Subsection 2.5.1 we have introduced the Tikhononv regularized Lagrangian:

$$\mathtt{L}^{1,\delta}_\varphi(\mu, \sigma) := -\sum_{e\in E} \frac{1}{2}(\mu_e + \delta)|\sigma_e|^2 + \sigma \cdot \nabla \varphi + \frac{1}{2}\sum_{e\in E} \mu_e,$$

which is (2.5.4) for $\Lambda = \nabla$ and $p = 1$ and the parameter $\delta > 0$ is a small Tikhononv parameter.
Consider now the functional:

$$\mathcal{L}^1_\delta(\varphi, \mu) := \sup_{\sigma \in \mathcal{H}(E)} \mathtt{L}^{1,\delta}_\varphi(\mu, \sigma).$$

With the same arguments as in (2.5.7),(2.5.8), $\mathcal{L}^1_\delta(\varphi, \mu)$ simplifies as follows:

$$\mathcal{L}^1_\delta(\varphi, \mu) = \sum_{e \in E} \frac{1}{2} \frac{|(\nabla \varphi)_e|^2}{(\mu_e + \delta)} + \frac{1}{2} \sum_{e \in E} \mu_e,$$

so that, we consider the following approximated minimization problem instead of the saddle point formulation for the Total Variation in (2.11.15):

$$\inf_{\mu \in \mathcal{H}(E)^+} \mathcal{L}^1_\delta(\varphi, \mu). \tag{2.11.16}$$

The KKT conditions for a minimizer (μ^*) of (2.11.16) satisfies:

$$\begin{cases} -\frac{|(\nabla \varphi)_e|^2}{(\mu^*_e + \delta)^2} + 1 - c_e = 0, & \forall\, e \in E \\ c_e \mu^*_e = 0, \quad c_e \geq 0, & \forall\, e \in E. \end{cases}$$

Thus, ${\mu^*}_{\bar{e}} = 0$ on some edge $\bar{e} \in E$ if and only if:

$$|(\nabla \varphi)_{\bar{e}}| \leq \delta, \tag{2.11.17}$$

and if ${\mu^*}_{\bar{e}} > 0$ we have that

$$|(\nabla \varphi)_{\bar{e}}| = \mu^*_{\bar{e}} + \delta. \tag{2.11.18}$$

Hence defining:

$$TV_\delta(\varphi) := \inf_{\mu \in \mathcal{H}(E)^+} \mathcal{L}^1_\delta(\varphi, \mu),$$

from (2.11.17), (2.11.18) we have:

$$TV_\delta(\varphi) = TV(\varphi) + \mathcal{O}(\delta).$$

and the accuracy on the sparsity of the gradient is controlled from above by δ. We are indeed motivated to consider the following approximated Total Variation as an opportune well approximated TV regularizer for some optimization problem, if δ is sufficiently small.
We have now all the ingredients for our EDMK scheme.
Let us consider the general situation of a Total Variation regularization for a general optimization problem on graphs:

$$\min_{\varphi \in \mathcal{H}(V)} F(\varphi) + \lambda TV(\varphi),$$

where $F : \mathcal{H}(V) \to \mathbb{R}$ is a differentiable function and $\lambda > 0$ is the Tikhonov regularization parameter.
We consider instead our regularized version:

$$\begin{aligned}&\min_{\varphi\in\mathcal{H}(V)} F(\varphi) + \lambda TV_\delta(\varphi) = \\ &= \min_{\substack{\varphi \in \mathcal{H}(V)\\ \mu \in \mathcal{H}(E)^+}} F(\varphi) + \lambda \left(\sum_{e\in E} \frac{1}{2} \frac{|(\nabla \varphi)_e|^2}{(\mu_e + \delta)} + \frac{1}{2} \sum_{e\in E} \mu_e \right).\end{aligned} \tag{2.11.19}$$

The main advantage of considering the approximated functional TV_δ instead of using the Total Variation, comes directly from (2.11.19). Indeed, having introduced the positive density variable μ, allows us to perform simultaneously the minimization in the pair (φ, μ). Moreover, the regularization parameters δ ensure the necessary differentiability for a simultaneous minimization with first or second order methods.
We now describe how to apply our techniques in three typical situations.

- **(Unconstrained TV regularization)**:
  This is the most typical situation and corresponds to problem (2.11.19) without adding any further constraint on φ. The proposed method is very similar to the case of 1-Harmonic functions(see Section 2.8). Indeed, we can subdivide in other two sub-cases:

  - **(Direct solvable problems)** This is the case for example of the classical Total Variation denoising (2.11.8) where it is possible to directly compute a solution of:

$$\lambda \Delta_{\frac{1}{\mu+\delta}} \varphi = -\partial_\varphi F(\varphi), \quad \forall\, \mu \in \mathcal{H}(E)^+. \tag{2.11.20}$$

    The corresponding version of the dynamics in (2.8.9) for problem (2.11.19) reads as follows:

$$\begin{aligned}\lambda \Delta_{\frac{1}{\mu(t)+\delta}} \varphi(t) &= -\partial_\varphi F(\varphi(t)) \\ \sigma_e(t) = \frac{(\nabla \varphi(t))_e}{(\mu_e(t) + \delta)}, &\quad \forall\, e \in E, \quad \textbf{(EDMK1)} \\ \partial_t \mu_e(t) = \mu_e(t)|\sigma_e(t)|^2 - \mu_e(t), &\quad \mu_e(0) = \mu_{0e} > 0, \quad \forall\, e \in E.\end{aligned} \tag{2.11.21}$$

    As for the time discretization we propose for simplicity the Explicit

Euler scheme:

$$\begin{cases} \lambda \Delta_{\frac{1}{\mu^k+\delta}} \varphi^k = -\partial_\varphi F(\varphi^k), \\ \sigma_e^k = \dfrac{(\nabla(\varphi^k))_e}{\mu_e^k + \delta}, \quad \forall\, e \in E \\ \mu_e^{k+1} = \mu_e^k + \Delta t_k \mu_e^k \left(|\sigma_e^k|^2 - 1 \right), \quad k = 0, \dots, k_{\max},\ e \in E \\ \mu_e^0 = \mu_{0e} > 0, \quad \forall\, e \in E. \end{cases} \tag{2.11.22}$$

We refer to Section (2.8) for other method of time discretization.

– **(Double "Gradient Flow" approach)** This is the case for example of complex inverse problems where the computation of the differential $\partial_\varphi F$ requires the solution of adjoints equations(Lagrange multipliers), thus, it is not possible to direct compute a solution of (2.11.20) but indeed we don't have any direct constraint on φ. Since (2.11.19) is a double convex minimization problem, we propose a double descending dynamics. The corresponding EDMK scheme reads now as the following double dynamics:

$$\partial_t \varphi(t) = -\partial_\varphi F(\varphi(t)) - \lambda \Delta_{\frac{1}{\mu(t)+\delta}} \varphi(t), \quad \varphi(0) = \varphi_0,$$

$$\sigma_e(t) = \frac{(\nabla\, \varphi(t))_e}{(\mu_e(t) + \delta)}, \quad \forall\, e \in E, \quad \textbf{(EDMK2)}$$

$$\partial_t \mu_e(t) = \mu_e(t) |\sigma_e(t)|^2 - \mu_e(t), \quad \mu_e(0) = \mu_{0e} > 0, \quad \forall\, e \in E.$$

As for the time discretization, taking inspiration from (2.11.3), we propose the following semi-implicit Proximal Forward-Backward Splitting scheme, which exhibits far superior stability properties with respect to the Explicit Euler scheme for this specific "Double Gradient Flow" approach(see [13],[40] for an exhaustive treatment):

$$\begin{cases} \tilde{\varphi}^k = \varphi^k - \Delta t_k \partial_\varphi F(\varphi^k), \\ \left(\mathbb{1} + \lambda \Delta t_k \Delta_{\frac{1}{\mu^k+\delta}} \right) \varphi^{k+1} = \tilde{\varphi}^k, \quad k = 0, \dots, k_{\max} \\ \varphi^0 = \varphi_0, \\ \sigma_e^k = \dfrac{(\nabla(\varphi^k))_e}{\mu_e^k + \delta}, \quad \forall\, e \in E \\ \mu_e^{k+1} = \mu_e^k + \Delta t_k \mu_e^k \left(|\sigma_e^k|^2 - 1 \right), \quad k = 0, \dots, k_{\max},\ e \in E \\ \mu_e^0 = \mu_{0e} > 0, \quad \forall\, e \in E. \end{cases}$$

- **(Constrained TV regularization)**:
  This application is not commonly found in literature, but in many practical situations, for example when the Total Variation is used as a regularization term in parameter identification inverse problems [26], there is the necessity to satisfy some further constraints for the physical feasibility of the variables involves in the optimization. Here we present two common situations often found in practice: the positivity constraint and the interval constraint on the design variable φ in (2.11.19).

  - **(The Positivity constraint)** This problem corresponds to (2.11.19) where we add the positivity constraint on φ, namely we consider the following problem:

$$\min_{\substack{\varphi \in \mathcal{H}(V) \\ \varphi \geq 0 \\ \mu \in \mathcal{H}(E)^+}} F(\varphi) + \lambda \left(\sum_{e \in E} \frac{1}{2} \frac{|(\nabla \varphi)_e|^2}{(\mu_e + \delta)} + \frac{1}{2} \sum_{e \in E} \mu_e \right).$$

    The approach to the EDMK scheme for this problem is the same as in the double "Gradient Flow" approach, with the only difference that, as in (2.8.9), we compose with the change of variable ($\mu(t) = |\xi(t)|^2, \varphi(t) = |\varepsilon(t)|^2$) to enforce the positivity, and then we perform a pull-back of the descending dynamics on the original variables $(\mu(t), \varphi(t))$(as in Subsection 2.8.2). The EDMK dynamics is the following:

$$\begin{gathered}
\partial_t \varphi(t)_v = -\varphi(t)_v \left(\partial_\varphi F(\varphi(t)) + \lambda \Delta_{\frac{1}{\mu(t)+\delta}} \varphi(t) \right)_v, \quad \forall\, v \in V \\
\varphi(0)_v = \varphi_{0_v} > 0, \quad \forall\, v \in V \\
\sigma_e(t) = \frac{(\nabla \varphi(t))_e}{(\mu_e(t) + \delta)}, \quad \forall\, e \in E, \quad \textbf{(EDMK3)} \\
\partial_t \mu_e(t) = \mu_e(t) |\sigma_e(t)|^2 - \mu_e(t), \quad \mu_e(0) = \mu_{0_e} > 0, \quad \forall\, e \in E.
\end{gathered}$$

    As in this case we propose the following semi-implicit Proximal Forward-

Backward Splitting scheme:

$$\begin{cases} \tilde{\varphi}^k = \varphi^k - \Delta t_k[\mathrm{Diag}(\varphi^k)]\partial_\varphi F(\varphi^k), \\ \left(\mathbb{1} + \lambda\Delta t_k[\mathrm{Diag}(\varphi^k)]\Delta_{\frac{1}{\mu^k+\delta}}\right)\varphi^{k+1} = \tilde{\varphi}^k, \quad k = 0,\dots,k_{\max} \\ \varphi_v^0 = \varphi_{0v} > 0, \quad \forall\, v \in V \\ \sigma_e^k = \dfrac{(\nabla(\varphi^k))_e}{\mu_e^k + \delta}, \quad \forall\, e \in E \\ \mu_e^{k+1} = \mu_e^k + \Delta t_k \mu_e^k \left(|\sigma_e^k|^2 - 1\right), \quad k = 0,\dots,k_{\max},\ e \in E \\ \mu_e^0 = \mu_{0e} > 0, \quad \forall\, e \in E. \end{cases}$$

– **(The Interval constraint)** This problem corresponds to (2.11.19) where we add an interval constraint on φ of the type:

$$a_v \le \varphi_v \le b_v, \quad \forall\, v \in V,$$

thus, we consider the following problem:

$$\min_{\substack{\varphi\,\in\,\mathcal{H}(V) \\ a_v \le \varphi_v \le b_v,\ \forall\, v \in V \\ \mu\,\in\,\mathcal{H}(E)^+}} F(\varphi) + \lambda\left(\sum_{e\in E}\frac{1}{2}\frac{|(\nabla\varphi)_e|^2}{(\mu_e+\delta)} + \frac{1}{2}\sum_{e\in E}\mu_e\right).$$

This kind of interval constraint can be treated in a similar way to the positivity constraint, projecting the descending dynamics along the flow generated by a sigmoidal vector field or equivalently by composing with the change of variable:

$$\varphi_v(t) = a_v + (b_v - a_v)\cos^2\left(\frac{\varepsilon_v(t)}{\sqrt{b_v - a_v}}\right), \quad v \in V,$$

and then performing a pull-back of the descending dynamics on the original variable φ. We refer to Subsection 2.8.2 for full details on the heuristics behind this techniques.
The positivity constraint for the density μ is treated as for (2.8.9) by composing with the quadratic map $\mu(t) = |\xi(t)|^2$.
Thus, defining the vectors $\mathtt{a} \in \mathcal{H}(V)$ and $\mathtt{b} \in \mathcal{H}(V)$ as:

$$\mathtt{a}_v = a_v,\ \forall\, v \in V,$$

and

$$\mathtt{b}_v = b_v,\ \forall\, v \in V,$$

we have the following descending EDMK dynamics:

$$\begin{aligned}
&\partial_t\varphi(t)_v = \\
&= -(\mathtt{b}_v-\varphi(t)_v)(\varphi(t)_v-\mathtt{a}_v)\left(\partial_\varphi F(\varphi(t)) + \lambda\Delta_{\frac{1}{\mu(t)+\delta}}\varphi(t)\right)_v, \quad \forall\, v \in V
\end{aligned}$$

$$\varphi(0)_v = \varphi_{0v},\ \mathtt{b}_v > \varphi_{0v} > \mathtt{a}_v, \quad \forall\, v \in V$$

$$\sigma_e(t) = \frac{(\nabla\,\varphi(t))_e}{(\mu_e(t)+\delta)}, \quad \forall\, e \in E, \quad \textbf{(EDMK4)}$$

$$\partial_t\mu_e(t) = \mu_e(t)|\sigma_e(t)|^2 - \mu_e(t), \quad \mu_e(0) = \mu_{0e} > 0, \quad \forall\, e \in E.$$

As in this case we propose the following semi-implicit Proximal Forward-Backward Splitting scheme:

$$\begin{cases}
\tilde{\varphi}^k = \varphi^k - \Delta t_k[\mathrm{Diag}((\mathtt{b}-\varphi^k)\odot(\varphi^k-\mathtt{a}))]\partial_\varphi F(\varphi^k), \\
\left(\mathbb{1} + \lambda\Delta t_k[\mathrm{Diag}((\mathtt{b}-\varphi^k)\odot(\varphi^k-\mathtt{a}))]\Delta_{\frac{1}{\mu^k+\delta}}\right)\varphi^{k+1} = \tilde{\varphi}^k, \\
\varphi^0_v = \varphi_{0v} > 0,\ \mathtt{b}_v > \varphi_{0v} > \mathtt{a}_v, \quad \forall\, v \in V \\
\sigma^k_e = \dfrac{(\nabla(\varphi^k))_e}{\mu^k_e+\delta}, \quad \forall\, e \in E \\
\mu^{k+1}_e = \mu^k_e + \Delta t_k\mu^k_e\left(|\sigma^k_e|^2 - 1\right), \quad e \in E \\
\mu^0_e = \mu_{0e} > 0, \quad \forall\, e \in E \\
k = 0, \dots, k_{\max}.
\end{cases}$$

Observe that in some sense the scheme in (2.11.21) is similar to the Osher-Bregman split iteration (2.11.14), since also in that case we have to solve for a linear laplacian system and update an iteration for some other variables.
The key point here in using the EDMK approach is not only the flexibility of our scheme, that can be used to solve more general TV regularization scenarios, but also, as observed for the EDMK scheme for 1-Harmonic functions, we can benefit from the dynamics of μ which admits a candidate Lyapunov functional. Thus here we can easily integrate an implicit time discretization scheme like the Implicit Euler scheme defined in Subsection (2.8). Moreover we have also the further advantage of the possibility to localize the effect of the Total Variation denoise. For example, one of the problem of the TV denoise is commonly known in literature as the "staircase" phenomena. In the contest of the TV denoise of images, this phenomena is much more evident when we have a region of the image that is already "clean", but indeed, the classical split Bregman iteration has no

possibility to concentrate the regularization in small prescribed area, unless to consider only a portion of the image and thus loosing all the information on the remaining parts. Consider a probability density $k \in \mathcal{H}(E)$:

$$0 \leq k_e \leq 1, \quad \forall\, e \in E,$$

and the following modified version of (2.11.19):

$$\min_{\substack{\varphi \in \mathcal{H}(V) \\ \mu \in \mathcal{H}(E)^+}} F(\varphi) + \lambda \left(\sum_{e \in E} \frac{1}{2} \frac{|(\nabla \varphi)_e|^2}{(\mu_e + \delta)} + \frac{1}{2} \sum_{e \in E} k_e \mu_e \right).$$

The probability density here can be concentrated in the region where we want more regularization, and set near zero in the regions where we don't need any regularization. This kind of Bayesian approach, known as the Space Variance approach has been recently introduced in [115], with far more sophisticated arguments.

Finally observe that by (2.5.12) we can easily extend all this results to the l_1 norm regularization.

Thus as in (2.5.12) we introduce the regularized l_1 norm:

$$\mathtt{l}_{1,\delta}(\varphi) := \inf_{\nu \in \mathcal{H}(V)^+} \sum_{v \in V} \frac{1}{2} \frac{|\varphi_v|^2}{(\nu_v + \delta)} + \frac{1}{2} \sum_{v \in V} \nu_v,$$

and instead of the following problem:

$$\min_{\varphi \in \mathcal{H}(V)} F(v) + \lambda \|\varphi\|_{l_1},$$

we consider the following approximated problem:

$$\begin{aligned} &\min_{\varphi \in \mathcal{H}(V)} F(v) + \lambda \mathtt{l}_{1,\delta}(\varphi) = \\ &= \min_{\substack{\varphi \in \mathcal{H}(V) \\ \nu \in \mathcal{H}(V)^+}} F(\varphi) + \lambda \left(\sum_{v \in V} \frac{1}{2} \frac{|\varphi_v|^2}{(\nu_v + \delta)} + \frac{1}{2} \sum_{v \in V} \nu_v \right). \end{aligned} \tag{2.11.23}$$

Also in this case we can introduce an EDMK scheme exactly as done for the TV regularization.

Observe that in this case the corresponding equation to (2.11.20) is far more easy to solve, it involves a diagonal matrix:

$$\lambda \operatorname{Diag}\left(\frac{1}{\nu + \delta} \right) \varphi = -\partial_\varphi F(\varphi), \quad \forall\, \nu \in \mathcal{H}(V)^+.$$

Thus the resulting EDMK scheme is far more easy to implement. We will see an application of this approach in Subsection 2.11.6.

2.11.5 The Discrete 1-D signal TV Denoising

In this subsection we will see an application of our EDMK scheme (2.11.21) for the numerical solution of a classical denoising problem often denoted as the ROF (Rudin-Osher-Fatemi) problem.
Given a noisy sampled digital signal $b = [b_1, ..., b_n] \in \mathbb{R}^n$ and a parameter $\lambda > 0$, consider the following discrete optimization problem:

$$\min_{\varphi=[\varphi_1,..,\varphi_n]\in\mathbb{R}^n} \frac{1}{2}\sum_{k=1}^{n} |\varphi_k - b_k|^2 + \lambda \sum_{i=1}^{n-1} |\varphi_{i+1} - \varphi_i|.$$

We can genuinely assign a differential structure to the collection of the n samples b by introducing an appropriate graph based counterpart.
Consider the $1D$-graph of n time samples $G = (V, E)$, $V = \{t_1, .., t_n\}$, $E = \{(t_i, t_{i+1}) \mid i = 1, .., n-1\}$, then the $1D$-ROF problem (2.11.5) rewrites as:

$$\min_{\varphi\in\mathcal{H}(V)} \frac{1}{2}\sum_{v\in V} |\varphi_v - b_v|^2 + \lambda \sum_{e\in E} |\,(\nabla\varphi)_e\,|.$$

As seen in Subsection 2.11.4, we will consider the following approximated optimization problem:

$$\min_{\varphi\in\mathcal{H}(V)} \min_{\mu\in\mathcal{H}(E)^+} \frac{1}{2}\sum_{v\in V} |\varphi_v - b_v|^2 + \frac{\lambda}{2}\sum_{e\in E} \frac{|\,(\nabla\varphi)_e\,|^2}{\mu_e + \delta} + \frac{\lambda}{2}\sum_{e\in E}\mu_e.$$

Observe that we are exactly in the case of the "direct solvable problems" of Subsection 2.11.4 and the corresponding equation to (2.11.20) is the following:

$$\left(\mathbb{1} + \lambda\Delta_{\frac{1}{\mu+\delta}}\right)\varphi = b, \quad \forall\,\mu \in \mathcal{H}(E)^+.$$

thus, the resulting EDMK scheme as in (2.11.21) reads as follows:

$$\left(\mathbb{1} + \lambda\,\Delta_{\frac{1}{\mu(t)+\delta}}\right)\varphi(t) = b, \quad \forall\, v \in V,$$

$$\partial_t\mu_e(t) = \mu_e(t)\frac{|(\nabla\,\varphi(t))_e|^2}{(\mu_e(t)+\delta)^2} - \mu_e(t), \quad \forall\, e \in E,$$

$$\mu_e(0) = \mu_{0e} > 0, \quad \forall\, e \in E.$$

We conclude this section with an application of our proposed EDMK scheme (2.11.5) with the Explicit Euler time discretization (2.11.22), for the TV denoise of a 128 samples very noisy digital signal (the noise is the 30 % of the original clean signal). For the numerical simulation, we set a small parameter $\delta = 1e-8$, a very large fixed time step $\Delta t = 0.8$, and a Tikhonov parameter $\lambda = 8.5$. Then, we let evolve the dynamics until:

$$err_{\mu^k}(\mu^{k+1}) = \frac{\|\mu^{k+1} - \mu^k\|_{l_2}}{\Delta t_k \|\mu^k\|_{l_2}} \leq 1e-7$$

In figure 2.13, we can see the comparison between the original clean signal (green), the noisy added signal (grey) and the denoised signal (red) computed with our EDMK solver (2.11.5).
In figure 2.14 we can see the convergence behaviour of err_{μ^k} versus the relative error of φ:

$$err_{\varphi^k}(\varphi^{k+1}) := \frac{\|\varphi^{k+1} - \varphi^k\|_{l_2}}{\Delta t_k \|\varphi^k\|_{l_2}}.$$

Even if the convergence is quite slow, we point out that qualitatively, there is no difference as soon as the error err_{μ^k} becomes less than $1e-4$. Nevertheless, the convergence is stable even if the time step is large and also the Tikhononv parameter λ.

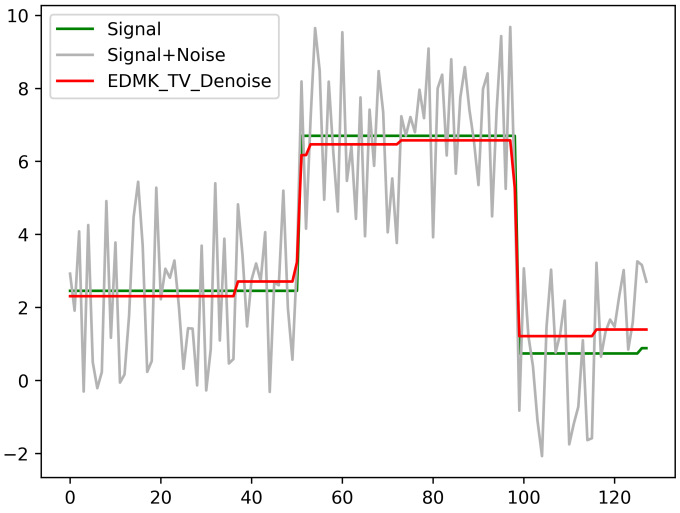

Figure 2.13: original clean signal (green), noisy added signal (grey), denoised signal (red)

2.11.6 Compressed Modes for the Graph Laplacian

Nowadays, in the era of big data, clustering and reducing order models techniques play a very important role in data analysis.
Spectral clustering and PCA are widely used techniques in data analysis and data mining, taking advantages from very efficient numerical algorithms directly inherited from the huge weaponry of numerical linear algebra.
Despite that, when one has to deal with big data, such techniques suffer from the lack of sparsity of their final outputs.
To overcome this problem, the compressed modes CM technique (often referred in literature as Sparse PCA [72]) was early introduced by Osher et al. in [106] for

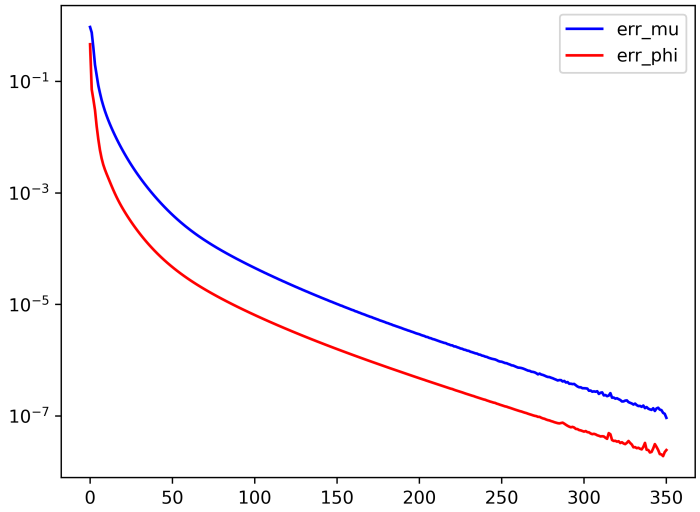

Figure 2.14: err_mu (blue) vs err_phi(red)

the laplacian matrix as an l_1 matrix norm Tikhonov-like regularization problem, in order to compute a sparse orthonormal approximated basis for the partial laplacian eigenvalue problem.
In this last subsection we will see an application of our EDMK technique for the l_1-norm in order to provide an alternative new algorithm to the standard Bregman-Osher split iteration technique to solve the CM for the graph laplacian problem.
Let $\mathcal{G} = (E, V)$ be an undirected graph, where E is the set of $m = |E|$ edges, V the set of $n = |V|$ nodes.
Set a number k of compressed modes and denote as $U \in \mathbb{R}^{n\times k}$, $U_{:,j} = u_j$, $j = 1, .., k$ the orthonormal basis of the k approximated compressed eigenvectors, then the CM for the graph laplacian problem is the following Tikhonov-like regularized optimization problem:

$$\min_{\substack{U \in \mathbb{R}^{n\times k} \\ U^T U = \mathbb{1}}} \frac{1}{2} U : \Delta U + \lambda ||U||_{1,1}, \tag{2.11.24}$$

where $A : B = \mathrm{tr}(A^T B)$ is the matrix scalar product, $||U||_{1,1} := \sum_{i,j} |U_{ij}|$ is the $l_{1,1}$ matrix norm and $\Delta = \nabla^T \nabla$ is the graph laplacian matrix defined in (2.4.1) with the weight c equal to 1 for simplicity, without loosing generality.
Since the $l_{1,1}$ norm of a matrix is the sum of the l_1-norm of it's columns, we can tackle problem (2.11.24) with our approximated regularized functional $\mathtt{1}_{1,\delta}$ defined in (2.5.12). Thus, as already observed in (2.11.23), we will consider the

following new optimization problem:

$$\min_{\substack{U \in \mathbb{R}^{n\times k} \\ U^T U = \mathbb{1}}} \min_{\substack{\nu \in \mathbb{R}^{n\times k} \\ \nu \geq 0}} \quad \frac{1}{2} U : \Delta U + \frac{\lambda}{2} U : (\nu_\delta)^{-*} \odot U + \frac{\lambda}{2} \nu : \mathbb{e}^{n\times k}, \tag{2.11.25}$$

where $\nu \in \mathbb{R}^{n\times k}$, $\nu_{ij} \geq 0$, $\mathbb{e}^{n\times k} \in \mathbb{R}^{n\times k}$, $\mathbb{e}_{ij}^{n\times k} = 1$, $\nu_\delta := \nu + \delta \mathbb{e}^{n\times k}$ and $(A \odot B)_{ij} := A_{ij} B_{ij}$, $A_{ij}^{-*} = \frac{1}{A_{ij}}$.

Optimization on the Stiefel Manifold: A Feasible Update Preserving Scheme

Problem (2.11.25) is an optimization problem on the Stiefel manifold of order k defined as:

$$S^{n\times k} := \{U \in \mathbb{R}^{n\times k} \,|\, U^T U = \mathbb{1}\}, n \geq k.$$

There is a wide literature about optimization on the Stiefel manifold, we will apply here a very beautiful technique presented in [143].
Let $f : S^{n\times k} \to \mathbb{R}$ a differentiable function and consider the following optimization problem:

$$\min_{U \in S^{n\times k}} f(U).$$

The Stiefel manifold inherits the Frobenius norm induced by the matrix scalar product, thus, it is natural to speak about the projection into it's tangent space. The most classical algorithm for optimization on the Stiefel manifold relies on the projected gradient descent, namely we look at the following ODE:

$$\partial_t U = -Prj_{T_U S^{n\times k}} \left(\nabla_U f(U) \right), \tag{2.11.26}$$

where $Prj_{T_U S^{n\times k}}$ denotes the projection into the tangent space of the Stiefel manifold at the point U and $\nabla_U f(U)$ is the gradient of the function f given by the Riesz representation theorem with respect to the matrix scalar product:.

$$Df(U) \cdot \Psi = \nabla_U f(U) : \Psi, \quad \forall \Psi \in T_U S^{n\times k}.$$

The ODE in (2.11.26), once opportunely discretized, define a local descent direction iteration scheme for the objective function f, but inevitably at every iterations of the algorithm, the candidate minimizer for f ends outside the manifold.
As a consequence, considering for example the Esplicit Euler discretization for (2.11.26), the proper projected gradient descent iteration reads as follows:

$$U_{s+1} = Prj_{S^{n\times k}} \left(U_s - dt\, Prj_{T_{U_s} S^{n\times k}} \left(\nabla_U f(U_s) \right) \right), \tag{2.11.27}$$

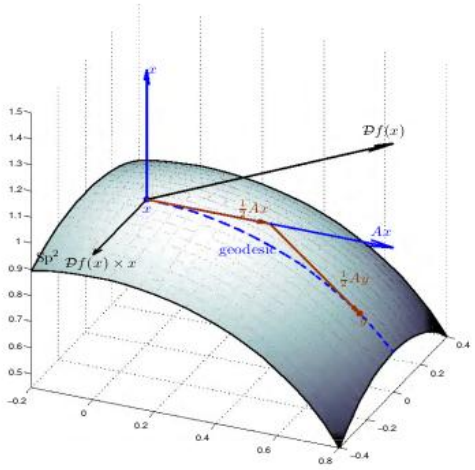

Figure 2.15: Projected Gradient(blue arrow) vs Update Preserving(red path)

where $Prj_{S^{n\times k}}$ is the minimum Frobenius norm projection into the the Steifel manifold of order k that can be easily computed via SVD as $\forall\, A \in \mathbb{R}^{n\times k}$:

$$Prj_{S^{n\times k}}(A) = \Phi\Psi^T,$$

where $A = \Phi\Lambda\Psi^T$ is the SVD factorization.
The scheme defined in (2.11.27) is one of the most classical example of an update non-preserving scheme. On the other hand, one might be interested in an update preserving scheme, e.g. an optimization scheme that remains inside the manifold at every iteration provided an initial point that lies inside the manifold.
Update preserving schemes are a case of direct interest for optimization on the Stiefeld manifold and are performed mainly via Cayley transform.
Differently from the standard projected gradient descent scheme (2.11.27), update preserving schemes moves "zig-zagging" along a geodesic. In Figure 2.15 we can see the difference between the projected gradient descent (blue arrow) and the update preserving scheme (red path) in a standard situation.
Following the work in [143], the starting point for an update preserving scheme on the Stiefel manifold is the projected gradient descent.
Using Lagrange multipliers or classical differential geometry arguments (see [143] and [130] for an exhaustive treatment) it is easy to see that:

$$Prj_{T_U S^{n\times k}}\left(\nabla_U f(U)\right) = H(U)\, U, \quad \forall\, U \in S^{n\times k},$$

where:

$$H(U) = \nabla_U f(U)\, U^T - U\ \nabla_U f(U)^T,$$

and clearly $H(U) = -H(U)^T$.
As a consequence, the ODE in (2.11.26) rewrites as:

$$\partial_t U = -H(U)U. \tag{2.11.28}$$

Observe now that if we use the Crank-Nicolson like scheme (or the mid point rule) to discretize (2.11.28) we have:

$$U_{s+1} = U_s - dt\, H\left(\frac{U_{s+1}+U_s}{2}\right)\left(\frac{U_{s+1}+U_s}{2}\right). \tag{2.11.29}$$

Rearranging (2.11.29) we obtain the following updating scheme:

$$U_{s+1} = \left(\mathbb{1} + \frac{dt}{2} H\left(\frac{U_{s+1}+U_s}{2}\right)\right)^{-1}\left(\mathbb{1} - \frac{dt}{2} H\left(\frac{U_{s+1}+U_s}{2}\right)\right) U_s. \tag{2.11.30}$$

Now, since

$$H\left(\frac{U_{s+1}+U_s}{2}\right) = -H\left(\frac{U_{s+1}+U_s}{2}\right)^T,$$

by the Cayley Transform Theorem we have that if

$$U_s^T U_s = \mathbb{1},$$

then

$$U_{s+1}^T U_{s+1} = \mathbb{1},$$

so that we remain inside the Stiefel manifold at every iteration.
The scheme in (2.11.30) can be further simplified as:

$$U_{s+1} = \left(\mathbb{1} + \frac{dt}{2} H\left(U_s\right)\right)^{-1}\left(\mathbb{1} - \frac{dt}{2} H\left(U_s\right)\right) U_s \tag{2.11.31}$$

and also in this case we have an update preserving scheme.
In [143] it is shown that the scheme defined in (2.11.31) is a descent direction scheme providing an opportune line search and time stepping policy. We will use this technique in our proposed numerical solution.

Numerical Solution

Consider our regularized optimization problem (2.11.25) and call:

$$f(U,\nu) = \frac{1}{2} U : \Delta U + \frac{\lambda}{2} U : (\nu_\delta)^{-*} \odot U + \frac{\lambda}{2}\nu : \mathbb{e}^{n\times k}, \tag{2.11.32}$$

with the same notations as in (2.11.25). In order to use the minimization scheme defined in (2.11.31) we need to compute the gradient of (2.11.32) with respect to U in the frobenius norm and the projection of the gradient into the Stiefel tangent space. It easy to see that:

$$\nabla_U f(U,\nu) = \Delta U + \lambda(\nu_\delta)^{-*} \odot U,$$

$$H(U) = \nabla_U f(U,\nu) U^T - U\, \nabla_U f(U,\nu)^T,$$

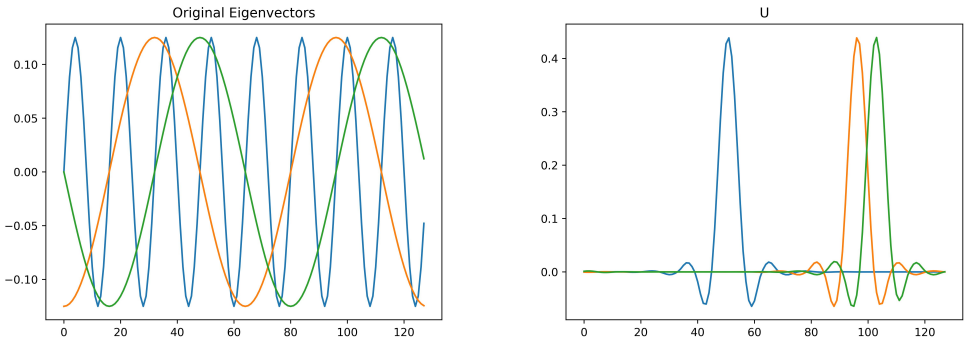

Figure 2.16: Original Eigenvectors (left), Compressed Eigenvectors (right)

Therefore, our discretized EDMK scheme for problem (2.11.25) becomes:

$$\begin{cases} \left(\mathbb{1} + \dfrac{dt}{2} H\left(U_s\right)\right) U_{s+1} = \left(\mathbb{1} - \dfrac{dt}{2} H\left(U_s\right)\right) U_s \\ \nu_{s+1} = \nu_s + \Delta t_s \, \nu_s \odot \left((\nu_\delta)_s^{-*} \odot U_s \odot U_s - \nu_s\right) \\ U_0^T U_0 = \mathbb{1} \\ \nu_0 > 0. \end{cases}$$

For our numerical example, we consider the cyclic $1D$-graph with n=128 nodes $G = (V, E)$, $V = \{v_1, .., v_n\}$ and

$$E = \begin{Bmatrix} (v_i, v_{i+1}) & i = 1, .., n-1 \\ (v_n, v_1) & i = n \end{Bmatrix}.$$

In Figure 2.16 we can see the comparison between some of the original cyclic $1D$-graph Laplacian matrix eigenvectors (the classical periodic sinusoidal functions) and some of the compressed modes computed with our EDMK scheme for $k = 20$, $\lambda = 0.01$.
As for the time discretization, we set a fixed time step $\Delta t = 1e-3$ and we let evolve the dynamics until:

$$err_{\nu^s}(\nu^{s+1}) = \max_{j=1,\dots,k} \left\{ \frac{\|\nu_{:,j}^{s+1} - \nu_{:,j}^s\|_{l_2}}{\Delta t_s \|\nu_{:,j}^s\|_{l_2}} \right\} \leq 1e-3$$

In Figure 2.17 we can see the comparison between the original k smallest laplacian eigenvalues and the k compressed eigenvalues i.e. the k smallest eigenvalues of the matrix $U^T \Delta U$ for $k = 20$.

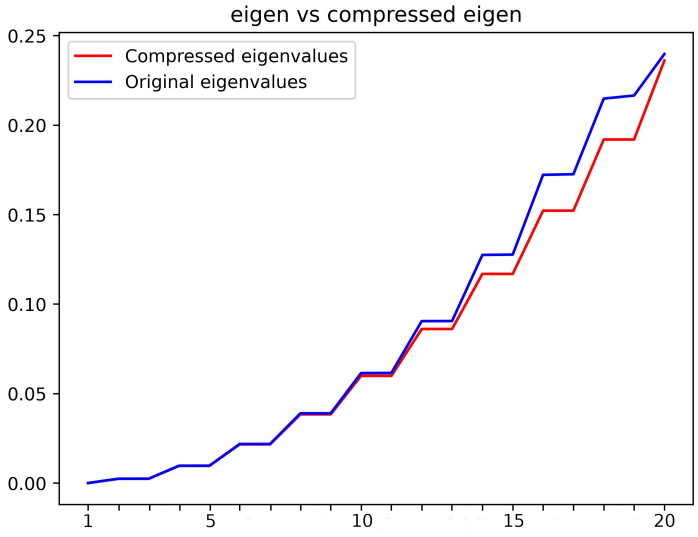

Figure 2.17: Original eigenvalues vs Compressed eigenvalues

3 Computing the graph p-Laplacian eigenpairs as constrained linear eigenpair via gradient flow of DMK dynamics

3.1 Introduction

The p-Laplace operator arises as a natural generalization of the Laplace-Beltrami operator in variational problems involving the p-norm of the gradient of an objective function $\|\nabla f\|_p$. Its numerous applications make it one of the most studied nonlinear operators both in the continuous and in the discrete settings In this chapter we focus our the study on the spectrum of the p-Laplace operator defined on graphs. The eigenpairs of a p-Laplacian are typically defined as the critical points/values of the family of Rayleigh quotients given by

$$\mathcal{R}_p(f) = \frac{\|\nabla f\|_p^p}{\|f\|^p},$$

where different norms at the denominator can be considered. The interest for nonlinear eigenpairs are varied, including data filtering, clustering, and partitioning, with other interesting applications in the field of optimal transportation problems [22, 27]. Within the field of variational filtering methods, in [25, 27] the authors show that the application of a nonlinear filter to a signal corresponds to computing a denoised signal that is a spectral approximation of the original one. Moreover, when using a regularizer of the form $F(x) = \|Ax\|_1$, possibly with additional structural properties of the linear operator A, the spectral decomposition corresponds to a linear decomposition of the signal in terms of the nonlinear eigenfunctions of the functional $F(x)$.
Another remarkable application of the p-Laplacian spectrum can be found in data clustering and partitioning. Indeed, different authors have addressed this problem in both the discrete [20, 35, 36, 72, 74, 134] and the continuous settings [84, 109]. It has been proved that the variational eigenvalues of the 1-Laplacian, and more generally the limit of the variational eigenvalues of the p-Laplacian as p goes to 1, provide good approximations of the Cheeger constants of the domain.

In particular for $p < 2$ such approximations improve the known relationships between the Cheeger constants and the Laplacian eigenvalues already observed by Cheeger himself [37]. We recall that Cheeger constants are used to quantify the number of clusters in the domain. More precisely, they evaluate how well a subset of the data can be splitted in a certain number of clusters. The smaller the k-th Cheeger constant is, the better the data can be clustered in k disjoint subsets. Considering the 1-Laplacian variational eigenvalues, it is possible to prove that the 1-st and the 2-nd variational eigenvalues match exactly the 1-st and the 2-nd Cheeger constants [35, 72, 74, 84, 109]. Moreover, the k-th variational eigenvalue can be bounded, both from above and from below, in terms of the higher order Cheeger constants with index "close" to k [36, 44, 134].

Analogous results relate the variational eigenvalues of the ∞-Laplacian with the packing radii of the domain [22, 24, 48, 78, 79]. The k-th packing radius of the domain is the largest radius that allows the inscription of k-disjoint balls in the domain. As in the $p = 1$ case, it is possible to show that the 1-st and the 2-nd variational eigenvalues of the ∞-Laplacian match the reciprocal of the first and the second packing radii of the domain. Moreover, the k-th packing radius can be approximated by the reciprocal of the k-th variational ∞-Laplace eigenvalue.

Despite the large number of applications, the study of the p-Laplacian eigenpairs still presents several open problems. Indeed, a number of properties of the linear ($p = 2$) Laplacian eigenfunctions are lost in the nonlinear ($p \neq 2$) case, yielding several critical issues and open problems. The first and probably most notable difficulty is consequential to the fact that the cardinality of the p-Laplacian spectrum is not known and can exceed the dimension of the space [6, 44, 145]. This clearly yields the loss of the notion of multiplicity of an eigenvalue and of independence of the eigenfunctions.

The introduction of the variational eigenpairs allows to partially overcome these difficulties. Variational eigenpairs are defined by a min max theorem that generalizes the classical Rayleigh-Ritz characterization of the eigenvalues of a symmetric matrix. As a consequence, the cardinality of the variational eigenvalues is always equal to the dimension of the space. Hence, the variational eigenvalues provide a partition of the p-Laplacian spectrum in non-empty subintervals. The position of a general eigenvalue in one of these intervals has some nontrivial implications as it affects the characteristic "frequency" of the corresponding eigenfunction [44, 134] . In addition, it is possible to define a notion of multiplicity for the variational eigenvalues which is consistent with the notion of multiplicity in the linear case $p = 2$ [36, 44, 128].

Clearly, the numerical approximation of the p-Laplacian eigenpairs presents the same difficulties in addition to the natural issues arising in all discretization processes. Among these, we have identified two fundamental issues that need to be addressed for the development of a robust and accurate numerical scheme and that are not or only partially tackled in the literature : i) develop consistent numerical algorithms, i.e., algorithms for which convergence toward solutions of

the eigenequation can be proved; ii) classification of the approximated eigenpairs in terms of the variational spectrum. Given the above mentioned difficulties and uncertainties, a scheme for which the consistency in the above sense can not be proved, may provide solutions that are not approximations of elements of the sought spectrum. On the other hand, with regard to the second point, we would like to observe that, to the best of our knowledge, no methods exist to identify the variational eigenvalues within a set of eigenpairs.

Notwithstanding the above difficulties and driven by the continuously excalating interest in data science, different algorithms for the numerical solution of the p eigenproblem have been proposed in the last few years [23, 72, 139]. In [139], the authors develop a scheme capable of computing a sequence of N eigenpairs as follows. Given the subspace L spanned by the first $k-1$ computed eigenfunctions ($L := \text{span}\{\tilde{f}_1, \dots, \tilde{f}_{k-1}\}$), the k-th eigenpair is found solving the following optimization problem:

$$\tilde{\lambda}_k = \min_{g \perp L} \operatorname*{local\,max}_{\tilde{f} \in \text{span}\{g, L\}} \mathcal{R}_p(\tilde{f})\,.$$

If the computed $\tilde{f}_k \notin L$, the authors show that $(\tilde{f}_k, \tilde{\lambda}_k)$ is a p-Laplacian eigenpair and that, assuming local differentiability of the map $g \to \operatorname*{local\,max}_{\tilde{f} \in \text{span}\{g, L\}} \mathcal{R}_p(\tilde{f})$, the eigenfunction $\tilde{f}_k$ has local minmax index of order $k-1$. Here the local minmax index is the number of local strictly decreasing directions of the p-Rayleigh quotient. However, there is no theoretical evidence for the existence of a sequence satisfying such properties. Indeed, with the exception of the smallest and largest variational ones, the p-eigenvalues may not be local maxima of the p-Rayleigh quotient on the linear subspace spanned by the corresponding eigenfunction (the latter possibly augmented by some other unknown eigenfunctions with smaller eigenvalues). The situation improves when looking for extremal eigenpairs. Indeed, for the nonlinear power method and the gradient flow scheme proposed in [72] and [23] to compute the extremal eigenpairs, it is possible to prove convergence. However, no a-priori information is available about the position in the spectrum of the approximated eigenpair. Moreover, neither method is suited to compute a full sequence of eigenpairs.

In this chapter we propose an original numerical scheme for the calculation of the eigenpairs of the p-Laplace operator and provide novel insights on the p-Laplacian eigenvalue problem on graphs that contribute to overcome some of the above-mentioned limitations of the previous efforts. In particular, we re-interpret the graph p-Laplacian eigenvalue problem as a constrained linear weighted Laplacian eigenproblem. The consequences of this reformulation are manifold. First, it becomes possible to assign a linear index to every p-Laplacian eigenvalue λ by simply assigning to it the corresponding index of the associated linear eigenvalue problem. Second, we are able to prove that, for any eigenpair (λ, f), the linear index of λ matches the Morse index of the p-Rayleigh quotient functional in f, providing thus additional information about the behaviour of the p-Rayleigh

quotient in a neighborhood of f. Based on this reformulation and inspired by the Dynamical-Monge-Kantorovich method introduced in [55–58], we consider the case of $p \in (2, \infty)$ and characterize the p-Laplacian eigenpairs as critical points of a family of energy functions defined on the domains of node and edge weights. Such energy functions are indexed from 1 to N, where N is the dimension of the graph, and thus provide a natural indexing for the eigenpair approximations. We are able to prove that the unique saddle point of the 1-st energy function corresponds to the unique first p-Laplacian eigenpair. Moreover, we prove that any differentiable saddle point of the k-th energy function corresponds to a p-Laplacian eigenpair having linear index equal to k. We then derive gradient flows for our energy functions and develop numerical algorithms for the computation of p-Laplacian eigenpairs. From a numerical point of view, our methods compute p-Laplacian eigenpairs as limits of sequences of linear eigenvalue problems, and we can then exploit the vast literature available for this last problem. Note that we are able to compute higher p-Laplacian eigenpairs without any prior information about the lower ones. Indeed, the choice of the index of the energy function prescribes a-priori the type of saddle point we converge to. Lastly, considering the first energy function, since we know that its unique saddle point corresponds to the unique 1-st p-Laplacian eigenpair, we can conclude that our method converges exactly to that eigenpair.
We point out that the energy functions here introduced are well defined also in the $p = \infty$ case. This leads us to conjecture the validity of our results also in the case $p = \infty$. We support this conjectrue by different numerical tests. However, the theoretical results that we prove in the case $p \in (2, \infty)$ cannot be extended in a straightforward manner to the case $p = \infty$. This will be the subject for a future work. We wish to conclude by observing that some very recent duality results [22, 77, 135] relate the p-Laplacian eigenvalue problem on the nodes of the graph to the q-Laplacian eigenvalue problem on the edges of the graph, where p and q are conjugate exponents. In particular, in [77, 135] the authors prove that there is a 1-to-1 correspondence between the non-zero eigenpairs of the node p-Laplacian and the edge q-Laplacian. Thus, extending some of our results to the edge q-Laplacian for $q > 2$, allows us to compute also the p-Laplacian eigenpairs for $p < 2$. Finally, we observe that the conjecture about the $q = \infty$ case on the edges of the graph corresponds to a conjecture about the graph 1-Laplacian eigenvalue problem.

3.2 Preliminaries and Notation

Let $\mathcal{G} = (E, V, \omega)$ be a non-oriented graph, where E is the set of edges, V is the set of nodes, and ω is a weight defined on the edges of the graph. For each pair of nodes u and v in V we have that the pair (u, v) is in E if and only if the pair (v, u) is in E. Also the weights are unique on each edge, i.e., $\omega_{uv} = \omega_{vu}$. We denote by $\mathrm{K} \in \mathbb{R}^{|E| \times |V|}$ the weighted incidence matrix of the graph, i.e., for each

$w \in V$:

$$\mathrm{K}\big((u,v),w\big) = \omega_{uv}\Big(\delta_v(w) - \delta_u(w)\Big)\,,$$

where $\delta_x(\cdot)$ denotes the indicator function of x. Then, having identified a subset of the nodes $B \subset V$ as the boundary of the graph, we say that the pair (λ, f) is a p-Laplacian eigenpair with homogeneous Dirichlet boundary conditions if it solves the following nonlinear equation:

$$\begin{cases} \frac{1}{2}\big(\mathrm{K}^T\,|\,\mathrm{K}\,f|^{p-2} \odot \mathrm{K}\,f\big)(u) = \lambda |f(u)|^{p-2} f(u) & \forall\, u \in V \setminus B \\ f(u) = 0 & \forall\, u \in B\,. \end{cases} \tag{3.2.1}$$

Then a simple argument allows to reformulate eq. (3.2.1) in terms of a generalized p-Laplacian eigenvalue problem as in [44]. Consider $\tilde{E}$ a subset of the edges obtained by selecting a unique direction for any edge (if $(u,v) \in \tilde{E}$ then $(v,u) \notin \tilde{E}$) and $\nabla \in \mathbb{R}^{|\tilde{E}| \times |V \setminus B|}$ the submatrix of K obtained by sampling the rows corresponding to $\tilde{E}$ and the columns corresponding to $V \setminus B$. Then for any $f \in \mathcal{H}_0(V) = \{f : V \to \mathbb{R} \mid f(u) = 0\ \forall\, u \in B\}$, define $\tilde{f} := f|_{V \setminus B}$ the restriction of f to the internal nodes. An easy computation shows that (λ, f) solves (3.2.1) if and only if $(\lambda, \tilde{f})$ solves the following equation:

$$\big(\nabla^T |\nabla \tilde{f}|^{p-2} \odot \nabla \tilde{f}\big)(u) = \lambda |\tilde{f}(u)|^{p-2} \tilde{f}(u) \qquad \forall\, u \in V \setminus B\,.$$

In particular, some trivial computations allow to prove that any p-Laplacian eigenpair with homogeneous Dirichlet boundary condition corresponds to a critical point/value of the following p-Rayleigh quotient defined on $\mathcal{H}(V \setminus B) := \{f : V \setminus B \to \mathbb{R}\}$:

$$\mathcal{R}_p(f) = \frac{\|\nabla f\|_p^p}{\|f\|_p^p} = \frac{\sum_{(u,v)\in\tilde{E}} |\nabla f(u,v)|^p}{\sum_{u \in V \setminus B} |f(u)|^p}\,.$$

Thus, throughout the whole chapter, we define the p-Laplace operator, or p-Laplacian, as follows:

Definition 3.2.1 (p-Laplace operator)**.**

$$\Delta_p f(u) := \big(\nabla^T |\nabla f|^{p-2} \odot \nabla f\big)(u) \qquad f \in \mathcal{H}(V \setminus B),\ u \in V \setminus B\,.$$

We remark that if $B = \emptyset$ our definition of Δ_p matches the classical definition of the p-Laplace operator by means of the incidence matrix [134]. On the other hand, when $B \neq \emptyset$ our p-Laplacian is included in the class of the generalized p-Laplace operators considered in [44, 110]. In addition, we point out that whenever $B \neq \emptyset$, then $\mathrm{Ker}(\nabla) = \{0\}$. In the sequel, given $f \in \mathcal{H}(V \setminus B)$ and the corresponding $\bar{f} \in \mathcal{H}_0(V)$ for economy of notation and with a small abuse of notation, we write

$$\nabla f(u,v) = K\bar{f}(u,v) = \omega_{uv}\big(\bar{f}(v) - \bar{f}(u)\big)$$

even if $(u,v) \notin \tilde{E}$. Note that in such a case, by definition of $\tilde{E}$, since only $\nabla f(v,u)$ is well defined we define $\nabla f(u,v) := -\nabla f(v,u)$ when $(u,v) \notin \tilde{E}$. Then,

the p-Laplace operator and the corresponding eigenvalue problem can be written as:

$$\Delta_p f(u) = \sum_{v \sim u} \omega_{uv} |\nabla f(v,u)|^{p-2} \nabla f(v,u) = \lambda |f(u)|^{p-2} f(u) \qquad \forall\, u \in V \setminus B\,. \tag{3.2.2}$$

We conclude this section by recalling the characterization of the first eigenpair of the p-Laplace operator as the minimum and the minimizer of $\mathcal{R}_p$ [44, 74]:

Theorem 3.2.2 (from [74]). *Let* $(f_1, \lambda_1) := (\arg\min, \min)_{f \in \mathcal{H}(V \setminus B)} \mathcal{R}_p(f)$. *Then:*

1. λ_1 *is simple, meaning that the associated eigenfunction* f_1 *is unique up to scalar factors;*
2. f_1 *is the only strictly positive eigenfunction, i.e. if* f *is an eigenfunction of* Δ_p *and* $f(v) > 0$ *for all* $v \in V \setminus B$, *then* $f = f_1$ *up to a multiplicative constant.*

Finally, we adopt the following definition of a connected graph in the presence of a boundary.

Definition 3.2.3 (Connected graph). *Given the graph boundary* $B \subset V$, *we say that the graph* $\mathcal{G}$ *is connected if the subgraph induced by* $V \setminus B$ *is connected.*

If not otherwise stated, in this manuscript we always assume the graph to be connected in the sense of the above definition.

3.3 An Equivalent Formulation of the p-Laplacian Eigenvalue Problem

In this section we consider a trivial reformulation of the p-Laplacian eigenvalue problem in terms of a constrained weighted Laplacian eigenvalue problem. Using such an equivalence, since the eigenvalues of the corresponding weighted Laplacian are finite, it is possible to assign to every p-Laplacian eigenvalue, λ, a linear index defined by the corresponding linear eigenavalue index. We prove that this index, which is theoretically computable, matches the Morse index of $\mathcal{R}_p$ in f, where f is the p-Laplacian eigenfunction corresponding to λ. We stress the fact that, here and in the following, we assume $p > 2$.
It is easy to observe that the pair (λ, f), solution of the p-Laplacian eigenequation (3.2.2), is an eigenpair of the p-Laplace operator if and only if (λ, f) is an eigenpair of the following constrained weighted Laplacian Dirichlet problem:

$$\begin{cases} \Delta_\mu f(u) = \big(\nabla^T \mathrm{diag}(\mu) \nabla f\big)(u) = \lambda \nu(u) f(u) & \forall\, u \in V \setminus B \\ \mu(uv) = |\nabla f(u,v)|^{p-2} & \forall\, (u,v) \in \tilde{E} \\ \nu(u) = |f(u)|^{p-2} & \forall\, u \in V \setminus B \end{cases}, \tag{3.3.1}$$

where $\mu \in \mathcal{M}^+(E)$ and $\nu \in \mathcal{M}^+(V \setminus B)$, with $\mathcal{M}^+(E)$ and $\mathcal{M}^+(V \setminus B)$ denoting the spaces of non-negative measures defined on the edges and on the internal nodes of the graph.

Definition 3.3.1.

$$\mathcal{M}^+(E) = \{\mu : \tilde{E} \to \mathbb{R}^+, \mu > 0\} \quad \textit{and} \quad \mathcal{M}^+(V \setminus B) = \{\nu : V \setminus B \to \mathbb{R}^+, \nu > 0\}\,.$$

Before proceeding with the task of calculating the Morse index of the p-Laplacian eigenpairs, we recall some facts about the linear Laplacian generalized eigenvalue problem weighted in μ and ν. Let $\mu \in \mathcal{M}^+(E)$ and $\nu \in \mathcal{M}^+(V \setminus B)$, we denote by $\mathrm{Diag}(\mu)$ and $\mathrm{Diag}(\nu)$ the diagonal matrices with entries given by the weights calculated on each edge and each node of the graph, i.e., $\mathrm{Diag}(\mu) = \mathrm{Diag}(\{\mu(uv), uv \in E\})$ and $\mathrm{Diag}(\nu) = \mathrm{Diag}(\{\nu(u), u \in V\})$. Consider the linear generalized eigenvalue problem

$$\Delta_\mu f(u) = \big(\nabla^T \mathrm{Diag}(\mu)\nabla f\big)(u) = \lambda\, \mathrm{Diag}(\nu) f(u) \quad \forall\, u \in V \setminus B\,. \tag{3.3.2}$$

We point out that the (μ, ν)-weighted Laplacian eigenvalue problem (3.3.2) can be degenerate if $\mathrm{Ker}(\mathrm{Diag}(\nu)) \cap \mathrm{Ker}(\Delta_\mu)$ is non empty. In this case, there would be only $N - \dim\big(\mathrm{Ker}(\mathrm{Diag}(\nu)) \cap \mathrm{Ker}(\Delta_\mu)\big)$ well defined, possibly infinite, eigenvalues. The previous statement is supported by the following discussion. First, we recall that (λ, f) is a generalized eigenpair of $(\Delta_\mu, \mathrm{Diag}(\nu))$ if it satisfies the eigenvalue equation

$$(\Delta_\mu - \lambda\, \mathrm{Diag}(\nu))\, f = 0\,. \tag{3.3.3}$$

From this definition it is obvious that, in the case $\mathrm{Ker}(\mathrm{Diag}(\nu)) \cap \mathrm{Ker}(\Delta_\mu) \neq \emptyset$, any value $\lambda \in \mathbb{R}$ is an eigenvalue corresponding to an eigenvector in $\mathrm{Ker}(\mathrm{Diag}(\nu)) \cap \mathrm{Ker}(\Delta_\mu)$. For this reason, we say that λ is a *well defined* eigenvalue if there exists $f \notin \mathrm{Ker}(\mathrm{Diag}(\nu)) \cap \mathrm{Ker}(\Delta_\mu)$ satisfying (3.3.3) (in which case we can equivalently ask $f \perp (\mathrm{Ker}(\mathrm{Diag}(\nu)) \cap \mathrm{Ker}(\Delta_\mu))$. Theorem 8.7.1 of [67] ensures that there exists a nonsingular matrix X such that the matrices $X^T \Delta_\mu X$ and $X^T\, \mathrm{Diag}(\nu) X$ are diagonal. Thus, the eigenvalues of $(\Delta_\mu, \mathrm{Diag}(\nu))$ are equal to the eigenvalues of the pair $(X^T \Delta_\mu X, X^T\, \mathrm{Diag}(\nu) X) =: (\mathrm{Diag}(\underline{a}, \underline{0}), \mathrm{Diag}(\underline{b}, \underline{0}))$, where $\underline{0}$ is the zero vector with dimension $\dim\big(\mathrm{Ker}(\mathrm{Diag}(\nu)) \cap \mathrm{Ker}(\Delta_\mu)\big)$. Thus, the number of well defined eigenvalues is $N - \dim(\mathrm{Ker}(\mathrm{Diag}(\nu)) \cap \mathrm{Ker}(\Delta_\mu))$ and their value is $\{a_i/b_i\}$, possibly taking the value ∞ if, for some i, $b_i = 0$. In this discussion we use Theorem 8.7.1 of [67]:

Theorem 3.3.2 (Theorem 8.7.1 of [67])**.** *Suppose that A and B are symmetric matrices and define $C(t) = tA + (1-t)B$. If there exists $t_0 \in [0,1]$ such that $C(t_0)$ is nonnegative definite and $\mathrm{Ker}\big(C(t_0)\big) = \mathrm{Ker}(A) \cap \mathrm{Ker}(B)$, then there exists a nonsingular X such that both $X^T A X$ and $X^T B X$ are diagonal.*

The well defined generalized eigenvalues can be characterized in terms of the Rayleigh quotient. To this aim, we introduce the following weighted seminorms

on the spaces $\mathcal{H}(\tilde{E}) := \{G : \tilde{E} \to \mathbb{R}\}$ and $\mathcal{H}(V \setminus B)$:

$$\|g\|_{2,\nu}^2 = \sum_u \nu_u |g(u)|^2, \quad g \in \mathcal{H}(V \setminus B) \quad \text{and} \quad \|G\|_{2,\mu}^2 = \sum_{(u,v)\in\tilde{E}} \mu_{uv} |G(u,v)|^2, \quad G \in \mathcal{H}(\tilde{E}).$$

The 2-Rayleigh quotient weighted in μ, ν given by:

$$\mathcal{R}_{2,\mu,\nu}(g) = \frac{\|\nabla g\|_{2,\mu}^2}{\|g\|_{2,\nu}^2} \quad g \in \mathcal{H}(V \setminus B)\,,$$

is well defined on $\big(\operatorname{Ker}(\operatorname{Diag}(\nu)) \cap \operatorname{Ker}(\operatorname{Diag}(\mu))\big)^{\perp}$ and takes values in $[0, \infty]$. Thus, the k-th well defined eigenvalue can be characterized as the solution of the following saddle-point problem:

$$\lambda_{(\mu,\nu),k} = \min_{A\in\mathcal{A}_k} \max_{f\in A} \mathcal{R}_{2,\mu,\nu}(f)\,,$$

where $\mathcal{A}_k := \{A \subset \mathbb{R}^{|V\setminus B|} \cap \operatorname{Ker}^{\perp}\big(\operatorname{Diag}(\nu) \cap \Delta_\mu\big) \mid \dim(A) \geq k\}$.
In addition, we will be using the following expanded definition of multiplicity for the well defined (μ,ν)-Laplacian eigenvalues:

Definition 3.3.3. *Let λ be a (μ,ν)-weighted Laplacian eigenvalue. The multiplicity of λ is*

$$\operatorname{mult}(\lambda) = \dim\{f \mid \Delta_\mu f = \lambda \operatorname{Diag}(\nu) f\}\,.$$

Note that, this definition of multiplicity of λ takes into account not only the number of times λ appears in the sequence of the well defined eigenvalues but also the dimension of the subspace $\operatorname{Ker}(\Delta_\mu) \cap \operatorname{Ker}(\operatorname{diag}(\nu))$. It finds application in the following result, whose straight-forward proof is provided in 3.6.

Lemma 3.3.4. *Let $(\lambda_{(\mu,\nu),k}, f_{(\mu,\nu),k})$ be the k-th eigenpair of the generalized (μ,ν)-Laplacian (3.3.2) and let m be the multiplicity of $\lambda_{(\mu,\nu),k}$. Then:*

$$\mathcal{MI}_f(\mathcal{R}_{2,\mu,\nu}) = k - 1\,, \quad \mathcal{MI}_f(-\mathcal{R}_{2,\mu,\nu}) = N - k - m + 1\,,$$

where $\mathcal{MI}_f(\mathcal{R}_{2,\mu,\nu})$ denotes the Morse index of $\mathcal{R}_{2,\mu,\nu}$ at f.

In essence, $\mathcal{MI}_f(\mathcal{R}_{2,\mu,\nu})$ is the number of decreasing local directions of $\mathcal{R}_{2,\mu,\nu}$ in f. More precisely the Morse index of a function ϕ at a point x, $\mathcal{MI}_x(\phi)$, is defined as the dimension of the largest subspace in which the Hessian matrix of ϕ at x is negative definite [see, e.g., 99]. We point out that, sometimes, the Morse index is used only in relation to Morse functions, i.e. functions whose critical points are all non degenerate, but, in general, this is not our case.
We return now to the p-Laplacian eigenproblem. Given an eigenpair (λ, f) and the corresponding weights μ and ν, we immediately observe that

$$f \in \operatorname{Ker}(\operatorname{Diag}(\nu))^{\perp} \subset \Big(\operatorname{Ker}(\Delta_\mu) \cap \operatorname{Ker}(\operatorname{Diag}(\nu))\Big)^{\perp}.$$

Moreover, if we assume w.l.o.g. that $\|f\|_p = 1$, then, by the definition of ν, $\|f\|_{2,\nu} = 1$. Thus, if we introduce the two spheres

$$S_p := \{g \in \mathcal{H}(V \setminus B) \,|\, \|g\|_p = 1\} \quad \text{and} \quad S_{2,\nu} := \{g \in \mathcal{H}(V \setminus B) \,|\, \|g\|_{2,\nu} = 1\},$$

we can state that if $f \in S_p$, then necessarily $f \in S_{2,\nu}$.
Let $T_f(S_p)$ and $T_f(S_{2,\nu})$ be the tangent spaces of the two spheres at point f. It is not difficult to observe that

$$T_f(S_p) = \{\xi \,|\, \langle \xi, |f|^{p-2} \odot f\rangle = 0\} = \{\xi \,|\, \langle \xi, \nu \odot f\rangle = 0\} = T_f(S_{2,\nu}).$$

Considering $\mathcal{R}_p$ and $\mathcal{R}_{2,\mu,\nu}$ as functions defined on the manifolds S_p and $S_{2,\nu}$, the next Lemma shows that it is possible to compare the Morse indices of $\mathcal{R}_p$ and $\mathcal{R}_{2,\mu,\nu}$ at point f. This allows us to relate $\mathcal{MI}_f(\mathcal{R}_p)$ to the linear index of λ, i.e., the position of λ in the spectrum of the associated linear eigenvalue problem, $\Delta_\mu f = \lambda \,\mathrm{Diag}(\nu) f$.

Lemma 3.3.5. *Given an eigenpair (λ, f) of the p-Laplacian and the weights $\nu = |f|^{p-2}$ and $\mu = |\nabla f|^{p-2}$. Assume that $(\lambda, f) = \left(\lambda_{(\mu,\nu),k}, f_{(\mu,\nu),k}\right)$ have multiplicity m. Then:*

$$\begin{aligned}\mathcal{MI}_f(\mathcal{R}_p) &= \mathcal{MI}_f(\mathcal{R}_{2,\mu,\nu}) = k - 1\,,\\ \mathcal{MI}_f(-\mathcal{R}_p) &= \mathcal{MI}_f(-\mathcal{R}_{2,\mu,\nu}) = N - k - m + 1\,.\end{aligned}$$

Proof. To prove the lemma it is enough to show that $\forall\, \xi \in T_f(S_p) = T_f(S_\nu)$ we have:

$$\frac{\partial^2}{\partial \epsilon^2}\left(\frac{\|\nabla(f+\epsilon\xi)\|_p^p}{\|f+\epsilon\xi\|_p^p}\right)\Big|_{\epsilon=0} = \frac{p(p-1)}{2}\frac{\partial^2}{\partial \epsilon^2}\left(\frac{\|\nabla(f+\epsilon\xi)\|_{2,\mu}^2}{\|f+\epsilon\xi\|_{2,\nu}^2}\right)\Big|_{\epsilon=0}.$$

Because of the equivalence of the p-Laplacian and weighted Laplacian eigenvalue problems, f is a critical point for both Rayleigh quotients $\mathcal{R}_p$ and $\mathcal{R}_{2,\mu,\nu}$, i.e., and hence their first derivative is zero:

$$\begin{aligned}0 &= \frac{\partial}{\partial \epsilon}\left(\frac{\|\nabla(f+\epsilon\xi)\|_p^p}{\|f+\epsilon\xi\|_p^p}\right)\Big|_{\epsilon=0} = \frac{p}{\|f\|_p^p}\left(\langle |\nabla f|^{p-2}\odot\nabla f, \nabla\xi\rangle - \frac{\|\nabla f\|_p^p}{\|f\|_p^p}\langle |f|^{p-2}\odot f, \xi\rangle\right)\\ 0 &= \frac{\partial}{\partial \epsilon}\left(\frac{\|\nabla(f+\epsilon\xi)\|_{2,\mu}^2}{\|f+\epsilon\xi\|_{2,\nu}^2}\right)\Big|_{\epsilon=0} = \frac{2}{\|f\|_{2,\nu}^2}\left(\langle \mu\odot\nabla f, \nabla\xi\rangle - \frac{\|\nabla f\|_{2,\mu}^2}{\|f\|_{2,\nu}^2}\langle \nu\odot f, \xi\rangle\right)\end{aligned} \tag{3.3.4}$$

We note that, since $\xi \in T_f(S_p) = T_f(S_\nu)$, we have:

$$\frac{\partial}{\partial\epsilon}\|f+\epsilon\xi\|_p^p = \frac{\partial}{\partial\epsilon}\|f+\epsilon\xi\|_{2,\nu}^2 = C\langle |f|^{p-2}\odot f, \xi\rangle = C\langle \nu\odot f, \xi\rangle = 0\,. \tag{3.3.5}$$

and for any $x, y \in \mathbb{R}$, we can calculate the first derivative of $x + \epsilon y$:

$$\frac{\partial |x+\epsilon y|^{p-2}(x+\epsilon y)}{\partial\epsilon}|_{\epsilon=0} = (p-2)|x|^{p-3}\frac{(x)^2}{|x|}y + |x|^{p-2}y = (p-1)|x|^{p-2}y\,. \tag{3.3.6}$$

Differentiating (3.3.4), using (3.3.5), and (3.3.6), and recalling that $|f+\epsilon\xi|^{p-2}\odot(f+\epsilon\xi)$ and $|\nabla(f+\epsilon\xi)|^{p-2}\odot\big(\nabla(f+\epsilon\xi)\big)$ are entrywise products, we obtain:

$$\begin{aligned}\frac{\partial^2}{\partial\epsilon^2}\left(\frac{\|\nabla(f+\epsilon\xi)\|_p^p}{\|f+\epsilon\xi\|_p^p}\right)\Bigg|_{\epsilon=0} &= \frac{p(p-1)}{\|f\|_p^p}\left(\langle|\nabla f|^{p-2}\odot\nabla\xi,\nabla\xi\rangle-\frac{\|\nabla f\|_p^p}{\|f\|_p^p}\langle|f|^{p-2}\odot\xi,\xi\rangle\right)\\ \frac{\partial^2}{\partial\epsilon^2}\left(\frac{\|\nabla(f+\epsilon\xi\|_{2,\mu}^2}{\|f+\epsilon\xi\|_{2,\nu}^2}\right)\Bigg|_{\epsilon=0} &= \frac{2}{\|f\|_{2,\nu}^2}\left(\langle\mu\odot\nabla\xi,\nabla\xi\rangle-\frac{\|\nabla f\|_{2,\mu}^2}{\|f\|_{2,\nu}^2}\langle\nu\odot\xi,\xi\rangle\right)\\ &= \frac{2}{\|f\|_p^p}\left(\langle|\nabla f|^{p-2}\odot\nabla\xi,\nabla\xi\rangle-\frac{\|\nabla f\|_p^p}{\|f\|_p^p}\langle|f|^{p-2}\odot\xi,\xi\rangle\right)\end{aligned} \tag{3.3.7}$$

which yields the desired equality. The conclusion follows from Lemma 3.3.4 . □

The results proved in this section show that, given a p-Laplacian eigenapair, the linear index of the (μ,ν)-eigenvalue provides information about the behaviour of the p-Rayleigh quotient in a neighborhood of the eigenfunction. However, it is not clear at this time how to properly exploit this information. This property will be used loosely in the next section but will be addressed more thoroughly in a future work.

3.4 Nonlinear Eigenpairs as Critical Points of a Family of Energy Functions

The previous section suggests to use the (μ,ν)-eigenvalue problem as much as possible. For this reason, and taking inspiration from the energy function defined in [57], we introduce the following family of energy functions $\mathcal{E}_{p,k}$, defined on $\mathcal{M}^+(E)\times\mathcal{M}^+(V\setminus B)$ and indexed by k, and such that their critical points identify p-Laplace eigenpairs:

$$\mathcal{E}_{p,k}(\mu,\nu) := \frac{1}{\lambda_{(\mu,\nu),k}} + \mathcal{M}_{E,p}(\mu) - \mathcal{M}_{V,p}(\nu)\,, \tag{3.4.1}$$

where $\lambda_{(\mu,\nu),k}$ is the k-th well defined eigenvalue of the weighted Laplacian eigenvalue problem (3.3.2) and the "mass functions" $\mathcal{M}_{V,p}(\nu)$ $\mathcal{M}_{E,p}(\mu)$ are given by:

$$\mathcal{M}_{V,p}(\nu) := \frac{p-2}{p}\sum_{u\in V\setminus B}\nu_u^{\frac{p}{p-2}}\,,\quad\text{and}\quad \mathcal{M}_{E,p}(\mu) := \frac{p-2}{p}\sum_{(u,v)\in\tilde{E}}\mu_{uv}^{\frac{p}{p-2}}\,.$$

We now first state the main results of this section and discuss their significance while postponing their proof to the end of the section. The first theorem shows that any differentiable saddle point of such energy functions corresponds to a p-Laplacian eigenpair.

Theorem 3.4.1. *Let $(\mu^*,\nu^*)\in\mathcal{M}^+(E)\times\mathcal{M}^+(V\setminus B)$ be a differentiable saddle point of the function $\mathcal{E}_{p,k}(\mu,\nu)$. Then, $\big(\lambda_{(\mu^*,\nu^*),k}^{\frac{p}{2}}, f_{(\mu^*,\nu^*),k}\big)$ is a p-Laplacian eigenpair.*

Observe that the hypothesis asking for $(\mu^*, \nu^*) \in \mathcal{M}^+(E) \times \mathcal{M}^+(V \setminus B)$ being a differentiable saddle point of the function $\mathcal{E}_{p,k}(\mu, \nu)$ is equivalent to assuming that $\lambda_{(\mu,\nu),k}$ is a simple eigenvalue of the generalized Laplacian eigenvalue problem (3.3.2). Indeed, since an eigenvalue is differentiable if and only if it is simple [83], Lemma 3.3.5 shows that $f_{(\mu^*,\nu^*),k}$ is a p-Laplacian eigenfunction such that

$$\mathcal{MI}_{f_{(\mu^*,\nu^*),k}}(\mathcal{R}_p) = k - 1 \qquad \mathcal{MI}_{f_{(\mu^*,\nu^*)}}(-\mathcal{R}_p) = N - k.$$

The second theorem asserts that if the boundary of the graph is not empty, $B \neq \emptyset$, for $k = 1$ the hypothesis of differentiability can be removed. Indeed, $\mathcal{E}_{p,1}$ has always a unique saddle point which corresponds to the unique first eigenpair of the p-Laplacian.

Theorem 3.4.2. *Let $B \neq \emptyset$ then the function $\mathcal{E}_{p,1}(\mu, \nu)$ admits a unique saddle point*

$$(\mu^*, \nu^*) = \operatorname*{arg\,max}_{\nu \in \mathcal{M}^+(V\setminus B)\setminus\{0\}} \operatorname*{arg\,min}_{\mu \in \mathcal{M}^+(E)} \mathcal{E}_{p,1}(\mu, \nu)\,.$$

Moreover, given $\lambda_{(\mu^*,\nu^*),1}$ the first eigenvalue of the Laplacian eigenvalue problem (3.3.2) weighted in (μ^*, ν^*), there exists an associated eigenfunction $f_{(\mu^*,\nu^*),1}$ such that the pair $(\lambda^{\frac{p}{2}}_{(\mu^*,\nu^*),1}, f_{(\mu^*,\nu^*),1})$ equals the first p-Laplacian eigenpair.

Observe that the functions $\mathcal{E}_{p,k}$ may be in general not well defined on the boundary of $\mathcal{M}^+(E) \times \mathcal{M}^+(V \setminus B)$ since the there could not exist k-well defined eigenvalues. However, the function $\mathcal{E}_{p,1}$ meets such kind of problems only for $(\nu, \mu) = (0, 0)$.
We would like also to remark that the assumption $B \neq \emptyset$ is not restrictive. Indeed, in the case $B = \emptyset$ the first p-Laplacian eigenpair is trivial as $\mathrm{Ker}(\nabla) = \mathrm{span}\{\underline{1}\}$ where $\underline{1}$ is the constant function equal to 1 on the nodes of the graph.
We would like to remark that the differentiability hypothesis in the above theorems is non trivial. Indeed, lack of continuity of the energy functions in (3.4.1) may occur when both $\mu \in \partial\mathcal{M}^+(E)$ and $\nu \in \partial\mathcal{M}^+(V \setminus B)$, where $\partial\mathcal{M}^+(E)$ and $\partial\mathcal{M}^+(V \setminus B)$ denote the boundary of $\mathcal{M}^+(E)$ and $\mathcal{M}^+(E)$. It is known [11] that in this case the generalized Laplacian eigenvalues may no longer be continuous. Moreover, the functions $\mathcal{E}_{p,k}(\mu, \nu)$ are not differentiable whenever $\lambda_{(\mu,\nu),k}$ is not simple [83]. In Fig. 3.1 we provide an example of such degeneracies in a p-Laplacian eigenpair problem.
Before proceeding with the proof of Theorem 3.4.1, we recall the following technical lemma. Assuming $\lambda_{(\mu,\nu),k}$ differentiable at the point (μ^*, ν^*), the next Lemma provides a classical characterization of the derivatives of $\lambda_{(\mu,\nu),k}$ with repect to μ and ν.

Lemma 3.4.3. *Let $\lambda^*_k = \lambda_{(\mu,\nu),k}$ be differentiable in (μ^*, ν^*) and assume the corresponding eigenfunction $f^*_k = f_{(\mu,\nu),k}$ to be unique. Then:*

$$\partial_\mu\Big((\lambda^*_k)^{-1}\Big) = -\frac{|\nabla f^*_k|^2}{(\lambda^*_k)^2 \|f^*_k\|^2_{2,\nu^*}} \qquad \text{and} \qquad \partial_\nu\Big((\lambda^*_k)^{-1}\Big) = \frac{|f^*_k|^2}{\|\nabla f^*_k\|^2_{2,\mu^*}}\,.$$

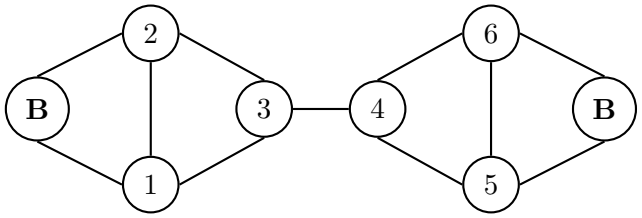

Figure 3.1: A graph with non-simple first eigenvalue. Assume $\nu_u = 1 \ \forall\, u \in V \setminus B$, then the graph is symmetric and the first eigenfunction of Δ_p, $f_{[p,p],1}$, is unique and necessarily agrees with the symmetry of the graph. This means that $\nabla f_{[p,p],1}(3,4) = 0$ and thus the density $\mu = |\nabla f_{[p,p],1}|^{p-2}$ of eq. (3.3.2) is zero on the edge $(3,4)$, splitting $\mathcal{G}$ in two connected components. As a result, $\lambda_{(\mu,\nu),1}$ is not simple and $\mathcal{E}_{p,1}$ is not differentiable.

Proof. The proof is straight-forward and uses the fact that if an eigenvalue is differentiable, then it is necessarily simple [83]. Hence, if $\lambda_{(\mu,\nu),k}$ is differentiable in μ_0, then $\lambda_{(\mu_0,\nu),k}$ is simple and the corresponding eigenfunction is uniquely defined. Thus, by the chain rule, it is enough to show that:

$$\partial_\mu \lambda_{(\mu,\nu),k} = \frac{\partial \mu_{uv} \Big(f_{(\mu,\nu),k}^T \nabla^T \mathrm{diag}(\mu) \nabla f_{(\mu,\nu),k} \Big)}{2 \| f_{(\mu,\nu),k} \|_{2,\nu}^2} = \frac{|\nabla f_{(\mu,\nu),k}(u,v)|^2}{2 \| f_{(\mu,\nu),k} \|_{2,\nu}^2} \,.$$

To prove the last equality, we differentiate both terms of the eigenvalue equation with respect to μ to obtain:

$$\begin{aligned} \partial_\mu \Big(\Delta_\mu f_k \Big) =& \partial_\mu \Big(\lambda_{(\mu,\nu),k} \mathrm{diag}(\nu) f_{(\mu,\nu),k} \Big) \\ \partial_\mu \big(\Delta_\mu \big) f_{(\mu,\nu),k} + \Delta_\mu \partial_\mu \big(f_{(\mu,\nu),k} \big) =& \partial_\mu \big(\lambda_{(\mu,\nu),k} \big) \mathrm{diag}(\nu) f_{(\mu,\nu),k} \\ & + \lambda_{(\mu,\nu),k} \mathrm{diag}(\nu) \partial_\mu \big(f_{(\mu,\nu),k} \big) \,. \end{aligned}$$

Multiplying by $f_{(\mu,\nu),k}$ and using the identities $\Delta_\mu f_{(\mu,\nu),k} = \Delta_\mu^T f_{(\mu,\nu),k} = \lambda_{(\mu,\nu),k} f_{(\mu,\nu),k}$ and $\Delta_\mu = \frac{1}{2} \nabla^T \mathrm{diag}(\mu) \nabla$ we obtain:

$$\begin{aligned} f_{(\mu,\nu),k}^T \partial_\mu \big(\Delta_\mu \big) f_{(\mu,\nu),k} + \lambda_{(\mu,\nu),k} f_{(\mu,\nu),k}^T \partial_\mu \big(f_{(\mu,\nu),k} \big) =& \partial_\mu \big(\lambda_{(\mu,\nu),k} \big) f_{(\mu,\nu),k}^T \mathrm{diag}(\nu) f_{(\mu,\nu),k} \\ & + \lambda_{(\mu,\nu),k} f_{(\mu,\nu),k}^T \mathrm{diag}(\nu) \partial_\mu \big(f_{(\mu,\nu),k} \big) \\ \frac{1}{2} f_{(\mu,\nu),k}^T \nabla^T \mathrm{diag}(e_{uv}) \nabla f_{(\mu,\nu),k} =& \partial_\mu \big(\lambda_{(\mu,\nu),k} \big) f_{(\mu,\nu),k}^T \mathrm{diag}(\nu) f_{(\mu,\nu),k} \,, \end{aligned}$$

where e_{uv} is the characteristic function of the edge (u,v). This concludes the proof of the first part of the theorem. The second part is obtained analogously. □

Now we are ready to present the proof of Theorem 3.4.1.

Proof of Theorem 3.4.1. The generalized k-th (μ,ν)-Laplacian eigenpair is a function of μ and ν. To simplify notation, when no ambiguity arises, in this proof

we write λ_k and f_k with no explicit reference to the dependence upon (μ, ν). In addition, we write $\lambda_k^* := \lambda_{(\mu^*,\nu^*),k}$ and $f_k^* := f_{(\mu^*,\nu^*),k}$, i.e., λ_k^* and f_k^* are the k-th (μ, ν)-Laplacian eigenvalue and eigenfunction evaluated at optimality.
Thanks to Lemma 3.4.3, the KKT conditions for the saddle points of the energy function $\mathcal{E}_{p,k}(\mu, \nu)$ can be written as:

$$\begin{cases} -\dfrac{|\nabla f_k^*(u,v)|^2}{(\lambda_k^*)^2 \|f_k^*\|_{2,\nu^*}^2} + {\mu_{uv}^*}^{\frac{2}{p-2}} - c_{uv} = 0 & \forall\, (u,v) \in \tilde{E} \\ \dfrac{|f_k^*(v)|^2}{\|\nabla f_k^*\|_{2,\mu^*}^2} - {\nu_v^*}^{\frac{2}{p-2}} + s_v = 0 & \forall\, v \in V \setminus B \\ c_{uv}\mu_{uv}^* = 0\,, \quad c_{uv} \geq 0 & \forall\, (u,v) \in \tilde{E} \\ s_v \nu_u^* = 0\,, \quad s_v \geq 0 & \forall\, v \in V \setminus B \\ \Delta_{\mu^*} f_k^* = \lambda_k^* \nu^* \odot f_k^* \end{cases}, \tag{3.4.2}$$

where $\tilde{E}$ is the subset of the edges obtained by selecting a unique direction for any edge (see Section 3.2). The constants $\{c_{uv}\}_{(u,v)\in\tilde{E}}$ and $\{s_v\}_{v\in V\setminus B}$ are suitable families of Lagrange multipliers. Since $c_{uv} \geq 0$, if $\mu_{uv}^* = 0$ the following equation

$$-\frac{|\nabla f_k^*(u,v)|^2}{(\lambda_k^*)^2 \|f_k^*\|_{2,\nu^*}^2} - c_{uv} = 0$$

admits only the solution $\nabla f_k^*(u,v) = 0$, $c_{uv} = 0$. Analogously $\nu_v^* = 0$ implies $f_k^*(v) = s_v = 0$. Hence equation (3.4.2) yields:

$$\begin{cases} \mu^* = \dfrac{|\nabla f_k^*|^{p-2}}{(\lambda_k^*)^{p-2} \|f_k^*\|_{2,\nu^*}^{p-2}} \\ \nu^* = \dfrac{|f_k^*|^{p-2}}{\|\nabla f_k^*\|_{2,\mu^*}^{p-2}} \\ \Delta_{\mu^*} f_k^* = \lambda_k^* \nu^* f_k^* \end{cases}. \tag{3.4.3}$$

Now we can write:

$$\begin{cases} \mu^* = c_\mu |\nabla f_k^*|^{p-2} \\ \nu^* = c_\nu |f_k^*|^{p-2} \end{cases} \quad \text{with} \quad \begin{cases} c_\mu = (\lambda_k^*)^{2-p} \|f_k^*\|_{2,\nu^*}^{2-p} \\ c_\nu = \|\nabla f_k^*\|_{2,\mu^*}^{2-p} \end{cases}.$$

Dividing the second equation in the previous expression by the first one we obtain:

$$\frac{c_\nu}{c_\mu} = \lambda_1^{p-2} \Big(\frac{\|f_k^*\|_{2,\nu^*}^2}{\|\nabla f_k^*\|_{2,\mu^*}^2} \Big)^{\frac{p-2}{2}} = (\lambda_k^*)^{\frac{p-2}{2}}\,.$$

Replacing the previously obtained expressions for μ^* and ν^* in the last equation of (3.4.3), dividing by c_μ, and using the ratio c_ν / c_μ just calculated, we obtain:

$$\sum_{v\sim u} \omega_{uv} |\nabla f_k^*(v,u)|^{p-2} \nabla f_k^*(v,u) = (\lambda_k^*)^{\frac{p}{2}} |f_k^*(u)|^{p-2} f_k^*(u)\,.$$

□

Next, we now turn our attention to the proof of Theorem 3.4.2 and the necessary preliminary results. The proof of the theorem is subdivided in two parts. The first part works on the weighted $[p,2]$-Laplacian eigenvalue problem and the second part extends these results to the p-Laplacian (or $[p,p]$-Laplacian) eigenproblem. Here we use square brackets to avoid confusion with the weighted (μ,ν) generalized Laplacian eigenproblem used before. Because the $[p,2]$-Laplacian is of independent interest [23, 62, 105] we decided to subdivide these two parts into two subsections. From know on, if not otherwise stated, we assume $B \neq \emptyset$.

3.4.1 The $[p,2]$-Laplacian Eigenvalue Problem

Let $\nu \in \mathcal{M}^+(V \setminus B)$ be a density on the nodes with $\nu \neq 0$ and consider the following $[p,2]$-Rayleigh quotient, which possibly can take the value $+\infty$:

$$\mathcal{R}_{p,2,\nu}(f) = \frac{\|\nabla f\|_p^p}{\|f\|_{2,\nu}^p} = \sum_{(u,v)\in\tilde{E}} |\nabla f(uv)|^p / \Big(\sum_{u\in V\setminus B} \nu_u |f(u)|^2 \Big)^{\frac{p}{2}} .$$

We assume $\mathcal{R}_{p,2,\nu}$ to be defined on the domain $\mathcal{H}(V \setminus B)$ and we name its critical point equation the $[p,2]$-Laplacian eigenvalue equation weighted in ν:

$$(\Delta_p f)(u) = \lambda\, \nu_u\, \|f\|_{2,\nu}^{p-2} f(u) \quad \forall\, u \in V \setminus B\,, \tag{3.4.4}$$

We provide now a characterization of the first eigenpair of the $[p,2]$-Laplacian as the minimal value and the minimum point of $\mathcal{R}_{p,2,\nu}$. In particular, we use the notation $(\lambda_{[p,2,\nu],1}, f_{[p,2,\nu],1})$ to indicate the weighted 1-th $[p,2]$-eigenpair, while we will denote by $(\lambda_{[p,p],1}, f_{[p,p],1})$ the first eigenpair of the p-Laplacian discussed in the preious sections (see Theorem 3.2.2). The next characterization of $(\lambda_{[p,2,\nu],1}, f_{[p,2,\nu],1})$ is analogue to the one holding for the classical p-Laplacian proposed in [74] and already reported in Thm 3.2.2. Also the proof of this characterization is very similar to the one used in [74] for the classical p-Laplacian eigenvalue problem. Before stating the characterization we recall the following maximum principle from [110] that we use in the proof. We point out that our definition of the p-Laplacian operator (see Def. 3.2.1), matches the definition of the generalized p-Laplacian operator used in the maximum principle in [110]. For ths reason, we report the theorem adapting the statement to our needs and notation.

Theorem 3.4.4 (from [110])**.** *If $f, g : V \to \mathbb{R}$ satisfy $\Delta_p f(u) > \Delta_p g(u)$, then $f(u) \geq g(u)$ for any $u \in V \setminus B$.*

Now we can prove that the first eigenvalue of the $[p,2]$-Laplacian is simple and positive and the corresponding unique first eigenfunction is the only one that is strictly positive on all internal nodes.

Theorem 3.4.5. *Let $\nu \neq 0$ and $\mathcal{G}$ be a connected graph. If $(\lambda_{[p,2,\nu],1}, f_{[p,2,\nu],1})$ is a first eigenpair of the $[p,2]$-Laplacian, then $\lambda_{[p,2,\nu],1} \geq 0$ and $f_{[p,2,\nu],1}(u) > 0 \quad \forall\, u \in V \setminus B$. Moreover $\lambda_{[p,2,\nu],1}$ is simple and $f_{[p,2,\nu],1}$ is the unique eigenfunction strictly greater than zero on every internal node.*

Proof. Observe that, for $\nu \neq 0$, the Rayleigh quotient $\mathcal{R}_{p,2,\nu}$ is always well defined if we admit that it takes values in $[0, \infty]$. Indeed, if $B \neq \emptyset$ then $\mathrm{Ker}(\nabla) = \emptyset$. If $B = \emptyset$, then $\mathrm{Ker}(\nabla) = \mathrm{span}(\underline{1})$, where $\underline{1}$ denotes the constant vector but for any $\nu \neq 0$, $\underline{1} \notin \mathrm{Ker}\big(\mathrm{Diag}(\nu)\big)$. In any case, for all $f \neq 0$ we have that $\min \mathcal{R}_{p,2,\nu} < \infty$. Let f_1 be a minimum point of $\mathcal{R}_{p,2,\nu}$ such that $\|f_1\|_{2,\nu} = 1$. An easy calculation shows that

$$\mathcal{R}_{p,2,\nu}(|f_1|) \leq \mathcal{R}_{p,2,\nu}(f_1)\,,$$

with equality if and only if $f_1 = \pm|f_1|$. Thus we can assume that $f_1(u) \geq 0 \;\forall\, u \in V \setminus B$. If $f_1(u) = 0$ for some $u \in V \setminus B$, then eq. (3.4.4) and the explicit expression of Δ_p in eq. (3.2.2) ensure that $f_1(v) = 0$ for any $v \sim u$. As a consequence of the connectedness of the graph, this implies $f_1 = 0$ for all $u \in V \setminus B$, from which $\|f_1\|_{2,\nu} = 0$, contradicting the initial hypothesis.
Now we can prove the second part of the theorem. We start from the last statement. Assume that there exists a positive eigenfunction $f_2 > 0$ such that $\mathcal{R}_{p,2,\nu}(f_2) = \lambda_2 > \lambda_1 = \mathcal{R}_{p,2,\nu}(f_1)$. Then there exists $t > 0$ such that

$$\lambda_2 f_2(u) > t\lambda_1 f_1(u) \;\forall\, u \in V \setminus B \quad \text{and} \quad \exists\, u_0 \in V \setminus B \text{ s.t. } t f_1(u_0) > f_2(u_0)\,.$$

Applying Theorem 3.4.4 to the functions tf_1 and f_2, we get a contradiction, proving that only positive eigenfunctions are associated to the first eigenvalue. We are left to prove that λ_1 is simple, i.e., the uniqueness of the corresponding eigenfunction f_1. Assume that there exist two positive eigenfunctions f_1 and f_2 relative to λ_1 with $\|f_1\|_{2,\nu} = \|f_2\|_{2,\nu} = 1$. Then, the function

$$g(u) = \big(f_1^2(u) + f_2^2(u)\big)^{\frac{1}{2}}\,,$$

has 2-norm given by $\|g\|_{2,\nu}^p = 2^{\frac{p}{2}}$ and its gradient satisfies:

$$\|\nabla g\|_p^p \leq 2^{\frac{p-2}{2}} \big(\|\nabla f_1\|_p^p + \|\nabla f_2\|_p^p\big)$$

with equality holding if and only if $\nabla f_1(u,v) = \nabla f_2(u,v) \;\forall\,(u,v) \in E$. To prove the last inequality, consider an edge (u,v) and use first the Cauchy Schwarz inequality applied to the two vectors $\big(f_1(u), f_2(u)\big)$ $\big(f_1(v), f_2(v)\big)$ and then Jensen inequality applied to the function $x \mapsto |x|^{\frac{p}{2}}$:

$$\begin{aligned}
|\nabla g(v,u)|^p &= \omega_{uv}^p \Big| \big(f_1(u)^2 + f_2(u)^2\big)^{\frac{1}{2}} - \big(f_1(v)^2 + f_2(v)^2\big)^{\frac{1}{2}} \Big|^p \\
&\leq \omega_{uv}^p \Big| \big(f_1(u) - f_1(v)\big)^2 + \big(f_2(u) - f_2(v)\big)^2 \Big|^{\frac{p}{2}} \\
&\leq \omega_{uv}^p 2^{\frac{p-2}{2}} \Big(\big|f_1(u) - f_1(v)\big|^p + \big|f_2(u) - f_2(v)\big|^p \Big) \\
&= 2^{\frac{p-2}{2}} \big(|\nabla f_1(v,u)|^p + |\nabla f_2(v,u)|^p\big)
\end{aligned}$$

where, by convexity of the function $|x|^{\frac{p}{2}}$, we have equality if and only if $f_1(u) - f_1(v) = f_2(u) - f_2(v)$. This means that

$$\lambda_1 2^{\frac{p}{2}} = \lambda_1 \|g\|_{2,\nu}^p \leq \|\nabla g\|_p^p \leq 2^{\frac{p-2}{2}} \big(\|\nabla f_1\|_p^p + \|\nabla f_2\|_p^p\big) = \lambda_1 2^{\frac{p}{2}}\,,$$

implying that in any edge $f_1(u) - f_1(v) = f_2(u) - f_2(v)$ and thus, by the connectedness of the graph, and the assumptions on f_1 and f_2 yields $f_1 = f_2$. □

Remark 3.4.6. *Observe that the same argument provides a characterization also for the first eigenpair of the (μ, ν)-Laplacian eigenvalue problem. In particular, let $\mu \in \mathcal{E}^+$ and let $\mathcal{G}_\mu$ be the subgraph of $\mathcal{G}$ obtained by removing the edges where $\mu = 0$. Assume that $\mathcal{G}_\mu$ is connected and observe that the first well defined eigenvalue can be written as:*

$$\lambda_{(\mu,\nu),1} = \min_{\|f\|_\nu = 1} \mathcal{R}_{2,\mu,\nu}(f)\,.$$

The same proof of Theorem 3.4.5 shows that $\lambda_1(\mu, \nu)$ is simple and the corresponding eigenfunction f_1 is uniquely characterized by the property of being strictly positive on any node. Finally note that in the case $\mathcal{G}_\mu$ is not connected, even if the "if and only if" condition does not hold, it is still possible to show that if we find a function f that satisfies the (μ, ν)-Laplacian eigenvalue equation and that is strictly positive on the internal nodes, then necessarily the corresponding eigenvalue is the first one, as the following corollary states.

Corollary 3.4.7. *Given $\mu \in \mathcal{E}^+ \neq 0$ and $\nu \in \mathcal{V} \setminus \mathcal{B}^+$ with $\nu \neq 0$. If (λ, f) is an eigenpair of the (μ, ν)-Laplacian such that $f(u) > 0$ for any $v \in V \setminus B$, then $\lambda = \lambda_{(\mu,\nu),1}$.*

Proof. The proof easily follows by observing that, even if the induced graph has been disconnected: $\mathcal{G}_\mu = \cup \mathcal{G}_i$, the (μ, ν)-spectrum is given by the union of the $(\mu|_{\mathcal{G}_i}, \nu|_{\mathcal{G}_i})$-spectra. Moreover, for any $\mathcal{G}_i$ where the $(\mu|_{\mathcal{G}_i}, \nu|_{\mathcal{G}_i})$-Laplacian eigenvalue problem is defined, i.e. $(\mu|_{\mathcal{G}_i}, \nu|_{\mathcal{G}_i}) \neq (0, 0)$, the first eigenfunction is characterized by

$$f_{(\mu|_{\mathcal{G}_i}, \nu|_{\mathcal{G}_i}),1}(u) > 0 \quad \forall\, u \in \mathcal{G}_i\,.$$

Thus, if f is an eigenfunction on $\mathcal{G}$ and $f > 0$, necessarily $f = \sum_i \alpha_i f_{(\mu|_{\mathcal{G}_i}, \nu|_{\mathcal{G}_i}),1}$ for some $\{\alpha_i > 0\}_i$, i.e. f corresponds to the first eigenvalue on any connected component. □

The $[p, 2]$-Laplacian eigenproblem as a (μ, ν)-Laplacian eigenproblem

Analogously to the p-Laplacian eigenvalue problem discussed in Section 3.3, also the $[p, 2]$-Laplacian eigenvalue problem can be reformulated in terms of a constrained weighted Laplacian eigenvalue problem. To this aim, we first rewrite the eigenvalue equation (3.4.4) as:

$$\nabla^T \left(|\nabla f|^{p-2} \odot \nabla f \right)(u) = \lambda\, \nu_u \|f\|_{2,\nu}^{p-2} f(u) \qquad \forall\, u \in V \setminus B.$$

Dividing both terms by $\|f\|_{2,\nu}^{p-2}$, it is straightforward to observe that (λ, f) is an eigenpair of the $[p, 2]$-Laplacian if and only if (λ, f) is an eigenpair of the con-

strained weighted Laplacian problem, i.e., it is solution of the following equation:

$$\begin{cases} \Delta_\mu f(u) := \nabla^T \left(\mathrm{Diag}(\mu)\nabla f\right)(u) = \lambda \nu_u f(u) & \forall\, u \in V \setminus B \\ \mu_{uv} = \dfrac{|\nabla f(u,v)|^{p-2}}{\|f\|_{2,\nu}^{p-2}} \geq 0 & \forall\ (u,v) \in \tilde{E} \end{cases}$$

3.4.2 Energy Function for the first eigenpair of the $[p,2]$-Laplacian

In this section we introduce a convex energy function whose minimum can be proved to correspond to the unique first eigenapair of the $[p,2]$-eigenvalue problem weighted in ν. The results and the techniques presented here are the starting point to prove Theorem 3.4.11.
Given a fixed density $\nu \in \mathcal{M}^+(V \setminus B)$ with $\nu \neq 0$, consider the following energy function:

$$\begin{aligned} \mathcal{L}_{1,E}(\mu) =& \frac{1}{\lambda_{(\mu,\nu),1}} + \mathcal{M}_{E,p}(\mu) = \sup_{\|f\|_{2,\nu}=1} \frac{\|f\|_{2,\nu}^2}{\|\nabla f\|_{2,\mu}^2} + \frac{p-2}{p} \sum_{(u,v)\in\tilde{E}} \mu_{uv}^{\frac{p}{p-2}} \\ =& \sup_{\|f\|_{2,\nu}=1} \frac{\sum\limits_{u\in V\setminus B} \nu_u f(u)^2}{\sum\limits_{(u,v)\in\tilde{E}} \mu_{uv} |\nabla f(uv)|^2} + \frac{p-2}{p} \sum_{(u,v)\in\tilde{E}} \mu_{uv}^{\frac{p}{p-2}} \end{aligned}$$

Observe that $\mathcal{L}_{1,E}$ is the μ-only part in $\mathcal{E}_{p,1}$ of eq. (3.4.1).
In the following Theorem we prove that the energy function $\mathcal{L}_{1,E}(\mu)$ admits a unique minimizer, μ^*, and that the first eigenfunction of Δ_{μ^*} corresponds to the unique first eigenpair of the $[p,2]$-Laplacian.

Theorem 3.4.8. *Let $\nu \in \mathcal{M}^+(V \setminus B)$ with $\nu \neq 0$ and assume μ^* is a minimum point of $\mathcal{L}_{1,E}(\mu)$ on $\mathcal{M}^+(E)$. Given $\lambda_1^* = \lambda_{(\mu^*,\nu),1}$, there exist f_1^* a (μ^*,ν)-eigenfunction associated to λ_1^* such that $\left((\lambda_1^*)^{p-1}, f_1^*\right)$, is the first $[p,2]$-eigenpair, i.e.:*

$$(\lambda_1^*)^{p-1} = \lambda_{[p,2,\nu],1} \qquad \text{and} \qquad f_1^* = f_{[p,2,\nu],1}\,.$$

Moreover

$$\mathcal{L}_{1,E}(\mu^*) = \frac{2p-2}{p} \lambda_{[p,2,\nu],1}^{-\frac{1}{p-1}}\,.$$

Proof. Observe first of all that the function $\mathcal{L}_{1,E}$ is strictly convex in $\mathcal{M}^+(E)$ and thus admits a unique minimum point. Moreover, using the characterization of $\lambda_{(\mu,\nu),1}$ by means of the (μ,ν)-Rayleigh quotient $\mathcal{R}_{2,\mu,\nu}$, the minimum problem of the function $\mathcal{L}_{1,E}$ can be written as a saddle point problem, i.e.:

$$\min_{\mu\in\mathcal{M}^+(E)} \mathcal{L}_{1,E} = \min_{\mu\in\mathcal{M}^+(E)} \max_{\|f\|_{2,\nu}=1} \frac{\|f\|_{2,\nu}^2}{\|\nabla f\|_{2,\mu}^2} + \frac{p-2}{p} \sum_{(u,v)\in\tilde{E}} \mu_{uv}^{\frac{p}{p-2}}\,.$$

From the minmax inequality, we can write:

$$\min_{\mu\in\mathcal{M}^+(E)} \mathcal{L}_{1,E} \geq \max_{\|f\|_{2,\nu}=1} \min_{\mu\in\mathcal{M}^+(E)} \frac{\|f\|_{2,\nu}^2}{\|\nabla f\|_{2,\mu}^2} + \frac{p-2}{p} \sum_{(u,v)\in\tilde{E}} \mu_{uv}^{\frac{p}{p-2}} . \tag{3.4.5}$$

Now, for a fixed f with $\|f\|_{2,\nu} = 1$, it is possible to compute the weight μ^f that realizes the minimum:

$$\mu^f = \arg\min_{\mu\in\mathcal{M}^+(E)} \frac{1}{\|\nabla f\|_{2,\mu}^2} + \frac{p-2}{p} \sum_{(u,v)\in\tilde{E}} \mu_{uv}^{\frac{p}{p-2}} .$$

Indeed, the KKT conditions for this constrained minimization problem are:

$$\begin{cases} -\dfrac{|\nabla f(u,v)|^2}{\|\nabla f\|_{\mu^f}^4} + \left(\mu_{uv}^f\right)^{\frac{2}{p-2}} - c_{uv} = 0 & \forall\,(u,v)\in\tilde{E} \\ c_{uv} \geq 0 \quad \text{and} \quad c_{uv}\mu_{uv}^f = 0 & \forall\,(u,v)\in\tilde{E} \end{cases} \tag{3.4.6}$$

where $\{c_{uv}\}$ is a family of edge-wise Lagrange multipliers that implement the non-negativity constraints.
Observe that if $\mu_{uv}^f =$, from the first equality in (3.4.6), then necessarily also $c_{uv} = 0$ and $|\nabla f(u,v)| = 0$. In particular, we see that μ^f satisfies the following equality:

$$\mu_{uv}^f = \frac{|\nabla f(u,v)|^{p-2}}{\|\nabla f\|_{\mu^f}^{2p-4}} \qquad \forall\,(u,v)\in\tilde{E} \tag{3.4.7}$$

Multiplying eq. (3.4.7) by $|\nabla f(u,v)|^2$ and summing over the edges we have:

$$\|\nabla f\|_{\mu^f}^{2p-2} = \|\nabla f\|_p^p . \tag{3.4.8}$$

Thus, if we replace (3.4.8) and (3.4.7) in (3.4.5) we obtain the following lower bound:

$$\begin{aligned} \min_{\mu\in\mathcal{M}^+(E)} \mathcal{L}_{1,E} &\geq \max_{\|f\|_\nu=1} \left(\frac{1}{\|\nabla f\|_p}\right)^{\frac{p}{p-1}} + \frac{p-2}{p}\frac{\|\nabla f\|_p^p}{\|\nabla f\|_{\mu^f}^{2p}} \\ &= \max_{\|f\|_\nu=1} \frac{2p-2}{p}\|\nabla f\|_p^{-\frac{p}{p-1}} = \frac{2p-2}{p}\lambda_{[p,2,\nu],1}^{-\frac{1}{p-1}} . \end{aligned}$$

On the other hand, consider the first $[p,2]$-Laplacian eigenvalue $\lambda_{[p,2,\nu],1}$ and the corresponding unique eigenfunction $f_{[p,2,\nu],1}$ with $\|f_{[p,2,\nu],1}\|_\nu = 1$. Then, consider μ^* defined by:

$$\mu^* = \lambda_{[p,2,\nu],1}^{\frac{2-p}{p-1}} |\nabla f_{[p,2,\nu],1}|^{p-2} .$$

Corollary (3.4.7) implies that $f_{[p,2,\nu],1}$ is the first eigenfunction of the (μ^*,ν)-eigenvalue problem with $\lambda_{(\mu^*,\nu),1} = \lambda_{[p,2,\nu],1}^{\frac{1}{p-1}}$. Thus we can write:

$$\min_{\mu\in\mathcal{M}^+(E)} \mathcal{L}_{1,E}(\mu) \leq \mathcal{L}_{1,E}(\mu^*) = \lambda_{(\mu^*,\nu),1}^{-1} + \frac{p-2}{p}\lambda_{[p,2,\nu],1}^{-\frac{1}{p-1}} = \frac{2p-2}{p}\lambda_{[p,2,\nu],1}^{-\frac{1}{p-1}} ,$$

which concludes the proof. □

Since, as mentioned before, the $[p,2]$ eigenvalue problem is of independent interest, before going back to the classical p-Laplacian eigenvalue problem we conclude this section by noting that, given a fixed density ν on the internal nodes, the class of energy functions

$$\mathcal{L}_{k,E}(\mu) = \frac{1}{\lambda_{(\mu,\nu),k}} + \mathcal{M}_{E,p}(\mu)$$

can be used to characterize $[p,2]$-Laplacian eigenpairs, in analogy with the (μ^*,ν^*) case of Theorem 3.4.1. We collect this result in the following Theorem whose proof is similar to the (μ^*,ν^*) case.

Theorem 3.4.9. *Let $\mu^* \in \mathcal{M}^+(E)$ be a differentiable minimizer of the function $\mathcal{L}_{k,E}(\mu)$. Then, $(\lambda^{p-1}_{(\mu^*,\nu),k}, f_{(\mu^*,\nu),k})$ is a $[p,2]$-Laplacian eigenpair.*

3.4.3 From the $[p,2]$-Laplacian to the p-Laplacian Eigenvalue Problem

This paragraph is dedicated to the proof of Theorem 3.4.2. To this aim, we start by observing that, analogously to the equivalence of the p-Laplacian eigenvalue problem with a generalized linear eigenvalue problem (eq. (3.3.1)), a pair (λ, f) is an eigenpair of the p-Laplacian operator if and only if it satisfies the following constrained weighted $[p,2]$-Laplacian eigenvalue problem:

$$\begin{cases} \Delta_p f(u) = \lambda \nu_u \|f\|^{p-2}_{2,\nu} f(u) & \forall\, u \in V \setminus B \\ \nu_u = \frac{|f(u)|^{p-2}}{\|f\|^{p-2}_{2,\nu}} & \forall\, u \in V \setminus B \end{cases}.$$

In Section 3.4.1 we have proved that, given a nonsingular weight function ν on the nodes, it is possible to characterize the first eigenpair of the $[p,2]$-Laplacian eigenvalue problem weighted in ν by the minimizer μ^*_ν of the function $\mathcal{L}_{1,E}(\mu)$ (see Theorem 3.4.8). Similarly, we introduce an energy function depending only on the variable ν given by:

$$\mathcal{L}_{1,V}(\nu) = \frac{2(p-1)}{p} \lambda^{-\frac{1}{p-1}}_{[p,2,\nu],1} - \frac{p-2}{p} \sum_{u \in V \setminus B} \nu(u)^{\frac{p}{p-2}}.$$

Observe that for any $\nu \neq 0$, from Theorem 3.4.8, we have the following equality:

$$\mathcal{L}_{1,V}(\nu) = \mathcal{L}_{1,E}(\mu^*_\nu) - \mathcal{M}_{V,p}(\nu) = \mathcal{E}_{p,1}(\mu^*_\nu, \nu),$$

Moreover, since $\mathcal{R}^{-1}_{p,2,0}(f) = 0$ for any $f \neq 0$, $\mathcal{L}_{1,V}$ can be extended in zero so that $\mathcal{L}_{1,V}(0) := 0$.
Now we want to show that there exists a unique critical point of $\mathcal{L}_{1,V}$ and that this critical point corresponds to the unique first eigenpair of the p-Laplacian operator. We start our goal by collecting some preliminary results needed in the proofs. First, in the next Lemma we address the differentiability of the function

$\nu \mapsto \lambda_{[p,2,\nu],1}$. Note that similar results are available in the continuous case for the regularity of the first p-Laplacian eigenfunction with respect to perturbations of the domain [88].

Lemma 3.4.10. *Let λ_1 and f_1 be the minimum value and the minimizer of $\mathcal{R}_{p,2,\nu}(f)$. Then the function $\lambda_1 : \nu \mapsto \lambda_{[p,2,\nu],1}$ and its first derivatives are continuous, i.e., $\lambda_1 \in C^1(\mathcal{M}^+(V \setminus B) \setminus \{0\}, \mathbb{R})$. Moreover:*

$$\frac{\partial \lambda_1}{\partial \nu}(\nu_0) = -\frac{p}{2} \frac{\lambda_1 |f_{[p,2,\nu_0],1}|^2}{\|f_{[p,2,\nu_0],1}\|^2_{2,\nu_0}} .$$

Proof. Recall the definition of the $[p, 2, \nu]$-Rayleigh quotient:

$$\mathcal{R}_{p,2,\nu}(f) := \frac{\|\nabla f\|_p^p}{\|f\|_{2,\nu}^p} = \frac{\sum\limits_{(u,v)\in\tilde{E}} |\nabla f(u,v)|^p}{\Big(\sum\limits_{u\in V\setminus B} \nu(u)|f(u)|^2\Big)^{\frac{p}{2}}}$$

Recall that, given $\nu \in \mathcal{M}^+(V \setminus B) \setminus \{0\}$, the first eigenvalue is characterized by

$$\lambda_1(\nu) := \min_f \mathcal{R}_{p,2,\nu}(f) = \mathcal{R}_{p,2,\nu}(f_{\nu,1}, \nu) .$$

The function that associates to a density ν the corresponding first eigenfunction, $f_\nu := f_{[p,2,\nu],1}$, of the $[p, 2]$-Laplacian weighted in ν, with $\|f_\nu\|_{2,\nu} = 1$ is well defined by Theorem 3.4.5 and continuous by the continuity of minimizers.
Now consider the variation of λ_1 near a point $\nu_0 \in \mathcal{M}^+(V \setminus B) \setminus \{0\}$. We have the following inequality:

$$\begin{aligned}\lambda_1(\nu_0) - \lambda_1(\nu) &= \mathcal{R}_{p,2,\nu_0}(f_{\nu_0}) - \mathcal{R}_{p,2,\nu}(f_\nu) \\ &\le \mathcal{R}_{p,2,\nu_0}(f_\nu) - \mathcal{R}_{p,2,\nu}(f_\nu) = \partial_\nu \mathcal{R}_{p,2,\nu_0}(f_\nu)(\nu_0 - \nu) + o(\|\nu_0 - \nu\|) ,\end{aligned}$$

which implies

$$\begin{aligned}&\limsup_{\nu\to\nu_0} \left(\lambda_1(\nu_0) - \lambda_1(\nu) - \partial_\nu \mathcal{R}_{p,2,\nu_0}(f_{\nu_0})(\nu_0 - \nu)\right) \\ &\qquad \le \limsup_{\nu\to\nu_0} \left(\partial_\nu \mathcal{R}_{p,2,\nu_0}(f_\nu) - \partial_\nu \mathcal{R}_{p,2,\nu_0}(f_{\nu_0})\right)(\nu_0 - \nu) = 0 .\end{aligned}$$

Similarly we can write:

$$\begin{aligned}\lambda_1(\nu_0) - \lambda_1(\nu) &= \mathcal{R}_{p,2,\nu_0}(f_{\nu_0}) - \mathcal{R}_{p,2,\nu}(f_\nu) \\ &\ge \mathcal{R}_{p,2,\nu_0}(f_{\nu_0}) - \mathcal{R}_{p,2,\nu}(f_{\nu_0}) = \partial_\nu \mathcal{R}_{p,2,\nu_0}(f_{\nu_0})(\nu_0 - \nu) + o\left(\|\nu_0 - \nu\|\right)\end{aligned}$$

which implies:

$$\liminf_{\nu\to\nu_0} \left(\lambda_1(\nu_0) - \lambda_1(\nu) - \partial_\nu \mathcal{R}_{p,2,\nu_0}(f_{\nu_0})(\nu_0 - \nu)\right) \ge 0 .$$

$$\partial_\nu \lambda_1(\nu_0) = \partial_\nu \mathcal{R}_{p,2,\nu_0}(f_{\nu_0}) = -\frac{p}{2} \frac{\lambda_1(\nu_0)|f_{\nu_0}|^2}{\|f_{\nu_0}\|^2_{2,\nu_0}}$$

□

The next theorem asserts the there exists a unique maximum point ν^* of the function $\mathcal{L}_{1,V}(\nu)$, which is everywhere nonzero and it identifies the unique first eigenpair of the p-Laplacian.

Theorem 3.4.11. *The maximizer ν^* of the function $\mathcal{L}_{1,V}(\nu)$ is unique and belongs to the interior of $\mathcal{M}^+(V \setminus B)$, i.e.,*

$$\nu^* \in \{\nu : V \setminus B \to \mathbb{R} \,|\, \nu_u > 0 \,\forall\, u \in V \setminus B\}\,.$$

Moreover:

1. *The first eigenpair $\left(\lambda_{[p,2,\nu^*],1}, f_{[p,2,\nu^*],1}\right)$ of the weighted $[p,2,\nu^*]$-Laplacian is related to the first eigenpair of the $[p,p]$-Laplacian by:*

$$\left(\lambda_{[p,2,\nu^*],1}^{\frac{p}{2(p-1)}}, f_{[p,2,\nu^*],1}\right) = \left(\lambda_{[p,p],1}, f_{[p,p],1}\right) \quad \textit{and} \quad \mathcal{L}_{1,V}(\nu^*) = \lambda_{[p,p],1}^{\frac{2}{p}}\,.$$

2. *No other internal critical points of the function $\mathcal{L}_{1,V}(\nu)$ exist.*

Proof. Observe that the first nonzero eigenvalue of the $[p,2,\nu]$-Laplacian given by:

$$\lambda_{[p,2,\nu],1} = \min_{f \neq 0} \frac{\|\nabla f\|_p^p}{\|f\|_{2,\nu}^p}\,,$$

where the $[p,2]$-Rayleigh quotient is admitted to take values in $[0,\infty]$ is always well defined from Theorem 3.4.5
Hence we can write:

$$\max_{\nu \in \mathcal{M}^+(V\setminus B)} \mathcal{L}_{1,V} = \max_{f \neq 0} \max_{\nu \in \mathcal{M}^+(V\setminus B)} \frac{2p-2}{p} \left(\frac{\|f\|_{2,\nu}^p}{\|\nabla f\|_p^p}\right)^{\frac{1}{p-1}} - \frac{p-2}{p} \sum_{u \in V\setminus B} \nu_u^{\frac{p}{p-2}}\,. \tag{3.4.9}$$

Assume f to be fixed and ν^f to realize the maxima:

$$\nu^f \in \operatorname*{arg\,max}_{\nu \in \mathcal{M}^+(V\setminus B)} \frac{2p-2}{p} \left(\frac{\|f\|_{2,\nu}^p}{\|\nabla f\|_p^p}\right)^{\frac{1}{p-1}} - \frac{p-2}{p} \sum_{u \in V\setminus B} \nu_u^{\frac{p}{p-2}}\,.$$

Then since the last is a constrained maximum problem, by the KKT conditions, there exist a family of Lagrange multipliers $\{c_u\}_{u \in V\setminus B}$ such that:

$$\begin{cases} \mathcal{R}_{p,2,\nu^f}^{-\frac{1}{p-1}}(f) \dfrac{|f(u)|^2}{\|f\|_{2,\nu^f}^2} - (\nu_u^f)^{\frac{2}{p-2}} + c_u = 0 & \forall\, u \in V \setminus B \\ c_u \nu_u^f = 0 \quad \text{and} \quad c_u \geq 0 & \forall\, u \in V \setminus B \end{cases}.$$

In particular, since whenever $\nu_u = 0$ necessarily also $f(u) = c(u) = 0$, The previous equation yields:

$$\nu_u^f = \left(\mathcal{R}_{p,2,\nu^f}(f)\right)^{-\frac{p-2}{2(p-1)}} \frac{|f(u)|^{p-2}}{\|f\|_{2,\nu^f}^{p-2}} \qquad \forall\, u \in V \setminus B\,. \tag{3.4.10}$$

Multiplying by $|f(u)|^2$ and summing over $u \in V \setminus B$, the $(2, \nu^f)$ seminorm of f can be written as

$$\|f\|_{2,\nu^f}^p = \big(\mathcal{R}_{p,2,\nu^f}(f)\big)^{-\frac{p-2}{2(p-1)}} \|f\|_p^p = \|f\|_p^{2p-2} / \|\nabla f\|_p^{p-2}. \tag{3.4.11}$$

In particular, (3.4.10) and (3.4.11) yield the following expression for the $p/(p-2)$-norm of ν^f:

$$\sum_{u \in V \setminus B} (\nu_u^f)^{\frac{p}{p-2}} = \frac{\|f\|_p^2}{\|\nabla f\|_p^2} \tag{3.4.12}$$

Finally if we replace the expressions from (3.4.11) and (3.4.12) in (3.4.9), we can now calculate the maximum of $\mathcal{L}_{1,V}$:

$$\max_{\nu \in \mathcal{M}^+(V \setminus B)} \mathcal{L}_{1,V} = \max_{f \neq 0} \frac{2p-2}{p} \Big(\frac{\|f\|_p^{2p-2}}{\|\nabla f\|_p^{2p-2}} \Big)^{\frac{1}{p-1}} - \frac{p-2}{p} \frac{\|f\|_p^2}{\|\nabla f\|_p^2} = \max_{f \neq 0} \frac{\|f\|_p^2}{\|\nabla f\|_p^2} = \lambda_{[p,p],1}^{-\frac{2}{p}}$$

and since the 1st p-Laplacian eigenfunction $f_{[p,p],1}$ realizes the maximum in f, from (3.4.10) the maximizer ν^* satisfies:

$$\nu^* = \lambda_{[p,p],1}^{-\frac{2(p-2)}{p^2}} \frac{|f_{[p,p],1}|^{p-2}}{\|f_{[p,p],1}\|_p^{p-2}} .$$

In addition we know that $f_{[p,p],1}(u) > 0$ for any $u \in V \setminus B$ (see Theorem 3.2.2), thus $\nu^* \in \mathrm{Int}(\mathcal{M}^+(V \setminus B))$ and it is the unique maximizer. To conclude the proof, we observe that if ν is a critical point of $\mathcal{L}_{1,V}$ with $\nu \in \mathrm{Int}(\mathcal{M}^+(V \setminus B))$, then from Lemma 3.4.10 we have

$$\begin{cases} \lambda_{[p,2,\nu],1}^{-\frac{1}{p-1}} \dfrac{|f_{[p,2,\nu],1}(u)|^2}{\|f_{[p,2,\nu],1}\|_{2,\nu}^2} - \nu(u)^{\frac{2}{p-2}} = 0 & \forall\, u \in V \setminus B \\ \Delta_p f_{[p,2,\nu],1} = \lambda_1(p,2,\nu) \|f_{[p,2,\nu],1}\|_{2,\nu}^{p-2} \nu \odot f_{[p,2,\nu],1} \end{cases},$$

i.e.:

$$\Delta_p f_{[p,2,\nu],1} = \lambda_{[p,2,\nu],1}^{\frac{p}{2(p-1)}} |f_{[p,2,\nu],1}|^{p-2} \odot f_{[p,2,\nu],1} .$$

But then, since $f_{[p,2,\nu],1}$ is the first $[p,2]$-Laplacian eigenfunction, Theorem 3.4.5 ensures that $f_{[p,2,\nu],1}(u) > 0$ for all $u \in V \setminus B$, and thus $f_{[p,2,\nu],1} = f_{[p,p],1}$, i.e. $\nu = \nu^*$. □

These results lead directly to the proof of Theorem 3.4.2 .

Proof of Theorem 3.4.2. From Theorems 3.4.11 and 3.4.8 there exists a unique (μ^*, ν^*), such that:

$$(\mu^*, \nu^*) = \operatorname*{arg\,max}_{\nu \in \mathcal{M}^+(V \setminus B) \setminus 0} \ \operatorname*{arg\,min}_{\mu \in \mathcal{M}^+(\mu)} \frac{1}{\lambda_1(\mu, \nu)} + \mathcal{M}_p(\mu) - \mathcal{M}_p(\nu) .$$

Thus (μ^*, ν^*) is the only, possibly non-differentiable, saddle point of the function $\mathcal{E}_{p,1}$:

$$\mathcal{E}_{p,1}(\mu, \nu) = \frac{1}{\lambda_1(\mu, \nu)} + \mathcal{M}_{E,p}(\mu) - \mathcal{M}_{V,p}(\nu)\,.$$

Moreover $\mu^* \in \arg\max_\mu \dfrac{1}{\lambda_{(\mu,\nu^*),1}} + \mathcal{M}_{E,p}(\mu)$, thus from Theorem 3.4.8 there exists a first eigenpair $\left(f_{(\mu^*,\nu^*),1}, \lambda_{(\mu^*,\nu^*),1}\right)$ of the (μ^*, ν^*) eigenvalue problem (3.3.2) such that

$$\left(f_{(\mu^*,\nu^*),1}, \lambda^{p-1}_{(\mu^*,\nu^*),1}\right) = \left(f_{[p,2,\mu^*],1}, \lambda_{[p,2,\mu^*],1}\right)$$

Finally, from Theorem 3.4.11,

$$\left(f_{[p,2,\mu^*],1}, \lambda^{\frac{p}{2(p-1)}}_{[p,2,\mu^*],1}\right) = \left(f_{[p,p],1}, \lambda_{[p,p],1}\right),$$

which concludes the proof. □

3.4.4 Discussion and open problems

We have observed that every p-Laplacian eigenpair can be considered as a linear eigenpair of a properly weighted Laplacian eigenproblem. This characterization allowed us to introduce a class of energy functions whose differentiable saddle points correspond to p-Laplacian eigenpairs. Now it is thus natural to investigate numerical methods for the computation of p-Laplacian eigenpairs based on gradient flows of the functions $\mathcal{E}_{p,k}(\mu, \nu)$. In the next section we present some preliminary numerical results showing that the these schemes actually deliver acceptable results in most situations. Nevertheless the problem of the lack of regularity of the functions $\mathcal{E}_{p,k}(\mu, \nu)$ in case of eigenvalues with multiplicity greater than 1 is still a stumbling block. Indeed, discontinuous energy functions prevent the convergence of the numerical schemes in many situations. These are evidenced by bounded oscillations of residuals and non-convergence of the algorithm.

With this aim in mind, before addressing some numerical results, we would like to add some notes and a short discussion on a number of open problems that are worth addressing in future research. The first observation we would like to mention is related to differentiable saddle points. Any p-Laplacian eigenpair (λ, f) corresponding to a smooth saddle point of the k-th energy function can be fully characterized in a neighborhood of f in terms of the behavior of the p-Rayleigh quotient. Indeed, the fact that (μ^*, ν^*) is a differentiable saddle point implies that the eigenvalue $\lambda_{[\mu^*,\nu^*],k}$ is simple, yielding $\mathcal{MI}_f(\mathcal{R}_p) = k-1$, $\mathcal{MI}_f(-\mathcal{R}_p) = N-k$ by Lemma3.3.5. As a consequence, differently from the local min-max algorithm presented in [139], with our approach we can compute directly a p-Laplacian eigenpair (λ, f) such that $\mathcal{MI}_f(\mathcal{R}_p) = k-1$, $\mathcal{MI}_f(-\mathcal{R}_p) = N-k$ without the

need of computing a whole sequence of p-Laplacian eigenpairs having linear index in $\{1, \dots, k-1\}$.

The second point we would like to stress is that the definition of the energy functions $\mathcal{E}_{p,k}(\mu, \nu)$ can be easily extended to the case $p = \infty$ by setting $p/p - 2 = 1$ in the expression of $M_{V,p}$ and $M_{E,p}$. We will see in the next section some preliminary numerical experiments supporting the validity of this observation and the effectiveness of gradient flow numerical methods in the case $p = \infty$. However, a more detailed study is needed to fully address this case, and this will be proposed in the future.

Finally, we would like to recall a duality result presented in [77, 135] and relating p-eigenpairs on the nodes to q-eigenpairs on the edges (p, q conjugate). This result allows the extension of our approach to the case $p \in [1, 2)$.

Consider the eigenvalue problem given by the critical point equation of the q-Rayleigh quotient $\mathcal{R}_q^E$ defined on the set of edge functions $\mathcal{H}(\tilde{E}) = \{G : \tilde{E} \to \mathbb{R}\}$ as:

$$\mathcal{R}_q^E(G) := \frac{\|\nabla^T G\|_q^q}{\|G\|_q^q}\,.$$

Any critical pair (value,point) (η, G) of $\mathcal{R}_q^E$ can be regarded as a q-eigenpair on the edges. Note that (η, G) is a q-eigenpair if it satisfies the nonlinear eigenvalue equation:

$$\left(\nabla \left|\nabla^T G\right|^{q-2} \nabla^T G\right)(uv) = \eta |G(uv)|^{q-2} G(uv) \qquad \forall\, u \in V \setminus B \tag{3.4.13}$$

In [77, 135] the authors show by duality that the nonzero critical values and points of $\mathcal{R}_q^E$ correspond to the nonzero critical values and points of $\tilde{\mathcal{R}}_p$, where p is the conjugate of q. In particular, the authors prove that if (λ, f) is an eigenpair of Δ_p with $\lambda \neq 0$, then $(\lambda^{\frac{q}{p}}, |\nabla f|^{p-2}\nabla f)$ is a q-eigenpair on the edges. Viceversa, if (η, G) is a q-eigenpair on the edges with $\eta \neq 0$, then $\left(\eta^{\frac{p}{q}}, |\nabla^T G|^{q-2}\nabla^T G\right)$ is a Δ_p-eigenpair. Using these facts, it is straightforward to observe that equation (3.4.13) can be reformulated in terms of a generalized eigenvalue problem defined on the function space $\mathcal{H}(\tilde{E})$. In particular we can consider the energy functions

$$\mathcal{E}_k^E(\nu, \mu) = \frac{1}{\eta_k(\mu, \nu)} + \mathcal{M}_q(\nu) - \mathcal{M}_q(\mu)\,, \tag{3.4.14}$$

where $k \geq \dim(\mathrm{Ker}(\nabla^T))$ and $\eta_{[\nu,\mu],k}$ is the k-generalized eigenvalue of the problem:

$$\nabla \mathrm{diag}(\nu) \nabla^T G = \eta \mu G\,.$$

Then, analogously to Thm. 3.4.1, it is trivial to observe that any differentiable saddle point of $\mathcal{E}_k^E$ corresponds to an edge q-eigenpair and hence, by duality, to a Δ_p-eigenapair. Moreover, when $p < 2$, $q > 2$, properties of saddle points of the functions (3.4.14) for $q > 2$ translate into properties of Δ_p-eigenpairs for $p < 2$. In particular, note that the conjecture about the validity of our strategy in the $q = \infty$ case corresponds to the extremal case $p = 1$.

3.5 Numerical evaluation of the saddle points

The computation of the saddle points of the energy functions $\mathcal{E}_{p,k}(\mu,\nu)$ is a constrained critical point problem. To incorporate in our fomulation the positivity constraint we follow the same procedure that turned out to be very successful in the solution of the L^1-Optimal Transport problem and discussed in [56, 113]. Thus, we perform the change of variable $\mu = \sigma_1^2$ and $\nu = \sigma_2^2$. Using the new variables, the energy functions $\mathcal{E}_{p,k}(\sigma_1^2, \sigma_2^2)$ become well defined everywhere in $\mathbb{R}^{|E|} \times \mathbb{R}^{|V|}$. We thus define a dynamics for the variables (μ,ν) as the gradient flow in the variables σ_1 and σ_2. To this aim we use the following time-derivatives:

$$\dot{\mu} = 2\sigma_1\dot{\sigma_1} = -2\sigma_1\frac{\partial \mathcal{E}_{p,k}(\sigma_1^2,\sigma_2^2)}{\partial \sigma_1} = -4\sigma_1^2\frac{\partial \mathcal{E}_{p,k}(\mu,\nu)}{\partial \mu} = -4\mu\frac{\partial \mathcal{E}_{p,k}(\mu,\nu)}{\partial \mu}$$

and

$$\dot{\nu} = 4\nu\frac{\partial \mathcal{E}_{p,k}(\mu,\nu)}{\partial \nu}\,.$$

Writing explicitly the partial derivatives and neglecting constant multiplicative factors, which turn out to be just an increase in the speed of the dynamics, we end up with the following gradient flow system:

$$\begin{cases} \dot{\mu} = \mu\left(\frac{|\nabla f_{[\mu,\nu],k}|^2}{\lambda_{[\mu,\nu],k}\|f_{[\mu,\nu],k}\|_\nu^2} - \mu^{\frac{2}{p-2}}\right) \\ \dot{\nu} = \nu\left(\frac{|f_{[\mu,\nu],k}|^2}{\|\nabla f_{[\mu,\nu],k}\|_\mu^2} - \nu^{\frac{2}{p-2}}\right) \\ \Delta_\mu f_{[\mu,\nu],k} = \lambda_{[\mu,\nu],k} f_{[\mu,\nu],k} \end{cases}.$$

We are then looking for the stationary equilibrium of the above dynamics. The first two algebraic-differential equations are discretized by means of a simple explicit Euler method with an empirically-determined constant time step size, τ. The third purely algebraic equation is solved by diagonalization of the μ-weighted linear Laplacian by means of standard Lapack routines. For simplicity, no effort has been done to exploit sparsity of the graph-related matrices, which could provide important computational efficiency improvements. Thus, when looking for the k-th eigenpair, starting from given initial values $\mu^0 = \mu_k^0$ and $\nu^0 = \nu_k^0$, the $n = 1, 2, \ldots$ approximations are calculated by solving:

$$\begin{aligned} &\text{calculate } (\lambda^{n+1}, f^{n+1}) \text{ solving:} && \Delta_{\mu^n} f = \lambda_{[\mu^n,\nu^n]} f \\ &\text{calculate } \mu^{n+1}\text{:} && \mu^{n+1} := \mu^n + \tau\mu^n\left(\frac{|\nabla f^{n+1}|^2}{(\lambda^{n+1})^2\|f^{n+1}\|_{\nu^n}^2} - (\mu^n)^{\frac{2}{p-2}}\right) \\ &\text{calculate } \nu^{n+1}\text{:} && \nu^{n+1} := \nu^n + \tau\nu^n\left(\frac{|f^{n+1}|^2}{\|\nabla f^{n+1}\|_{\mu^n}^2} - (\nu^n)^{\frac{2}{p-2}}\right). \end{aligned}$$

Convergence towards equilibrium is considered achived when the error, defined as:

$$\text{err} = \|\Delta_p f^{n+1} - (\lambda^{n+1})^{\frac{p}{2}}|f^{n+1}|^{p-2}f^{n+1}\|_\infty \tag{3.5.1}$$

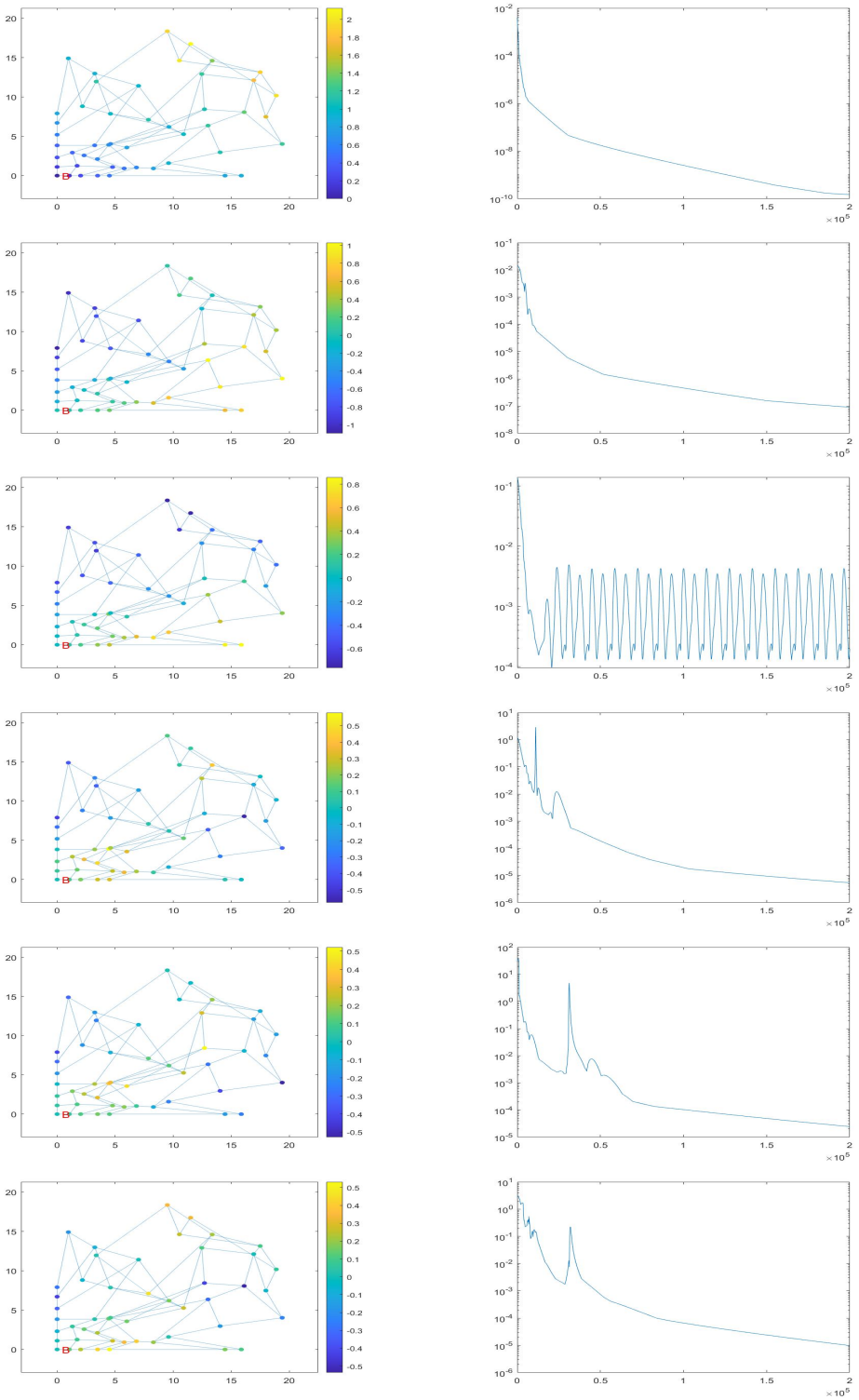

Figure 3.2: Left panel: first six eigenfunctions as calculated by the proposed method for $p = 6$. The graph nodes are randomly distributed with edge lengths equal to the reciprocal of the weights. The nodal values of the eigenfunctions are plotted with the color-code shown on the right of the figure for $k = 1, \ldots, 6$ (top to bottom). For each k the right panel reports the behavior of the error defined in eq. (3.5.1) as a function of time steps (iterations) n.

is below a given tolerance.
Figure 3.2 shows the experimental results obtained on a graph of 49 vertices with weights randomly chosen between 0.1 and 1.1. The graph is plotted by distributing the nodes randomly in space with edge lengths equal to the reciprocal of the weights. The results are relative to a value of $p = 6$. The first 6 eigenfunctions (left panels) and relative convergence behaviour are reported. We note that convergence towards equilibrium for $k = 1$ and $k = 2$ is smooth and fast. However, for $k = 3$ strong oscillations when the error reaches 10^{-4} appear and convergence is completely absent. For $k > 3$ the initial oscillations disappear quickly and convergence of the discrete gradient flow proceeds smoothly after that.
We must recall here that for $k = 1$ Theorem 3.4.2 ensures that the energy function $\mathcal{E}_{p,1}$ has only one saddle point and the proposed algorithm is expected to converge. However, for $k > 1$ nothing is known. In particular, if the eigenvalues are not simple, the energy function loses continuity, and the ODE trajectories identified by the gradient flow intersect, potentially leading to an oscillatory behaviour of the discrete method.
For $k = 3$ the initial oscillations clearly noticeable in the convergence profile are due to the jumping back and forth between energy levels relative to different values of k of the numerically calculated trajectories. In this case the gradient flow stagnates. In other cases we observe experimentally an oscillatory behaviour which actually converges towards stationarity. This behaviour can be justified empirically postulating that the time step becomes large enough to jump over the discontinuity point and, by chance the numerical scheme picks an appropriate trajectory and carries the calculations to convergence. However, unlike in the linear ($p = 2$) case, we have no means at the moment to identify the position in the spectrum towards which we converge.

3.6 Technical results

Proof of Lemma 3.3.4. Let us complete f to a ν and Δ_μ-orthogonal basis by taking a basis of eigenfucntions, i.e. take $\{f_i\}_{i=1}^N$ as follows: $\{f_i\}_{i=1}^{k-1}$ are eigenvectors relative to the first $k-1$ well defined eigenvalues, $f = f_k$ and $\{f_i\}_{i=k}^{k+m-1}$ are eigenvectors relative to λ_k, including a base of the subspace $\mathrm{Ker}(\Delta_\mu) \cap \mathrm{Ker}(\nu)$, $\{f_i\}_{i=k+m}^N$ are the eigenvectors relative to the well defined eigenvalues $\lambda_i > \lambda_k$. The eigenvectors relative to the well defined eigenvalues, except the base of $\mathrm{Ker}(\Delta_\mu) \cap \mathrm{Ker}(\nu)$, are chosen in $\big(\mathrm{Ker}(\Delta_\mu) \cap \mathrm{Ker}(\nu)\big)^\perp$. Observe that $T_f(S_{2,\nu}) = \mathrm{span}\{f_i\}_{i\neq k}$, indeed $Tg_f(S_{2,\nu}) = \{\xi, |, \langle \nu \odot f, \xi\rangle = 0\}$, and $\{f_i(\mu,\nu)\}_i$ is a ν-othogonal base of the space. Hence, the following implications hold:

$$\frac{\partial^2}{\partial\epsilon^2}\left(\frac{\|\nabla(f+\epsilon\xi)\|_{2,\mu}^2}{\|f+\epsilon\xi\|_{2,\nu}^2}\right)\Big|_{\epsilon=0} < 0 \quad \Longleftrightarrow \quad \xi \in \mathrm{span}\{f_i(\mu,\nu)|\, i<k\}\,,$$

$$\frac{\partial^2}{\partial\epsilon^2}\left(\frac{\|\nabla(f+\epsilon\xi)\|_{2,\mu}^2}{\|f+\epsilon\xi\|_{2,\nu}^2}\right)\Big|_{\epsilon=0} > 0 \quad \Longleftrightarrow \quad \xi \in \mathrm{span}\{f_i(\mu,\nu)|\, i>k+m-1\}\,.$$

To prove the last statement, let $\xi = \sum_{i\neq k} \alpha_i f_i(\mu,\nu)$ and recall that if $i \neq j$, then $\langle \mu \odot \nabla f_i, \nabla f_j\rangle = 0$ and $\langle \nu \odot f_i, f_j\rangle = 0$. Hence, using (3.3.7), we can provide the following equality that allows easily to conclude the proof of the lemma:

$$\begin{aligned}\frac{\partial^2}{\partial \epsilon^2}\left(\frac{\|\nabla(f+\epsilon\xi\|_{2,\mu}^2}{\|f+\epsilon\xi\|_{2,\nu}^2}\right)\Big|_{\epsilon=0} &= \frac{2}{\|f\|_{2,\nu}^2}\sum_{i\neq k}\sum_{j\neq k}\alpha_i\alpha_j\Big(\langle \mu\odot\nabla f_i,\nabla f_j\rangle - \lambda_k\langle \nu\odot f_i, f_j\rangle\Big)\\ &= \frac{2}{\|f\|_{2,\nu}^2}\sum_{i\neq k}\alpha_i^2\Big(\langle \mu\odot\nabla f_i,\nabla f_i\rangle - \lambda_k\langle \nu\odot f_i, f_i\rangle\Big)\end{aligned}$$

In the last equality observe that if f_i is an eigenfunction corresponding to an eigenvalue λ_i with $f_i \notin \operatorname{Ker}\big(\operatorname{diag}(\nu)\big) \cap \operatorname{Ker}\big(\Delta(\mu)\big)$, then

$$\Big(\langle \mu\odot\nabla f_i,\nabla f_i\rangle - \lambda_h\langle \nu\odot f_i, f_i\rangle\Big) = \|f_i\|_{2,\nu}^2\big(\lambda_i-\lambda_k\big)\,,$$

i.e., f_i is an increasing or a decreasing direction of $\mathcal{R}_{2,\mu,\nu}$ in f according to the inequalities $\lambda_i > \lambda_k$ or $\lambda_i < \lambda_k$. Moreover if $f_i \in \operatorname{Ker}(\Delta_\mu) \cap \operatorname{Ker}\big(\operatorname{diag}(\nu)\big)$ it is trivial to observe that f_i is neither an increasing nor a decreasing direction of $\mathcal{R}_{2,\mu,\nu}$ in f, i.e.:

$$\Big(\langle \mu\odot\nabla f_i,\nabla f_i\rangle - \lambda_h\langle \nu\odot f_i, f_i\rangle\Big) = 0\,.$$

□

Conclusions

In this thesis we have presented different new techniques for the numerical solution of a rather large class of problems.
Moreover, we have shown several numerical applications underlying the efficiency and robustness of our proposed algorithms, not only for the identifiability of the parameters governing the piezometric heads and water fluxes dynamics in WDS, but also for other more general problems, coming from different fields of application.
These ideas are strictly connected to the main purpose of this thesis, i.e. the numerical modeling of WDS via the p-Laplace operator, and surprisingly all the other applications proposed both in the second and in the third chapter, are somehow related to the solution of similar problems, interconnected by the EDMK scheme, in all of it's variants.
This shows also the extremely power of convex duality to rewrite a complex problem in a simplified one, which can be possibly solved with more performing techniques.
Moreover, the high flexibility of our EDMK scheme leads also to apply our techniques to non standard scenarios, where other methods fails to be opportunely adapted. This is the case for example of the proposed scheme for the Total Variation regularization in presence of positivity and interval constraints, where the standard techniques based on the Bregman iteration is in general not directly usable.
Another advantage of our techniques in the framework of the WDS model calibration problem of Chapter 1 is that, differently from the standard approach where is necessary a complete knowledge of all the pipes physical properties(e.g. diameters, materials etc., see [81] and [86]), our proposed algorithm doesn't relies on any particular constitutive laws, but rather it is specifically designed to retrieve the constitutive law governing WDS.
Observe that, working with a general weight w and exponent p for any edge, allows us to perform the model calibration also in the case where partial diameters and materials data are known. The Total Variation regularization, based on the Line Graph(see Chapter 1 Section 1.5.4) automatically enforces a local constant behaviour of the design parameters on the connected components of the graph. Thus, it naturally reconstructs the missing data along the topology of the graph, and leads us to genuinely carry out the model calibration also in the presence of

partial data.
This is in some sense the strong idea which motivates and interlaces Chapter 1 with Chapter 2.
On the other hand, similar considerations can be done for the case of the p-Laplacian eigenproblem in Chapter 3. In this case the connection with the WDS problem is not only given by the p-Laplace operator itself, but also from the necessity to provide some tools in order to further analyze the results, using for example the eigenfunctions of the p-Laplacian operator given by the weights and exponents distribution derived from the model calibration. This eigenfunctions provide strong geometrical informations on the spatial distribution of the data and will be used in future developments of kernel based method for reduced order models and physical based data classification on WDS.

Bibliography

[1] EPANET 2.2 documentation. https://epanet22.readthedocs.io.

[2] *Obstacle problem*, pages 47–56. Vieweg+Teubner, Wiesbaden, 2008.

[3] G. Alberti and M. Santacesaria. CalderÓn's inverse problem with a finite number of measurements. *Forum of Mathematics, Sigma*, 7, 10 2019. doi: 10.1017/fms.2019.31.

[4] G. Allaire. Conception optimale de structures. Springer, 2007.

[5] L. Ambrosio, N. Gigli, and G. Savaré. *Gradient Flows in Metric Spaces and in the Space of Probability Measures*. Lectures in Mathematics ETH Zürich. Birkhäuser, 2. ed edition. ISBN 978-3-7643-8722-8 978-3-7643-8721-1. OCLC: 254181287.

[6] S. Amghibech. Eigenvalues of the discrete p-Laplacian for graphs. *Ars Combinatoria*, 67:283–302, 04 2003.

[7] S. Arora, E. Hazan, and S. Kale. The multiplicative weights update method: a meta-algorithm and applications. *Theory of Computing*, 8(1):121–164, 2012. URL http://dblp.uni-trier.de/db/journals/toc/toc8.html#AroraHK12.

[8] S. Arridge, P. Maass, O. Öktem, and C.-B. Schönlieb. Solving inverse problems using data-driven models. *Acta Numerica*, 28:1–174, 2019. doi: 10.1017/S0962492919000059.

[9] R. C. Aster, B. Borchers, and C. H. Thurber. Chapter ten - nonlinear inverse problems. In R. C. Aster, B. Borchers, and C. H. Thurber, editors, *Parameter Estimation and Inverse Problems (Second Edition)*, pages 239–252. Academic Press, Boston, second edition edition, 2013. ISBN 978-0-12-385048-5. doi: https://doi.org/10.1016/B978-0-12-385048-5.00010-0. URL https://www.sciencedirect.com/science/article/pii/B9780123850485000100.

[10] O. Awe, S. Okolie, and O. Fayomi. Review of water distribution systems modelling and performance analysis softwares. *Journal of Physics: Conference Series*, 1378(2):022067, dec 2019. doi: 10.1088/1742-6596/1378/2/022067. URL https://doi.org/10.1088/1742-6596/1378/2/022067.

[11] Z. Bai, J. Demmel, J. Dongarra, A. Ruhe, and H. van der Vorst. *Templates for the Solution of Algebraic Eigenvalue Problems*. Society for Industrial and Applied Mathematics, 2000. doi: 10.1137/1.9780898719581. URL https://epubs.siam.org/doi/abs/10.1137/1.9780898719581.

[12] G. Bal. Introduction to inverse problems. *Lecture Notes-Department of Applied Physics and Applied Mathematics, Columbia University, New York*, 2012.

[13] A. Beck and M. Teboulle. A fast iterative shrinkage-thresholding algorithm for linear inverse problems. *SIAM Journal on Imaging Sciences*, 2(1):183–202, 2009.

[14] M. Belkin, I. Matveeva, and P. Niyogi. Tikhonov regularization and semi-supervised learning on large graphs. In *2004 IEEE International Conference on Acoustics, Speech, and Signal Processing*, volume 3, pages iii–1000, 2004. doi: 10.1109/ICASSP.2004.1326716.

[15] R. Bergmann, R. Herzog, M. S. Louzeiro, D. Tenbrinck, and J. Vidal-Núñez. Fenchel duality theory and a primal-dual algorithm on riemannian manifolds, 2020.

[16] V. Bonifaci. A laplacian approach to $$\ell _1$$-norm minimization. *Computational Optimization and Applications*, 79(2):441–469, mar 2021. doi: 10.1007/s10589-021-00270-x. URL https://doi.org/10.1007%2Fs10589-021-00270-x.

[17] G. Bouchitté and G. Dal Maso. Integral representation and relaxation of convex local functionals on $bv(\omega)$. *Annali della Scuola Normale Superiore di Pisa - Classe di Scienze*, Ser. 4, 20(4):483–533, 1993. URL http://www.numdam.org/item/ASNSP_1993_4_20_4_483_0/.

[18] G. Bouchitté, G. Buttazzo, and P. Seppecher. Mathématiques/mathematics shape optimization solutions via monge-kantorovich equation. *Comptes Rendus de l'Académie des Sciences-Series I-Mathematics*, 324(10):1185–1191, 1997.

[19] X. Bresson, X.-C. Tai, T. F. Chan, and A. Szlam. Multi-class transductive learning based on l 1 relaxations of cheeger cut and mumford-shah-potts model. *Journal of mathematical imaging and vision*, 49(1):191–201, 2014.

[20] T. Bühler and M. Hein. Spectral clustering based on the graph p-laplacian. In *Proceedings of the 26th Annual International Conference on Machine Learning*, ICML '09, page 81–88, New York, NY, USA, 2009. Association for Computing Machinery. ISBN 9781605585161. doi: 10.1145/1553374.1553385. URL https://doi.org/10.1145/1553374.1553385.

[21] L. Bungert and M. Burger. Asymptotic profiles of nonlinear homogeneous evolution equations of gradient flow type. *Journal of Evolution Equations*, 20:1061–1092, 2019.

[22] L. Bungert and Y. Korolev. Eigenvalue problems in l^∞: optimality conditions, duality, and relations with optimal transport. *Comm. American Math. Soc.*, 2(08):345–373, 2022.

[23] L. Bungert, M. Burger, and D. Tenbrinck. Computing nonlinear eigenfunctions via gradient flow extinction. In J. Lellmann, M. B. 0001, and J. Modersitzki, editors, *Scale Space and Variational Methods in Computer Vision - 7th International Conference, SSVM 2019, Hofgeismar, Germany, June 30 - July 4, 2019, Proceedings*, volume 11603 of *Lecture Notes in Computer Science*, pages 291–302. Springer, 2019. ISBN 978-3-030-22368-7. doi: 10.1007/978-3-030-22368-7_23. URL https://doi.org/10.1007/978-3-030-22368-7_23.

[24] L. Bungert, Y. Korolev, and M. Burger. Structural analysis of an l-infinity variational problem and relations to distance functions. *Pure and Applied Analysis*, 2, 01 2020. doi: 10.2140/paa.2020.2.703.

[25] L. Bungert, M. Burger, A. Chambolle, and M. Novaga. Nonlinear spectral decompositions by gradient flows of one-homogeneous functionals. *Anal. PDE*, 14(3):823–860, 2021.

[26] M. Burger. Parameter identification. *Winter School Inverse Problems 2005*, 2005.

[27] M. Burger, G. Gilboa, M. Moeller, L. Eckardt, and D. Cremers. Spectral decompositions using one-homogeneous functionals. *SIAM J. Imaging Sci.*, 9(3):1374–1408, 2016.

[28] J. Calder. The game theoretic p-laplacian and semi-supervised learning with few labels. *Nonlinearity*, 32(1):301, 2018.

[29] A. Candelieri, A. Ponti, and F. Archetti. On the distributional characterization of graph models of water distribution networks in wasserstein spaces. *Preprint*, 2021.

[30] E. Casas. *The Influence of the Tikhonov Term in Optimal Control of Partial Differential Equations*, pages 73–94. Springer International Publishing,

Cham, 2018. ISBN 978-3-319-97613-6. doi: 10.1007/978-3-319-97613-6_5. URL https://doi.org/10.1007/978-3-319-97613-6_5.

[31] M. Castro-Gama, Q. Pan, A. Jonoski, and D. Solomatine. A graph theoretical sectorization approach for energy reduction in water distribution networks. *Procedia Engineering*, 154:19–26, 2016.

[32] A. Chambolle and T. Pock. A first-order primal-dual algorithm for convex problems with applications to imaging. *Journal of Mathematical Imaging and Vision*, 40(1):120–145, 2011. URL http://dblp.uni-trier.de/db/journals/jmiv/jmiv40.html#ChambolleP11.

[33] A. Chambolle, V. Caselles, M. Novaga, D. Cremers, and T. Pock. An introduction to total variation for image analysis. working paper or preprint, Nov. 2009. URL https://hal.science/hal-00437581.

[34] A. Chambolle, M. Goldman, and M. Novaga. Fine properties of the subdifferential for a class of one-homogeneous functionals, 2013.

[35] K. C. Chang. Spectrum of the 1-laplacian and cheeger's constant on graphs. *Journal of Graph Theory*, 81(2):167–207, 2016.

[36] K. C. Chang, S. Shao, and D. Zhang. Nodal domains of eigenvectors for 1-Laplacian on graphs. *Adv. Math.*, 308:529–574, 2017.

[37] J. Cheeger. *A Lower Bound for the Smallest Eigenvalue of the Laplacian*, pages 195–200. Princeton University Press, Princeton, 2015. doi: doi: 10.1515/9781400869312-013.

[38] T. Y.-J. Chen, J. A. Beekman, S. D. Guikema, and S. Shashaani. Statistical modeling in absence of system specific data: Exploratory empirical analysis for prediction of water main breaks. *Journal of Infrastructure Systems*, 25(2):04019009, 2019. doi: 10.1061/(ASCE)IS.1943-555X.0000482. URL https://ascelibrary.org/doi/abs/10.1061/%28ASCE%29IS.1943-555X.0000482.

[39] W.-C. Cheng, N.-S. Hsu, W.-M. Cheng, and W. W.-G. Yeh. A flow path model for regional water distribution optimization. *Water Resources Research*, 45(9), 2009. doi: https://doi.org/10.1029/2009WR007826. URL https://agupubs.onlinelibrary.wiley.com/doi/abs/10.1029/2009WR007826.

[40] P. L. Combettes and V. R. Wajs. Signal recovery by proximal forward-backward splitting. *Multiscale Modeling & Simulation*, 4(4):1168–1200, 2005.

[41] A. Corbo Esposito and G. Piscitelli. Pseudo-orthogonality for graph 1-laplacian eigenvectors and applications to higher cheeger constants and data clustering. *Frontiers of Mathematics in China*, 17, 09 2021. doi: 10.1007/s11464-021-0961-2.

[42] E. B. Curtis and J. A. Morrow. *Inverse Problems for Electrical Networks*. WORLD SCIENTIFIC, 2000. doi: 10.1142/4306. URL `https://www.worldscientific.com/doi/abs/10.1142/4306`.

[43] M. F. Daniele Boffi, Franco Brezzi. *Mixed Finite Element Methods and Applications*. Springer, 1991.

[44] P. Deidda, M. Putti, and F. Tudisco. Nodal domain count for the generalized graph p-laplacian. *Applied and Computational Harmonic Analysis*, 64:1–32, 2023. ISSN 1063-5203. doi: https://doi.org/10.1016/j.acha.2022.12.003. URL `https://www.sciencedirect.com/science/article/pii/S1063520322001002`.

[45] S. Efromovich and V. Koltchinskii. On inverse problems with unknown operators. *IEEE Transactions on Information Theory*, 47(7):2876–2894, 2001. doi: 10.1109/18.959267.

[46] I. Ekeland and R. Témam. *Convex Analysis and Variational Problems*. Society for Industrial and Applied Mathematics, 1999. doi: 10.1137/1.9781611971088. URL `https://epubs.siam.org/doi/abs/10.1137/1.9781611971088`.

[47] A. Elmoataz, M. Toutain, and D. Tenbrinck. On the p-laplacian and ∞-laplacian on graphs with applications in image and data processing. *SIAM Journal on Imaging Sciences*, 8(4):2412–2451, 2015. doi: 10.1137/15M1022793. URL `https://doi.org/10.1137/15M1022793`.

[48] L. Esposito, B. Kawohl, C. Nitsch, and C. Trombetti. The neumann eigenvalue problem for the ∞-laplacian. *Rendiconti Lincei - Matematica e Applicazioni*, 26, 05 2014. doi: 10.4171/RLM/697.

[49] E. Esser, X. Zhang, and T. Chan. A general framework for a class of first order primal-dual algorithms for convex optimization in imaging science. *SIAM J. Imaging Sciences*, 3:1015–1046, 01 2010. doi: 10.1137/09076934X.

[50] L. Evans. The 1-laplacian, the infinity-laplacian and differential games. *Perspectives in Nonlinear Partial Differential Equations: In Honor of Haim Brezis*, 446:245, 10 2009. doi: 10.1090/conm/446/08634.

[51] L. C. Evans and W. Gangbo. Differential equations methods for the monge-kantorovich mass transfer problem. *Memoirs of the American Mathematical Society*, 137(653):1–66, 1999.

[52] L. C. Evans and R. E. Gariepy. *Measure theory and fine properties of functions : textbooks in mathematics*. CRC Press, New York, 2015.

[53] T. S. Evans and R. Lambiotte. Line graphs, link partitions, and overlapping communities. *Physical Review E*, 80(1), jul 2009. doi: 10.1103/physreve.80.016105. URL `https://doi.org/10.1103%2Fphysreve.80.016105`.

[54] E. Facca and M. Benzi. Fast iterative solution of the optimal transport problem on graphs, 2020.

[55] E. Facca, F. Cardin, and M. Putti. Towards a stationary monge–kantorovich dynamics: The physarum polycephalum experience. *SIAM Journal on Applied Mathematics*, 78(2):651–676, 2018.

[56] E. Facca, S. Daneri, F. Cardin, and M. Putti. Numerical solution of Monge–Kantorovich equations via a dynamic formulation. *J. Sci. Comput.*, 82:68, 02 2020. doi: 10.1007/s10915-020-01170-8.

[57] E. Facca, F. Cardin, and M. Putti. Branching structures emerging from a continuous optimal transport model. *J. Comp. Phys.*, 447:110700, 2021. ISSN 0021-9991. doi: https://doi.org/10.1016/j.jcp.2021.110700.

[58] E. Facca, F. Piazzon, and M. Putti. Transport energy. *Appl. Math, Optim. ,submitted*, 2021.

[59] E. Facca, F. Piazzon, and M. Putti. Computing the l^1 optimal transport density: a fem approach. *In Preparation*, 2022.

[60] E. Facca, F. Piazzon, and M. Putti. l^1 transport energy. *Applied Mathematics & Optimization*, 86(2):1–40, 2022.

[61] G. B. Folland. *Real analysis : modern techniques and their applications / Gerald B. Folland*. Pure and applied mathematics (Wiley). Wiley, New York, 1984. ISBN 0471809586.

[62] G. Franzina and P. D. Lamberti. Existence and uniqueness for a p-laplacian nonlinear eigenvalue problem. *Electronic Journal of Differential Equations*, 2010(26):1–10, 2010.

[63] J. Friedman. Some geometric aspects of graphs and their eigenfunctions. *Duke Math. J.*, 69(3), 1993. ISSN 00127094. doi: 10.1215/S0012-7094-93-06921-9.

[64] P. Getreuer. Rudin-osher-fatemi total variation denoising using split bregman. *Image Processing On Line*, 2:74–95, 05 2012. doi: 10.5201/ipol.2012.g-tvd.

[65] O. Giustolisi, A. Simone, and L. Ridolfi. Network structure classification and features of water distribution systems. *Water Resources Research*, 53 (4):3407–3423, 2017.

[66] O. Giustolisi, F. G. Ciliberti, L. Berardi, and D. B. Laucelli. A novel approach to analyze the isolation valve system based on the complex network theory. *Water Resources Research*, 58(4):e2021WR031304, 2022.

[67] G. H. Golub and C. F. Van Loan. *Matrix computations*. JHU press, 2013.

[68] S. Guastavino and F. Benvenuto. Convergence rates of spectral regularization methods: A comparison between ill-posed inverse problems and statistical kernel learning. *SIAM Journal on Numerical Analysis*, 58(6): 3504–3529, 2020. doi: 10.1137/19M1256038. URL `https://doi.org/10.1137/19M1256038`.

[69] D. N. Hào and T. N. T. Quyen. Convergence rates for tikhonov regularization of coefficient identification problems in laplace-type equations. *Inverse Problems*, 26(12):125014, nov 2010. doi: 10.1088/0266-5611/26/12/125014. URL `https://doi.org/10.1088/0266-5611/26/12/125014`.

[70] D. Hauer and J. Mazon. The dirichlet-to-neumann operator associated with the 1-laplacian and evolution problems. *Calculus of Variations and Partial Differential Equations*, 61, 02 2022. doi: 10.1007/s00526-021-02149-5.

[71] B. He, F. Ma, S. Xu, and X. Yuan. A generalized primal-dual algorithm with improved convergence condition for saddle point problems. *SIAM Journal on Imaging Sciences*, 15(3):1157–1183, 2022. doi: 10.1137/21M1453463. URL `https://doi.org/10.1137/21M1453463`.

[72] M. Hein and T. Bühler. An inverse power method for nonlinear eigenproblems with applications in 1-spectral clustering and sparse pca, 2010.

[73] M. Herrera, E. Abraham, and I. Stoianov. A graph-theoretic framework for assessing the resilience of sectorised water distribution networks. *Water Resources Management*, 30(5):1685–1699, 2016.

[74] B. Hua and L. Wang. Dirichlet p-laplacian eigenvalues and cheeger constants on symmetric graphs. *Advances in Mathematics*, 364:106997, 04 2020. doi: 10.1016/j.aim.2020.106997.

[75] D. Jang, H. Park, and G. Choi. Estimation of leakage ratio using principal component analysis and artificial neural network in water distribution systems. *Sustainability*, 10(3):750, 2018.

[76] Y. Jin, Q. Shen, X. Wu, J. Chen, and Y. Huang. A Physics-Driven Deep-Learning Network for Solving Nonlinear Inverse Problems. *Petrophysics* -

The SPWLA Journal of Formation Evaluation and Reservoir Description, 61(01):86–98, 02 2020. ISSN 1529-9074. doi: 10.30632/PJV61N1-2020a3. URL https://doi.org/10.30632/PJV61N1-2020a3.

[77] J. Jost and D. Zhang. Discrete-to-continuous extensions: piecewise multilinear extension, min-max theory and spectral theory. *arXiv preprint arXiv:2106.04116*, 2021.

[78] P. Juutinen and P. Lindqvist. On the higher eigenvalues for the ∞-eigenvalue problem. *Calculus of Variations and Partial Differential Equations*, 23(2):169–192, 2005.

[79] P. Juutinen, P. Lindqvist, and J. Manfredi. The ∞-eigenvalue problem. *Archive for Rational Mechanics and Analysis*, 148:89–105, 1999.

[80] U. S. Kamilov, H. Mansour, and B. Wohlberg. A plug-and-play priors approach for solving nonlinear imaging inverse problems. *IEEE Signal Processing Letters*, 24(12):1872–1876, 2017. doi: 10.1109/LSP.2017.2763583.

[81] S. Kara, I. E. Karadirek, A. Muhammetoglu, and H. Muhammetoglu. Hydraulic modeling of a water distribution network in a tourism area with highly varying characteristics. *Procedia Engineering*, 162:521–529, 2016. ISSN 1877-7058. doi: https://doi.org/10.1016/j.proeng.2016.11.096. URL https://www.sciencedirect.com/science/article/pii/S1877705816334051. International Conference on Efficient & Sustainable Water Systems Management toward Worth Living Development, 2nd EWaS 2016.

[82] B. Karney and D. McInnis. Transient analysis of water distribution systems. *Journal - American Water Works Association*, 82:62–70, 07 1990. doi: 10.1002/j.1551-8833.1990.tb06992.x.

[83] T. Kato. *Perturbation theory for linear operators*, volume 132. Springer Science & Business Media, 2013.

[84] B. Kawohl and V. Fridman. Isoperimetric estimates for the first eigenvalue of the p-laplace operator and the cheeger constant. *Commentationes Mathematicae Universitatis Carolinae*, 44(4):659–667, 2003. URL http://eudml.org/doc/249207.

[85] J. Kepner and J. R. Gilbert, editors. *Graph Algorithms in the Language of Linear Algebra*, volume 22 of *Software, environments, tools*. SIAM, 2011. ISBN 978-0-89871-990-1.

[86] B. Kizilöz. Prediction model for the leakage rate in a water distribution system. *Water Supply*, 21(8):4481–4492, 06 2021. ISSN 1606-9749. doi: 10.2166/ws.2021.194. URL https://doi.org/10.2166/ws.2021.194.

[87] Q. T. Kolt, S. J. Kilner, and D. L. Farnsworth. A table of legendre-transformation pairs with methodologies for construction, authentication, and approximation of pairs, 2022.

[88] P. D. Lamberti. A differentiability result for the first eigenvalue of the p-Laplacian upon domain perturbation. In V. Lakshmikantham, R. Agarwal, and D. O'Regan, editors, *Nonlinear analysis and applications: to V. Lakshmikantham on his 80th birthday*, volume 1, pages 741–754. Kluwer Academic Publishers, 2003.

[89] P. Lee, T. Kim, and S. Kim. Accurate and efficient numerical solutions for elliptic obstacle problems. *Journal of Inequalities and Applications*, 2017: 34, 02 2017. doi: 10.1186/s13660-017-1309-z.

[90] S.-S. Leu and Q.-N. Bui. Leak prediction model for water distribution networks created using a bayesian network learning approach. *Water resources management*, 30(8):2719–2733, 2016.

[91] M. Levi, F. Santagati, A. Tabacco, and M. Vallarino. Poincaré inequalities on graphs. *Analysis Mathematica*, 49(2):529–544, mar 2023. doi: 10.1007/s10476-023-0215-5. URL `https://doi.org/10.1007%2Fs10476-023-0215-5`.

[92] J. L. Lions and G. Stampacchia. Variational inequalities. *Communications on Pure and Applied Mathematics*, 20(3):493–519, 1967. doi: https://doi.org/10.1002/cpa.3160200302. URL `https://onlinelibrary.wiley.com/doi/abs/10.1002/cpa.3160200302`.

[93] H. Liu, D. Savić, Z. Kapelan, M. Zhao, Y. Yuan, and H. Zhao. A diameter-sensitive flow entropy method for reliability consideration in water distribution system design. *Water Resources Research*, 50(7):5597–5610, 2014. doi: https://doi.org/10.1002/2013WR014882. URL `https://agupubs.onlinelibrary.wiley.com/doi/abs/10.1002/2013WR014882`.

[94] S. Lunz, A. Hauptmann, T. Tarvainen, C.-B. Schönlieb, and S. Arridge. On learned operator correction in inverse problems. *SIAM Journal on Imaging Sciences*, 14(1):92–127, 2021. doi: 10.1137/20M1338460. URL `https://doi.org/10.1137/20M1338460`.

[95] R. Löhner and H. Antil. Revisiting calderon's problem, 2019.

[96] F. Mantlik. Partial differential operators depending analytically on a parameter. *Annales de l'Institut Fourier*, 41(3):577–599, 1991. doi: 10.5802/aif.1266. URL `http://www.numdam.org/articles/10.5802/aif.1266/`.

[97] N. Masuda and F. Meng. Dynamical stability of water distribution networks. *Proceedings of the Royal Society A*, 475(2230):20190291, 2019.

[98] F. Meng, G. Fu, R. Farmani, C. Sweetapple, and D. Butler. Topological attributes of network resilience: A study in water distribution systems. *Water research*, 143:376–386, 2018.

[99] J. Milnor. Morse theory.(am-51), volume 51. In *Morse Theory.(AM-51), Volume 51*. Princeton university press, 2016.

[100] N. Moosavian and B. J. Lence. Flow-uniformity index for reliable-based optimal design of water-distribution networks. *Journal of Water Resources Planning and Management*, 146(3):04020005, 2020. doi: 10.1061/(ASCE)WR.1943-5452.0001161. URL https://ascelibrary.org/doi/abs/10.1061/%28ASCE%29WR.1943-5452.0001161.

[101] J. L. Mueller and S. Siltanen. *Linear and nonlinear inverse problems with practical applications*. SIAM, 2012.

[102] O. Nachum and B. Dai. Reinforcement learning via fenchel-rockafellar duality, 2020.

[103] T. M. Nguyen, T. M. Nguyen, N. Ho, A. L. Bertozzi, R. Baraniuk, and S. Osher. A primal-dual framework for transformers and neural networks. In *The Eleventh International Conference on Learning Representations*, 2023. URL https://openreview.net/forum?id=U_T8-5hClV.

[104] S. Osher, M. Burger, D. Goldfarb, J. Xu, and W. Yin. An iterative regularization method for total variation-based image restoration. *Multiscale Modeling & Simulation*, 4(2):460–489, 2005. doi: 10.1137/040605412.

[105] M. Ôtani. On certain second order ordinary differential equations associated with Sobolev-Poincaré-type inequalities. *Nonlinear Anal. Theory Methods Appl.*, 8(11):1255–1270, 1984.

[106] V. Ozoliņš, R. Lai, R. Caflisch, and S. Osher. Compressed modes for variational problems in mathematics and physics. *Proceedings of the National Academy of Sciences*, 110(46):18368–18373, oct 2013. doi: 10.1073/pnas.1318679110. URL https://doi.org/10.1073%2Fpnas.1318679110.

[107] A. Pagano, C. Sweetapple, R. Farmani, R. Giordano, and D. Butler. Water distribution networks resilience analysis: A comparison between graph theory-based approaches and global resilience analysis. *Water Resources Management*, 33(8):2925–2940, 2019.

[108] N. Palod, V. Prasad, and R. Khare. Reliability-based optimization of water distribution networks. *Water Supply*, 22(2):2133–2147, 10 2021. ISSN 1606-9749. doi: 10.2166/ws.2021.363. URL https://doi.org/10.2166/ws.2021.363.

[109] E. Parini. The second eigenvalue of the p-Laplacian as goes to 1. *Int. J. Differ. Equ.*, 2010, 2010.

[110] J.-H. Park. On a resonance problem with the discrete p-Laplacian on finite graphs. *Nonlinear Anal. Theory Methods Appl.*, 74(17):6662–6675, 2011. ISSN 0362-546X. doi: https://doi.org/10.1016/j.na.2011.06.046. URL https://www.sciencedirect.com/science/article/pii/S0362546X11004652.

[111] S. Park and P. V. Hentenryck. Self-supervised primal-dual learning for constrained optimization, 2022.

[112] L. Perelman, M. Housh, and A. Ostfeld. Robust optimization for water distribution systems least cost design. *Water Resources Research*, 49(10):6795–6809, 2013. doi: https://doi.org/10.1002/wrcr.20539. URL https://agupubs.onlinelibrary.wiley.com/doi/abs/10.1002/wrcr.20539.

[113] F. Piazzon, E. Facca, and M. Putti. Computing the l^1 optimal transport density: a fem approach. *arXiv preprint arXiv:2304.14047*, 2023.

[114] A. Ponti, A. Candelieri, I. Giordani, and F. Archetti. A novel graph-based vulnerability metric in urban network infrastructures: The case of water distribution networks. *Water*, 13(11):1502, 2021.

[115] M. Pragliola, L. Calatroni, A. Lanza, and F. Sgallari. On and beyond total variation regularization in imaging: The role of space variance. *SIAM Review*, 65(3):601–685, 2023. doi: 10.1137/21M1410683. URL https://doi.org/10.1137/21M1410683.

[116] T. D. Prasad and N.-S. Park. Multiobjective genetic algorithms for design of water distribution networks. *Journal of Water Resources Planning and Management*, 130(1):73–82, 2004. doi: 10.1061/(ASCE)0733-9496(2004)130:1(73). URL https://ascelibrary.org/doi/abs/10.1061/%28ASCE%290733-9496%282004%29130%3A1%2873%29.

[117] D. N. Raad, A. N. Sinske, and J. H. van Vuuren. Comparison of four reliability surrogate measures for water distribution systems design. *Water Resources Research*, 46(5), 2010. doi: https://doi.org/10.1029/2009WR007785. URL https://agupubs.onlinelibrary.wiley.com/doi/abs/10.1029/2009WR007785.

[118] V. Rabinovich. Parameter dependent differential operators on graphs and their applications. *Applicable Analysis*, 100(3):493–512, 2021. doi: 10.1080/00036811.2019.1608963. URL https://doi.org/10.1080/00036811.2019.1608963.

[119] M. Raissi, P. Perdikaris, and G. Karniadakis. Physics-informed neural networks: A deep learning framework for solving forward and inverse problems involving nonlinear partial differential equations. *Journal of Computational Physics*, 378:686–707, 2019. ISSN 0021-9991. doi: https://doi.org/10.1016/j.jcp.2018.10.045. URL https://www.sciencedirect.com/science/article/pii/S0021999118307125.

[120] R. T. Rockafellar. *Convex analysis*. Princeton Mathematical Series. Princeton University Press, Princeton, N. J., 1970.

[121] M. T. Schaub and S. Segarra. FLOW SMOOTHING AND DENOISING: GRAPH SIGNAL PROCESSING IN THE EDGE-SPACE. In *2018 IEEE Global Conference on Signal and Information Processing (GlobalSIP)*. IEEE, nov 2018. doi: 10.1109/globalsip.2018.8646701. URL https://doi.org/10.1109%2Fglobalsip.2018.8646701.

[122] A. Scheidegger, L. Scholten, M. Maurer, and P. Reichert. Extension of pipe failure models to consider the absence of data from replaced pipes. *Water Research*, 47(11):3696–3705, 2013. ISSN 0043-1354. doi: https://doi.org/10.1016/j.watres.2013.04.017. URL https://www.sciencedirect.com/science/article/pii/S0043135413003461.

[123] K. Sebbagh, A. Safri, and M. Zabot. Pre-localization approach of leaks on a water distribution network by optimization of the hydraulic model using an evolutionary algorithm. *Proceedings*, 2(11), 2018. ISSN 2504-3900. doi: 10.3390/proceedings2110588. URL https://www.mdpi.com/2504-3900/2/11/588.

[124] U. Shamir. Optimal design and operation of water distribution systems. *Water Resources Research*, 10(1):27–36, 1974. doi: https://doi.org/10.1029/WR010i001p00027. URL https://agupubs.onlinelibrary.wiley.com/doi/abs/10.1029/WR010i001p00027.

[125] Q. Shuang, H. J. Liu, and E. Porse. Review of the quantitative resilience methods in water distribution networks. *Water*, 11(6), 2019. ISSN 2073-4441. doi: 10.3390/w11061189. URL https://www.mdpi.com/2073-4441/11/6/1189.

[126] R. Sitzenfrei, M. Möderl, and W. Rauch. Graph-based approach for generating virtual water distribution systems in the software VIBe. *Water Supply*, 10(6):923–932, 12 2010. ISSN 1606-9749. doi: 10.2166/ws.2010.579. URL https://doi.org/10.2166/ws.2010.579.

[127] R. Sitzenfrei, Q. Wang, Z. Kapelan, and D. Savić. Using complex network analysis for optimization of water distribution networks. *Water resources research*, 56(8):e2020WR027929, 2020.

[128] M. Struwe. *Variational methods*, volume 991. Springer, 2000.

[129] P. B. Sáez and B. E. Rittmann. Model-parameter estimation using least squares. *Water Research*, 26(6):789–796, 1992. ISSN 0043-1354. doi: https://doi.org/10.1016/0043-1354(92)90010-2. URL `https://www.sciencedirect.com/science/article/pii/0043135492900102`.

[130] H. D. Tagare. Notes on optimization on stiefel manifolds. 2011.

[131] A. Tarantola. *Inverse problem theory and methods for model parameter estimation*. SIAM, 2005.

[132] E. Todini. Looped water distribution networks design using a resilience index based heuristic approach. *Urban Water*, 2(2):115–122, 2000. ISSN 1462-0758. doi: https://doi.org/10.1016/S1462-0758(00)00049-2. URL `https://www.sciencedirect.com/science/article/pii/S1462075800000492`. Developments in water distribution systems.

[133] B. A. Tolson, M. Asadzadeh, H. R. Maier, and A. Zecchin. Hybrid discrete dynamically dimensioned search (hd-dds) algorithm for water distribution system design optimization. *Water Resources Research*, 45(12), 2009. doi: https://doi.org/10.1029/2008WR007673. URL `https://agupubs.onlinelibrary.wiley.com/doi/abs/10.1029/2008WR007673`.

[134] F. Tudisco and M. Hein. A nodal domain theorem and a higher-order cheeger inequality for the graph p-laplacian. *Journal of Spectral Theory*, 8 (3):883–908, 2018.

[135] F. Tudisco and D. Zhang. Nonlinear spectral duality. *arXiv preprint arXiv:2209.06241*, 2022.

[136] G. Uhlmann. 30 years of calderón's problem. *Séminaire Laurent Schwartz—EDP et applications*, pages 1–25, 2012.

[137] A.-J. Ulusoy, I. Stoianov, and A. Chazerain. Hydraulically informed graph theoretic measure of link criticality for the resilience analysis of water distribution networks. *Applied network science*, 3(1):1–22, 2018.

[138] H. Whitney. A set of topological invariants for graphs. *American Journal of Mathematics*, 55(1):231–235, 1933. ISSN 00029327, 10806377. URL `http://www.jstor.org/stable/2371125`.

[139] X. Yao and J. Zhou. Numerical methods for computing nonlinear eigenpairs: Part i. iso-homogeneous cases. *SIAM J. Sci. Comput.*, 29:1355–1374, 2007.

[140] X. Yao and J. Zhou. Unified convergence results on a minimax algorithm for finding multiple critical points in banach spaces. *SIAM Journal on Numerical Analysis*, 45(3):1330–1347, 2007. doi: 10.1137/050627320. URL `https://doi.org/10.1137/050627320`.

[141] A. Yazdani and P. Jeffrey. Water distribution system vulnerability analysis using weighted and directed network models. *Water Resources Research*, 48(6), 2012. doi: https://doi.org/10.1029/2012WR011897. URL https://agupubs.onlinelibrary.wiley.com/doi/abs/10.1029/2012WR011897.

[142] W. Yin, S. Osher, D. Goldfarb, and J. Darbon. Bregman iterative algorithms for l(1)-minimization with applications to compressed sensing. *Siam Journal on Imaging Sciences - SIAM J IMAGING SCI*, 1, 01 2008. doi: 10.1137/070703983.

[143] W. Zaiwen and Y. Wotao. A feasible method for optimization with orthogonality constraints. *Mathematical Programming*, dec 2013. doi: 10.1007/s10107-012-0584-1. URL https://doi.org/10.1007/s10107-012-0584-1.

[144] F. Zeng, K. Li, X. Li, and E. W. Tollner. Impact of planning horizon on water distribution network design. *Water Supply*, 22(3):2863–2873, 12 2021. ISSN 1606-9749. doi: 10.2166/ws.2021.431. URL https://doi.org/10.2166/ws.2021.431.

[145] D. Zhang. Homological eigenvalues of graph p-Laplacians. *arXiv:2110.06054*, 2021.

[146] M. Zhu and T. Chan. An efficient primal-dual hybrid gradient algorithm for total variation image restoration. *UCLA CAM Report*, 05 2008.